



**UNIVERSITY OF LEEDS**

# **Characterisation of the Phenotypic and Functional Repertoire of Monocytes in Idiopathic Pulmonary Fibrosis**

---

**Emily Ruth Fraser**

**Submitted in accordance with the requirements  
for the degree of Doctor of Philosophy**

The University of Leeds  
Faculty of Medicine and Health  
School of Medicine  
Leeds Institute of Biomedical and Clinical Sciences

March 2019

The candidate confirms that the work submitted is her own and that appropriate credit has been given within the thesis where reference has been made to the work of others.

This copy has been supplied on the understanding that it is copyright material and that no quotation from the thesis may be published without proper acknowledgement.

© 2018 "The University of Leeds" and Emily Fraser.

The right of Emily Fraser to be identified as Author of this work has been asserted by her in accordance with the Copyright, Design and Patents Act 1988.

## Acknowledgements

I would like to thank my supervisors for all their support and helpful advice throughout my research and during the writing of this thesis. I would also like to thank members of my group, in particular, Adel Benlahrech, who spent many hours teaching me the art of flow cytometry and other laboratory skills. Without his technical and scientific expertise, alongside his endless patience and willingness to help, completing this work would have been tremendously difficult. I am grateful to Karl Blirando, who took the time to teach me RNA extraction and quantitative PCR. Karl undertook the majority of the qPCR assays presented in this thesis. I would like to thank Dr Rachel Benamore and Dr Victoria St Noble, thoracic radiologists, who helped devise the CT scoring system and graded the CT scans in this project. Many thanks to Dr Rachel Hoyles for helping me to develop my clinical understanding of IPF and other fibrotic lung diseases, as well as allowing me to recruit patients from her clinic. Lastly, I would like to thank my family and friends for the endless encouragement and support throughout.

Supervisor: Professor Sir Alexander F Markham

Co-supervisors: Doctor Rashida Anwar and Professor Ling-Pei Ho (Oxford)

*This thesis represents studies carried out at the MRC Human Immunology Unit, University of Oxford; supervised by Prof Ling-Pei Ho. All studies were funded by grants secured by Prof Ho.*

## Abstract

Idiopathic pulmonary fibrosis (IPF) is a chronic fibroproliferative disease characterised by the accumulation of scar tissue within the lung parenchyma. The pathogenic mechanisms underlying the disease remain incompletely understood but involve aberrations in repair pathways. The role of macrophages in IPF has gained interest due to their recognised contribution in orchestrating repair. In health, lineage tracing has revealed that lung macrophages are established in early development and undergo self-renewal. Following injury however, these populations become depleted and there is evidence from murine models that infiltrating monocytes differentiate into macrophages and potentiate fibrogenic processes. I hypothesised that monocytes may be phenotypically and functionally distinct in IPF and contribute to the process of fibrotic over-repair.

To test this, peripheral blood monocytes from IPF patients were immunophenotyped and the expression of genes and proteins associated with inflammatory and repair processes were analysed. Given that IPF exclusively affects the lung tissue, monocytes were differentiated into macrophages using autologous serum to determine whether they expressed pro-repair characteristics. I examined key macrophage functions including ROS generation, phagocytosis and efferocytosis. Lastly, I assessed the influence of monocyte-derived macrophages (MDMs) on fibrogenic endpoints.

My data revealed that monocyte levels were higher in IPF patients and correlated with fibrotic burden on CT. CD64 was increased on IPF monocytes and a higher proportion of CD64<sup>+</sup>CD163<sup>-</sup> cells underwent early apoptosis. IPF MDMs on day 7 showed greater retention of the monocyte marker CD14, alongside lower CD64 and CD86 expression. ROS generation, phagocytosis and efferocytosis were impaired in IPF MDMs. qPCR of Day 7 MDMs revealed up-regulation of both pro-injury genes, *TNF $\alpha$*  and *STAT1*, and pro-repair genes including *GR*, *PPAR- $\gamma$* , *LGALS3* and *AREG*. Both IPF and control MDMs increased fibroblast proliferation and expression of *HAS2*, *IL-6* and *MCP-1* but differences were not observed between groups. MDMs collectively inhibited the process of EMT in an epithelial cell line.

The increase in monocyte levels and correlation with fibrotic extent suggests a role for these cells in the pathogenesis of IPF. Impaired efferocytosis and the up-regulation of genes associated with both injurious and reparative processes in IPF MDMs may potentiate tissue damage and promote fibrogenesis *in vivo*.

# List of Contents

<b>Acknowledgements</b>	<b>i</b>
<b>Abstract</b>	<b>ii</b>
<b>List of Contents</b>	<b>iii</b>
<b>List of Figures</b>	<b>x</b>
<b>List of Tables</b>	<b>xvi</b>
<b>List of Abbreviations</b>	<b>xviii</b>
<b>1 Introduction</b>	<b>1</b>
<b>1.1 Idiopathic Pulmonary Fibrosis (IPF)</b>	<b>1</b>
1.1.1 Background	1
1.1.2 Clinical Features	2
1.1.3 Diagnostic Features	3
1.1.4 Acute Exacerbations	6
1.1.5 Pharmacological treatment of IPF	7
<b>1.2 Pathophysiology of IPF</b>	<b>8</b>
1.2.1 Models of lung fibrosis	8
1.2.2 Alveolar epithelial cell injury	9
1.2.3 Genetic susceptibility to lung fibrosis	10
1.2.4 Environmental factors and the 'Second hit' hypothesis	12
1.2.5 Role of microbes as cofactors in IPF	13
1.2.6 TGF $\beta$ and its role in fibrogenesis	14
1.2.7 Inflammatory responses in IPF	16
1.2.8 Oxidative stress	18
1.2.9 Fibroblast activation in IPF	20
1.2.10 Epithelial-mesenchymal transition (EMT)	21
1.2.11 Adaptive immune responses in IPF	22
<b>1.3 Monocytes and Macrophages</b>	<b>24</b>
1.3.1 Monocyte subsets	24
1.3.2 Macrophage ontogeny	26

1.3.3	Lung macrophage populations	27
1.3.4	Monocyte-derived-macrophages and polarised subsets	28
1.3.5	Monocytes and macrophages in inflammation and repair	32
1.3.6	The role of monocytes and macrophages in fibrogenesis	34
<b>1.4</b>	<b>Project aims</b>	<b>37</b>
<b>2</b>	<b>Materials and Methods</b>	<b>38</b>
<b>2.1</b>	<b>Patients and participants</b>	<b>38</b>
<b>2.2</b>	<b>Clinical information</b>	<b>39</b>
<b>2.3</b>	<b>Laboratory methods</b>	<b>40</b>
2.3.1	Media	40
2.3.2	Extraction of peripheral blood mononuclear cells (PBMCs)	40
2.3.3	Serum preparation	40
2.3.4	Monocyte isolation	41
2.3.5	Generation of monocyte-derived macrophages (MDMs)	41
<b>2.4</b>	<b>Flow cytometry</b>	<b>41</b>
2.4.1	Phenotypic and cytokine staining of monocytes within PBMCs and MDMs	42
	Intracellular staining (ICS):	42
<b>2.5</b>	<b>Monocyte-derived macrophage studies</b>	<b>44</b>
2.5.1	Phagocytosis assays	44
2.5.2	ROS assay	45
2.5.3	Inflammasome assay	46
<b>2.6</b>	<b>ELISA</b>	<b>46</b>
2.6.1	IL-1 $\beta$	46
2.6.2	M-CSF	46
<b>2.7</b>	<b>Apoptosis assays</b>	<b>47</b>
<b>2.8</b>	<b>Neutrophil efferocytosis assay</b>	<b>47</b>
2.8.1	Isolation of neutrophils	47
2.8.2	Preparation of MDMs	47
2.8.3	Efferocytosis experiment	48
<b>2.9</b>	<b>RNA extraction</b>	<b>48</b>
<b>2.10</b>	<b>Quantitative PCR (qPCR)</b>	<b>49</b>
<b>2.11</b>	<b>Fibroblast studies</b>	<b>54</b>
2.11.1	Culturing primary fibroblasts	54

2.11.2	Co-culture and transwell experiments	55
2.11.3	Immunofluorescence	55
<b>2.12</b>	<b>Epithelial-mesenchymal transition/mesenchymal-epithelial transition (EMT/MET) studies</b>	<b>56</b>
<b>2.13</b>	<b>Cryopreservation and thawing of samples</b>	<b>57</b>
<b>2.14</b>	<b>Statistical analysis</b>	<b>57</b>

### **3 Monocyte phenotype in stable and acute exacerbations of**

<b>IPF</b>		<b>58</b>
<b>3.1</b>	<b>Introduction</b>	<b>58</b>
<b>3.2</b>	<b>Hypothesis and Aims</b>	<b>60</b>
<b>3.3</b>	<b>Methods</b>	<b>61</b>
3.3.1	Participant samples	61
3.3.2	Isolation and preparation of peripheral blood mononuclear cells (PBMCs)	61
3.3.3	Flow cytometry and gating strategy	62
3.3.4	RNA extraction and qPCR analysis	64
<b>3.4</b>	<b>Results</b>	<b>65</b>
3.4.1	Patient characteristics	65
3.4.2	Monocyte levels were increased in IPF compared to age-matched controls	68
3.4.3	The proportions of classical, intermediate and non-classical monocytes were similar between stable IPF patients and controls	70
3.4.4	CD64 expression was increased in both classical and non-classical monocyte subsets in IPF	71
3.4.5	CD14 monocytes from AEIPF displayed a distinct profile consistent with M2 polarisation	73
3.4.6	Expression of M1/M2 genes differed in monocytes from patients with stable IPF compared to aged-matched healthy controls	80
3.4.7	CD163 expression was down-regulated by LPS but retained following TLR7/8 stimulation	83
3.4.8	IL-10 expression was attenuated in monocytes from patients with AEIPF in response to stimulation with LPS	85
3.4.9	CD163+ monocytes showed enhanced cytokine/chemokine responses to LPS and r848 compared to their CD163- counterparts	87

3.5	<b>Discussion</b>	<b>90</b>
<b>4</b>	<b>Fibrotic burden, anti-fibrotic treatment and monocytes in</b>	
	<b>IPF</b>	<b>97</b>
4.1	<b>Introduction</b>	<b>97</b>
4.2	<b>Hypothesis and aims</b>	<b>99</b>
4.3	<b>Methods</b>	<b>100</b>
4.3.1	Development of a computed tomography (CT) fibrosis score	100
4.3.2	Patient characteristics and monocyte profiling	101
4.3.3	Lung function data collection and the composite physiologic index (CPI)	101
4.4	<b>Results</b>	<b>102</b>
4.4.1	Patient characteristics	102
4.4.2	The Total CT Fibrosis Score (TFS) was highly reproducible between radiologists	103
4.4.3	Validation of the TFS against lung function parameters CPI, FVC and TLCO	105
4.4.4	Monocyte levels correlated positively with the TFS but not with lung function parameters	106
4.4.5	Cell surface markers CD64, CD163, CCR7, CD62L on monocytes and the CD163/CD64 ratio did not correlate significantly with the TFS or lung function indices	108
4.4.6	Patients with AEIPF have a higher burden of lung fibrosis than patients with stable disease	111
4.4.7	Pirfenidone attenuates CD64 expression on monocytes	112
4.5	<b>Discussion</b>	<b>116</b>
<b>5</b>	<b>Phenotypic and functional characteristics of monocyte-derived macrophages from IPF patients</b>	<b>120</b>
5.1	<b>Introduction</b>	<b>120</b>
5.2	<b>Hypothesis and aims</b>	<b>122</b>
5.3	<b>Methods</b>	<b>123</b>
5.3.1	Participant samples	123



5.3.2	Generation of monocyte-derived macrophages (MDMs)	123
5.3.3	Dexamethasone assay	124
5.3.4	Flow cytometry and gating strategy	124
5.3.5	ELISA for M-CSF	125
5.3.6	Functional assays	125
5.3.7	RNA extraction and qPCR	126
<b>5.4</b>	<b>Results</b>	<b>126</b>
5.4.1	Participant demographics	126
5.4.2	CD14 expression was down-regulated and CD68 up-regulated during the differentiation of monocytes to macrophages in culture	127
5.4.3	Monocytes from IPF patients showed evidence of delayed differentiation in ex vivo culture	129
5.4.4	Monocytes from IPF patients differentiated into phenotypically distinct MDMs	130
5.4.5	MDMs from AEIPF and stable patients on Prednisolone showed up-regulation of CD163 after 7 days' ex vivo culture	132
5.4.6	CD64 <sup>+</sup> monocytes exhibit preferential apoptosis in IPF patients	135
5.4.7	RNA expression of key inflammatory and reparative genes differs significantly between IPF and control MDMs	139
5.4.8	M-CSF was increased in the serum of IPF patients	148
5.4.9	The production of reactive oxygen species (ROS) is impaired in IPF MDMs compared to controls	149
5.4.10	IL-1 $\beta$ secretion in response to inflammasome activation does not differ between IPF and control MDMs	151
<b>5.5</b>	<b>Discussion</b>	<b>153</b>
<b>6</b>	<b>The influence of MDMs on fibrogenic end-points</b>	<b>160</b>
<b>6.1</b>	<b>Introduction</b>	<b>160</b>
<b>6.2</b>	<b>Hypothesis and aims</b>	<b>163</b>
<b>6.3</b>	<b>Methods</b>	<b>164</b>
6.3.1	Participant samples	164
6.3.2	Generation of human lung fibroblasts	164
6.3.3	Generation of monocyte-derived macrophages	164
6.3.4	Preparation of A549 cells for use in EMT and MET experiments	164
6.3.5	Co-culture experiments	165

6.3.6	Flow cytometry, gating strategy and analysis	166
6.3.7	RNA extraction and qPCR	167
<b>6.4</b>	<b>Results</b>	<b>168</b>
6.4.1	Participant demographics	168
6.4.2	MDMs decrease $\alpha$ SMA expression in primary lung fibroblasts	168
6.4.3	MDMs increase fibroblast proliferation	171
6.4.4	MDMs induce the expression of fibroblast genes associated with an activated phenotype	173
6.4.5	Optimisation of an A549 cell-based EMT assay	177
6.4.6	MDMs inhibit the loss of E-cadherin on A549 cells	179
6.4.7	MDMs potentiate mesenchymal-epithelial transition (MET) in A549 cells	181
<b>6.5</b>	<b>Discussion</b>	<b>184</b>
<b>7</b>	<b>Phagocytosis and neutrophil efferocytosis by monocyte-derived macrophages in IPF</b>	<b>191</b>
<b>7.1</b>	<b>Introduction</b>	<b>191</b>
<b>7.2</b>	<b>Hypothesis and aims</b>	<b>192</b>
<b>7.3</b>	<b>Methods</b>	<b>193</b>
7.3.1	Participant samples	193
7.3.2	Sample processing	193
7.3.3	Phagocytosis	194
7.3.4	Neutrophil isolation	194
7.3.5	Neutrophil preparation	195
7.3.6	MDM preparation	196
7.3.7	Efferocytosis assay	196
7.3.8	Gating strategy	197
7.3.9	RNA extraction and qPCR	198
<b>7.4</b>	<b>Results</b>	<b>198</b>
7.4.1	Participant demographics	198
7.4.2	MDMs from IPF patients showed evidence of impaired phagocytosis	198
7.4.3	Defective phagocytosis in IPF was linked to macrophage differentiation and not observed in monocytes	201
7.4.4	Neutrophil isolation using negative selection was the preferred	

	method for the efferocytosis assay	203
7.4.5	Efferocytosis was impaired in MDMs from IPF patients	205
7.4.6	The expression of genes involved in phagocytosis was decreased in IPF MDMs	206
<b>7.5</b>	<b>Discussion</b>	<b>208</b>
<b>8</b>	<b>Final discussion and future direction</b>	<b>213</b>
8.1	Final discussion	213
8.2	Future work	221
	<b>Appendix</b>	<b>223</b>

## List of Figures

Figure 1- 1. Graphical representation of the differing clinical courses observed in patients with IPF. ....	2
Figure 1- 2. Computed tomography images of a normal and IPF lung. ....	4
Figure 1- 3. The histopathological appearances of healthy and IPF lung tissue. ....	6
Figure 1- 4 Radiological appearances of AEIPF. ....	7
Figure 1- 5. Alveolar cell injury and the precipitation of a profibrotic cascade. ....	10
Figure 1- 6. The major TGF $\beta$ signalling pathways in fibroblasts. ....	15
Figure 1- 7. Proposed mechanisms leading to fibrogenesis in IPF. ....	18
Figure 1- 8. Fibroblasts in models of pulmonary fibrosis are thought to derive from three sources. ....	21
Figure 1- 9. Diagrammatic representation of epithelial-mesenchymal transition. ....	22
Figure 1- 10. The contribution of tissue-resident (embryonically derived) and monocyte-derived macrophages (MDMs) varies between organs. ....	27
Figure 1- 11. Macrophage polarisation. ....	31
Figure 1- 12. The role of monocytes in the repair process. ....	34
Figure 3-1. Gating strategy to identify freshly isolated monocytes within PBMCs and their cell surface markers. ....	63
Figure 3-2. Gating strategy to classify monocyte subsets and the proportions of each subset in IPF patients and controls. ....	64
Figure 3-3. Monocyte levels in IPF patients and aged-matched controls. ....	69
Figure 3-4. The percentage of classical, intermediate and non-classical monocyte subsets within the total monocyte population in stable IPF (IPF), healthy controls (HC) and acute exacerbations of IPF (AEIPF). ....	70

Figure 3-5. The expression (MFI) of cell surface receptors associated with inflammatory ('M1) and reparative functions ('M2') in stable IPF (IPF) and control (HC) monocytes.	72
Figure 3-6. The expression of receptors (MFI) associated with reparative (M2) and inflammatory (M1) phenotypes on monocytes from participants with stable IPF (IPF), AEIPF and controls.	75
Figure 3-7. Expression of genes associated with inflammatory (M1) and reparative (M2) functions in monocytes from controls, stable IPF and AEIPF.	77
Figure 3-8. The expression of M1/M2 genes in monocytes extracted from PBMCs in stable IPF patients and aged-matched controls.	81
Figure 3-9. The expression of CD163 and CD64 by control (HC), stable IPF (IPF) and AEIPF (AE) monocytes following stimulation with LPS and the TLR7/8 agonist, r848.	84
Figure 3-10. Cytokine expression by monocytes from stable IPF patients (IPF), controls (HC) and those with acute exacerbations of IPF (AEIPF).	86
Figure 3-11. Comparison of cytokine expression by CD163+ and CD163- monocytes in response to LPS and r848 stimulation in controls and stable IPF patients.	89
Figure 4-1. Computed tomography (CT) images of a normal (left) and IPF lung (right).	98
Figure 4-2. Correlations in the scoring of fibrotic components on CT by two radiologists who were blinded to each other.	104
Figure 4-3. Correlation between the Total CT Fibrosis Score and lung function parameters.	105
Figure 4-4. The correlation of monocyte levels (represented as % of PBMCs) with the Total CT Fibrosis Score and the individual fibrotic components that make up the total score.	107
Figure 4-5. The relationship of monocyte percentage (of PBMCs) and lung function values.	108

Figure 4-6. Correlations between the CPI, Total CT Fibrosis Score (TFS) and cell surface receptors CD163, CD64, CD62L, CCR7 and the CD163/CD64 ratio to look at M2/M1 balance in different severities of disease. ....	111
Figure 4-7. Comparison of the Total CT Fibrosis Score and CT scores of ground-glass opacification (GGO) and consolidation in patients with stable disease and AEIPF. ...	112
Figure 4-8. The clinical parameters and monocyte percentages of patients off and on Pirfenidone (No Pirf/Pirf). ....	113
Figure 4-9. Comparison of the expression of cell surface receptors CD163, CD64 and CD62L on monocytes from treatment-naïve patients (No Pirf), those on Pirfenidone (Pirf) and controls (HC).....	115
Figure 5-1. The major macrophage phenotypes associated with inflammatory (M1) and reparative/resolution (M2) processes. ....	122
Figure 5-2. Gating strategy for MDM phenotyping. ....	125
Figure 5-3. Monocytes change morphologically and phenotypically as they differentiate into macrophages. ....	128
Figure 5-4. Expression of the monocyte marker CD14 and the macrophage marker CD68 on day 7 monocyte-derived macrophages (MDMs) from stable IPF patients and controls. ....	129
Figure 5-5. Expression of CCR7 on human monocytes and following differentiation into macrophages.....	131
Figure 5-6. The expression of cell surface receptors associated with inflammatory ('M1) and reparative ('M2') macrophage phenotypes on MDMs from stable IPF patients and age-matched controls. ....	132
Figure 5-7. Intensity of receptor expression (MFI) on MDMs from IPF patients not on prednisolone (No Pred) compared to those on prednisolone treatment (Pred).....	134
Figure 5-8. Morphological appearances and expression of M1 and M2 receptors on day 7 MDMs differentiated in the absence (Dex-) and presence of Dexamethasone (Dex+). ....	135

Figure 5-9. The expression of CD64 on monocytes and day 7 MDMs from IPF and control participants. ....	136
Figure 5-10. The proportion of apoptotic monocytes (Annexin V <sup>+</sup> +/-7AAD) within the total monocyte population on days 1, 3 and 5 of culture. ....	138
Figure 5-11. Percentage of CD64 <sup>+</sup> CD163 <sup>-</sup> and CD64 <sup>+</sup> CD163 <sup>+</sup> monocytes in apoptosis on day 1 ex vivo culture. ....	139
Figure 5-12. Gene expression of soluble factors and proteins in IPF and control MDMs. ....	143
Figure 5-13. Gene expression of transcription factors and nuclear receptors in IPF and control MDMs. ....	145
Figure 5-14. Gene expression of cell surface receptors in IPF and control MDMs. ...	146
Figure 5-15. The concentration of M-CSF in serum from IPF patients was significantly higher than healthy controls. ....	148
Figure 5-16. Assay comparing ROS generation by IPF and control MDMs following stimulation with hydrogen peroxide (H <sub>2</sub> O <sub>2</sub> ). ....	150
Figure 5-17. Activation of the NLRP3 inflammasome triggers release of IL-1 $\beta$ . ....	151
Figure 5-18. IL-1 $\beta$ secretion following activation of the NLRP3 inflammasome in MDMs. ....	152
Figure 5-19. Diagrammatic representation of the main genes up-regulated and down-regulated in IPF MDMs compared to controls. ....	155
Figure 5-20. The major macrophage phenotypes associated with inflammatory and reparative/resolution activities. ....	156
Figure 6-1. Fibroblast activity during tissue homeostasis and following injury and disease states. ....	161
Figure 6-2. Gating strategy for fibroblast (ELF) analysis following co-culture with MDMs. ....	167
Figure 6-3. The influence of TGF $\beta$ 1 and MDMs on the expression of $\alpha$ SMA by primary human lung fibroblasts (ELF). ....	170

Figure 6-4. The influence of MDMs on fibroblast proliferation using the cell tracer VPD (violet proliferation dye) as a comparative measure.....	172
Figure 6-5. Gene expression of cytokines, chemokines and growth factors associated with activated fibroblast phenotypes in fibroblasts cultured alone (ELF <sup>nil</sup> ), with IPF MDMs (ELF <sup>IPF</sup> ) or control MDMs (ELF <sup>HC</sup> ) for 72 hours via a transwell.....	174
Figure 6-6. The expression of ECM genes and genes associated and activated/invasive fibroblast phenotypes in fibroblasts cultured alone (ELF <sup>nil</sup> ), with IPF MDMs (ELF <sup>IPF</sup> ) or control MDMs (ELF <sup>HC</sup> ) for 72 hours via a transwell.....	175
Figure 6-7. The morphological appearance and expression of EMT markers in A549 cells cultured in the absence and presence of TGFβ.....	178
Figure 6-8. The influence of IPF and control MDMs on E-cadherin and fibronectin expression (MFI) in A549 cells. ....	180
Figure 6-9. The influence of IPF and control MDMs on E-cadherin and fibronectin expression (MFI) in A549 cells following direct co-culture. ....	181
Figure 6-10. The influence of MDMs on mesenchymal-epithelial transition (MET) in A549 cells following indirect co-culture. ....	183
Figure 6-11. The influence of MDMs on mesenchymal-epithelial transition (MET) in A549 cells following direct co-culture. ....	184
Figure 7-1. Graphical representation of the experimental protocol used for neutrophil efferocytosis assay.....	197
Figure 7-2. Gating strategy used for neutrophil efferocytosis assay. ....	197
Figure 7-3. Phagocytosis assay utilising fluorescent latex beads and effect of the phagocytosis inhibitor Cytochalasin D on apparent bead uptake.....	200
Figure 7-4. Phagocytosis using the pHrodo® assay. ....	201
Figure 7-5. Phagocytic ability of monocytes from IPF patients and healthy age-matched controls as they differentiate into macrophages over 7 days. ....	202



Figure 7-6. The percentage of MDMs participating in efferocytosis using neutrophils isolated with CD15 microbeads (positive selection) compared to those isolated with the MACSxpress® kit (negative selection). .....	204
Figure 7-7. FACs plots demonstrating the purity of the neutrophils following isolation using the MACSxpress® neutrophil isolation kit.....	204
Figure 7-8. The proportion of neutrophils that had undergone cell death or were in the process of apoptosis 18h post isolation was assessed via flow cytometry. ....	205
Figure 7-9. The proportion of MDMs phagocytosing neutrophils in IPF and age-matched controls. ....	206
Figure 7-10. The gene expression of key scavenger receptors and <i>MERTK</i> in IPF and control MDMs. ....	207
Figure 7-11. Mechanisms by which impaired efferocytosis could potentiate the pathophysiology of IPF.....	212

## List of Tables

Table 1-1. The radiological criteria for a diagnosis of UIP.....	4
Table 1-2. The histopathological criteria for a diagnosis of UIP. ....	5
Table 2-1. Media used in experiments. ....	40
Table 2-2. List of flouochrome-conjugated monoclonal antibodies used to characterise cells in this study. ....	43
Table 2-3. Isotype control mAbs used in the study. ....	44
Table 2-4. The components and quantities of reagents used in the Reverse Transcriptase (RT) master mix for each RNA sample.....	49
Table 2-5. Details of genes and primer sequences used for the characterisation of monocytes (chapter 3).....	50
Table 2-6. Details of genes and primer sequences used for the characterisation of MDMs (chapter 5).....	52
Table 2-7. Details of genes and primer sequences used for the characterisation of primary human lung fibroblasts (ELF) following transwell co-culture with MDMs (chapter 6). ....	53
Table 2-8. Details of phagocytic genes and primer sequences (chapter 7). ....	54
Table 2-9. Details of the three housekeeping genes used in the analysis of gene expression as endogenous controls.....	54
Table 3-1. Phenotypic and cytokine panel used to characterise fresh and cultured monocytes. ....	63
Table 3-2. Details of controls and IPF patients from which monocyte RNA was extracted.....	65
Table 3-3. The demographics of IPF and control participants involved in the characterisation of monocytes.....	66
Table 3-4. Clinical details of patients sampled with AEIPF. ....	67

Table 3-5. List of genes analysed in freshly isolated monocytes from controls, stable IPF and AEIPF. ....	79
Table 3-6. Full list of genes analysed in freshly isolated monocytes extracted from PBMCs from aged-matched healthy controls and stable IPF patients not on steroid therapy. ....	82
Table 4-1. The demographics of patients involved in the characterisation of monocytes. ....	102
Table 5-1. Demographic details of patients and controls participating in MDM phenotyping. ....	126
Table 5-2. Demographic details of patients and controls participating in MDM functional assays and RNA analysis. ....	127
Table 5-3. The full list of genes analysed on day 7 MDMs from IPF patients and aged-matched healthy controls (HC). ....	147
Table 6-1. Demographics of IPF patients and healthy controls involved in fibroblast and EMT experiments. N=nintedanib; P=Pirfenidone; N/A – data not applicable to healthy controls. ....	168
Table 6-2. Genes analysed in primary human fibroblasts (ELF) following transwell co-culture with IPF and control MDMs (ELF <sup>IPF</sup> and ELF <sup>HC</sup> ) compared to fibroblasts cultured in isolation (ELF <sup>nil</sup> ). ....	176
Table 7-1. Demographic details of IPF patients and controls sampled for the efferocytosis and phagocytosis assays and the expression of phagocytic genes. ....	198
Table 7-2. Neutrophil purity and issues with three different methods of isolation. ....	203

## List of Abbreviations

7AAD	7-amino-actinomycin
AE	Acute exacerbation
AEC	Alveolar epithelial cells
AEIPF	Acute exacerbation of IPF
AM	Alveolar macrophage
BAL(F)	Broncho-alveolar lavage (fluid)
BM	Bone marrow
BSA	Bovine serum albumin
CAFs	Cancer-associated fibroblasts
CCL	Chemokine ligand
CCR	Chemokine receptor
CD	Cluster of differentiation
COPD	Chronic obstructive pulmonary disease
CPI	Composite physiologic index
CRP	C-reactive protein
CS	Corticosteroid
CT	Computed tomography
CTGF	Connective tissue growth factor
DAMPs	Damage-associated molecular patterns
Dex	Dexamethasone
DMSO	Dimethyl sulfoxide
ECM	Extracellular membrane
EDTA	Ethylene-diamine-tetra-acetic acid
ELF	Explant lung fibroblasts (human)
ELISA	Enzyme-linked immunosorbent assay
EMT	Epithelial-mesenchymal transition
ER	Endoplasmic reticulum
ESR	Erythrocyte sedimentation rate
FACS	Fluorescence-activated cell sorting
FAFs	Fibrosis-associated fibroblasts
FCS	Foetal calf serum
FEV1	Forced expiratory volume in 1 second
FGF	Fibroblast growth factor
FSC	Forward scatter
FVC	Forced vital capacity
GGO	Ground glass opacification
GM-CSF	Granulocyte-macrophage colony-stimulating factor
GWAS	Genome-wide association study
HC	Healthy control
HHV	Human herpes virus
HLA	Human leukocyte antigen
HRCT	High-resolution computed tomography
ICS	Intracellular cytokine staining
IFN	interferon
Ig	Immunoglobulin

IL	Interleukin
ILD	Interstitial lung disease
IM	Interstitial macrophage
IPF	Idiopathic pulmonary fibrosis
KO	Knock-out
LC	Langerhan cell
LPS	Lipopolysaccharide
M-CSF	Macrophage colony-stimulating factor
mAB	Monoclonal antibody
MACS	Magnetic activated cell sorting
MCP-1	Monocyte chemotactic protein-1
MDM	Monocyte-derived macrophage
MET	Mesenchymal-epithelial transition
MFI	Mean fluorescence intensity
MMP	Matrix metalloproteinase
NLRP	Nucleotide-binding oligomerisation domain-like receptors
PAMP	Pathogen-associated molecular pattern
PBMC	Peripheral blood mononuclear cell
PBS	Phosphate buffered saline
PDGF	Platelet-derived growth factor
PFTs	Pulmonary function tests
Pred	Prednisolone
PRR	Pattern recognition receptor
qPCR	Quantitative polymerase chain reaction
r848	Resiquimod
RA	Rheumatoid arthritis
ROS	Reactive oxygen species
RPM	Revolutions per minute
RT	Reverse transcriptase
SLE	Systemic lupus erythematosus
SMA	Smooth muscle actin
SSC	Side scatter
STAT	Signal transducer and activator of transcription
TAMs	Tumour-associated macrophages
TFS	Total CT fibrosis score
TGF	Transforming growth factor
TLCO	Transfer factor of the lung for carbon monoxide
TLR	Toll-like receptor
TNF	Tumour necrosis factor
Treg	Regulatory T cell
UIP	Usual interstitial pneumonitis
UPR	Unfolded protein response
VEGF	Vascular endothelial growth factor
VPD	Violet proliferation dye

# 1 Introduction

## 1.1 Idiopathic Pulmonary Fibrosis (IPF)

### 1.1.1 Background

Idiopathic pulmonary fibrosis (IPF) is a chronic fibroproliferative disease exclusively affecting the lungs. It is characterised by the irreversible accumulation of scar tissue that gradually replaces the normal lung parenchyma and leads to symptoms of exercise intolerance and dyspnoea. As the fibrosis progresses, exertional hypoxia and pulmonary hypertension can develop and respiratory failure and death usually ensue [1]. IPF has been classified as a rare disease but evidence from national UK databases indicates that the incidence is increasing; at present, there are estimated to be 7-9/100,000 new cases per year in the UK and a prevalence of 15-25/100,000 (BTS registry annual report 2013/14). This however may be an underestimation as a recent US study examining Medicare claims over ten years found a far higher prevalence of 93.7/100,000 [2, 3].

By definition, the aetiology of IPF is unknown but the pathological process is likely to arise due to environmental stimuli triggering an injurious response within a genetically predisposed individual. Men are more commonly affected, with a ratio of 3:2. The reasons for this are unclear although it may be related to risk factors which include smoking and exposure to wood and metal dusts [2]. Possible disease triggers such as viruses and gastro-oesophageal reflux (GOR) have been investigated and appear to be associated with IPF in a subset of patients, although direct causality has not been proven [1]. More recently, there has been greater focus on the genetic contribution following the identification of specific mutations found in familial forms of pulmonary fibrosis. Mutations in genes encoding telomerase and surfactant, and polymorphisms in the *MUC5B* gene amongst others, have shed light on pathogenic pathways and led to the discovery that the frequencies of these mutations are significantly higher in the IPF population. Indeed, a familial link in patients with IPF is seen in anywhere between 2-20% of cases [4]. Age is an important risk factor with an average age of onset of 70 (BTS registry 2013/14).

Until recently, there have been no effective therapeutic strategies to target the relentless nature of the disease and the median life expectancy following diagnosis is between 2 - 5 years. It is anticipated that the availability of two novel anti-fibrotic drugs, Pirfenidone and Nintedanib, should improve this prognosis by slowing down the progression of the disease [5]. However, evidence for use of these therapies is derived from patients with mild to moderate disease (forced vital capacity (FVC) 50-80% predicted) and in those

with advanced disease, there remains an absence of therapeutic options [6, 7]. Furthermore, there is no treatment to improve outcome for patients who suffer episodes of acute worsening of their disease (termed acute exacerbation), which carries a mortality of over 50% [8].

### 1.1.2 Clinical Features

The disease is characterised clinically by insidious and progressive breathlessness, with the history often predating the diagnosis by many months and often years [9]. Cough is a common symptom and may be the presenting complaint. Over time, symptoms deteriorate, and exertional and subsequently resting hypoxaemia can develop, which may result in secondary pulmonary hypertension, exacerbating dyspnoea further. IPF is a highly heterogeneous disease, however, with some patients surviving long term with only minimally progressive symptoms whilst others decline rapidly into respiratory failure only months after presentation. Patients may experience a stepwise deterioration in symptoms and lung physiology, with periods of relative disease stability in between (Fig 1-1) [10]. At the time of diagnosis, it rarely possible to determine the disease course a patient will take and therefore careful follow-up and monitoring of pulmonary function tests (PFTs) are essential, particularly in the first 18 months, to ascertain the nature of the disease and enable early intervention if necessary [5, 7]

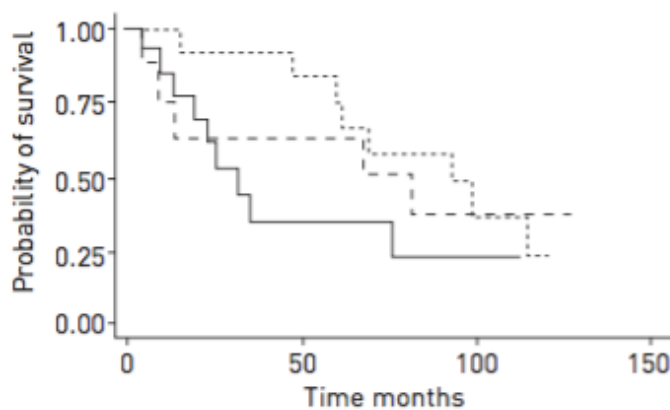


**Figure 1- 1. Graphical representation of the differing clinical courses observed in patients with IPF.** Survival following diagnosis differs significantly between patients, with some pursuing an aggressive disease course (solid line), whilst others remain stable for longer periods with improved survival (dashed and dotted lines). Adapted from Saini G, *et al.* [10].

Physical examination typically reveals the presence of ‘velcro’ crackles on auscultation, predominantly bilaterally and in the lower zones of the chest. Clubbing is present in 50% [1]. The presence of features suggestive of connective tissue disease effectively excludes the diagnosis of IPF. PFTs usually show a restrictive defect with an FEV1/FVC ratio of greater than 70%, unless there is co-existent airways disease. The lung volumes are reduced alongside the gas transfer for carbon monoxide (TLCO). Co-existent

emphysema may be present in up a third of patients and artificially inflate the functional vital capacity whilst disproportionately lowering the TLCO [11].

### **1.1.3 Diagnostic Features**

Usual interstitial pneumonia (UIP) is a term that encompasses a number of specific histological and radiological features most classically associated with IPF. UIP is not unique to this disease however, and it can be seen in the context of connective tissue disease (in particular rheumatoid disease), sarcoidosis, drug toxicity, asbestosis and chronic hypersensitivity pneumonitis. Thus, careful exclusion of these conditions is necessary before a diagnosis of IPF can be made [12].

The radiological appearances of UIP include a basal subpleural distribution of disease, the presence of honeycombing with or without traction bronchiectasis, reticular abnormality (fine fibrosis) and an absence of any features considered inconsistent with UIP such as the presence of extensive ground glass (inflammatory) changes and nodularity (Fig 1-2). If all UIP features are present, a 'definite diagnosis' of IPF can be made in a patient without a known cause of UIP. In a significant proportion of patients however, typical CT features are not present and the ATS/ERS/JRS/ALAT statement provides guidelines enabling a definite, probable or possible diagnosis of the disease to be made depending on the radiological features present (Table 1-1). The NICE Clinical Guidelines published in 2013 also acknowledge the diagnostic difficulty that can occur and recommend that all suspected cases of IPF be reviewed by a multi-disciplinary team with expertise in interstitial lung disease, including a consultant radiologist, pathologist and specialist ILD chest physician [7].



<b>UIP Pattern (all four features)</b>	<b>Possible UIP (all three features)</b>	<b>Inconsistent with UIP pattern (any of the following)</b>
<b>Subpleural, predominantly basal distribution of disease</b>	Subpleural, predominantly basal distribution of disease	Disease in predominantly upper or mid -zone distribution
<b>Reticular abnormality (fine fibrosis)</b>	Reticular abnormality	Disease clustered around bronchioles and vasculature
<b>Honeycombing with or without traction bronchiectasis</b>	Absence of features listed as inconsistent with a UIP pattern (see third column)	Extensive ground glass abnormality
<b>Absence of features listed as inconsistent with a UIP pattern (see third column)</b>		Profuse micronodules
<b>Subpleural, predominantly basal distribution of disease</b>	all three features	Discrete cysts (multiple, bilateral, away from areas of honeycombing
<b>UIP Pattern (all four features)</b>		Diffuse air trapping
		Consolidation

**Table 1-1. The radiological criteria for a diagnosis of UIP.**  
Adapted from the ATS/ERS/JRS/ALAT Statement for IPF 2011[13]

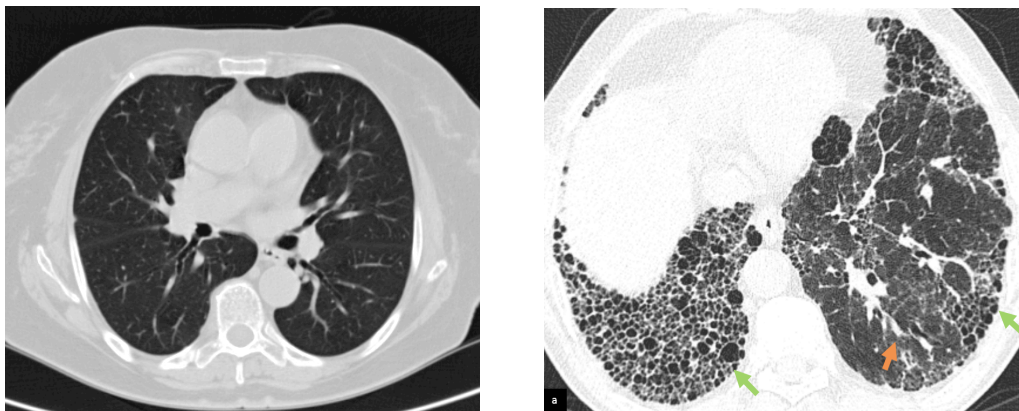


**Figure 1- 2. Computed tomography images of a normal and IPF lung.**  
Normal lung (left) and IPF lung (right). Green arrows demonstrate areas of honeycombing and orange arrow shows area of reticulation.

In cases of diagnostic uncertainty, a surgical lung biopsy may be appropriate in patients who are able to tolerate the procedure. The histopathological features of UIP comprise spatial and temporal heterogeneity with patches of new and established fibrosis

4

interspersed with areas of normal lung tissue. The presence of fibroblastic foci is pathognomonic of the disease. They consist of aggregates of proliferating fibroblasts and myofibroblasts that secrete components of the extracellular matrix and precede fibrotic change (Fig 1-3). Inflammatory cell infiltrates may be present in small numbers, but if a prominent feature, suggest an alternative diagnosis to UIP. Alveolar walls become thickened with excessive collagen deposition leading to architectural distortion and destruction. These areas of fibrotic cystic change are referred to as honeycombing and represent end-stage fibrosis. Similar to the radiological criteria, histological findings have also been categorised to provide a guide as to the probability of UIP (Table 1-2).

<b>UIP Pattern (all four criteria)</b>	<b>Probable UIP Pattern</b>	<b>Possible UIP Pattern (all three criteria)</b>	<b>Not a UIP Pattern (any of the six criteria)</b>
<b>Evidence of marked fibrosis, architectural distortion +/- honeycombing in a predominantly subpleural distribution</b>	Evidence of marked fibrosis, architectural distortion +/- honeycombing	Patchy or diffuse lung fibrosis, with or without interstitial inflammation	Marked interstitial inflammatory cell infiltrate away from honeycombing
<b>Patchy areas of fibrosis</b>	Absence of either patchy fibrosis or fibroblastic foci, but not both	Absence of other criteria for UIP (see UIP pattern column)	Hyaline membranes or organising pneumonia (except in cases of acute exacerbation)
<b>Fibroblastic foci</b>	Absence of features against a diagnosis of UIP (see fourth column)	Absence of features against a diagnosis of UIP (see fourth column)	Presence of granulomas
<b>Absence of features against a diagnosis of UIP (see fourth column)</b>	OR Honeycomb changes only		Predominantly airway centered changes  Other features suggestive of an alternative diagnosis

**Table 1-2. The histopathological criteria for a diagnosis of UIP.**  
Adapted from the ATS/ERS/JRS/ALAT Statement for IPF 2011[13].

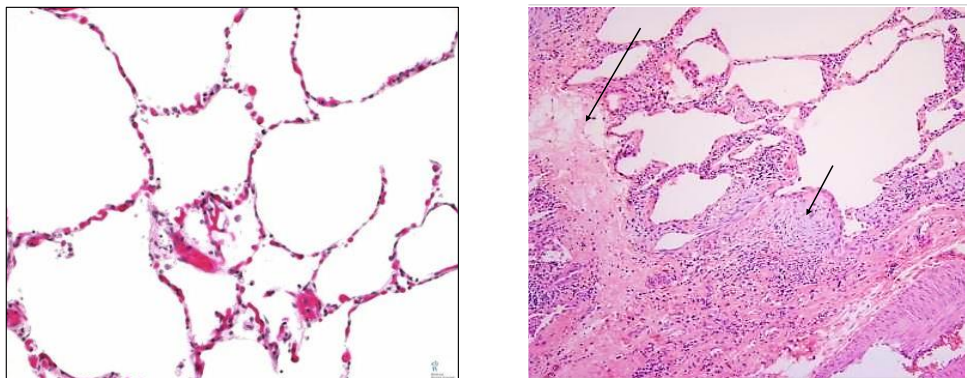


**Figure 1- 3. The histopathological appearances of healthy and IPF lung tissue.**

Histological section of healthy lung showing thin-walled alveoli (left) contrasted with the typical features of UIP (right). The histological sample on the right shows dense fibrosis with collagen bundles (long arrow), fibroblastic foci (short arrow) underneath a layer of abnormal hyperplastic alveolar epithelium.

### 1.1.4 Acute Exacerbations

Patients with IPF are often elderly and therefore susceptible to the common causes of acute respiratory decline such as heart failure and pneumonia and there is evidence that IPF increases the risk of pulmonary emboli. Patients with IPF may also experience an acute worsening or exacerbation of their disease resulting in increased breathlessness and hospital admission in the majority of cases. Acute exacerbations (AE) carry an exceptionally poor prognosis with a 3-month mortality of over 50% and a significant step-down in functional status in those who survive. The term ‘acute exacerbation’ has been defined by consensus opinion as: a worsening of dyspnoea over 30 days or less, new airspace changes on HRCT (Fig 1-4), and exclusion of other causes such as heart failure, pulmonary emboli and infection [14, 15]. More recently, the necessity of excluding infection has been questioned due to the realisation that it is often not clinically feasible to exclude it with certainty (bronchoscopy often contraindicated on the basis of low oxygen saturations for example) and the increasing evidence that infection may act as an initial trigger for an acute deterioration in the disease process [15]. In a subgroup analysis following the STEP-IPF trial (Sildenafil Trial of Exercise Performance in IPF), investigators analysed the outcomes of patients with ‘Definite acute exacerbations’, (in which infection and alternative causes for decline had been excluded), to patients with ‘Suspected acute exacerbations’ who had identical features of AE but without the stringent exclusion of associated causes. No differences between the two groups were demonstrated, including quality of life measures, six minute walk test, lung function parameters or mortality [16]. Thus ‘Acute Exacerbation’ is probably best considered a term that describes a clinical and radiological decline that is likely to be caused by a

number of triggers (of which infection is probably the most common), but in a proportion of patients may be a truly idiopathic phenomenon.

At present, relatively little is understood regarding the pathogenesis of AE and it is unclear whether these events represent an acceleration of the disease process or a separate pathological event within a predisposed diseased lung [14]. The histological picture is that of diffuse alveolar damage, which is an acute and nonspecific reaction of the lung to a multitude of injurious agents and is characterised by the presence of hyaline membrane formation and oedema following endothelial and alveolar cell injury [17].

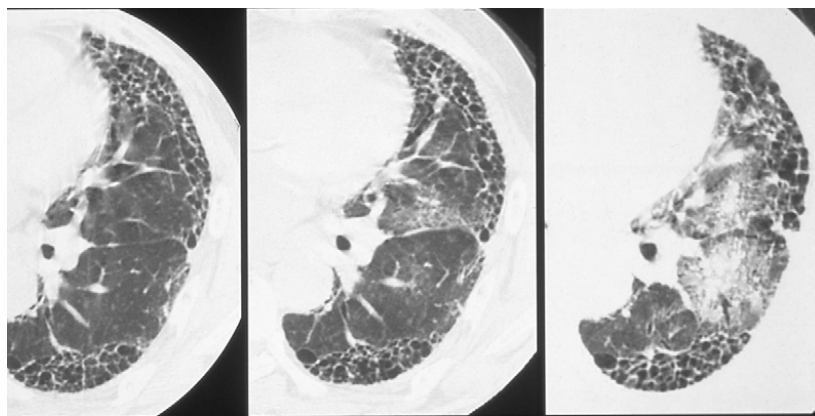


**Figure 1- 4 Radiological appearances of AEIPF.**

Progressive CT changes in a patient with stable IPF (left), early exacerbation and more severe exacerbation. Acute exacerbations are defined radiologically as new airspace changes indicated by the presence of ground glass opacification and/or multi-focal consolidation.

### **1.1.5 Pharmacological treatment of IPF**

Pharmacological management of patients with IPF has changed significantly over the past few years with the development and subsequent licencing of two anti-fibrotic agents, Pirfenidone and Nintedanab. Large, international, randomised controlled trials were undertaken to assess the efficacy of these agents and a reduction in the rate of lung function decline after one year was demonstrated with both agents. In addition, following adjudication of the acute exacerbation data, Nintedanab use was found to be associated with a reduced incidence of this complication. Extension studies looking at the long-term safety of Pirfenidone indicate an emerging mortality benefit in these who continue on the drug long term (4.1 for details) [18-20].

Pirfenidone was the first orally available anti-fibrotic drug approved for use in the UK by NICE in 2013 for patients with mild-moderate IPF [21]. Its exact mechanism of action is unknown but in a murine model of fibrosis, administration of Pirfenidone led to a reduction in the production of key profibrotic cytokines including TGF  $\beta$ , IL-1  $\beta$  and FGF. A decrease in lung collagen content and fibrosis scores was demonstrated and proliferation of fibroblasts was attenuated indicating that Pirfenidone acts by inhibiting important fibrogenic pathways [22]. Nintedanib is an intracellular triple tyrosine kinase inhibitor that binds competitively to receptors to VEGF, PDGF and FGF blocking downstream signalling pathways. These growth factors are recognised mediators of fibrogenic pathways and, as with Pirfenidone, the administration of Nintedanib following bleomycin lung injury in mice resulted in reduced inflammation and fibrosis. The inhibition of fibroblast function is thought to be the main mechanism by which Nintedanib modulates the disease processes in IPF [23].

Treatment for acute exacerbation is currently very limited and entirely without an evidence base. Antibiotics are invariably prescribed to treat possible infection, regardless of the clinical findings, and in the majority of cases, patients are treated with high-dose prednisolone, usually in the form of pulsed methylprednisolone for three days. The rationale behind its use is the notion that the deterioration in the disease may in part be caused by a superimposed inflammatory component within the scarred lung. Whilst a subset of patients respond to steroid therapy, in the majority of cases it does not appear to change the course of the decline [24].

## **1.2 Pathophysiology of IPF**

### **1.2.1 Models of lung fibrosis**

Uncovering mechanisms involved in the development of IPF has been a slow and difficult process although important discoveries have been made in recent years. Light has been shed on some of the major pathogenic pathways, resulting in the development of effective therapeutic agents. Part of the difficulty in understanding the pathogenesis of the disease is the lack of a representative animal model. Bleomycin is most commonly used to induce murine lung fibrosis but the pathological consequences poorly replicate the IPF lung. Bleomycin-induced lung injury results in a period of dense inflammation that precedes fibrotic change and the fibrosis itself often recedes over time as restorative mechanisms are activated to return tissue to health [25, 26]. In IPF, the role of

inflammation remains controversial and the presence of a significant inflammatory cell infiltrate on histology contravenes a diagnosis of UIP [13]. Furthermore, in IPF the fibrosis is progressive and irreversible with no sign of regression [27]. In the last two decades, the central paradigm that fibrosis only arises as a result of chronic inflammation has been overturned and experimental models have demonstrated that fibrosis can develop independently of inflammation [28]. Thus, whilst the use of bleomycin-induced lung injury has contributed to our understanding of fibrosis generally, it has limited usefulness in enabling investigators to unravel the processes occurring in IPF specifically.

The prevailing hypotheses surrounding the pathogenesis of IPF have thus been largely derived from a number of indirect sources of which clinical research has played a major contribution. Epidemiological and clinical studies have defined the characteristics of the disease, its natural history, and the environmental factors associated with its development [2, 27, 29-31]. Investigating the genetic mutations that underlie familial forms of lung fibrosis has advanced our understanding of the disease considerably and genome-wide studies involving patients with IPF and other fibrotic lung diseases have identified polymorphisms in similar genes to those seen in genetic forms of the disease [4, 32-36]. The role of immune cells and soluble mediators have been evaluated through BAL fluid and blood analysis [37-43]. Examination of IPF lung tissue, when available, has contributed to current concepts and validated animal model data [44-47]. Furthermore, the failure of drugs with isolated molecular targets (such as TNF $\alpha$  and IFN $\gamma$ ) to inhibit disease processes has shed light on some of the redundant and non-redundant molecular pathways in IPF and highlighted the complexity of the disease [48, 49]. However, whilst these combined approaches have furthered our knowledge of the disease substantially, the precise pathogenic mechanisms involved (and how to inhibit them) remain elusive.

### **1.2.2 Alveolar epithelial cell injury**

Selman *et al.* (2001) [50] first put forward the hypothesis that IPF was initiated by injury to the alveolar epithelium resulting in an aberrant healing response leading to the accumulation of extracellular tissue. This proposition has subsequently become the prevailing theory and is supported by genetic work showing that mutations and polymorphisms within alveolar epithelial cells (AEC) genes are linked to the development of lung fibrosis (see below) [4, 32]. In IPF, the alveolar epithelium is grossly abnormal and fibroblastic foci are often seen in close proximity to denuded, apoptotic or

hyperplastic alveolar epithelium. It is postulated that AECs provide the primary source of profibrotic cytokines, chemokines and growth factors mediating fibrotic responses [28, 51]. Indeed, studies have demonstrated that AECs can synthesise PDGF, TGF $\beta$  and TNF $\alpha$  in abundance [51]. These mediators in turn are thought to induce the migration, proliferation and activation of fibroblasts resulting in the production of excessive extracellular matrix (ECM) and eventual destruction of lung architecture (Fig 1-5) [52].

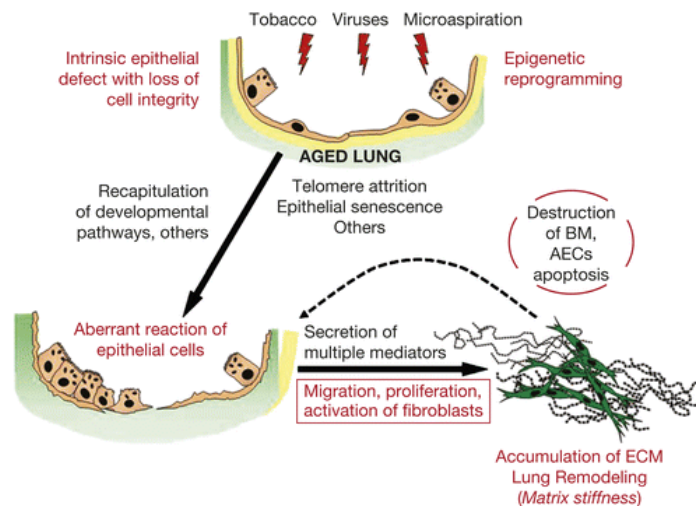


**Figure 1- 5. Alveolar cell injury and the precipitation of a profibrotic cascade.**

In IPF it is postulated that AEC injury induced by external triggers results in loss of cellular integrity and defective regenerative responses. Alterations in AECs that occur in aging, including telomere shortening, cellular senescence and impaired autophagy, predispose to aberrant activation of the AEC. The secretion of soluble mediators by AEC subsequently results in the local proliferation, migration and differentiation/activation of fibroblasts into collagen-secreting myofibroblasts leading to the deposition and accumulation of ECM. Adapted from Selman *et al.* [52]

### 1.2.3 Genetic susceptibility to lung fibrosis

To elucidate the pathogenic pathways in IPF, there has been a focus on examining familial forms of the disease. Conditions such as Hermansky-Pudlak syndrome (HPS) and dyskeratosis congenita have a clear genetic basis and are associated with pulmonary fibrosis. Mutations and polymorphisms in genes have been identified that are predominantly expressed by type II alveolar epithelial cells, supporting the hypothesis that this cell type is a key player in the pathogenesis of the disease [4, 32, 35, 53]. These cells produce surfactant, essential for reducing surface tension and enabling alveolar inflation. They also regenerate the epithelium, and are capable of differentiating and replenishing type I AECs [54]. HPS is caused by mutations in genes encoding proteins involved in lysosomal intracellular trafficking resulting in the pathologic accumulation of lipid-protein complexes within cells such as type II AECs (AECII), which eventually leads

to pulmonary fibrosis in the 4<sup>th</sup> and 5<sup>th</sup> decades [53]. Mutations in genes encoding surfactant protein C and A2 have also been uncovered in familial forms of pulmonary fibrosis. These result in the aggregation or misfolding of surfactant proteins within the endoplasmic reticulum (ER) and subsequent retention within the cell. This leads to ER stress and its key function in the synthesising, folding and packaging of proteins becomes compromised [55]. Activation of pathways that aim to increase the ER capacity are subsequently triggered, such as the unfolded protein response (UPR). However, when demand outweighs this capacity, proteins such as IRE1a are trans-autophosphorylated triggering both apoptotic and profibrotic pathways [56]. Patients with IPF have increased markers of UPR and biopsy samples reveal histological evidence of an abnormal hyperplastic and denuded alveolar epithelial cell layer [56]. The causes of ER stress in sporadic cases have not been identified with certainty but proteins from Herpesviruses have been found to co-localise with proteins involved in UPR implicating viruses as potential triggers [36] (Section 1.2.5).

IPF is rarely encountered in young patients and is generally viewed as a disease of older age. Individuals in the 8<sup>th</sup> and 9<sup>th</sup> decade may show UIP changes at the bases of their lungs on CT that often confer no clinical significance and can be attributed to an aging lung [57]. Mutations in genes *TERC* and *TERT*, which code for telomerase enzyme components, form the genetic basis of dyskeratosis congenita, a disease which is characterised by premature aging [58]. Telomerases elongate telomeres, which are repetitive DNA sequences positioned at the ends of chromosomes. Telomeres shorten with every cell cycle and eventually reach a critical point resulting in either cellular senescence or a DNA damage response leading to apoptosis [59]. Researchers thus questioned whether age-related gene mutations may play a role in the development of pulmonary fibrosis [33, 36, 60]. Genetic sequencing of familial cases subsequently identified that approximately 8% were associated with telomerase mutations [34]. Whilst only 1% of sporadic cases revealed similar mutations, a further study found that a significant proportion of IPF patients have shortened telomeres within AECs [33]. The significance of this finding is unclear but following AEC injury, short telomeres may compromise the ability of these cells to proliferate and regenerate damaged areas resulting in activation of DNA damage responses and pro-apoptotic pathways [33, 61]. Shortened telomeres may also partly explain the presence of seemingly benign UIP changes seen in individuals at the extreme of age.

A large genome-wide association study looking at familial and sporadic cases of pulmonary fibrosis was undertaken in 2011 to look at possible genetic risk factors for the



development of the disease. High frequencies of specific single nucleotide polymorphisms (SNP) were noted in genes including *MUC5B*, which encodes mucin (a major constituent of mucous); *DSP*, which encodes desmoplakin (a component of desmosomes that are important for cell-cell adhesion), and genes influencing telomere length. Furthermore, the *MUC5B* SNP correlated with increased expression within the tissue of patients compared with controls [32]. The pathological significance of these polymorphisms has yet to be elucidated but indicates that genetic factors influence host susceptibility to pulmonary fibrosis.

#### **1.2.4 Environmental factors and the ‘Second hit’ hypothesis**

Genetic mutations and polymorphisms are not enough to directly induce fibrotic lung disease. ER stress was demonstrated in transgenic mice expressing a mutant form of surfactant protein C in AECII resulting in the protein misfolding within the cell, but these mice did not develop lung fibrosis in the absence of a second profibrotic stimulus. When bleomycin was given however, these mice developed exaggerated fibrosis [62]. The ‘second hit’ hypothesis has thus become established in the pathogenesis of IPF, which proposes that an additional environmental insult is required for disease development and progression. Potential triggers include microbes, smoking and mechanical ventilation [2, 63-65]. Microaspiration due to gastro-oesophageal reflux may also be a precipitating factor in disease development. A study using oesophageal manometry to measure reflux episodes found that IPF patients had a significantly higher number of events than healthy controls [66]. Furthermore, measurement of BAL pepsin, a marker of gastric aspiration, was elevated in patients with AEIPF suggesting that aspiration may contribute to the development of acute exacerbations [67]. A retrospective analysis looking at the placebo arm of three IPF clinical trials compared patients on acid suppression with those who were not and found that the use of anti-acid therapy was associated with a slower decline in FVC over time and fewer acute exacerbations [68]. To further evaluate the potential contribution of reflux in disease progression, a clinical trial is ongoing comparing lung function decline in IPF patients who have undergone fundoplication to those managed conservatively (clinical trial number NCT01982968).

### 1.2.5 Role of microbes as cofactors in IPF

The role of microbes in the pathogenesis of IPF has been investigated in a number of studies. Air-borne viruses that infect the respiratory tract and instigate alveolar epithelial damage have been implicated as both initiating and propagating cofactors [69-76]. Human herpes viruses (HHV) in particular are postulated to provide the 'second hit' required for the development of IPF. This hypothesis has been supported by a number of studies that have demonstrated a high prevalence of these viruses in patients with IPF including a study by Tang *et al.* (2003), which identified herpesviruses (Cytomegalovirus, Epstein Barr Virus, HHV-7 and HHV-8) via PCR in 32 out of 33 IPF lung biopsies compared to only 36% of controls [74]. A more recent study found that HHV viral proteins were present within AECs in 65% of IPF tissue samples and co-localised with proteins associated with the UPR [77]. Herpes viruses infect epithelial cells causing ER stress leading to activation of the UPR, which the virus may manipulate to its replication advantage. Epithelial cellular integrity becomes compromised which can lead to the activation of apoptotic pathways [76]. Given that ER stress and UPR are features of both genetic and sporadic forms of lung fibrosis there is thus a mechanistic explanation for the role of viruses in triggering profibrotic responses in genetically susceptible individuals. Viral encounter in older age may also increase susceptibility to IPF due to the cellular changes that occur with aging such as genomic instability, mitochondrial dysfunction and epigenetic modification that may reduce the ability of AEC to respond and clear infection. Of relevance to this, elderly but not young mice infected with a murine herpes virus went on to develop severe fibrosis following bleomycin lung injury [73]. Bacterial colonisation may also drive fibrogenesis. A study by Molyneux *et al.* (2014) measured bacterial DNA within BAL fluid from IPF patients and controls, and found that IPF patients had double the bacterial burden and those with the greatest load had increased risk of disease progression (signified by a fall in FVC of >10% over 6 months) [63].

It must be noted however that studies implicating microbes in the pathogenesis of IPF are mostly small and retrospective [64]. Furthermore, whilst an association has been established this is not the same as a causal relationship and within the abnormal IPF lung, host defence mechanisms are likely to be impaired. It is possible, albeit less likely, that the persistence of microbes is due to defective host clearance and they are bystanders rather than cofactors in disease pathogenesis.

### 1.2.6 TGF $\beta$ and its role in fibrogenesis

Injury to the alveolar epithelium is thus postulated to initiate an aberrant repair process that is uncontrolled and progressive. Whether this is due to a chronic or repetitive injury initiating temporally and spatially distinct fibrotic responses, or an isolated precipitant capable of triggering a cascade of profibrotic cellular events that subsequently become self-perpetuating, is unclear. The exact mechanisms by which AEC damage triggers fibrogenic responses are also poorly understood but studies indicate that numerous defective pathways are involved and the contribution of each are likely to differ depending on genetic predisposition and environmental exposures of the individual [78-80]. Certain pathological processes and cytokines are however recognised to play dominant roles in disease pathogenesis and the activation of TGF $\beta$  in particular is recognised as a key mediator in driving fibrogenesis [78, 81].

TGF $\beta$  incorporates a superfamily of growth factors consisting of TGF $\beta$  isoforms (from which the name derives), bone morphogenetic proteins (BMPs), activins and inhibitins. These proteins play key roles in growth and development and are implicated in a range of physiological and pathological processes including wound healing, immune regulation, angiogenesis, fibrosis, epithelial mesenchymal transition (EMT) and oncogenesis [82]. Of the three major isoforms of TGF $\beta$  (comprising TGF $\beta$ 1, TGF $\beta$ 2 and TGF $\beta$ 3), TGF $\beta$ 1 is associated most closely with fibrogenesis and aberrant regulation. Its over-production has been implicated in a range of fibrotic diseases including liver cirrhosis, glomerulosclerosis, systemic sclerosis and IPF [83-85]. TGF $\beta$  was found to be highly expressed in fibrotic lung tissue from IPF patients [86] and when Sime *et al.* (1997) generated rats to over-express the growth factor, severe lung fibrosis developed that was ameliorated by TGF $\beta$  inhibition [72]. TGF $\beta$ 1 mediates the recruitment, proliferation and activation of fibroblasts into collagen-secreting myofibroblasts. TGF $\beta$  is also implicated in the recruitment of circulating fibrocytes which may contribute to the fibroblast pool in IPF [87-90]. Furthermore, it enhances fibrotic pathways by stimulating the expression of pro-fibrogenic cytokines such as PDGF, IL-1 $\beta$  and IL-13. TGF $\beta$  is produced by most bone marrow derived cells including macrophages, T cells and neutrophils but also by epithelial cells including those lining the alveoli. It is secreted in a latent form, bound to latency-associated peptide (LAP) and a TGF $\beta$ -binding protein, and can be cleaved to its activated form by a variety of conditions including acidic pH, increased tissue stiffness and oxidative stress, plus mediators such as MMP2 and MMP9, thrombospondin-1 and integrins such as  $\alpha$ v $\beta$ 6 [81].

TGF $\beta$  interacts with a heteromeric complex of transmembrane receptors (designated type I and type II) which results in the phosphorylation of transcription factors known as Smads that shuttle between the cytoplasm and nucleus. Upon activation of TGF $\beta$  receptors, Smad proteins accumulate in the nucleus to regulate transcription. TGF $\beta$  can also signal via Smad-independent pathways, including MAP Kinase, Rho-like GTPases and phosphatidylinositol-3-kinase (PI3K) (Fig 1-6) [82, 91]. Depending on the TGF $\beta$  ligand and the nature of its interaction with its receptors, combinatorial signalling pathways can be induced providing a mechanistic explanation for the pleiotropic activities of TGF $\beta$  [82]. Indeed, TGF $\beta$  can play a dual role in a number of processes. In cancer for example, it is recognised to inhibit tumour development through its potent negative effect on epithelial cell proliferation although it may also promote metastases through EMT; facilitating the detachment and migration cancerous cells [92]. Inhibition of TGF $\beta$  may require caution therefore as whilst fibrotic over-repair is undesirable, ameliorating the effects of TGF $\beta$  may lead to defects in wound healing, immune regulation and other physiological processes. To date, clinical trials using agents to inhibit the activity of TGF $\beta$  have met with disappointing outcomes, including a recent pilot study using a monoclonal antibody targeting all three isoforms in IPF (clinical trial number GC1008) [93, 94] [94].

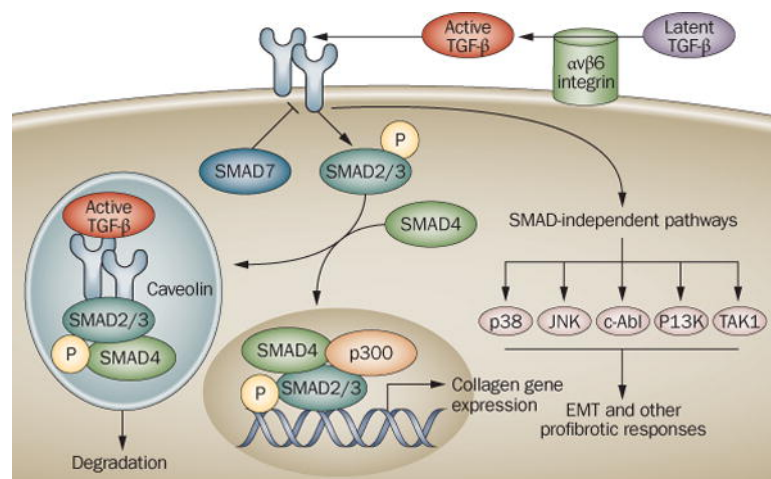


**Figure 1- 6. The major TGF $\beta$  signalling pathways in fibroblasts.**

TGF $\beta$  is secreted in a latent form and is cleaved to an activated form by a variety of conditions including acidic pH, increased tissue stiffness and integrins such as  $\alpha$ v $\beta$ 6 [81]. Activated TGF $\beta$  binds to Type I and II transmembrane receptors resulting in the recruitment and phosphorylation of Smad 2/3. Phosphorylated Smad 2/3 then forms a complex with Smad 4 and translocates to the nucleus where it binds to Smad-binding DNA elements leading to transcription of TGF $\beta$  responsive target genes. Smad 7 is a physiological inhibitor of Smad signalling. TGF $\beta$  can also signal via Smad-independent pathways, including MAP Kinase, Rho-like GTPases and phosphatidylinositol-3-kinase (PI3K). Adapted from Varga *et al.* [94].

### 1.2.7 Inflammatory responses in IPF

The role of inflammation in IPF has been contested in recent years. There are a number of reasons for this, which include the paucity of immune cells found within histological sections, the absence of significant ground glass opacification (radiological evidence of inflammation) on CT, and a lack of clinical response to corticosteroids and other immunomodulatory agents [5, 95-97]. IPF is characterised by uncontrolled fibroproliferation rather than chronic inflammation but evidence for an inflammatory component which assists in driving fibrotic processes does exist. BALF from IPF patients demonstrates a cytokine milieu that is high in pro-inflammatory cytokines including IL-1 $\beta$ , TNF $\alpha$  and IL-6 [98-100]. Furthermore, neutrophils are the predominant immune cell type in the BAL and increasing numbers correlate adversely with prognosis [101]. Whilst CT findings do not support a major inflammatory component, limited areas of ground glass change are not inconsistent with the diagnostic criteria and may represent isolated areas of early injury [102, 103]. Indeed, if the prevailing hypothesis is correct and damage directed at the AECII initiates the disease process, the absence of any inflammatory response would be surprising. The relationship between inflammation and fibrosis is closely interconnected with many 'inflammatory' cytokines and mediators capable of inducing fibrotic responses following high or prolonged release.

TNF $\alpha$ , IL-1 $\beta$  and IL-6 are key examples and all were found to be elevated in IPF patients. TNF $\alpha$  in particular has dual inflammatory and fibrotic function and numerous studies have demonstrated that up-regulation of its expression is linked to lung fibrosis. In IPF, alveolar macrophages (AMs) were found to spontaneously produce higher levels of TNF $\alpha$  compared to controls and in a related study, mRNA levels of TNF $\alpha$  were increased in lung tissue with immunohistochemistry (IHC) staining localising the cytokine to AMs, interstitial macrophages (IMs) and AECs [104]. In addition, transgenic mice over-expressing TNF $\alpha$  developed progressive pulmonary fibrosis [105] and intradermal injections of TNF $\alpha$  resulted in the focal accumulation of fibroblasts and collagen. Interestingly, this dermal fibrotic response was accompanied by an infiltrate of polymorphonuclear leukocytes early on but these cells were absent by day 7, indicating an initial inflammatory and subsequent fibrotic phase associated with TNF $\alpha$  administration [106]. TNF $\alpha$  has also been demonstrated to stimulate production of plasminogen-activator inhibitor-1 (PAI-1), which inhibits the activity of the fibrinolytic mediator plasmin. This protein also plays an important role in matrix degradation and stimulates the production of anti-fibrotic mediators COX-2 and PGE2. In keeping with

this, PAI-1 was found to be elevated in the BALF of IPF patients compared to controls [107, 108].

IL-1 $\beta$  is also associated with acute inflammatory responses and the development of pulmonary fibrosis [109]. IL-1 $\beta$  is most recognised for its role as a major inflammatory cytokine predominantly released by innate immune cells such as macrophages and monocytes following activation of pattern-recognition receptors (PRRs) by danger associated molecular patterns (DAMPs) and pathogen-associated molecular patterns (PAMPs) [110]. Acute release of IL-1 $\beta$  following injury results in rapid recruitment of neutrophils to sites of inflammation, increased production of chemokines and cytokines such as TNF $\alpha$  and IL-6 and the triggering of pyroptosis, a form of inflammatory cell death often seen in the context of infected cells [111, 112]. Sustained release of IL-1 $\beta$  however, as demonstrated in a rat model transfected to over-express IL-1 $\beta$  in the lung, resulted in the production of pro-fibrotic cytokines PDGF and TGF $\beta$  and the development of pulmonary fibrosis [109]. More pertinently, IL-1 $\beta$  was found to be increased in the BAL fluid and lung tissue from IPF patients and mRNA levels were increased in the alveolar macrophages [98, 113].

IL-6 plays an important role in the acute phase response, but like IL-1 $\beta$  it is also closely linked to fibrogenic processes [114-116]. Mouse models have demonstrated that by inhibiting the *trans*-signalling pathway of IL-6, pulmonary fibrosis was attenuated following bleomycin injury [100]. *In vitro* studies have revealed that IL-6 can directly mediate the differentiation of fibroblasts to collagen-secreting myofibroblasts [100, 117]. Of relevance, the highest levels of serum IL-6 were found in patients with acute exacerbations, events postulated to represent an acceleration of the disease process [118]. Furthermore, dermal fibroblasts in fibrotic areas from patients with systemic sclerosis expressed *IL-6* mRNA 30-fold higher than unaffected areas [119]. IL-6 has also been implicated in chronic airways remodelling seen in COPD and asthma, and blockade of IL-6 by the monoclonal antibody Tocilizumab has proven clinical efficacy in the treatment of rheumatoid arthritis [99, 120].

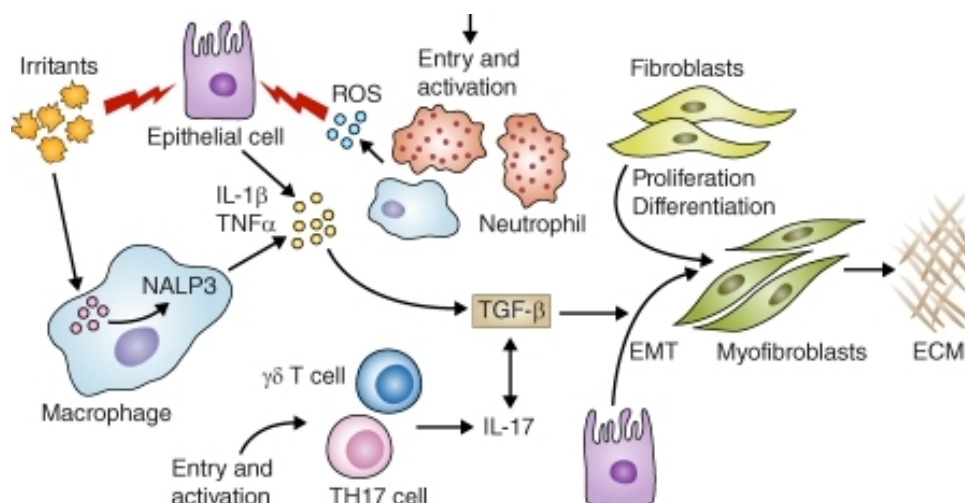


**Figure 1- 7. Proposed mechanisms leading to fibrogenesis in IPF.**

Irritants such as tobacco smoke, viruses and bile acids induce alveolar epithelial cell damage and activate inflammatory pathways including the NLRP3 inflammasome. Release of inflammatory mediators such as TNF $\alpha$ , IL-1 $\beta$  and ROS results in the recruitment of neutrophils and other leukocytes to the site of injury and stimulates the production of TGF $\beta$ . TGF $\beta$  mediates the recruitment, proliferation and activation of fibroblasts into collagen-secreting fibroblasts which promote extracellular matrix formation. Adapted from Wynn. [79].

Cytokines are produced by a wide range of cells including fibroblasts and epithelial cells and these may represent the major reservoir in IPF. However, numerous studies have also demonstrated that macrophages from IPF patients express higher levels of these soluble factors compared to controls [98, 121]. Furthermore, the preponderance of neutrophils within the BAL suggests that whilst inflammatory cells may not be the predominant mediators in IPF pathogenesis, they are likely to contribute to the profibrotic environment through the release of cytokines, chemotactic factors and reactive oxygen species (Fig 1-7) [122].

### 1.2.8 Oxidative stress

Oxidative stress is induced by the excessive production of reactive oxygen species (ROS) or the depletion of anti-oxidants, creating an imbalance that results in molecular and cellular abnormalities. Low-level generation of ROS by cells is physiological and molecules serve as signalling mediators to influence cellular processes [123]. Excessive or unopposed ROS activity however triggers a DNA damage response leading to apoptosis or necrosis of AECs and activation of pro-fibrogenic pathways [124]. ROS can also up-regulate fibrogenic mediators directly, enhancing release of TGF $\beta$  from its latency-associated protein and stimulating the NLRP3 inflammasome to release IL-1 $\beta$  (Fig 1-7) [125]. ROS is produced by a wide range of cell types including epithelial,

mesenchymal and endothelial cells although innate immune cells such as neutrophils, macrophages and monocytes generate high levels in response to stimulation [79, 126]. Research has revealed that aging is associated with enhanced ROS responses indicating that the lung may become more susceptible to oxidative stress with advancing years [127]. Furthermore, lung tissue may be particularly vulnerable due to high oxygen tensions that enhance oxidative insults alongside exposure to agents such as tobacco smoke, asbestos and other pollutants. These external factors can cause oxidative stress directly through the generation of oxygen and nitrogen intermediates and indirectly through the activation of inflammatory responses [124, 128].

Bleomycin, used to induce lung fibrosis in murine models increases free radical content that has been shown to stimulate fibroblast proliferation, myofibroblast differentiation and collagen secretion [129, 130]. Given that oxidative stress is mechanistically linked to fibrosis development, its role in IPF has been evaluated over the years in a number of studies. Free radicals of oxygen are difficult to measure directly, but researchers have looked at the products of oxidative reactions, such as modified proteins, lipids and DNA for evidence of oxidative stress. One study found that the levels of lipid peroxidation were significantly higher in both the bronchoalveolar lavage (BAL) fluid and sera from IPF patients. [128]. Another study measured biomarkers of oxidative stress, 8-isoprostrane and hydrogen peroxide ( $H_2O_2$ ), in the exhaled air from IPF patients and found that they were higher than controls, with  $H_2O_2$  negatively correlating with lung function severity [131]. There is also evidence that anti-oxidant generation is impaired in IPF with lower levels of glutathione found in the serum and lung fluid from patients with the disease [128]. Furthermore, the major anti-oxidant enzyme, extracellular superoxide dismutase, was found to be depleted in fibrotic areas from IPF lung tissue [132]. Taken together, there is sufficient evidence to indicate that a dysregulation of the oxidant/anti-oxidant balance exists in IPF and contributes to the pathogenesis of the disease. An early phase clinical trial using the anti-oxidant N-acetyl cysteine (NAC) suggested that administration may slow lung function decline although this was not validated in a larger phase III clinical trial (PANTHER-IPF) [133]. Thus, whilst anti-oxidant therapy may improve oxidative stress, the multitude of aberrant pathways involved in the development of the disease are likely to supersede small improvements made in any one component.



### 1.2.9 Fibroblast activation in IPF

Fibroblasts differentiate into myofibroblasts, which are the key effector cells in all fibrotic responses, responsible for the laying down of collagen-rich extracellular matrix. The origin of these cells in IPF is controversial and whilst the majority are likely to be recruited from the resident stromal population, there is evidence that they may also stem from the process of EMT (see below), and from circulating haematopoietic cells known as fibrocytes (Fig 1-8) [89, 90, 134]. During homeostasis, fibroblasts are relatively quiescent serving to support and maintain the tissue architecture. Following injury, they transiently differentiate into myofibroblasts and acquire contractile characteristics identifiable by the production of  $\alpha$ SMA [135]. This enables cells to migrate towards the site of injury where they establish a provisional matrix and contract the edges of the wound. The release of soluble factors such as TGF $\beta$ , PDGF, CDGF, IL-4 and IL-13 during injury mediate this differentiation process and these cytokines are all implicated in the pathogenesis of IPF [79, 80, 126]. In contrast to normal wound healing, myofibroblasts in IPF do not return to a resting state or undergo programmed cell death but continue to proliferate and accumulate in the lung tissue laying down excessive ECM leading to the destruction of the lung architecture. Studies have found that IPF fibroblasts are not only resistant to apoptotic signals but also operate under autonomous control [136, 137]. Unlike cancer cells, they are not of monoclonal origin but genomic studies indicate that IPF fibroblasts share similarities with malignant cells particularly seen at the level of translational control [138]. Contributing to the activated phenotype of fibroblasts may be the ECM itself, which in IPF becomes stiffened and contains excessive amounts of connective tissue, matrix metalloproteinases (MMPs), growth factors and morphogens. An elegant study by Parker *et al.* (2014) using decellularised ECM from controls and IPF patients found that both control and IPF fibroblasts seeded on of IPF matrix developed a genomic profile enriched for ECM proteins. Interestingly, they found that the matrix itself exerted the greatest influence on the pathological gene expression in fibroblasts rather than the origin of the fibroblasts themselves [44]. This study thus suggests that the development of an abnormal matrix in IPF may itself provide positive feedback signal propagating myofibroblast activity further.

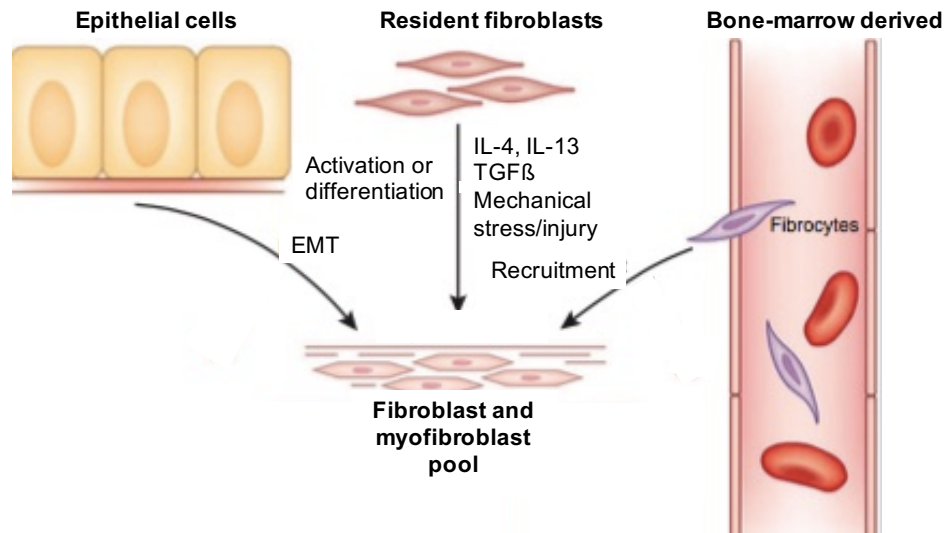


**Figure 1- 8. Fibroblasts in models of pulmonary fibrosis are thought to derive from three sources.** The predominant population stems from the local recruitment and proliferation of resident fibroblasts. Cells with fibroblast properties may also may descend from epithelial cells through the process of epithelial to mesenchymal transition (EMT) and from bone marrow derived precursor cells called fibrocytes. Adapted from Wynn. [80].

### 1.2.10 Epithelial-mesenchymal transition (EMT)

EMT is the process by which epithelial cells transdifferentiate into cells with mesenchymal characteristics. During EMT, epithelial cells down-regulate E-cadherin and other molecules involved in cell-cell junctions, lose apical-basal polarity and reorganise their cytoskeleton to enable them to acquire motility. It is usually a transient phenomenon and the term mesenchymal-epithelial transition (MET) refers to the reverse process. It was originally observed during embryonic development and later during physiological processes such as wound healing [92]. Triggers for EMT include hypoxia, inflammation, disruption of cellular contact and ER stress (Fig 1-9). The role of EMT in promoting cancer progression through the down-regulation of cellular adhesion molecules and the acquisition of an invasive phenotype facilitating metastasis is firmly established, but more recently its role in lung fibrosis has been investigated. The accumulation of collagen-producing myofibroblasts has been suggested to be partly contributed by the process of EMT [139-141]. Evidence for this comes from a number of studies which demonstrated the co-expression of epithelial and mesenchymal markers on AECs within histological sections. Mice studies involving the labelling of alveolar epithelial cells with green fluorescent protein (GFP) and subsequent bleomycin-induced lung injury also showed that the AECs stained positive for mesenchymal markers such as vimentin and fibronectin [139, 140, 142]. These findings however have not been

consistently reported and the contribution EMT plays in fibrosis remains uncertain. It is also unclear whether the process results in the generation of fibroblasts that actually contribute to matrix formation, and if so, whether their involvement is significant [141].

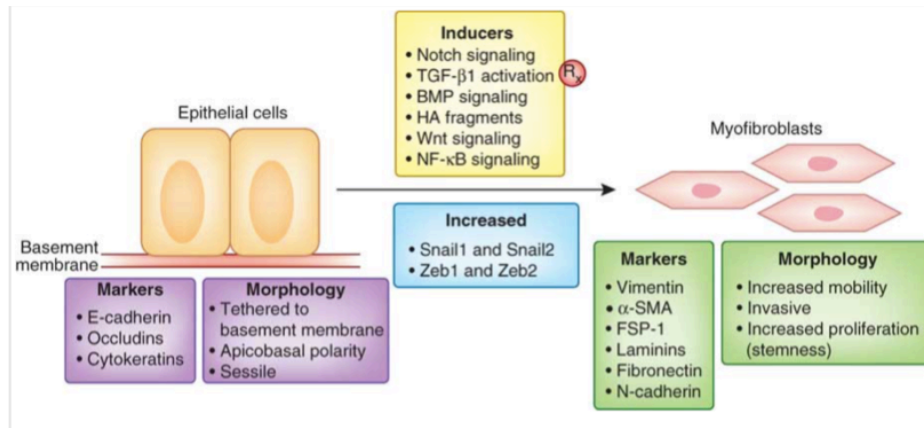


**Figure 1- 9. Diagrammatic representation of epithelial-mesenchymal transition.**

Epithelial cells can transdifferentiate into cells with mesenchymal characteristics. This process involves the down-regulation of cellular adhesion molecules and loss of apical-basal polarity. Reorganisation of the cytoskeleton occurs and cells become motile. Markers associated with epithelial cells such as E-cadherin, occludins and cytokeratin are down-regulated whilst those associated with mesenchymal cells such as vimentin,  $\alpha$ SMA and fibronectin are up-regulated. HA – Hyaluronic acid; FSP-1 - fibroblast-specific protein. Taken from Wynn *et al.* [80]

### 1.2.11 Adaptive immune responses in IPF

There is growing evidence that the adaptive immune system also plays a role in IPF. Perturbations have been demonstrated in the phenotype and functional repertoire of T and B cells, and circulating autoantibodies and immune complexes have been identified in a significant proportion of patients with the disease [143]. Histological lung sections from IPF patients demonstrate the presence of lymphocytic aggregates, known as tertiary lymphoid structures. These consist of clusters of T cells lying alongside mature dendritic cells that lie close to fibroblastic foci [144, 145] Non-proliferating CD20+ B cells have also been found in a subset of these aggregates, clustered within the centre [146]. High levels of circulating B-lymphocyte stimulating factor, which promotes B cell survival and maturation, was also identified in IPF serum. Furthermore, CXCL13, a chemokine that mediates the homing of B-cells to inflammatory foci, was increased in the blood and lung tissue from IPF patients. [146, 147].

Peripheral circulating T cells from IPF patients differed from controls, and CD4 lymphocytes demonstrated autoreactive clonal expansion when stimulated by fibrotic, but not healthy lung tissue. This suggests that self-antigens exist within the IPF lung and stimulate self-reactive T cells when presented by antigen-presenting cells [148]. Expression of the costimulatory receptor, CD28, which provides a 'second signal' for the activation of naïve CD4 lymphocytes, was found to be reduced in IPF. Of relevance, CD4+CD28- cells were also found to produce higher levels of pro-inflammatory cytokines including IL-1 $\beta$  and IL-6. Down-regulation of this co-receptor in IPF patients was associated with worsening lung function and reduced survival [149]. Regulatory T cells (Tregs) have also been investigated in IPF. Tregs play an important role in immune homeostasis and the maintenance of self-tolerance and are identified by their high expression of CD25 and the transcription factor FoxP3. Two studies reported that Tregs were reduced in IPF [150, 151], and one of these found that their suppressive function was impaired in vitro. A further study, however, reported the opposite finding with increased Treg levels measured in IPF patients. The authors of this study found that circulating Tregs in IPF were phenotypically different to controls and expressed the membrane-bound protein semaphorin 7a (Sema 7a+), which has been associated with enhanced fibrotic responses. This was demonstrated following the adoptive transfer of Sema 7a+ Tregs into mice resulting in increased lung collagen that was absent in mice injected with Sema 7a- Tregs [152]. Conversely, a further study found that Treg depletion in mice resulted in an exaggerated fibrotic response in a TGF $\beta$ -induced model of lung fibrosis [153]. The function and phenotype of Tregs can be influenced by the cytokine milieu and local environment [143, 154] and given the results of the above studies, it is possible that Tregs play a dual role in fibrosis development depending on the external factors modulating their activity.

A loss of self-tolerance and the development of autoreactive lymphocytes may also contribute to disease pathogenesis. Investigators have identified antibodies to a range of self-antigens including vimentin, cytokeratin 8,18 and 19, HSP70 and collagen V [155-159]. In contrast to autoimmune diseases such as systemic lupus erythematosus (SLE) and rheumatoid arthritis (RA) where autoantibodies and immune complexes can be linked mechanistically to disease pathogenesis [160, 161], their presence in IPF does not fit so neatly with our current understanding of disease mechanisms. Furthermore, mice depleted in lymphocytes develop pulmonary fibrosis following bleomycin injury whilst immunosuppressive agents such as Azathioprine do not alter the disease course [162, 163]. Thus, it is unlikely that abnormalities in the adaptive immune system drive the disease process. However, given that IPF is a heterogeneous disease resulting from

a variable combination of genetic and environmental factors, aberrations in T and B cell responses may play a fibrosis-promoting role in a proportion of patients diagnosed with the disease.

## 1.3 Monocytes and Macrophages

### 1.3.1 Monocyte subsets

Human monocytes comprise between 5-10% of circulating nucleated cells and are most commonly subdivided into three groups according to the expression of the LPS co-receptor CD14, and the FcγIII receptor, CD16 [164-166]. Significant controversies exist regarding the functional repertoires that define each subset and the role they play in response to injury. Mouse monocytes are more clearly defined and can be broadly divided into two subsets based on Ly6C expression. High expression is seen in monocytes which are released from the bone marrow (BM) in a CCR2-dependent manner and recruited early to sites of infection or inflammation. Analogous to Ly6C<sup>hi</sup> monocytes is the 'Classical' subset in humans, which represents around 90% of the monocyte population and is defined by high CD14 expression and an absence of CD16 [36]. Mouse studies reveal that release of Ly6C<sup>hi</sup> monocytes from the BM is under diurnal control by the circadian gene *Bmal1*. It has been suggested that their presence in the circulation during steady state may be part of a mechanism of 'anticipatory inflammation' to enable innate cells to respond rapidly to injury when it arises [167]. Recent work however suggests that Ly6C<sup>hi</sup> monocytes play a more active role in maintaining homeostasis and continuously traverse the endothelium in both directions surveying the tissue for antigens. Ly6C<sup>hi</sup> monocytes transport antigens to draining lymph nodes where they present them to cognate T cells without differentiating into macrophages. Following injury, Ly6C<sup>hi</sup> monocytes are recruited into the tissue in high numbers where local signals trigger the differentiation of these cells into 'inflammatory' macrophages [168] signified by an increase in size and cytoplasmic complexity. These monocyte-derived-macrophages (MDMs) undergo apoptosis after inflammation subsides or mature into macrophages with different phenotypic and functional characteristics that then assist in repair and resolution processes [164, 168-170].

Ly6C<sup>lo</sup> monocytes represent a distinct subpopulation and exhibit crawling behaviour over the endothelium suggesting a surveillance function [171]. They remove cellular debris and particulates and are important in viral responses, inducing TLR7 pathways and

recruiting inflammatory cells to the area [169, 172]. Gene profiling studies have found that the human equivalent to these cells are the 'Non-classical' or 'Patrolling' monocytes which are distinguished by high CD16 and low CD14 expression [166]. A third human subset has been described in more recent years which expresses both CD14 and CD16 and these cells are termed 'Intermediate monocytes'. They express high levels of HLA-DR and are considered important in antigen presentation [173]. This subset is reported to possess high inflammatory potential, producing elevated levels of ROS and cytokines such as TNF $\alpha$  and IL-1 $\beta$  in response to stimulation. Intermediate monocyte levels are increased in a number of disease states including rheumatoid arthritis and in the immediate aftermath following stroke and acute coronary syndrome [174-176]. Indeed, there is evidence to suggest that intermediate monocytes promote unstable plaque formation leading to coronary artery occlusion [177].

This description of monocyte subsets is likely to be overly simplistic and more recent research has highlighted the heterogeneity and functional complexity of monocytes. Much of the work based on monocyte subsets has been extrapolated from murine studies and the accuracy of these functional descriptions has been questioned. A study by Mukherjee *et al.* (2015) for example looked at human monocytes and found that non-classical subsets were increased in sepsis and decreased in patients receiving treatment with anti-inflammatory agents such as glucocorticoids [178]. Non-classical monocytes were also found to produce the highest levels of TNF $\alpha$  and IL-1 $\beta$  upon stimulation [176]. Furthermore, new techniques such as single-cell RNA sequencing have revealed the existence of additional monocyte populations which express unique sets of genes that have the potential to affect the cell cycle, differentiation and trafficking [179].

The process by which monocyte subsets evolve is also contentious. There is evidence from mouse studies that Ly6C<sup>lo</sup> monocytes represent terminally differentiated cells derived from the differentiation of Ly6C<sup>hi</sup> monocytes after BM egress [170]. A recent study by Patel *et al.* (2017) suggests that human monocytes may undergo a similar process within the circulation. Deuterium-labelled glucose was administered to healthy volunteers to study monocyte kinetics which identified the emergence of classical monocytes after 24 hours followed by the sequential appearance of intermediate and non-classical monocytes over 7 days [164]. Other studies however suggest that monocyte differentiation occurs much earlier on during bone marrow development with lineage tracing techniques providing evidence that monocyte progenitors become committed to specific fates prior to entering the circulation [180, 181]. In support of this, a study by Askenase *et al.* (2015) found monocytes isolated from the BM following T

*gondii* infection exhibited a regulatory phenotype and produced high levels of IL-10 and prostaglandin E<sub>2</sub> following stimulation. The authors demonstrated that the transcriptional reprogramming of monocyte progenitors occurred in response to IFN $\gamma$ -producing natural killer cells within the BM [182]. It is thus probable that some monocyte progenitors are primed early on to differentiate into cells with committed fates (mediated or influenced by external triggers) whilst other monocyte subgroups become moulded by their external environment as they mature following BM egress.

The broad spectrum of monocyte functionality has only recently started to be unravelled. In addition to their roles in innate responses, monocytes influence the adaptive immune system in their capacity as APCs and support the differentiation of specific T cell subsets (including Tregs, T follicular cells and cytotoxic CD8 cells) as well as inhibiting T cell proliferation and promoting regulatory T cell development [168].

### **1.3.2 Macrophage ontogeny**

Macrophages are usually classified according to the tissue in which they reside and represent a heterogeneous group of cells. Indeed, recent commentary has questioned whether it is appropriate to classify macrophages as a single group following compelling research that has challenged the central dogma that macrophages uniformly arise from a haematopoietic origin and revealed that the majority of tissue resident macrophages are in fact embryonically derived, with cell populations becoming established shortly after birth. Fate-mapping models indicate that these cell populations are long-lived and possess the unique ability to self-renewal, with minimal contribution from circulating bone marrow precursors. [170, 171, 183]. Furthermore, mouse knock out (KO) studies have revealed that resident lung macrophage populations are almost normal in the absence of haematopoietic stem cell progenitors (HSCPs). Evidence for this in humans has been found in patients with severe monocytopenia due to a GATA2 mutation. Analysis of tissue macrophages and epidermal Langerhans cells (LC) revealed that populations were largely preserved, indicating the shared prenatal ontogeny with mice [184].

Further evidence comes from haematopoietic stem cell recipients where host LCs are present years after transplant illustrating the long lived-nature of these cells [185]. The relative contribution of embryonically derived and haematopoietic macrophages does however depend on the type of tissue. Whilst LC and other tissue resident macrophages exist almost independently of blood borne precursors, mouse studies show that

monocyte derived macrophages are essential to replenish gut and dermal macrophages during steady state (Fig 1-10) [186, 187].

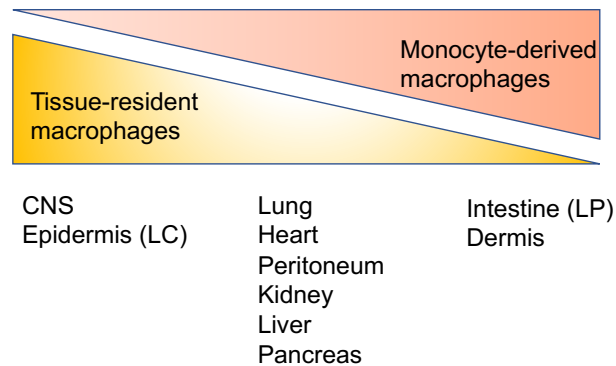


**Figure 1- 10. The contribution of tissue-resident (embryonically derived) and monocyte-derived macrophages (MDMs) varies between organs.**

Macrophages located in the central nervous system (CNS) and Langerhans cells (LC) within the epidermis are established prenatally from the foetal yolk sac. Monocytes constantly replenish macrophage populations in the lamina propria (LP) and dermis. In the lung, heart, peritoneum, kidney, liver and pancreas the ontogeny of macrophages has not been fully established although a population comprised of both tissue-resident and MDMs is considered likely. Adapted from Italiani *et al.* [187].

### 1.3.3 Lung macrophage populations

Alveolar and interstitial macrophages represent two distinct populations within the lung and are named according to their anatomical localisation. Alveolar macrophages are established prenatally, are long-lived cells capable of self-renewal and proliferation following lung injury [188]. They are positioned strategically within the airways and alveolar space and interact with the epithelium to maintain lung homeostasis. They are poor at presenting antigens to T cells and aid in clearing apoptotic cells and cellular debris thereby limiting unnecessary inflammatory responses [189]. Recent work looking at the transcriptional profile of tissue resident (embryonically derived) macrophages from different organs found that whilst a core macrophage signature exists, depending on the tissue type, these cells possess a unique transcriptional profile [190]. This enables tissue resident macrophages to perform the specialised and diverse functions required, such as the clearance of pulmonary surfactant by alveolar macrophages or maintenance of the epithelial barrier by Langerhans cells.

Less is known about the ontogeny and function of interstitial macrophages located within the lung tissue itself. However, in contrast to alveolar macrophages, interstitial macrophages from the lung, heart, gut and skin were found to have more closely overlapping transcriptional profiles regardless of their tissue origin [191]. This suggests



a common monocytic origin, although recent evidence suggests that lung interstitial macrophages may represent a hybrid population comprised of both tissue resident (embryonically derived) macrophages and MDMs, with the relative contribution of each depending on prior exposures. For example, in a mouse model of influenza-induced lung injury, areas depleted of macrophages were later repopulated by the remaining resident cells with little contribution from blood borne monocytes [192]. Bleomycin lung injury however induced the recruitment of monocyte-derived macrophages that persisted long after the resolution of fibrosis. Over time, these became almost indistinguishable from tissue resident macrophages [193]. Furthermore, radiation-induced lung macrophage depletion, with the remaining cells exhibiting reduced capacity for proliferation, led to the recruitment and permanent replenishment of monocyte-derived macrophages into lung niches [194].

These studies indicate that the type of lung injury and its effect on tissue resident macrophages (i.e. transient or permanent depletion) influence the subsequent contribution of MDMs to the long-term population [194]. Aging may also influence the cellular origin of the lung macrophage pool as whilst tissue resident cells are capable of self-renewal, it is unclear whether this ability extends to advanced old age. It is possible that these cells reach senescence resulting in the replacement of embryonically-derived macrophages by blood-borne precursors [195]. In cases where lung injury is chronic or repetitive, as is postulated to be the case in IPF, resident populations may become depleted with reduced ability for self-renewal and the contribution of monocyte derived macrophages could then become significant [127]. These cells, with a lineage distinct from their embryonic counterparts, may adopt characteristics of resident cells but may also retain distinct functional and cytokine repertoires that influence and possibly perpetuate the processes of repair and matrix deposition [193].

#### **1.3.4 Monocyte-derived-macrophages and polarised subsets**

The original belief that macrophages were derived and replenished solely from blood monocytes was developed in the 1960s before the advent of sophisticated lineage mapping techniques [185]. Whilst now somewhat outdated, these early studies remain important as they identified the essential roles monocytes and their tissue-based counterparts play in inflammation and repair. These studies also demonstrated how highly adaptable these cells are, with the capacity to differentiate and perform a diverse range of functions according to environmental cues. This cellular plasticity was first noted during *in vitro* studies when it was discovered that the phenotype and function of

macrophages, differentiated from monocytes, could be modulated depending on the type of stimuli given in vitro [196-199]. Th1 cytokines (IFN $\gamma$ ) result in macrophages with enhanced microbicidal activity that secrete high levels of pro-inflammatory cytokines such as IL-1, IL-6 and IL-23 as well as nitric oxide, important in host defence and early response to tissue injury [200]. These cells were designated 'M1' or 'classical' macrophages and are associated with high expression of receptors such as CD64 (an Fc  $\gamma$ -receptor to IgG), CD86 and CCR7, a lymph node homing receptor. Stimulation of the IFN $\gamma$  receptor triggers JAK-mediated tyrosine phosphorylation leading to dimerisation of the transcription factor STAT1 (signal transducer and activator of transcription). This binds to the promoter regions within genes to increase the expression of genes encoding *NOS2*, MHC class II molecules and *IL-12*, amongst others [201]. In contrast, stimulation by Th2 cytokines IL-4 and IL-13 resulted in macrophages with anti-inflammatory, reparative and regulatory properties. These cells were correspondingly labelled M2 or 'alternatively activated' macrophages and are recognised to play an important role in the later stages of tissue repair and immune modulation (Figure 1.3) [200, 202]. These cells are characterised by cell surface receptors that include the haemoglobin scavenger receptor CD163, the mannose receptor CD206 and CD200R [203]. Expression of the enzyme arginase-1 which competes with nitric oxide synthase produced by inflammatory macrophages is also increased. M2 macrophages produce higher levels of IL-10 and TGF $\beta$  in response to stimulation [197]. Many of the genes associated with M2 macrophages are regulated by STAT6 and interferon regulatory factor 4 (IRF4) [198].

Over the years, the M2 categorisation has been further subdivided into M2a, M2b and M2c to more clearly define macrophages according to their phenotypic characteristics and roles in repair and immunomodulation [196, 197]. The stimuli used to induce these subsets results in the expression of genes and proteins that only partially overlap with each other, demonstrating that 'M2' polarisation incorporates a diversity of phenotypes. IL-4 was first used to polarise cells to M2 and as such cells are defined as M2a. Receptor binding of IL-4 activates JAK1 and JAK3 leading to STAT6 activation and translocation. IL-4 promotes macrophage fusion and decreases phagocytosis [204]. M2b macrophages are activated by immune complexes and participate in crosstalk with B cells. Binding of immunoglobulins to Fc receptors (Fc $\gamma$ R) results in LPS-activated cells switching off IL-12 production and increasing IL-10 secretion and antigen presentation. M2c incorporates corticosteroids (CS) and IL-10 as stimuli. CS diffuses through the lipid membrane and binds to the glucocorticoid receptor (GR), which then translocates to the nucleus to influence gene transcription. Analysis of corticosteroid-stimulated monocytes showed

induction of *il-10*, *CD163*, *CD206*, *IL1R2*, thrombospondin 1 (*THBS1*), complement component 1 subunit A (*c1qa*) and TSC22 domain family, member 3 (*dsipi*) [198]. Long-term exposure to steroids reduces monocyte adherence, spreading, and apoptosis and increases phagocytic capacity [205]. Up-regulation of IL-10 results in inhibition of Th1 responses and pro-inflammatory cytokine production through the activation of STAT3 mediated pathways [187].

Macrophage-colony stimulating factor (M-CSF) is recognised for its role in maintaining tissue resident macrophage populations and promoting the survival and differentiation of monocyte-derived cells [206]. More recently, M-CSF has been classified as an M2 stimulus and upon binding to its receptor induces signalling pathways that up-regulate *IL-10* and *ARG1* whilst decreasing expression of *IL-1 $\beta$*  [207, 208]. In contrast, Granulocyte-colony stimulating factor (GM-CSF) promotes the development of dendritic cells and elicits M1-type responses in macrophages. Following stimulation with LPS and IFN $\gamma$ , GM-CSF cultured macrophages produced high levels of TNF, IL-18, IL-1 $\beta$  and IL-6 compared to M-CSF cultured cells which generated low level pro-inflammatory cytokines and high IL-10 [209]. However, neither factor induces a strongly polarised response and for in vitro work M-CSF is usually administered alongside IL-4, IL-10 or TGF $\beta$  to generate a prototypic M2 phenotype [194, 208, 210]. M-CSF and GM-CSF instead are thought predominantly to prime cells for M2 or M1 responses, respectively, and modulate the cellular response to subsequent stimuli. However, depending on the nature of additional factors, a partial overlap of M1 and M2 phenotypes may be seen [210] (Fig 1-11).

Tumour associated macrophages (TAMs) represent a distinct macrophage subtype. Their identification followed the observation that tumour growth was promoted by macrophages isolated from metastatic lesions but not from healthy tissue [211]. Further research into the role of TAMs has revealed that they can play a dual role in tumour development depending on the stage of cancer, tissue type and other environmental factors. TAMs promote tumour growth through several mechanisms. The generation of reactive oxygen and nitrogen species enhances genetic instability and mutations within malignant cells. The production of growth factors such as EGF by TAMs provides a permissive environment for cancer stem cells to proliferate [212]. TAMs may also facilitate metastasis through the production of high levels of proteolytic enzymes that degrade the extracellular matrix [213]. It is recognised that TAMs inhibit adaptive immune responses through the production of immunosuppressive factors such as IL-10, TGF $\beta$  and prostaglandins and the promotion of regulatory T cell activity [214-216]. Conversely, tumour models also show that TAMs may be beneficial in certain cancers and potentiate

the action of chemotherapy drugs and monoclonal antibody therapies via antibody-dependent cellular cytotoxicity and phagocytosis [217]. TAMs have a unique transcriptional profile and although they exhibit a phenotypic profile similar to M2 macrophages with high expression of CD163 and CD206, they also express M1-associated genes such as *NOS2* and *IL-12* [218]. Chemoattractants involved in monocyte recruitment such as MCP-1 and M-CSF are produced by TAMs themselves within cancer tissue. M-CSF has also been demonstrated to modulate the transcriptional profile of MDMs towards an immunosuppressive, tumour-promoting phenotype [219]. Indeed, several clinical trials are underway to evaluate the effect of blocking M-CSF signalling on tumour progression [217].

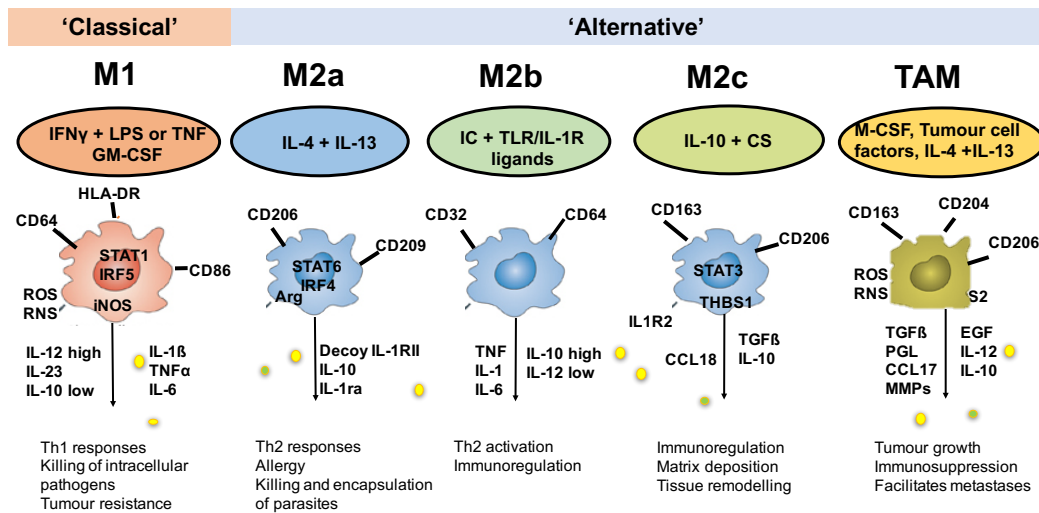


**Figure 1- 11. Macrophage polarisation.**

Macrophage subtypes can be categorised according to the type of stimulation used during the differentiation process which induces defined phenotypic and functional characteristics in vitro. 'M1' macrophages are polarised by Th1 cytokines such as IFN $\gamma$  and LPS and exhibit inflammatory activity important in host defence and tumour resistance. M2 macrophages represent a broader category of macrophages that are activated by Th2 cytokines alongside other factors including immune complexes (ICs), TLR ligands, corticosteroids (CS) and M-CSF. They have been further subdivided into Ma, Mb, Mc and TAMs in attempt to more clearly define phenotypes within a heterogeneous group. Macrophage polarisation and classification has arisen predominantly through in vitro work and does not necessarily reflect the phenotype and function of macrophages in vivo which are likely to share characteristics of different subgroups. Phenotyping of tumour associated macrophages (TAMs) for example has shown that whilst M2 characteristics predominant, certain M1 genes are also upregulated and reactive oxygen and nitrogen species (ROS and NOS) and produced in high concentration. Adapted from Martinez *et al.* [196] and Montovani *et al.* [217].

As knowledge of macrophage biology expanded and genomic analysis was employed it became clear that describing macrophages according to this polarised classification rarely typified the macrophage populations in vivo. Indeed, it is now recognised that macrophages often exhibit features of both types and possess a degree of plasticity

enabling them to perform diverse and contrasting functions in response to different environmental cues [199, 209, 220]. However, whilst the M1 and M2 paradigm may be overly simplistic and difficult to apply, it can be useful for describing the phenotypic characteristics of macrophage populations seen in certain disease states that have localised or systemic polarised responses. Acute tissue injury and tuberculosis for example have been characterised by an IFN $\gamma$ -induced pro-inflammatory 'M1' response [221-224], whereas murine studies show that chronic parasitic infestation is dominated by an 'M2' macrophage response similar to that seen following IL-4 stimulation *in vitro*. Mice infected with schistosomiasis initially mount an inflammatory response to try and eradicate the organisms. When this fails however, T helper and other immune cells secrete IL-4 which results in sustained polarisation of macrophages eventually leading to hepatic fibrosis after eggs lodge in the liver vasculature [225, 226]. Thus, prolonged or inappropriate macrophage polarisation induced by a persistent trigger may hamper the return to homeostasis and contribute to the disease process.

### **1.3.5 Monocytes and macrophages in inflammation and repair**

It has long been established that monocytes and macrophages play a key role in the repair process and exhibit distinct and differing phenotypic and functional characteristics depending on the stage of the process. Following initial injury, monocytes are rapidly recruited via chemokine gradients to the site of damage where they extravasate into the tissue and exhibit pro-inflammatory characteristics [126, 227]. They release cytokines to promote further inflammatory cell recruitment, produce high levels of reactive oxygen species to counteract microbial activity and help clear the area of cellular debris. Following the initial inflammatory response to injury, macrophages start to display regulatory and reparative activities and eliminate neutrophils through apoptosis and phagocytosis [228]. Macrophages involved in post-inflammatory stages of repair generate factors such as TGF $\beta$ , VEGF and insulin-like growth factor. These factors assist in fibroblast recruitment, proliferation and differentiation into myofibroblasts. Myofibroblasts are the major effector cells in repair and secrete structural proteins and other matrix components leading to the deposition of a collagen-rich scaffold over which endothelial and mesenchymal cells migrate to regenerate damaged tissue [229]. In rodent studies, it has been demonstrated that macrophages during this phase of repair assist in matrix formation through the expression of mediators that enhance the production of Lysyl Hydroxylase-2, an enzyme that facilitates the cross-linking of collagen fibrils [230]. Macrophages also express arginase-1, which in mice converts

arginine to ornithine. This is then metabolised to proline, a key amino acid required for the generation of collagen [231]. In the reparative stages, macrophages secrete inhibitory mediators such as IL-10 and express cell surface markers including PD-L1 and 2 that are essential for dampening inflammatory responses that may otherwise result in further cellular damage (Fig 1-12) [200, 232] .

Macrophages are also essential in the resolution phase of repair, induce apoptosis in redundant inflammatory and stromal cells, and produce factors to degrade excessive ECM components laid down during earlier stages of repair [232]. The process of ingesting apoptotic and aged cells (efferocytosis) modifies macrophage functionality. In a model of reversible biliary fibrosis, macrophages were found to co-localise with apoptotic cholangiocytes and in vitro assays revealed that following efferocytosis of these apoptotic cells, macrophages produced high levels of matrix metalloproteinases (MMPs) that degrade matrix components [232, 233].

During wound healing, it is unclear whether monocyte and macrophage subsets with differing phenotypes are drafted in sequentially or whether cells present during the early phases of injury adapt their functional repertoire according to the phase of repair [126]. Research provides evidence for both mechanisms. In a study of experimental myocardial ischemia, early infiltrating inflammatory monocytes were identified by expression of cell surface receptors Ly-6C<sup>hi</sup>, CCR2<sup>hi</sup> and CX3CR1<sup>lo</sup>, and isolation of immature tissue macrophages demonstrated high levels of IL-6 and TNF $\alpha$ . Three days after the initial injury response however, the phenotype of the infiltrating monocytes switched to Ly6C<sup>lo</sup>, CCR2<sup>lo</sup>, CX3CR1<sup>hi</sup>, suggesting that sequential recruitment of different monocyte populations occurred at specific time points [234]. In contrast to this, reversible liver fibrosis using CCl4-induced injury identified macrophage populations during the recovery phase of injury derived from circulating inflammatory monocytes, that underwent a phenotypic switch following the ingestion of cellular debris within the tissue [235].

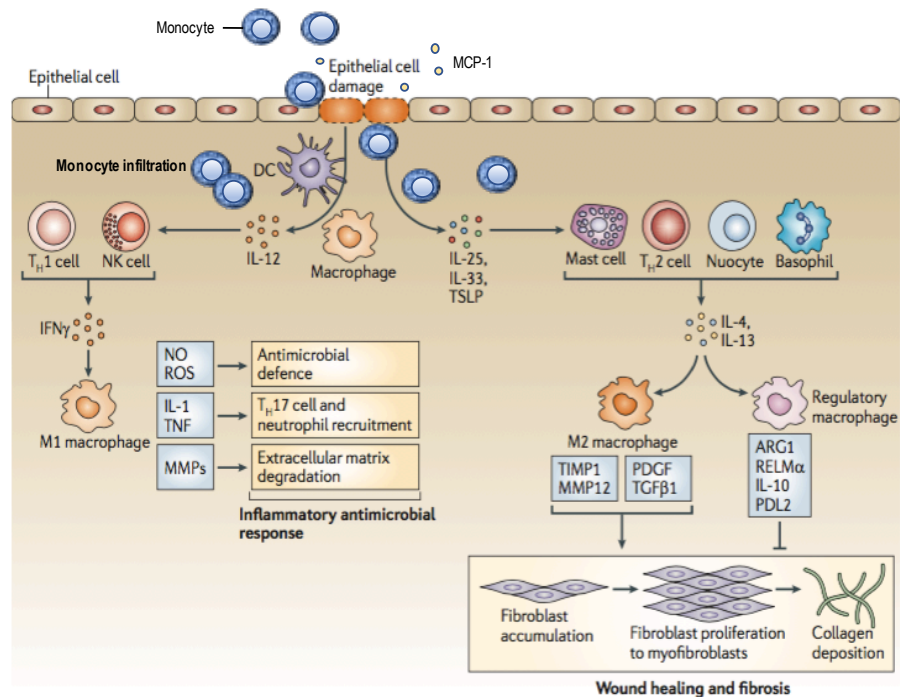


**Figure 1- 12. The role of monocytes in the repair process.**

Following injury, monocytes and macrophages with inflammatory activities flood the tissue. They recruit neutrophils through the release of mediators such as IL-1 and TNF and secrete mediators such as nitric oxide (NO) and reactive oxygen species (ROS) to counteract invading organisms. They also produce matrix metalloproteinases (MMPs) to assist in clearing the damaged area and phagocytose cellular debris. Following the inflammatory phase, macrophages assist in tissue remodelling through the secretion of factors such as TGF $\beta$  and PDGF leading to the recruitment and activation of fibroblasts. They also produce mediators, including MMPs and tissue inhibitors of MMPs (TIMPs), that assist in collagen deposition and the construction of an extracellular scaffold through which cells can migrate to repopulate denuded tissue. Towards the end of the repair process, macrophages possess a regulatory phenotype (induced in part by the process of efferocytosis) and release factors such as IL-10 and programmed death ligand 2 (PDL2) which inhibit further inflammatory activity and assist in returning the tissue to homeostasis. Aberrations in the activities of macrophages during any stage of the repair process may lead to healing responses that are delayed or exuberant with excessive collagen deposition. Adapted from Murray and Wynn [200].

### 1.3.6 The role of monocytes and macrophages in fibrogenesis

Tissue repair is a tightly coordinated sequence of cellular events and aberrations in the process can lead to delayed tissue regeneration or excessive collagen deposition. Macrophages (both monocyte-derived and tissue resident) are key players in orchestrating wound healing and undertake dual and opposing roles during different phases of repair, capable of both promoting fibrosis and enhancing its clearance. Thus, imbalances in the number or function of these cells have been postulated to contribute to the development of diseases characterised by excessive scar formation, including IPF [25, 151, 193, 236, 237]. In support of this, an array of cytokines and chemokines including TNF $\alpha$ , IL-1 $\beta$ , CCL18 and IL-13 that potentiate fibrogenesis in mouse models have been found to be elevated in the BAL fluid from IPF patients [40, 98, 105, 238].

These same mediators are recognised to modulate macrophage phenotype and alter functionality in vitro, supporting the hypothesis that lung macrophages may be aberrantly activated to potentiate fibrosis in this disease.

The opposing roles played by monocytes and macrophages during the course of normal healing has been demonstrated in cellular depletion studies. In a model of cutaneous injury, it was found that depleting monocytes in the early inflammatory stage resulted in delayed wound debridement, granulation tissue and epithelialisation [239]. A study by Gibbons *et al.* (2011) used bleomycin to induce lung fibrosis in mice, and found that depleting monocytes and macrophages with liposomal clodronate when lung fibrosis was maximal (around week 3) hastened fibrosis resolution. Depleting these cells during the recovery phase six weeks later however resulted in the persistence of fibrotic tissue [25]. These findings were mirrored in a murine model of reversible liver fibrosis where researchers found that depleting macrophage populations late in the repair process also delayed fibrosis resolution [235]. The phenotype of cells involved in the fibroproliferative phase following bleomycin injury was not identified with certainty but a reduction in the expression of M2 markers Arginase-1 and Ym1 was noted following macrophage depletion.

Determining the phenotype of macrophages that specifically contribute to fibrosis may have important therapeutic implications and a number of studies have sought to identify pro-fibrogenic populations in the context of lung fibrosis [39-41, 240]. In vitro studies show that M2-differentiated macrophages produce higher levels of cytokines such as TGF $\beta$ , CTGF and IGF-1 which activate fibroblasts and promote collagen production. In vivo, chronic schistosomiasis infection induces M2-polarised responses resulting in the development of hepatic fibrosis. Therefore, it has been postulated that macrophages in IPF may exhibit a similar M2 profile that contributes to fibrogenesis. In support of this, IPF macrophages isolated from BAL fluid were found to express higher levels of CD163 and CD206 alongside arginase I and chitinase 3-like 1 protein; mediators implicated in fibroproliferative responses [25, 39, 241, 242]. Furthermore, IL-13 and CCL18 were also found to be elevated in the AMs from patients with IPF and other fibrotic lung diseases. CCL18 stimulates collagen production in fibroblasts and levels of this chemokine correlated with lung function decline as well as exacerbation risk in IPF [40]. Other studies however, suggest that a single polarised population is unlikely to be driving fibrotic responses and there is evidence that IPF macrophages also produce higher levels of inflammatory mediators such as TNF $\alpha$ , IL-1 $\beta$  and reactive oxygen species [98, 128, 243]. Indeed, persistent inflammatory responses by macrophages are recognised



to induce fibrotic sequelae. In chronic Hepatitis C infection for example, sustained activation of the NLRP3 inflammasome results in IL-1 $\beta$  release which potentiates hepatic fibrosis [244].

Whilst the phenotype of macrophages in IPF cannot be neatly categorised, there is sufficient evidence that these cells differ in comparison to healthy controls and may contribute to the disease process [25, 39, 40]. However, the majority of studies to date have analysed alveolar macrophages obtained from BAL fluid and little is known about the potential role of either monocytes or interstitial macrophages (which are thought to be derived from both embryonic and bone marrow precursors) in the disease. Furthermore, studies reveal that the ontology of lung macrophages differs significantly following lung injury and in response to bleomycin instillation, there is evidence that monocyte-derived macrophages drive fibrotic responses. In a model where a monocyte tracking system was established, Misharin *et al.* (2017) [193] found that tissue resident macrophages predominated within the lung during homeostasis although following injury the population become heterogeneous with monocyte-derived cells. When necroptosis was induced in monocytes upon entry to the lung, fibrosis was ameliorated. Transcriptomic profiling of MDMs during the fibrotic stage of bleomycin injury revealed up-regulation of genes that were causally linked to fibrosis development. Whilst the bleomycin model poorly recapitulates the pathological processes occurring in IPF, the chronicity of tissue injury and elevated levels of the major monocyte chemoattractant protein-1 (MCP-1) in both the BAL and serum of IPF patients [245, 246] suggests a role for monocytes in the disease.

## 1.4 Project aims

Given the essential roles monocytes play in wound healing after injury and the evidence from animal studies that they replenish empty macrophage niches, there are surprisingly few studies that have focused on phenotypic and functional differences that exist between monocytes from IPF patients and healthy controls. Therefore, the aims of this study were:

- i. To characterise monocytes from IPF patients with stable and acute exacerbations of disease and determine whether the immunophenotype of these cells changes with different severities of disease.
- ii. To explore the phenotypic characteristics of monocytes from IPF patients as they differentiate into macrophages *ex vivo*.
- iii. To determine whether functional differences exist between monocyte-derived-macrophages from IPF patients compared to controls, including the influence of these cells on fibrogenic end-points.

## **2 Materials and Methods**

### **2.1 Patients and participants**

This was a cross-sectional study examining the phenotypic and functional characteristics of monocytes from patients with IPF between January 2015 and April 2017.

Patient samples were acquired during specialist ILD clinics or during in-patient stays in cases of AEIPF. Age and sex matched healthy volunteers were recruited predominantly from orthopaedic pre-assessment clinics. Additional samples were obtained from volunteers at the University. The study was approved by the South Central-Oxford C Research Ethics Committee (REC ref: 14/SC/1060, appendix 1) and all subjects provided informed consent.

Patients recruited within the study had a definite or probable diagnosis of IPF according to the 2011 ATS/ERS/JRS/ALAT guidelines [13]. Patient and control demographics are supplied in the results section in each chapter.

Exclusion criteria for both patients and controls were as follows:

- 1) The presence of coexistent lung disease (excluding emphysema if occupying less than 25% of the lung volume)
- 2) Co-existent inflammatory disease or active cancer
- 3) Active or recurrent infection
- 4) Current smokers
- 5) Participants on greater than 10mg of prednisolone (with stable disease)

Disease severity was assessed by the use of 4 well-validated indices and is discussed in detail in section 4.1:

- 1) Forced vital capacity (FVC)
- 2) Composite physiological index (CPI) [247]
- 3) Transfer factor for carbon monoxide (TLCO)
- 4) CT fibrosis scores

An acute exacerbation was defined as:

- 1) Deterioration in dyspnoea over 30 days or less
- 2) New airspace infiltrates on HRCT (with or without evidence of infection)
- 3) Exclusion of pulmonary emboli and heart failure

This definition of acute exacerbation (AE) was based on accepted criteria [14] but modified to include instances where the disease may have been exacerbated by infection. The decision to include these cases was based on the recent understanding that microorganisms are likely to trigger acute decline in a significant proportion of patients with a diagnosis of AEIPF [24, 64, 248]. Examination of clinical trial data found that patients with AE who had infection investigated and excluded, followed a similar clinical course as those who had not. It was therefore reasoned that excluding cases where infection had not been definitively excluded would be arbitrary and might artificially skew the findings [15, 249].

## **2.2 Clinical information**

For monocyte phenotyping studies, lung function tests were undertaken on the same day as blood sampling in all but 5 cases, which were performed a maximum of three months beforehand due to reasons of practicality. In instances of acute exacerbation, the most recent values obtained as an outpatient were recorded (all within a 12-month period of sampling). Demographics, previous smoking status and clinical data including use of anti-fibrotic agents, other medications and past medical history were recorded in an anonymised database to ensure controls and IPF patients were well matched.

## 2.3 Laboratory methods

### 2.3.1 Media

Name	Composition
R10	RPMI-1640 (Sigma Aldrich) + 10% FCS + 1% L-Glutamine and 1% Pen/Strep
R0	RPMI-1640 (Sigma Aldrich) + 1% L-Glutamine and 1% Pen/Strep
FACS / MACS buffer	500ml PBS + 2% FCS + 2ml 0.5M EDTA
Saponin buffer	200ml PBS + 2g BSA + 2ml FCS + 1g Saponin
D10	DMEM (Sigma Aldrich) + 10% FCS + 1% L-Glutamine and 1% Pen/Strep
D0	DMEM (Sigma Aldrich) + 1% L-Glutamine and 1% Pen/Strep

**Table 2-1. Media used in experiments.**

RPMI-Roswell Park Memorial Institute 1640 medium; FCS- foetal calf serum; pen/strep- Penicillin Streptomycin; PBS- Phosphate Buffered Saline; EDTA-Ethylenediaminetetraacetic acid; DMEM- Dubecco's Modified Eagle's Medium.

### 2.3.2 Extraction of peripheral blood mononuclear cells (PBMCs)

Blood samples were collected in 9ml tubes containing Lithium Heparin (Greiner bio-one 455084) and processed within 4 hours. Peripheral blood mononuclear cells (PBMCs) were extracted using Ficoll density gradient separation. Blood was diluted in an equal volume of R10 (Table 2-1) followed by layering of 25ml aliquots over 15ml of Lymphoprep™ (Axis-Shield 1114544). Samples were centrifuged at 20000rpm for 20 minutes without a break enabling separation of the different cellular layers. PBMCs were removed from the Lymphoprep™ interface layer using a Pasteur pipette. Cells were then washed in R10. PBMCs were then counted under the microscope (Nikon) using FastRead disposable cell counting chambers (Immune Systems, BVS100) and a 9:1 dilution of trypan blue (Sigma T6146).

### 2.3.3 Serum preparation

At the time of sampling, all participants had blood taken for serum using serum separator tubes (BD Vacutainer SST Tube 367977). Tubes were centrifuged at 3000rpm for 5

minutes to separate the serum which was removed using a Pasteur pipette and transferred to a mini-Falcon tube. Samples were heat-inactivated at 56°C for 30 minutes then left to cool to room temperature. Serum was aliquoted for monocyte differentiation assays and stored at -20°C for future analysis of soluble factors.

#### **2.3.4 Monocyte isolation**

Monocytes were isolated from PBMCs by positive selection using CD14 microbeads (Miltenyi Biotec 130-050-201) according to the manufacturer's instructions. PBMCs were counted, washed in MACS buffer (Table 2-1) and re-suspended in 80µl of buffer plus 20µl of microbeads per  $10^7$  PBMCs. Cells were then incubated at 4°C for 15 minutes, washed in MACS buffer and centrifuged at 1600 rpm for 10 minutes. Cells were reconstituted in 500µl buffer and passed through a 30µm cell filter and LS column. Purity was assessed using fluorescence-conjugated antibodies to CD3, CD19, CD15, CD16 and CD14, and found to be consistently above 98%.

#### **2.3.5 Generation of monocyte-derived macrophages (MDMs)**

Monocytes were cultured in X-vivo (Lonza BE04-380Q) supplemented with 10% autologous serum at a concentration of  $1 \times 10^6$ /ml. 50ng/ml human M-CSF (Miltenyi Biotec 130-093-963) was added on day 0 to aid survival. Cells were plated onto low-adherence plates (Corning CLS3471-24EA) and cultured at 37°C with 5% CO<sub>2</sub> for 6 or 7 days depending on the experimental protocol. Media was replenished on day 4 with removal of 20% of media followed by addition of 40% fresh media. On day 6 or 7, depending on the assay, plates were removed from the incubator and placed on ice for 20 minutes. Cells were then harvested by gentle pipetting into mini-Falcon tubes, washed and counted.  $1 \times 10^5$  cells were placed into round bottomed 96 well plates for flow cytometric phenotypic staining. Flat bottomed 96 well plates were used for phagocytosis, ROS and inflammasome assays.

### **2.4 Flow cytometry**

Monoclonal antibodies used are listed in Table 2-2 and 2-3. Prior to experiments antibodies were titrated to ensure optimal results. All cultured cells were incubated with a fixable viability stain (Zombie Aqua, Biolegend 423102) for 15 minutes to enable

exclusion of dead cells from subsequent analysis. Cells were surface stained within 100µl of FACS buffer (Table 2-1) and intracellular staining was undertaken in 100µl of a permeability buffer. Frequency-minus-one samples were used to establish the gating strategy except for experiments where auto-fluorescence was a concern. In these instances, isotype controls were used. For each experiment, cells were acquired using a standardized experimental template on a 4-laser, 18-colour flow cytometer (BD LSRFortessa™, LSRII). Data was analysed using Flowjo v10 software (Tree star, Inc).

#### **2.4.1 Phenotypic and cytokine staining of monocytes within PBMCs and MDMs**

**PBMCs:** Following isolation of PBMCs, cells were plated into 96 well plates and stained immediately for phenotypic analysis or cultured at 37°C overnight in R10 media in the presence of either LPS (1µg/ml, Sigma L2630), r848 (TLR 7/8 agonist, 1µg/ml, Invivogen 144875-48-9) or left unstimulated for comparative purposes. Cytokine analysis was conducted after a 20-hour stimulation period with Brefeldin A (10µg/ml, Sigma B7651) added at 16 hours.

**Surface staining:**  $5 \times 10^5$  PBMCs and  $1 \times 10^5$  MDMs in 100 µl of FACS buffer were transferred to 96 well plates and incubated with fluorochrome-conjugated monoclonal antibodies (mAb) in the dark at 4°C for 20 minutes. They were then washed twice in FACS buffer and fixed with Stabilising Fixative (BD 339860) for 15 minutes.

**Intracellular staining (ICS):** Following fixation, PBMCs were permeabilised with Permeability Buffer I (BD 557885), and incubated with mAbs in the dark for 30 minutes at room temperature. They were then washed once in Permeability Buffer I, twice with FACS buffer and re-suspended in Stabilising Fixative. For ICS of MDMs, fibroblasts and A549 cells, Saponin buffer (Table 2-1) was used rather than Permeability Buffer I. Following incubation with mAb, cells were washed twice in Saponin buffer and once in FACS buffer prior to fixation.

<b>Antibody</b>	<b>Fluorochrome</b>	<b>Clone</b>	<b>Isotype</b>	<b>Supplier</b>	<b>Catalogue number</b>
Anti-Annexin V	FITC	VAA-33	Mouse IgG2a, k	eBiosciences	BMS147FI
Anti-CCR7	BV421	G043H7	Mouse IgG2a, k	Biolegend	353208
Anti-CD14	PE-Cy7	HCD14	Mouse IgG1, k	Biolegend	325618
Anti-CD14	FITC	61D3	Mouse IgG1, k	eBioscience	11-0149-42
Anti-CD15	BV-650	W6D3	Mouse IgG1, k	Biolegend	323034
Anti-CD15	PerCP-Cy5.5	W6D3	Mouse IgG1, k	Biolegend	323020
Anti-CD15	PE	HI98	Mouse IgM, k	Biolegend	301906
Anti-CD16	AF700	3G8	Mouse IgG1, k	Biolegend	302026
Anti-CD163	BV605	GHI/61	Mouse IgG1, k	Biolegend	333622
Anti-CD163	APC-Cy7	GHI/61	Mouse IgG1, k	Biolegend	333616
Anti-CD19	PE	HIB19	Mouse IgG1, k	Biolegend	302294
Anti-CD200R	APC	OX-108	Mouse IgG1, k	Biolegend	329308
Anti-CD206	APC-Cy7	15-Feb	Mouse IgG1, k	Biolegend	321120
Anti-CD3	FITC	HIT3a	Mouse IgG2a, k	eBioscience	11-0039
Anti-CD36	APC-Cy7	5-271	Mouse IgG2a, k	Biolegend	336214
Anti-CD62L	FITC	DREG-56	Mouse IgG1, k	Biolegend	304804
Anti-CD64	PerCP-Cy5.5	10.1	Mouse IgG1, k	Biolegend	305024
Anti-CD64	BV421	10.1	Mouse IgG1, k	Biolegend	305020
Anti-CD68	PE-Cy7	Y1/82A	Mouse IgG2b, k	Biolegend	333816
Anti-CD86	PE	IT2.2	Mouse IgG2b, k	Biolegend	305406
Anti-E-cadherin	APC	67A4	Mouse IgG1	Abcam	ab99885
Anti-fibronectin	AF488	F1	Rabbit IgG	Abcam	ab198933
Anti-HLA-DR	AF488	L243	Mouse IgG2a, k	Biolegend	307620
Anti-HLA-DR	PE	L243	Mouse IgG2a, k	Biolegend	307605
Anti-HLA-DR	PerCP-Cy5.5	L243	Mouse IgG2a, k	Biolegend	307630
Anti-IL-10	APC	JES3-19F1	Rat IgG2a, k	Biolegend	506807
Anti-IL-4	APC	8D4-8	Mouse IgG1, k	Biolegend	500714
Anti-IL-6	APC	MQ2-13A5	Rat IgG1, k	Biolegend	501112
Anti-IL17A	PerCP-Cy5.5	BL168	Mouse IgG1, k	Biolegend	512314
Anti-MCP-1	FITC	2H5	Armenian Hamster IgG	eBioscience	11-7096-81
Anti-N-cadherin	PE	8C11	Mouse IgG1	Abcam	ab93525
Anti- $\alpha$ SMA	AF594	1A4	Mouse IgG2a, k	Abcam	ab202368
Anti-Vimentin	FITC	VAA-33	IgG2a, k	eBioscience	BMS147FI
Cell viability	7-AAD	N/A	N/A	Biolegend	420404
Cell viability	Zombie Aqua	N/A	N/A	Biolegend	423102

**Table 2-2. List of flourochrome-conjugated monoclonal antibodies used to characterise cells in this study.**



Antibody	Fluorochrome	Clone	Supplier	Catalogue number
Mouse IgG2a, k	AF594	10D7A7B2	Abcam	ab178001
Mouse F(ab') <sub>2</sub> IgG1	APC	15H6	Abcam	ab37391
IgG2b	PE-Cy7	MPC-11	Biolegend	400326
IgG1, k	APC-Cy7	MOPC-21	Biolegend	400128
Mouse IgG1	PE	B11/6	Abcam	ab91357
Mouse IgG1, k	APC	P3.6.2.8.1	eBioscience	17-4714-42
Mouse IgG2b, k	PE	BMG2b	eBioscience	12-4732-42
Mouse IgG1, k	PerCP-Cy5.5	MOPC-21	Biolegend	400149
Mouse IgG1, k	FITC	P3.6.2.8.1	eBioscience	11-4714-42
Mouse IgG1, k	BV605	MOPC-21	Biolegend	400161

Table 2-3. Isotype control mAbs used in the study.

## 2.5 Monocyte-derived macrophage studies

### 2.5.1 Phagocytosis assays

To test phagocytosis, two assays were utilised:

- 1) *Yellow-green carboxylate-modified polystyrene latex bead assay* (Sigma L4655). 1µm beads were incubated with cells at a ratio of 1 cell to 30 beads for 2 hours. Prior to the assay, 100 000 cells/200µl were seeded onto flat-bottomed 96 well plates. To assess the extent of non-specific binding of beads on the cell surface, a phagocytosis inhibitor was used. 30nM cytochalasin D (Sigma C2618) was added to control wells 30 minutes before the addition of latex beads. Optimisation experiments were performed prior to the assays to ascertain the optimal number of beads per cell, the concentration of cytochalasin required and the impact of LPS on phagocytosis. Samples were analysed by flow cytometry. The emission and excitation range of the latex beads is 470nm and 505nm, respectively.
- 2) *pHrodo® Green E. coli bioparticle assay* (Molecular Probes P35366). Due to the issues that arose from non-specific cell surface binding when using latex beads, the pHrodo assay was subsequently utilised. This kit employs a bioparticle conjugated to a novel fluorogenic compound that only emits light in conditions of

low pH. Therefore, only after ingestion by the MDM and uptake into the acidic environment of the lysosome does a positive signal appear, eliminating concerns regarding non-specific binding. For each patient sample, two wells within a flat bottomed 96 well plate were used, each containing 100,000 cells. Into one of the two wells per sample, Cytochalasin D was added for 30 minutes to serve as a negative control. The plate was then spun and the media discarded and replaced with a 100µl of pHrodo solution. This was prepared by adding 2ml of PBS to a vial of pHrodo Green E. coli Bioparticles® and vortexing well to ensure a homogeneous suspension. The plate was placed in the incubator for 30 minutes, followed by subsequent centrifugation and replacement of the media by the viability dye Aqua Zombie for a further 15 minutes. Samples were then washed in FACS buffer and transferred on ice for immediate acquisition on the flow cytometer (LSRII). The fluorescent bioparticles have an excitation/emission range of 509/533nm.

### **2.5.2 ROS assay**

This assay utilises the compound CM-H2DCFDA (Molecular Probes C6827) which is normally non-fluorescent but passively diffuses into the cell where cellular esterases cleave acetate groups and render the product responsive to oxidation. Induction of oxidative stress subsequently results in a highly fluorescent adduct, which is retained in the cell and allows comparative quantification of in vitro ROS activity. Optimisation assays were carried out to determine the optimal length of the assay and concentration of CM-H2DCFDA and hydrogen peroxide (H<sub>2</sub>O<sub>2</sub>) required.

The experiment was carried out according to the manufacturer's protocol. MDMs were cultured in X-vivo without phenol red (Lonza BE04-743Q) supplemented with Gentamicin, L-glutamine and 10% autologous serum. On day 7 cells were harvested, counted and suspended in a single cell solution of PBS. 1x10<sup>5</sup> MDMs in 100µl of PBS were placed in a flat-bottomed 96 well plate. A vial of CM-H2DCFDA was reconstituted with DMSO immediately before use then added to each well at a concentration of 5 µM. Cells were incubated in the dark for 30 minutes at 37°C then washed in X-vivo. Oxidative stress was induced using 0.03% H<sub>2</sub>O<sub>2</sub> for 1 hour. Cells were then washed and incubated with a viability dye for 10 minutes before being placed on ice and acquired immediately on the LSRII. Experimental controls included cells not exposed to CM-H2DCFDA or H<sub>2</sub>O<sub>2</sub> to ascertain background levels of ROS generation.

### **2.5.3 Inflammasome assay**

**Sample preparation:** MDMs were cultured as previously described and harvested on day 6.  $1 \times 10^5$  MDMs were used per experimental condition (undertaken in duplicate) within a 96 well plate. Conditions were as follows: unstimulated cells, cells stimulated with LPS alone (1:10000), Nigericin alone (1:1000, Invivogen tlr-nig-5) and 'test' cells that were stimulated with both LPS and Nigericin in order to induce inflammasome activation and IL-1 $\beta$  release. LPS was added first for 16h followed by Nigericin for 30 minutes. The plate was then centrifuged and the supernatant removed, spun twice to remove any remaining cells and stored at -20°C for future IL-1 $\beta$  testing using an ELISA-based assay (section 2.6).

## **2.6 ELISA**

### **2.6.1 IL-1 $\beta$**

IL-1 $\beta$  was measured using a quantitative sandwich ELISA. The assay was undertaken according to the manufacturer's protocol (R&D Human IL-1 beta/IL-1F2 Quantikine ELISA Kit, DLB50). Supernatant samples collected from the inflammasome assay (section 2.7), and IL-1 $\beta$  standards were added in duplicate to a microplate pre-coated with a monoclonal antibody to IL-1 $\beta$ . After an incubation period of 2 hours, the plate was washed three times in wash buffer and 200 $\mu$ l of an enzyme-linked polyclonal antibody to IL-1 $\beta$  (Human IL-1 $\beta$  conjugate) was added to the wells for 1 hour. The wells were then aspirated and washed three times with wash buffer and a substrate solution added for 20 minutes resulting in colouration of the wells proportionate the amount of IL-1 $\beta$  present in the supernatant and standards. Stop solution was then added to terminate the reaction and the optical density of each well was measured using a microplate reader set at a wavelength of 450 nm with correction to 570 nm.

### **2.6.2 M-CSF**

M-CSF was measured using a quantitative sandwich ELISA. The assay was undertaken according to the manufacturer's protocol (R&D Human M-CSF Quantikine ELISA kit, DMC00B). The assay follows the same steps described above for IL-1 $\beta$  with an initial incubation period of 2 hours followed by washing and the addition of the M-CSF conjugate for 2 further hours.

## **2.7 Apoptosis assays**

Positively selected monocytes ( $5 \times 10^5/\text{ml}$ ) suspended in media (X-vivo and 10% autologous serum) were plated in triplicate into 24 well plates (1ml per well) and incubated at  $37^\circ\text{C}$  for 24 hours, 72 hours or 5 days. At each of the time points, cells were harvested by placing plates on ice for 20 minutes followed by gentle scraping and suction using a Pasteur pipette. Cells were collected into a mini-falcon tube, centrifuged and transferred to a 96 well plate. Cells were then washed once in PBS, followed by binding buffer (eBioscience BMS500BB) diluted 1 in 10 in distilled water, and then incubated with  $5\mu\text{l}$  Annexin V (FITC-conjugated, eBioscience BMS500FI-100) in  $100\mu\text{l}$  diluted binding buffer for 10 minutes in the dark, at room temperature. Cells were washed again in binding buffer, re-suspended in  $200\mu\text{l}$  of binding buffer and stained with 7-AAD. Samples were then transferred on ice for immediate acquisition on the LSRII flow cytometer.

For assays looking at the phenotype of cells undergoing apoptosis, the M1 marker CD64 (BV421, Biolegend) and M2 marker CD163 (APC-Cy7, Biolegend) were selected. Cells were harvested as described above and transferred onto 96 well plates where they were initially immunostained with  $2\mu\text{l}$  of CD64 and  $2\mu\text{l}$  CD163 and incubated at  $4^\circ\text{C}$  for 20 minutes in  $100\mu\text{l}$  FACS buffer. Following washing in FACS buffer and PBS, the above protocol was followed.

## **2.8 Neutrophil efferocytosis assay**

### **2.8.1 Isolation of neutrophils**

Neutrophils were isolated from whole blood using the MACSxpress isolation kit (Miltenyi Biotec 130-104-434). The protocol is detailed in section 7.3.4.

### **2.8.2 Preparation of MDMs**

Monocytes were cultured in X-vivo with 10% autologous serum as per previous experiments and  $1.5 \times 10^6$  cells were plated into 12 well culture plates (Corning 3613). On day 7 cells were harvested into mini-falcon tubes and washed in PBS. The cell tracer

Violet Proliferation Dye (VPD, Molecular probes C34557) was used at a concentration of 1 $\mu$ M to label cells (section 7.3.6 for details).

### **2.8.3 Efferocytosis experiment**

Aged neutrophils (between 18-20 hours' post venesection) were added to MDMs at a ratio of 1:3. Cells were incubated at 37°C for 2 hours then fixed with Stabilising Fixative. Cells were acquired on the LSRII. Cell populations positive for both tracer dyes were taken to be indicative of neutrophil efferocytosis by MDMs (section 7.3.7).

## **2.9 RNA extraction**

Positively selected monocytes were isolated, quantified and centrifuged to remove the supernatant. Monocytes were re-suspended in RLT to aid cell disruption and passed through a QIAshredder (Qiagen 79654) to homogenise the cellular material. The lysate was frozen at -80°C for later RNA extraction. A monocyte aliquot was taken after positive selection to test the purity of the isolated population.

RNA extraction was undertaken using the RNeasy Mini Kit (Qiagen 74104). Briefly, the cell lysate was thawed and an equal volume of 70% ethanol was added. The solution was placed into an RNeasy spin column with a collection tube in place and centrifuged at 10,000rpm for 15 seconds. The flow-through was discarded and 700 $\mu$ l of RW1 buffer was added to the spin column and then centrifuged again. The flow-through was again discarded and 500 $\mu$ l of RPE buffer added to the column and the sample centrifuged at 10,000rpm for 15 seconds. This step was repeated with centrifugation for 2 minutes. The spin column was then placed in a new collection tube and 30 $\mu$ l of RNase-free water added directly to the spin column membrane and centrifuged for 1 minute at 10,000rpm to elute the RNA. Aliquots were removed to assess RNA integrity using nanodrop and Agilent technology and the remainder of the sample frozen at -80°C for qPCR.

## 2.10 Quantitative PCR (qPCR)

Complementary DNA (cDNA) was synthesised from RNA using High Capacity cDNA RT Kit (Applied Biosystems, Cat 4368813). The reverse transcription (RT) master mix was prepared on ice using the components tabulated below (Table 2-4).

Component in RT Master Mix	Volume per sample (µl)
10X RT Buffer	2
25X dNTP Mix (100mM)	0.8
10X RT Random Primers	2
MultiScribe™ Reverse Transcriptase	1
Total volume	5.8

**Table 2-4. The components and quantities of reagents used in the Reverse Transcriptase (RT) master mix for each RNA sample.**

1µg of RNA was diluted with 14.2µl of RNase-free water in an Eppendorf tube. 5.8µl of RT master mix was then added and the sample centrifuged briefly to spin down contents. Tubes were then transferred to a thermal cycler where they were incubated at 25°C for 10 minutes, 37°C for 120 minutes and 85°C for 5 minutes. Samples were removed and placed on ice for subsequent qPCR.

cDNA samples were diluted to a concentration of 2ng/µl using nuclease-free water. 5µl cDNA was transferred to a 384 well plate and samples were run in duplicate. Into each well, 5µl of 2X Fast SYBR® Green Master Mix (Applied Biosystems, cat no 4385616) and of 1µl of primer (5µM) were added. The plate was sealed and centrifuged at 1500rpm for 4 minutes. The amplification reactions were performed in a 7500 Fast Real-Time PCR system (Applied Biosystems). Fast mode was selected which consisted of a cycle on hold for 20 seconds at 95°C, then 40 cycles for 3 seconds at 95°C and finally 60°C for 30 seconds. The delta-delta C<sub>t</sub> method ( $2^{-\Delta\Delta C_t}$ ) was used to determine the relative expression of genes normalised to three endogenous controls; β-actin, cyclophilin and β2-microglobulin. Details of genes and primer sequences used in experiments are documented in Tables 2-5 to 2-9.

Gene	Accession number	Forward primer	Reverse primer	Amplicon length	Protein Transcript	Design / Reference
<b>TGFβ1</b>	NM_000660.5	CAATTCCTGGCGAT ACCTCAG	GCACAACCTCCGG TGACATCAA	86	Transforming growth factor, beta 1	PrimerBank ID: 260655621c3
<b>IL-10</b>	NM_000572	TACGGCGCTGT CATCGATT	GGCTTTGTAGATG CCTTCTCTTG	103	Interleukin-10 (IL-10)	Roche Online
<b>CD206</b>	NM_002438.3	GGGTTGCTATCACT CTCTATGC	TTTCTTGTCTGTT GCCGTAGTT	126	CD206, Mannose Receptor	PrimerBank ID: 145312260c2
<b>Cd200R1</b>	NM_138806	GACCAGAGAGGGT CTCACCA	TTGAAGCGGCCA CTAAGAAG	164	CD200 receptor 1	Roche Online
<b>COX-2</b>	NM_000963	ATGCTGACTATGGC TACAAAAGC	TCGGGCAATCAT CAGGCAC	90	Cyclooxygenase-2 (COX-2)	Roche Online
<b>TGM2</b>	NM_004613	GCCACTTCATTTTGC TCTTCAA	TCCTTCCGAGT CCAGGTACA	67	Transglutaminase 2 (TGM2)	Roche Online
<b>CD163</b>	NM_004244.5 + V2	GCGGGAGAGTGGGA AGTGAAAG	GTTACAATCACA GAGACCGCT	89	High affinity scavenger receptor for the hemoglobin-haptoglobin complex	PrimerBank ID: 344179109c2
<b>C1QA</b>	NM_015991.2 V1-2	GCATCCAGTTGGAG TTGACA	ACAGAGCACCAG CCATCC	71	Complement component 1, q subcomponent, A chain	Roche Online
<b>DSIPI</b>	V 1-5	GTTTCCAGGTAAG TTAACAATTGA	CGCCCCTACTTTT CCAATC	73	TSC22 domain family member 3, TSC22D3	Roche Online
<b>THBS1</b>	NM_003246.2	CAATGCCACAGTTC CTGATG	TGGAGACCAGCC ATCGTC	76	Thrombospondin 1	Roche Online
<b>TNFα</b>	NM_000594	GGCCAAGCCCTGGT ATGAG	TAGTCGGGCCGA TTGATCTC	92	Tumour necrosis Factor alpha (TNFα)	Roche Online
<b>IL-6</b>	NM_000600.3	CCTGAACCTTCCAA AGATGGC	TTCACCAGGCAA GTCTCCCTCA	75	Interleukin 6 (interferon, beta 2)	Primer Bank ID: 224831235c2
<b>CXCL10</b>	NM_001565	TCCACGTGTTGAGA TCATTGC	TCTTGATGGCCTT CGATTCTG	79	Chemokine (C-X-C motif) ligand 10	Roche Online
<b>GBP1</b>	NM_002053.2	CCAGTGCTCGTGAA CTAAGGA	TGTCATGTGGATC TCTGATGC	76	Guanylate binding protein 1	Roche Online
<b>VEGF-A</b>	All 10 variants	CCAGGAAAGACTGA TACAGAACG	TCAGGTTTCTGG ATTAAGGACTG	96	Vascular endothelial growth factor A (VEGF-A)	Roche Online
<b>CCR2</b>	NM_001123041 .2	CCACATCTCGTTCT CGGTTTATC	CAGGGAGCACCG TAATCATAATC	88	C-C motif chemokine receptor 2	Roche Online
<b>CD14</b>	NM_000591.3 V2-4	ACGCCAGAACCTTG TGAGC	GCATGGATCTCC ACCTCTACTG	122	CD14, co-receptor for bacterial LPS	PrimerBank ID: 291575162c1
<b>IL1R2</b>	NM_004633.3	CACATAGAGAGCGC CTACCC	GGCACTTCAATGT AGTTCTCATTATT	89	Interleukin 1, receptor type 2	Roche Online
<b>IDO1</b>	NM_002164	GCCAGCTTCGAGAA AGAGTTG	ATCCCAGAACTAG ACGTGCAA	96	Indoleamine 2,3-dioxygenase 1 (IDO1)	Roche Online
<b>FGL2</b>	NM_006682.2	GCTTCTTTTGCCTAT TGCGT	TGGATGGCAAAT GTTCAAAG	110	fibrinogen like 2	Roche Online

**Table 2-5. Details of genes and primer sequences used for the characterisation of monocytes (chapter 3).**

Gene	Accession number	Forward primer	Reverse primer	Amplicon length	Protein Transcript	Design / Reference
<i>TNF<math>\alpha</math></i>	NM_000594	GGCCAAGCCCTGG TATGAG	TAGTCGGGCCGA TTGATCTC	92	Tumour necrosis Factor alpha (TNF $\alpha$ )	Roche Online
<i>IL-1<math>\beta</math></i>	NM_000576	TTCGACACATGGGA TAACGAGG	TTTTTGCTGTGA GTCCCGGAG	84	Interleukin-1 beta (IL-1 $\beta$ )	PrimerBank ID:27894305c3
<i>IL-6</i>	NM_000600.3	CCTGAACCTTCCAA AGATGGC	TTCACCAGGCCAA GTCTCCTCA	75	Interleukin-6 (IL-6)	Roche Online
<i>COX-2</i>	NM_000963	ATGCTGACTATGGC TACAAAAGC	TCGGGCAATCAT CAGGCAC	90	Cyclooxygenase-2 (COX-2)	Roche Online
<i>CD64</i>	NM_000566.3	AGCTGTGAAACAAA GTTGCTCT	GGTCTTGCTGCC CATGTAGA	75	CD64- Fc-Gamma Receptor I A1	Primer Bank ID: 31334a1
<i>HLA-DR</i>	NM_019111.4	AGTCCCTGTGCTAG GATTTTTCA	ACATAAACTCGC CTGATTGGTC	131	major histocompatibility complex, class II, DR alpha	Primer Bank ID: 301171411c1
<i>STAT1</i>	NM_007315.3 Va&b	CGGCTGAATTCGG CACCT	CAGTAACGATGA GAGGACCTT	81	Signal Transducer And Activator Of Transcription 1 (STAT1)	PrimerBank ID: 189458859c3
<i>IRF5</i>	NM_00109863 0	GGGCTTCAATGGG TCAACG	GCCTTCGGTGTA TTTCCTCG	138	Interferon Regulatory Factor 5 (IRF5)	PrimerBank ID: 148833495c1
<i>IDO1</i>	NM_002164	GCCAGCTTCGAGA AAGAGTTG	ATCCCAGAACTA GACGTGCAA	96	indoleamine 2,3-dioxygenase 1 (IDO1)	Roche Online
<i>VEGF-A</i>	All 10 variants	CCAGGAAAGACTG ATACAGAACG	TCAGGTTTCTGG ATTAAGGACTG	96	Vascular Endothelial Growth Factor (VEGF-A)	Roche Online
<i>IGF-1</i>	NM_001111283 .1	TGTGGAGACAGGG GCTTTTA	ATCCACGATGCC TGTCTGA	84	Insulin-like Growth Factor-1 (IGF-1)	Roche Online
<i>AREG</i>	NM_001657.3	GTGGTGCTGTCCG TCTTGATA	CCCCAGAAAATG GTTCCACGCT	97	AREG/ amphiregulin	PrimerBank ID: 22035683c1
<i>TGF<math>\beta</math></i>	NM_000660.5	CAATTCCTGGCGAT ACCTCAG	GCACAACCTCCGG TGACATCAA	86	Transforming Growth Factor beta (TGF $\beta$ )	Roche Online
<i>CCL18</i>	NM_002988.2	GCTCTGCTGCCTC GTCTATAACC	GGGCTGGTTTCA GAATAGTCAACT	72	Chemokine CCL18	High CCL18/PARC Expression in Articular Cartilage
<i>CCL22</i>	NM_002990.4	ATTACGTCGGTTAC CGTCTGC	TCCCTGAAGGTT AGCAACACC	100	Chemokine CCL22	PrimerBank ID: 300360575c2
<i>CD206</i>	NM_002438.3	GGGTTGCTATCACT CTCTATGC	TTTCTTGCTGTT GCCGTAGTT	126	CD206, Mannose receptor	PrimerBank ID: 145312260c2
<i>CD209</i>	NM_005076.4 V1-8	AATGGCTGGAACG ACGACAAA	CAGGAGGCTGC GGACTTTTT	68	CD209 (DC Sign)	PrimerBank ID: 15281077a1
<i>IL-4R</i>	NM_000418.3 V1.3.4.5	CACCTATGCAGTCA ACATTTGGA	GATGCGGAGGGA GGGTTCTA	88	IL-4 Receptor (IL-4R)	PrimerBank ID: 56788410c3
<i>STAT3</i>	NM_139276.2 V1-3	CAGCAGCTTGACA CACGGTA	AAACACCAAAGT GGCATGTGA	150	Signal Transducer And Activator Of Transcription 3 (STAT3)	PrimerBank ID: 47080104c1
<i>STAT6</i>	NM_00117807 8.1 V1-5	CGAGTAGGGGAGA TCCACCTT	GCAGGAGTTTCT ATCAAGCTGTG	92	Signal Transducer And Activator Of Transcription 6 (STAT6)	PrimerBank ID: 296010867c2
<i>IRF4</i>	NM_002460 V1 & 2	ACCCGGAAATCCC GTACCA	GGCAACCATTTT CACAAGCTG	84	Interferon Regulatory Factor 4 (IRF4)	PrimerBank ID: 305410879c3
<i>PPAR<math>\gamma</math></i>	NM_138712.3 V1-5	ACCAAAGTGCAATC AAAGTGGA	ATGAGGGAGTTG GAAGGCTCT	100	Peroxisome Proliferator-activated Receptor-gamma (PPAR $\gamma$ )	PrimerBank ID: 116284372c2
<i>LGALS3</i>	NM_002306.3 V1 & 3	GTGAAGCCCAATG CAAACAGA	AGCGTGGGTTAA AGTGAAGG	76	Galectin-3 (LGALS3)	PrimerBank ID: 294345474c2
<i>INHA</i>	NM_002192.3	AGACAGCTCTTACC ACATGATACAA	TCTCCTCTTCCAG CAAATCTCTTT	78	Inhibin alpha subunit (INHA)	Roche Online
<i>IL-10</i>	NM_000572	TACGGCGCTGTCAT CGATT	GGCTTTGTAGAT GCCTTCTCTTG	103	Interleukin -10 (IL-10)	Roche Online



Gene	Accession number	Forward primer	Reverse primer	Amplicon length	Protein Transcript	Design / Reference
<b>CD163</b>	NM_004244.5 + V2	GCGGGAGAGTGGAAGTGAAG	GTTACAAATCACAGAGACCGCT	89	CD163 - High affinity scavenger receptor for the hemoglobin-haptoglobin complex	Roche Online
<b>CD273/PDL-2</b>	NM_025239.3	ACCCTGGAATGCAACTTTGAC	AAGTGGCTCTTTCACGGTGTG	109	CD273/Programmed cell death ligand 2 (PDL2)	PrimerBank ID: 190014604c2
<b>CD274/PDL-1</b>	NM_014143.3 V1&4	TGGCATTGCTGAA CGCATT	TGCAGCCAGGTC TAATTGTTTT	120	CD274/Programmed cell death ligand 1 (PDL1)	PrimerBank ID: 292658763c1
<b>IL-10R<math>\beta</math></b>	NM_000628.4	ATGAGCATTACAGAC TGGGTAAAC	TTTTAGGGGCTAA GAAACGCAT	123	IL-10 Receptor beta (IL-10R $\beta$ )	PrimerBank ID: 24430214c2
<b>GR/NR3C1</b>	NM_000176.2 V1-8	ACAGCATCCCTTTC TCAACAG	AGATCCTTGGCA CCTATTCCAAT	99	Glucocorticoid Receptor (GR)/Nuclear Receptor Subfamily 3 Group C Member 1 (NR3C1)	PrimerBank ID: 324021682c1
<b>ATF3</b>	NM_001674.3 V1,3-5,7-8	CCTCTGCGCTGGA ATCAGTC	TTCTTTCTCGTCG CCTCTTTTT	111	Activating Transcription Factor 3 (ATF3)	PrimerBank ID: 346223459c1
<b>CD14</b>	NM_000591.3 + V2-4	ACGCCAGAACCTT GTGAGC	GCATGGATCTCC ACCTCTACTG	122	CD14, co-receptor for bacterial LPS	PrimerBank ID: 291575162c1
<b>CSF1-R</b>	NM_005211.3 V1, 2 & 4	TCCAAAACACGGG GACCTATC	CGGGCAGGGTCT TTGACATA	91	Colony stimulating Factor-1 Receptor (CSF1-R)	PrimerBank ID: 195947380c2

**Table 2-6. Details of genes and primer sequences used for the characterisation of MDMs (chapter 5).**

Gene	Accession number	Forward primer	Reverse primer	Amplicon length	Protein Transcript	Design / Reference
<b>FGF2</b>	NM_002006.4	AGAAGAGCGACCC TCACATCA	CGGTTAGCACACA CTCCTTTG	82	FGF2 - Fibroblast growth factor 2	PrimerBank ID: 153285460c1
<b>FGF7</b>	NM_002009	TCCTGCCAACTTTG CTCTACA	CAGGGCTGGAACA GTTACAT	123	FGF7 - Fibroblast growth factor 7	PrimerBank ID: 219842354c1
<b>PDGF-A</b>	NM_002607.5	GCAAGACCAGGAC GGTCATTT	GGCACTTGACACT GCTCGT	135	PDGF $\alpha$ - Platelet derived growth factor alpha	PrimerBank ID: 197333758c1
<b>VEGF-A</b>	All 10 variants	CCAGGAAAGACTG ATACAGAACG	TCAGGTTTCTGGAT TAAGGACTG	96	VEGF $\alpha$ - Vascular endothelial growth factor alpha	Roche Online
<b>CTGF</b>	NM_001901.2	AAAAGTGCATCCGT ACTCCCA	CCGTCGGTACATAC TCCACAG	109	CTGF - Connective tissue growth factor	PrimerBank ID: 9898635c3
<b>HGF</b>	NM_001010931	GCTATCGGGTAAA GACCTACA	CGTAGCGTACCTCT GGATTGC	99	HGF - Hepatocyte growth factor	PrimerBank ID: 58533162c1
<b>IGF-1</b>	NM_001111283.1	TGTGGAGACAGGG GCTTTTA	ATCCAGCATGCTG TCTGA	84	IGF-1 - Insulin-like growth factor 1 (somatomedin C)	Roche Online
<b>IL-6</b>	NM_000600.3	CCTGAACCTTCCAA AGATGGC	TTCACCAGGCAAG TCTCTCA	75	IL-6 - Interleukin 6 (interferon, beta 2)	Primer Bank ID: 224831235c2
<b>MCP-1 (CCL2)</b>	NM_002982	TCAAAGTGAAGCTC GCACTCT	GTGACTGGGGCAT TGATTG	129	MCP-1 (CCL2) - Monocyte chemoattractant protein-1	Roche design
<b>TGF<math>\beta</math>1</b>	NM_000660.5	CAATTCCTGGCGAT ACCTCAG	GCACAACCTCCGGT GACATCAA	86	TGF $\beta$ 1 - Transforming growth factor, beta 1	PrimerBank ID: 260655621c3
<b>COL1A1</b>	NM_000088.3	GTGCGATGACGTG ATCTGTGA	CGGTGGTTTCTTG GTCGGT	119	Collagen Type I alpha 1 chain	PrimerBank ID: 110349771c2
<b>COL3A1</b>	NM_000090.3	TTGAAGGAGGATG TTCCCATCT	ACAGACACATATTT GGCATGGTT	83	Collagen Type III alpha 1 chain	PrimerBank ID: 110224482c2
<b>COL5A1</b>	NM_000093.4	TACCCTGCGTCTGC ATTTCC	GCTCGTTGTAGATG GAGACCA	97	Collagen Type V alpha 1 chain	PrimerBank ID: 89276750c2
<b>COL6A1</b>	NM_001848.2	ACACCGACTGCGCT ATCAAG	CGGTACCACAATC AGTACTT	90	Collagen Type VI alpha 1 chain	PrimerBank ID: 87196338c2
<b>FIBRONECTIN1</b>	NM_212482.2	AGGAAGCCGAGGT TTTAACTG	AGGACGCTCATAA GTGTCACC	106	Fibronectin	PrimerBank ID: 47132556c2
<b>MMP2</b>	NM_004530	TACAGGATCATTGG CTACACACC	GGTCACATCGCTCC AGACT	90	MMP2 - Matrix metalloproteinase 2 (Gelatinase A)	PrimerBank ID: 189217851c1
<b>MMP9</b>	NM_004994	TGTACCGCTATGGT TACACTCG	GGCAGGGACAGTT GCTTCT	97	MMP9 - Matrix metalloproteinase 9 (Gelatinase B)	PrimerBank ID: 74272286c1
<b>MMP11</b>	NM_005940.4	CCGCAACCGACAG AAGAGG	ATCGCTCCATACCT TTAGGGC	145	MMP11 - Matrix metalloproteinase 11	PrimerBank ID: 58331147c1
<b>PAI-1</b>	NM_000602.4	ACCGCAACGTGGTT TTCTCA	TTGAATCCCATAGC TGCTTGAAT	109	PAI-1 - Plasminogen activator inhibitor type 1	PrimerBank ID: 383286746c1
<b>UPA</b>	NM_001145031.2	TTGCTCACCACAAC GACATT	GGCAGGCAGATGG TCTGTAT	94	Urokinase-type plasminogen activator	Roche design
<b>TGM2</b>	NM_004613	GCCACTTCATTTTG CTCTTCAA	TCCTCTCCGAGTC CAGGTACA	67	TGM2 - Transglutaminase 2	Roche Online
<b>TIMP1</b>	NM_003254	CTTCTGCAATTCGG ACCTCGT	ACGCTGGTATAAGG TGGTCTG	79	Tissue inhibitor of metalloproteinase 1	PrimerBank ID: 73858576c1
<b>S100A4</b>	NM_002961	GATGAGCAACTTG GACAGCAA	CTGGGCTGCTTATC TGGGAAG	123	S100 calcium-binding protein A4	PrimerBank ID: 4506765a1
<b>HAS2</b>	NM_005328.2	TTATTACCTCAATTT TGGAACTGC	TCAGGATACATAGA AACCTCTCACAA	123	Hyaluronan synthase 2	Roche Design
<b>CD44</b>	20 variants	CTGCCGCTTTGCAG GTGTA	CATTGTGGGCAAG GTGCTATT	109	CD44 - Cognate receptor for hyaluronan	PrimerBank ID: 48255942c1

**Table 2-7. Details of genes and primer sequences used for the characterisation of primary human lung fibroblasts (ELF) following transwell co-culture with MDMs (chapter 6).**

Gene	Accession number	Forward primer	Reverse primer	Amplicon length	Protein Transcript	Design / Reference
<b>MSR1</b>	NM_138715.2 V1-3	GCAGTGGGATCAC TTTCACAA	AGCTGTCATTGAG CGAGCATC	85	MSR-1 - Macrophage scavenger receptor 1	Primer Bank ID: 109148505c1
<b>MARCO</b>	NM_006770.3	TGTCCGTCAGGAT TGTCGG	CTGTCATCGCAA ATTGTCCC	86	MARCO - Macrophage receptor with collagenous structure	Primer Bank ID: 56237031c3
<b>CD36</b>	NM_001001548.2 V1-5	CTTTGGCTTAATGA GACTGGGAC	GCAACAAACATCA CCACACCA	134	CD36/Thrombospondin receptor	Primer Bank ID: 188536061c3
<b>MERKT</b>	NM_006343	GTGCAGCGTTCAG ACAATGG	TCGATGTAGATGG GATCAGACAC	83	MerTK - c-mer proto-oncogene tyrosine kinase	PrimerBank ID: 66932917c3

**Table 2-8. Details of phagocytic genes and primer sequences (chapter 7).**

Gene	Accession number	Forward primer	Reverse primer	Amplicon length	Protein Transcript	Design / Reference
<b>CYCLOPHILIN-A</b>	NM_021130.3	ATGCTGGACCC AACACAAAT	TCTTTCACCTTTG CCAAACACC	97	Cyclophilin A	Roche Online
<b>BETA-2-MICROGLOBULIN</b>	NM_004048	TGACTTTGTCA CAGCCCAAGAT A	AATGCGGCATCT TCAAACCT	78	Beta-2-Microglobulin	PrimerBank ID: 37704380c1
<b>BETA-ACTIN</b>	NM_001101	CCTGGCACCCA GCACAAT	GCCGATCCACA CGGAGTACT	69	Beta-Actin	PrimerBank ID: 4501885a1

**Table 2-9. Details of the three housekeeping genes used in the analysis of gene expression as endogenous controls.**

## 2.11 Fibroblast studies

### 2.11.1 Culturing primary fibroblasts

Primary human lung fibroblasts were obtained from surgical pneumonectomy explants. Optimisation experiments were undertaken to ensure that fibroblasts from different donors had similar characteristics and responses to stimulation. Subsequently, fibroblasts from a single source were selected for use in all assays to ensure consistency and enable comparison. Fibroblasts between passage 2 – 7 were used for assays and cryopreserved in liquid nitrogen when not in use. Fibroblasts were cultured in D10 (Table 2-1) in sterile T75 flasks (Corning 430725U). Media was changed every 3 days and cells were split into 3 flasks every 3-5 days using trypsin-EDTA to detach cells (Gibco 25300054).

### 2.11.2 Co-culture and transwell experiments

Fibroblasts were harvested using trypsin-EDTA and then washed in D10 to neutralise trypsin activity. To identify fibroblasts and study relative proliferative capacity, cells were labelled with the cell tracer dye VPD (section 6.3.6 for details). This was undertaken by washing fibroblasts in PBS to remove traces of serum and re-suspending cells within a mini-falcon tube at a concentration of  $10^6$ /ml of PBS. VPD ( $1\mu\text{M}$ ) was added and fibroblasts incubated at  $37^\circ\text{C}$  in a water bath for 10 minutes. The tracer dye was then removed by washing cells twice in 10ml of D10. Cells were re-counted and suspended in fresh media consisting of DMEM containing 2.5% FCS, 2% Pen-Strep and 2% L-Glutamine (D2.5).  $5 \times 10^4$  of fibroblasts in 1ml of media were seeded onto 12-well plates and left to adhere overnight.

Co-culture experiments were undertaken by adding MDMs ( $2 \times 10^5$  in  $500\mu\text{l}$  media) directly to the wells containing fibroblasts. To study the effect of secreted mediators on fibroblast characteristics, indirect co-culture assays were performed using a  $0.4\ \mu\text{m}$  transwell insert to separate cell populations (Corning EK-680175). The transwell was placed into the well above the fibroblast layer and  $500\mu\text{l}$  of media containing  $2 \times 10^5$  MDMs added to the upper chamber. Plates were cultured at  $37^\circ\text{C}$ , 5%  $\text{CO}_2$  for 72 hours.

Following incubation, cells were harvested with trypsin-EDTA, washed in D10 then surface stained with HLA-DR to identify MDMs. Cells were then fixed and permeabilised for ICS staining with  $\alpha\text{SMA}$ . For transwell experiments, the insert was discarded and fibroblasts were stained for  $\alpha\text{SMA}$  without initial surface staining. Cells were analysed via flow cytometry on the LSRII using a standardised template.

For studies looking at the effect of MDMs on RNA expression in fibroblasts, transwell inserts were used containing MDMs within the upper chamber. After 72 hours, the inserts were discarded and the media removed from the wells. Fibroblasts were processed by adding  $500\mu\text{l}$  RLT (Qiagen 79216) to the well for 5 minutes. The cellular solution was then pipetted into Eppendorf tubes and frozen at  $-80^\circ\text{C}$  for later RNA extraction.

### 2.11.3 Immunofluorescence

$5 \times 10^3$  fibroblasts were seeded on to a Perkin-Elmer Cell Carrier black clear-bottom 96 well plate and allowed to attach overnight at  $37^\circ\text{C}$  5%  $\text{CO}_2$ .  $5 \times 10^4$  MDMs or monocytes were then added to the wells and incubated for 72 hours. As a positive control,  $10\text{ng/ml}$

human TGF $\beta$  (hTGF $\beta$ , Miltenyi Biotec 130-095-067) was added to wells containing fibroblasts without MDMs. On day 3, Media was aspirated from the wells, cells washed with PBS and fixed with 4% formaldehyde for 20 minutes at room temperature. Cells were then permeabilised with 0.2% TritonX-100 for 10 minutes, blocked with 3% FCS for 60 minutes and incubated with  $\alpha$ SMA or an isotype control overnight at 4C. Wells were washed 3 times in PBS and a secondary antibody applied (Biolegend, Alexa 488 anti-mouse, 1:500) for 1 hour at room temperature. Cells were then counterstained with DAPI and images acquired on a Zeiss Axiovert S100 microscope.

## **2.12 Epithelial-mesenchymal transition/mesenchymal-epithelial transition (EMT/MET) studies**

Low-passage (passage 4-6) A549 cells (ATCC® CCL-185™) were used. Epithelial and mesenchymal markers were measured at baseline via flow cytometry to ensure that there was no evidence of EMT prior to co-culture and transwell assays. A549 cells were labelled with the cell tracer VPD, as described previously, and aliquots were frozen down and thawed for each assay.

A549 cells were seeded onto 12 well plates ( $1.25 \times 10^4$  for EMT studies,  $2.5 \times 10^4$  for MET studies) in R10. EMT was induced in cells using 5ng/ml of hTGF $\beta_1$  and cells were subsequently incubated for 72 hours at 37°C. Cells were then visualised under the microscope to assess degree of confluency and morphological appearances. Media was then replaced with RPMI containing a lower concentration of FCS (2.5%).  $2 \times 10^5$  MDMs were added either directly to the well or onto the upper chamber of a 0.4  $\mu$ m transwell. Plates were incubated for 6 days (this time period was determined following optimisation experiments), with a partial media change (20% removed, 40% added) on day 3.

Following incubation, transwell inserts were discarded and cells harvested using trypsin-EDTA. Cells were surface stained with mAbs to HLA-DR (co-cultures only), E-cadherin and N-cadherin, and then fixed. ICS for fibronectin, SMA and vimentin was then undertaken and results obtained via flow cytometry.

## 2.13 Cryopreservation and thawing of samples

A549 cells and fibroblasts for cryopreservation were centrifuged at 1500rpm for 8 minutes to obtain a cellular pellet. The supernatant was then removed and the cells were resuspended at  $1-2 \times 10^6$ /ml in freezing media [10% dimethyl sulphoxide (DMSO, Sigma D8418-100ML) in FCS]. Cells were frozen in 1ml aliquots in labelled cryovials (Alpha laboratories LW3332) and transferred in a freezing container (CoolCell®SV2, Biocision cat no BCS-172) to a -80°C freezer. For long-term storage, cells were transferred on dry ice to liquid nitrogen.

Cells were thawed by placing cryovials in a 37°C water bath until the freezing media had almost melted (around 1 minute). Cells were then pipetted drop by drop from the cryovial into a mini-falcon tube containing 10ml of R10 (for A549 cells) or D10 (for fibroblasts) prewarmed to 37°C. Tubes were centrifuged at 1500rpm for 8 minutes and the supernatant discarded. Cells were then resuspended in 10ml of R10/D10 and centrifuged once again at 1500rpm for 8 minutes to remove traces of DMSO. Cells were then resuspended in media, counted and the concentration determined for planned experiments.

## 2.14 Statistical analysis

GraphPad Prism version 7.00 for Windows (La Jolla California USA, [www.graphpad.com](http://www.graphpad.com)) was used for all statistical analysis. D'Agostino–Pearson omnibus normality test was used to determine the distribution of data. For comparison of data sets that showed normal distribution, the Student t-test was used. Mann-Whitney test was applied for data that was not normally distributed. To compare multiple data sets that were normally distributed, one-way ANOVA with Tukey's correction for multiple comparisons was used. Multiple data sets that were not normally distributed were analysed using Kruskal-Wallis test with Dunn's correction for multiple comparisons. Paired data sets were analysed using the paired t-test or Wilcoxon test when data did not show a normal distribution. Data correlations were undertaken using Pearson test and to determine whether systemic deviation existed in the scoring of CT scans by independent radiology assessors, Bland-Altman plots were used. A p-value of less than 0.05 was considered significant. For work involving patient samples, error bars on graphs represent standard deviation (SD). For studies examining cell lines and cell explants, error bars represent standard error of the mean (SEM), unless stated otherwise.

## **3 Monocyte phenotype in stable and acute exacerbations of IPF**

### **3.1 Introduction**

In recent years, there has been a growing interest into the potential role of monocytes in the development of particular diseases. Pathogenic processes where macrophages are noted to play a prominent role, such as in the formation of atherosclerotic plaques and inflammatory conditions such as rheumatoid arthritis (RA), have been of particular focus [169, 234, 250, 251]. Perturbations in the proportions of the traditional monocyte subsets have been demonstrated leading to hypotheses that skewing of monocyte populations may either predispose to disease or accentuate its progression. Atherosclerosis for example appears to be linked to CD16<sup>+</sup> monocytes with numbers positively correlating with traditional risk factors such as hyperlipidaemia and body mass index (BMI) [177]. In a large prospective cohort study looking at monocyte subsets in 951 patients undergoing elective angiography, investigators found that high numbers of classical (CD14<sup>+</sup>CD16<sup>-</sup>) monocytes were associated with an increased risk of myocardial infarction, stroke and cardiovascular death [173]. Non-classical monocytes have also been found to be elevated in patients with systemic lupus erythematosus (SLE) and RA, with frequency correlating with other indicators of disease activity and severity [169, 252].

Monocytes can also be defined by the relative expression of other cell surface receptors. In particular, CD64 (FCγRI), is upregulated in a number of inflammatory and autoimmune diseases. CD64 is an FC receptor that binds IgG, mediates the phagocytosis of antibody bound cells, internalises immune complexes and stimulates inflammatory cytokine production [250, 251, 253]. CD64 expression on monocytes correlated with indices of disease severity in RA as well as biochemical markers of inflammation such as the C-reactive protein (CRP) and erythrocyte sedimentation rate (ESR) in psoriatic arthritis. CD64 normalised following successful response to treatment and its role as a biomarker for disease activity has been proposed [250, 253].

Monocytes differentiated into macrophages in the presence of polarising agents result in subpopulations of cells with distinct phenotypes that have been linked to specific in vivo functions. LPS and IFNγ polarise monocyte-derived-macrophages (MDMs) to an inflammatory phenotype (referred to as 'M1') that release mediators such as TNFα, IL-6

### Chapter 3: Monocyte phenotype in stable and acute exacerbations of IPF

and IL-1 $\beta$  in response to stimulation. In contrast, cytokines such as IL-4, IL-10 and IL-13 result in macrophages with anti-inflammatory phenotypes associated with reparative and immunomodulatory activities. These are referred to as 'M2' populations which have been further subdivided to incorporate groups of cells with a range of activities (detailed in 1.3.4) [196, 197, 199, 202, 203]. Whilst in recent years this categorisation of MDMs based on defined forms of stimulation has been criticised as being poorly reflective of in vivo events, it may still have utility in enabling the identification and comparison of different cell populations [196]. Fibrosis for example is linked to 'M2' reparative macrophage activity and phenotypes associated with these cells have been defined in a number of animal and human studies [78-80, 126, 204, 227, 254, 255]. What is less well researched however is whether receptors associated with macrophage phenotypes are also present on monocytes and if so, whether they differ in health and disease.

Monocytes respond to pathogen-associated molecular patterns (PAMPs) and danger-associated molecular patterns (DAMPs) through pattern recognition receptors (PRRs) including toll-like receptors (TLRs) located on their cell surface and within endosomes. Bacterial and viral ligands stimulate TLR pathways resulting in the release of chemical mediators to aid recruitment and activation of cells to orchestrate inflammatory and reparative responses [256, 257]. Inappropriate production and sustained release of inflammatory mediators such as MCP-1, IL-6 and TNF $\alpha$ , however, can result in perpetuating tissue damage. Over-expression of cytokines TNF $\alpha$ , IL-1 $\beta$  and IL-6 led to the development of lung fibrosis in rodent models [100, 109, 121]. Interestingly, high levels of inflammatory cytokines have been demonstrated in the lung tissue and BALF of IPF patients, including TNF $\alpha$  and IL-1 $\beta$  [98]. The prevailing hypothesis that a repetitive or chronic stimulus drives a profibrotic response in IPF [64] has led some to question the role of viruses as aetiological agents [64, 73]. Alveolar epithelial cell (AEC) damage induced by pathogens that infect the respiratory tract may be a mechanism by which fibrogenic processes are mediated, and sustained activation of monocytes and macrophages in response to PAMPs may also play an important role. Alveolar macrophages taken from IPF patients exhibited enhanced IL-1 $\beta$  release in response to stimulation compared to controls indicating that macrophage populations in IPF exhibit differential responses to stimuli [98].

Surprisingly, there have been few studies looking at the role of monocytes in idiopathic pulmonary fibrosis despite significant research efforts examining polarised macrophage responses in the context of injury and repair in lung fibrosis [25, 39, 41, 240, 258]. Studies



## Chapter 3: Monocyte phenotype in stable and acute exacerbations of IPF

on alveolar macrophages in IPF patients have demonstrated high expression of the M2 markers CD163 and CD206 [25, 39], although published works on monocytes, which number only a handful, has not looked in detail at their phenotypic and polarisation characteristics [236, 259-261]. In addition, some of the data needs to be interpreted with caution. The profibrotic mediator periostin for example, was found to be increased in IPF monocytes, but the control group had only three subjects, limiting any conclusions that can be drawn [260]. Another study published in 2010 found that CD163 was increased on monocytes in patients with progressive disease but this receptor is also upregulated by steroids which are often administered to patients with deteriorating symptoms and may have been a confounding factor [236]. A wide-ranging study examining the phenotypic characteristics of monocytes from patients with IPF, including AEIPF, in comparison to age and sex matched controls, has not yet been performed.

The focus of this part of the study was to examine the immune phenotype of monocytes from IPF patients to evaluate if they differed from age-matched controls. The cytokine response of monocytes to ligands inducing bacterial and viral pathways was also investigated. In addition to traditional monocyte subsets, markers more commonly associated with polarised macrophage responses were used to determine whether monocytes from IPF patients showed an inflammatory, reparative or more activated phenotype than controls.

### 3.2 Hypothesis and Aims

I hypothesised that monocytes from patients with IPF are distinct from age-matched healthy controls and exhibit characteristics indicative of a reparative phenotype that are further enhanced during AEIPF.

To test this hypothesis, I undertook the following:

- i. Characterised monocyte subsets from IPF patients with stable disease and with acute exacerbations and compared the findings to age-matched healthy controls.
- ii. Determined the effects of representative viral and bacterial pathogen associated molecular patterns (PAMPS) on monocyte cytokine production and polarisation markers.

## Chapter 3: Monocyte phenotype in stable and acute exacerbations of IPF

- iii. Investigated the expression of genes associated with inflammatory and reparative processes in freshly isolated monocytes from IPF patients compared to healthy controls

### 3.3 Methods

#### 3.3.1 Participant samples

Samples were collected from January 2015 to February 2016 from Oxford University Hospitals NHS Trust. Patient samples were acquired during specialist Interstitial Lung Disease (ILD) clinics or during in-patient stays. Age and sex-matched healthy volunteers were recruited from orthopaedic pre-assessment clinics or from the University and screened for smoking, the presence of co-existent inflammatory conditions and lung disease. Medical history and current medications were documented.

#### 3.3.2 Isolation and preparation of peripheral blood mononuclear cells (PBMCs)

Blood samples were collected in heparinised tubes and Ficoll separation was used to extract PBMCs (section 2.3.2). Cells were then transferred to 96 well plates for immediate immunostaining of monocytes using mAbs and plated in triplicate where PBMCs were stimulated overnight with LPS, r848 or without stimulation for control purposes. Brefeldin was added after 16 hours for 4 hours and the cells were then surface stained, fixed and permeabilised to assess cytokine responses (section 2.4.1, mAb panel Table 2-2 and 2-3). Absolute monocyte counts were calculated by measuring the starting volume of blood, PBMC count following extraction and monocyte and live cell counts identified by flow cytometric analysis. The following formula was used:

$$\text{Cells/ml blood} = \frac{\text{PBMC count}}{\text{ml blood}} \times \frac{\text{monocyte number (event count)}}{\text{live cells (event count)}}$$

### 3.3.3 Flow cytometry and gating strategy

To identify monocytes within PBMCs, three cell surface receptors were used; CD14, CD15 and CD16. CD15 was included in the staining panel to enable the exclusion of low-density neutrophils remaining within PBMCs following the process of density-gradient separation, and to ensure that CD16+ cells were representative of monocyte subsets rather than neutrophils. The gating strategy to identify phenotypic markers on monocytes is demonstrated in Figure 3-1. Doublet cells and cellular debris were first excluded based on FSC-H/FSC-A and SSC/FSC appearances, respectively. Monocytes were then identified by CD14 expression. Samples stained for CD14, CD15 and CD16 only were used to establish the gating for the phenotypic marker of interest (Figure 3-1). The gates were then applied to 'test' samples containing all the phenotypic markers (Table 3-1). PBMCs that were stained immediately after isolation showed a viability of greater than 97% in optimisation studies and so the viability dye was not routinely used for fresh cells but included for all cultured samples. To measure cytokine expression, cells cultured overnight without stimulation were used to establish the gating for the cytokine of interest then applied to the stimulated samples.

To identify the traditional monocyte subsets based on expression of CD14 and CD16, the gating strategy demonstrated in Figure 3-2, was used as described in the literature [165, 262-264]. Classical monocytes were defined as CD14<sup>hi</sup> CD16<sup>neg</sup> and in cases where the FACS plots did not show clear demarcation between the classical and intermediate populations, CD16 histograms were generated to aid with the gating of the subsets. The geometric mean fluorescence intensity (MFI) was used to represent the intensity of receptor expression on each of the monocyte subsets.

### Chapter 3: Monocyte phenotype in stable and acute exacerbations of IPF

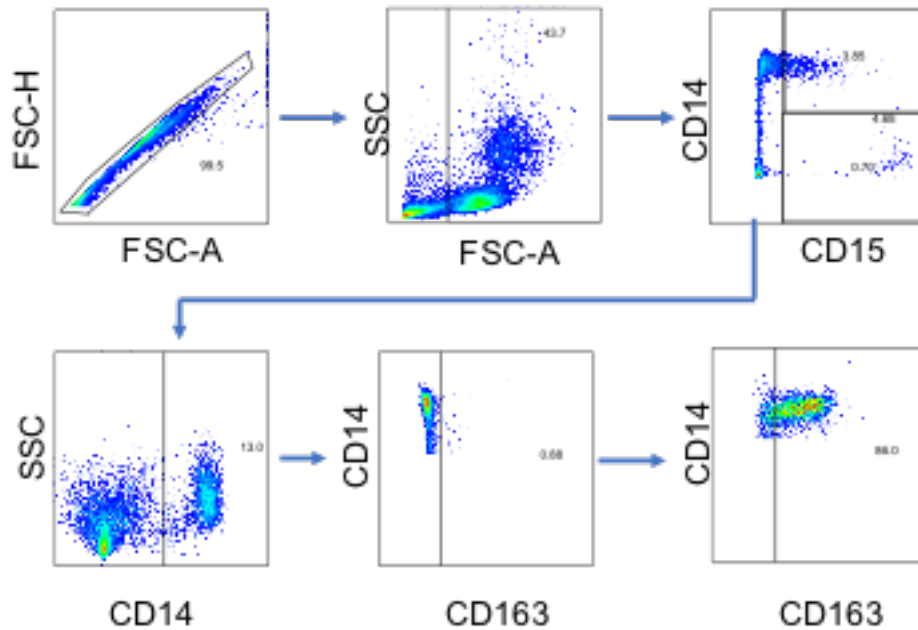


**Figure 3-1. Gating strategy to identify freshly isolated monocytes within PBMCs and their cell surface markers.**

From the top left: Singlet gate, cells (removal of cell debris), gating out of CD15 positive cells, identification of CD14 cells, gating of CD163 on CD14+ cells on a sample without CD163 staining and the gating applied to a test sample enabling the percentage CD163+ cells to be calculated.

	BV510	BV421	BV605	BV650	FITC	PerCP-Cy5.5	PE-Cy7	APC	AF700	APC-Cy7
Fresh PBMC staining	-	-	-	CD15	-	-	CD14	-	CD16	-
	-	CCR7	CD163	CD15	CD62L	CD64	CD14	CD86	CD16	CD206
20h staining following LPS and r848 stimulation	Viability	-	-	CD15	-	-	CD14	-	CD16	-
	Viability	-	CD163	CD15	IL-4	CD64	CD14	IL-10	CD16	CD206
	Viability	CCR7	CD163	CD15	MCP-1	CD64	CD14	IL-6	CD16	CD206

**Table 3-1. Phenotypic and cytokine panel used to characterise fresh and cultured monocytes.**

For each participant sample, cells were stained with CD14, CD15 and CD16 only to establish the gating of the phenotypic markers and this was then applied to 'test' samples containing all the markers of interest.

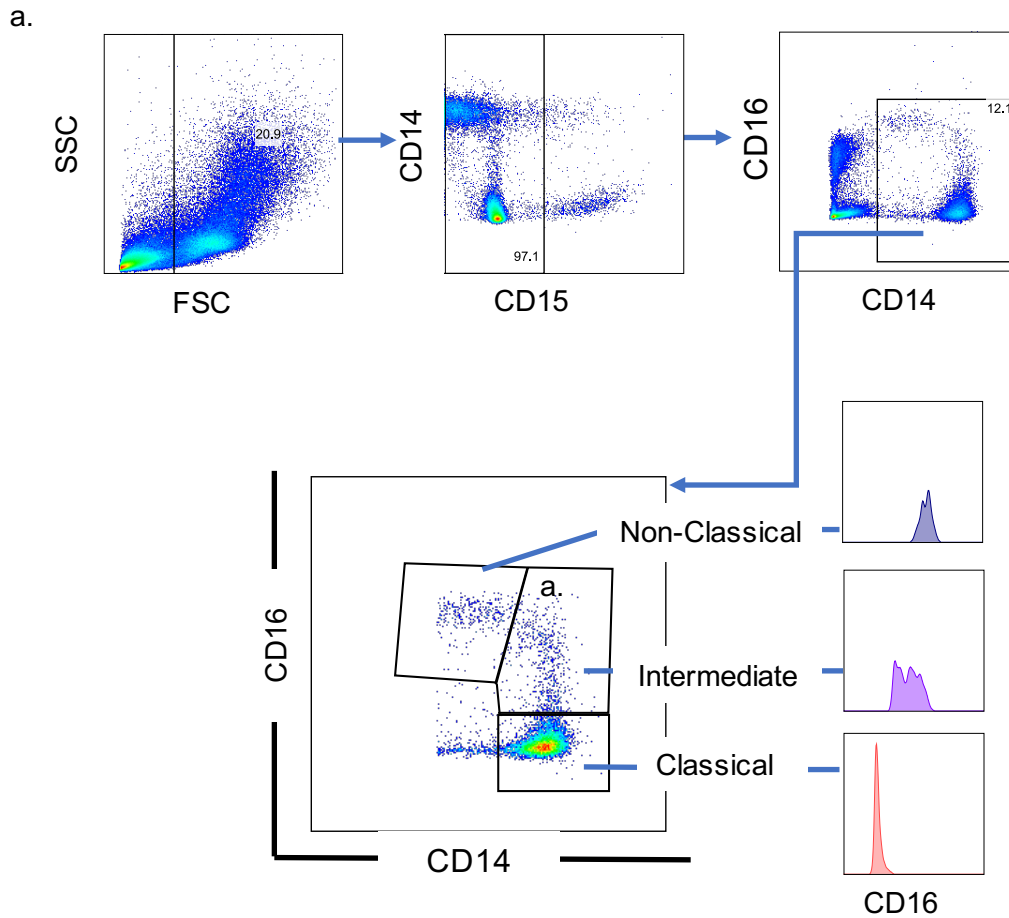


**Figure 3-2. Gating strategy to classify monocyte subsets and the proportions of each subset in IPF patients and controls.**

Classical monocytes were classified as CD14 high and CD16 negative based on FACS plots and histograms for CD16. Intermediate cells express both CD14 and CD16 whilst non-classical population were CD14 low and CD16 positive.

### 3.3.4 RNA extraction and qPCR analysis

To consolidate the monocyte phenotypic findings, RNA was extracted from CD14 positively selected monocytes (section 2.9) to ascertain if differences existed in the transcription of 20 genes recognised to play key roles in inflammatory and reparative processes [126, 196] (Table 2-5). qPCR (Section 2.10) was performed on RNA from 8 controls, 7 stable patients and 7 with AEIPF. The fold change over three housekeeping genes (*cyclophilin A*,  *$\beta$ 2-microglobulin* and  *$\beta$ -actin*) was used to determine the relative expression of the genes of interest.

## Chapter 3: Monocyte phenotype in stable and acute exacerbations of IPF

The purity of monocytes used for gene expression analysis was assessed by flow cytometry. A panel of fluorochrome-conjugated antibodies was used to identify monocytes (CD14), T cells (CD3), B cells (CD19), and neutrophils (CD15 and CD16). The percentage of monocytes after positive selection was around 99% (Table 3-2).

Group (n)	Mean age (range)	Gender (% male)	% Definite diagnosis	% on steroid treatment	% on Pirfenidone	Monocyte purity	Mean RIN (Range)
Controls (8)	67.3 (50-72)	87	N/A	0	N/A	98.6 (98.6-98.7)	9.5 (8.9-10)
Stable IPF (7)	70.8 (57-83)	100	71	0	29 (1 patient stopped 6 weeks prior)	99.2 (97.8-99.8)	10 (9.5-10)
AEIPF (7)	71.4 (52-80)	75	71	100	57	99.3 (98.6-99.8)	10 (9.7-10)

**Table 3-2. Details of controls and IPF patients from which monocyte RNA was extracted.**

The purity of positively selected monocytes was assessed via flow cytometry. RIN - RNA Integrity number (range 1-10 with 10 indicating RNA with the highest integrity).

## 3.4 Results

### 3.4.1 Patient characteristics

Patients recruited into this part of the study were representative of a typical IPF cohort [2, 12, 265]; the majority were male (81%), in their sixth to eighth decade, and with varying severities of IPF as indicated by the range of lung function parameters (Table 3-3).

The clinical details of patients with acute exacerbations are listed in Table 3-4. 50% of the patients had at least one previous admission with AEIPF within the past 12 months and were on maintenance corticosteroids (prednisolone) on admission. All patients with AEIPF had new multifocal ground glass opacification on CT scan and 40% of patients had a history consistent with possible co-existent infection (although not evident biochemically or radiologically). One patient had clinical features suggestive of possible cardiac failure complicating his presentation. The mortality from AE was similar to

### Chapter 3: Monocyte phenotype in stable and acute exacerbations of IPF

published data [14, 16, 266] at 50% within 6 months and 80% within 18 months of hospital admission.

Demographics	All patients	CPI <40	CPI 40-59	CPI 60+	AEIPF	CPI N/A	Controls
Number of samples	57	12	28	5	10	2	26
% Male	81	92	79	80	80	50	69
Mean age	72.8	71.6 (64-78)	73.4 (57-80)	69 (65-74)	70.7 (52-80)	83 (79,87)	65 (44-81)
% Definite	51	42	61	20	50	50	N/A
% Probable	49	58	39	80	50	50	N/A
% on Anti-fibrotics	46	25	39	100	50	0	N/A
Number on Prednisolone/ Methylprednisolone (dose)	4 (+10 AEIPF)	0	3 (5-10 mg)	0	10 5 on Pred (15-30mg) 5 on MP (1g)	1 (5mg)	N/A
Mean FVC	71.2 (47.6-123.7)	87.8 (71.4-123.7)	69.7 (49.1-89.5)	63.3 (58.7-77.2)	60.9 (47.6-71)	60.4 (57.8-63)	N/A
Mean TLCO	47.6 (18.4-89.9)	73.6 (57-89.9)	44.7 (31.1-61.2)	26.1 (24.7-27.1)	31.4 (18.4-46)	N/A	N/A
Mean FEV1	73 (40-107.5)	86.5 (70.3-107.5)	71.6 (40-99.5)	63.3 (58.7-77.2)	65.9 (45.1-86)	68.4 (63-73.7)	N/A
Mean CPI	47 (14.7-6.1)	26 (14.7-37.4)	48.4 (40.5-59.1)	63.1 (62.4-63.9)	60.7 (51.6-67.1)	N/A	N/A

**Table 3-3. The demographics of IPF and control participants involved in the characterisation of monocytes.**

Anti-fibrotic therapy - Pirfenidone in all cases. (FVC - Forced vital capacity, TLCO - Transfer factor for carbon monoxide, FEV1- Forced expiratory volume in 1 second, CPI - composite physiologic index, N/A – not applicable/information not available, Pred – Prednisolone, MP – Methylprednisolone).

### Chapter 3: Monocyte phenotype in stable and acute exacerbations of IPF

Sample code and date	Time since diagnosis (years)	Length of symptoms prior to sampling (weeks)	No. of previous admissions for exacerbations	No. of days on Prednisolone prior to sampling	Pirfenidone treatment Prior?	CT findings	Additional cause for decline	Outcome
01BWAE 13/01/2015	5	6	3	Maintenance Prednisolone	Yes	New patchy GG	Possible infection	Home for palliation RIP 19/06/2015
02AEAE 20/01/2015	2.8	3	1	Maintenance Prednisolone	Yes	Widespread GG	No	RIP 7/3/2015
03NKAE 24/01/2015	2.5	2	1	Maintenance Prednisolone	Yes	New GG Progressive HC	No	Home RIP 11/3/2016
04PFAE 17/04/2015	5	5	0	14	No	Widespread GG Patchy consolidation	No	Hospital RIP 24/4/15
05JFAE 01/05/2015	4.5	3	0	5	No (nintedinab)	Widespread GG Progressive HC	No	Home RIP 19/8/2015
06PBAE 19/06/2015	0	3	0	2	No	Patchy GG Progressive HC	No	Home
07CBAE 09/07/2015	4	2	0	6	No	Airspace opacification GG	Likely CCF in addition	Home for palliation RIP 20/10/2015
08HHAE 18/07/2015	3.7	4	2	Maintenance Prednisolone	No	Progressive HC Multifocal GG	Yes-infection	Improvement and home RIP 30-9-2016
09RSAE 18/08/2015	2.4	1	0	5	Yes	New GG	Yes – infection	Initial improvement RIP 3/11/2016
10JDAE 21/01/2016	3.5	4	2	Maintenance Prednisolone	Yes	Little GG Small patch of consolidation	Possibly infection	Home Palliative care

**Table 3-4. Clinical details of patients sampled with AEIPF.**

All patients had CT evidence of acute exacerbation and were treated with high dose corticosteroids. At 18 months following hospital admission and sampling, the mortality was 80%. GG- *ground glass*; HC *honeycombing*, CCF- *congestive cardiac failure*



### **3.4.2 Monocyte levels were increased in IPF compared to age-matched controls**

Using flow cytometry to identify monocytes within PBMCs, I first questioned whether differences in monocyte proportions existed between IPF patients and age-matched controls.

I found that the percentages of monocytes within PBMCs were increased in stable IPF patients compared to controls ( $p=0.020$ , Fig 3-3a). Furthermore, the expression (MFI) of CD14 was also higher in IPF monocytes ( $p=0.004$ , Fig 3-3b). Comparing patients with stable disease to those with AEIPF, the highest percentage of monocytes within PBMCs was seen in AEIPF ( $p<0.002$ , Fig 3-3c). The increase in the percentage of monocytes was not due to a proportionate decrease in other mononuclear cells within PBMCs but due to an overall increase in circulating blood monocytes. Figure 3-3e shows that the numbers of monocytes per ml of blood were elevated in stable IPF patients compared to controls ( $p=0.003$ ).

### Chapter 3: Monocyte phenotype in stable and acute exacerbations of IPF

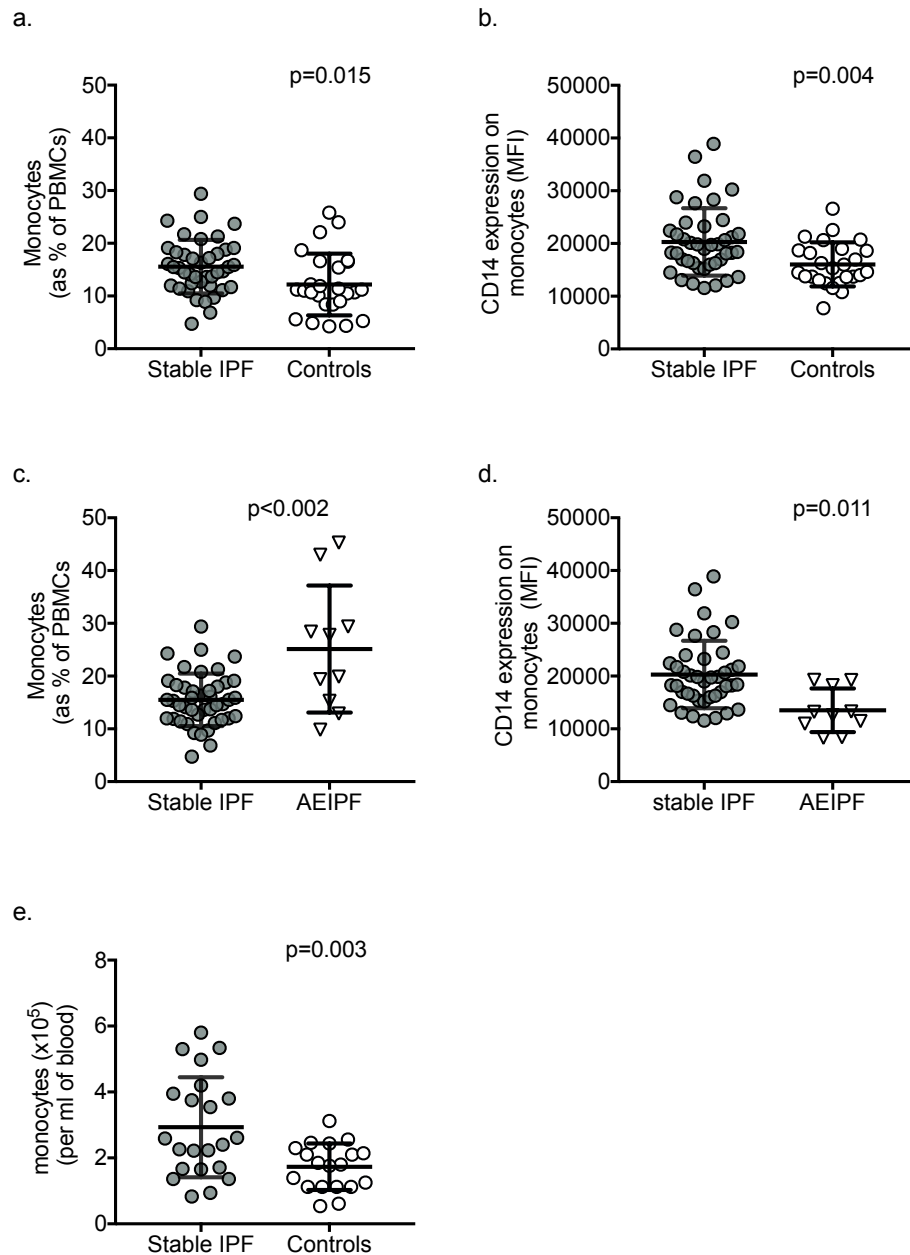


**Figure 3-3. Monocyte levels in IPF patients and aged-matched controls.**

PBMCs were extracted from whole blood and stained with mAbs for flow cytometric analysis to identify the percentage and MFI of CD14+ monocytes within PBMCs in controls, stable IPF and AEIPF. The Mean(SD) are illustrated in the graphs and quoted below. a) The percentage of monocytes within PBMCs in stable IPF was higher than in age-matched healthy controls [15.50%(4.98) vs 12.54%(6.34) IPF n=41 controls n=26]. (b) The MFI of CD14 on monocytes was also higher in IPF compared to controls [20291(6384) vs 16035(4171) n=41 and 26 respectively]. (c) The percentage of monocytes within PBMCs in AEIPF was increased compared to in stable patients [25.12%(12.02), vs 15.50%(4.98) AEIPF n=10, stable IPF n=41]. (d) The MFI of CD14 was lower in AEIPF compared to stable IPF [13510(4125) vs 20291(6384) n=10 and 41]. (e) Monocytes per ml of blood were increased in stable IPF compared to controls (2.93%(1.52) vs 1.73%(0.70) n=22 and 19]. Data not available for AEIPF group. D'Agostino-Pearson omnibus normality test and Student t-test or Mann-Whitney test used for all analyses. P values <0.05 taken to indicate statistical significance.

### 3.4.3 The proportions of classical, intermediate and non-classical monocytes were similar between stable IPF patients and controls

To examine whether IPF patients exhibited differences in the proportions of traditionally defined monocyte subsets [165, 166] compared to controls, I measured the percentages of classical, intermediate and non-classical monocytes within the total monocyte population.

There was no difference in the proportions of classical, intermediate and non-classical monocytes in the stable patient cohort compared to controls. However, as shown in Figure 3-4, classical monocytes were elevated in the AEIPF group compared to controls ( $p=0.034$ ) and a proportionate decrease in the non-classical population was observed in AEIPF compared to both stable IPF and controls ( $p=0.012$  for AEIPF vs IPF and  $p=0.002$  for AEIPF vs controls).

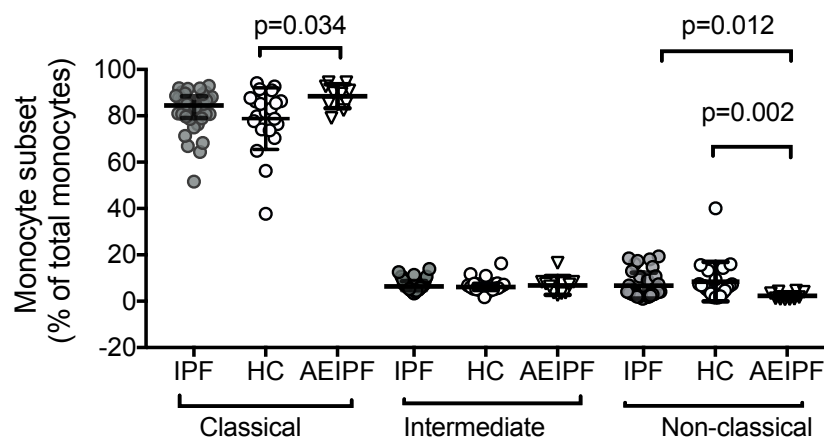


**Figure 3-4. The percentage of classical, intermediate and non-classical monocyte subsets within the total monocyte population in stable IPF (IPF), healthy controls (HC) and acute exacerbations of IPF (AEIPF).**

PBMCs isolated from whole blood were stained with mAb to CD14 and CD16 to identify the percentage of classical ( $CD14^{hi} CD16^{neg}$ ), intermediate ( $CD14^{+}CD16^{+}$ ) and non-classical subsets ( $CD14^{lo}CD16^{+}$ ) within the total monocyte population. Classical monocytes were increased in AEIPF compared to HC [88.4%(5.2) vs 78.8%(13.3)] and non-classical monocytes were lower in AEIPF compared to IPF and HC [2.3%(1.5) vs 6.7%(5.6) vs 8.4(8.5)]. IPF  $n=36$ , HC= 21, AEIPF=10. Mean(SD) has been quoted here and illustrated on graphs. One-way ANOVA with corrections for all multi-wise comparisons stated were performed using Dunn's method (section 2.14).

#### **3.4.4 CD64 expression was increased in both classical and non-classical monocyte subsets in IPF**

To determine whether the phenotype of monocytes within the traditional monocyte subsets differed between stable IPF patients and controls, I analysed the expression of cell surface receptors associated with M1 (inflammatory) and M2 (reparative) macrophage responses in each of the subsets. CD64, CD86 and CCR7 were selected as receptors associated with inflammatory and activated states [220, 250, 251, 253] alongside CD62L, a cell surface adhesion molecule that facilitates the migration of monocytes to sites of inflammation [267]. CD206 and CD163 were selected as markers recognised to be up-regulated in 'M2' macrophages [196, 268, 269].

CD64 was significantly elevated in both classical and non-classical subgroups in IPF patients compared to controls ( $p=0.005$  and  $0.042$ , respectively, Fig 3-5a). A reduction in the expression of both CD62L and CCR7 was observed in the intermediate monocyte subset in IPF patients ( $p=0.030$  and  $p=0.043$ , respectively, Fig 3-5b-c). However, expression of these markers did not differ significantly between stable patients and controls when measured on monocytes as a collective group without division into subsets as illustrated in Figure 3-6d-e. Comparing the expression of receptors between the monocytes subsets, the MFI of CD64 was higher in classical and intermediate subsets and decreased in non-classical monocytes in both IPF and control monocytes (both Adj- $p<0.001$ , Fig 3-5a). High expression of CD62L was also noted on classical monocytes compared to non-classical monocytes (both IPF and controls Adj- $p<0.001$ , Fig 3-5b). Differences in the MFI of CCR7 and CD86 between monocyte subsets were not observed in IPF and controls (Fig 3-5c-d).

CD163 expression did not differ significantly between IPF and control monocytes, and was expressed at highest intensity in the classical and intermediate subsets in both groups (Fig 3-5e). CD206 was expressed on monocytes at a very low level and showed a trend towards increased expression in the intermediate and non-classical subsets (Fig 3-5f).

### Chapter 3: Monocyte phenotype in stable and acute exacerbations of IPF

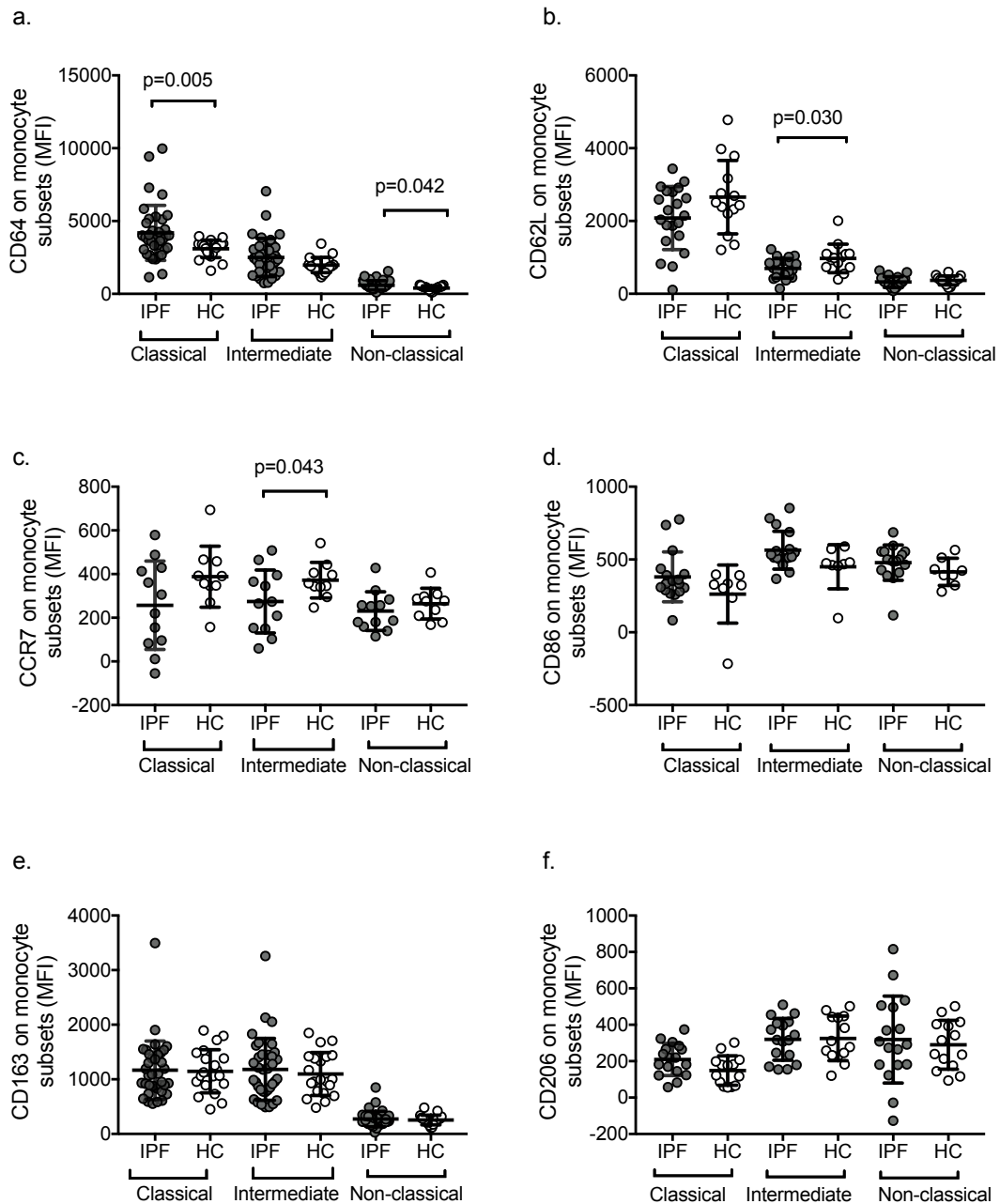


**Figure 3-5. The expression (MFI) of cell surface receptors associated with inflammatory ('M1) and reparative functions ('M2') in stable IPF (IPF) and control (HC) monocytes.**

Flow cytometry was used to assess the expression of 'M1' markers CD64, CD62L, CCR7 and CD86 and 'M2' receptors CD163 and CD206 on classical ( $CD14^{hi} CD16^{neg}$ ), intermediate ( $CD14^{+}CD16^{+}$ ) and non-classical monocyte subsets ( $CD14^{lo}CD16^{+}$ ). Mean MFI (SD) are described here and illustrated on graphs. (a) CD64 expression was increased on classical and non-classical monocytes from IPF patients compared to controls [Classical subset 4185(1888) vs 3091(582) and non-classical 590.8(318) vs 402.8(150.3)  $n=36$  and 21 respectively]. CD64 expression was higher on classical and intermediate monocyte subsets in both IPF and controls [classical vs non-classical monocytes in IPF: MFI mean(SD) 4185(1888) vs 590.8(318.1) and controls: 3091(581.8) vs 402.8(150.3), both Adj- $p<0.001$ ]. (b) CD62L expression was lower in the intermediate subset in IPF monocytes compared to controls [250(163.6) vs 371.8(81.5)  $n=21$  and 14]. Expression of CD62L was increased in the classical subset compared to non-classical monocytes in both

## Chapter 3: Monocyte phenotype in stable and acute exacerbations of IPF

IPF and control monocytes [2081(867) vs 324.9(147.8) and 2655(1009) vs 369.3 (123.1) for IPF and HC, both Adj-p<0.001]. (c) CCR7 expression was lower in the intermediate monocyte subset in IPF [698.5(270.2) vs 972(391.7) n=10 and 13]. (d) Differences in expression of CD86 were not seen in IPF and HC monocyte subsets (n=17 and 8 for IPF and HC respectively). (e-f) Expression of 'M2' receptors CD163 and CD206 on monocyte subsets did not differ significantly. (IPF and controls: CD163 n=36 and 21; CD206 n=17 and 14). D'Agostino and Pearson omnibus normality test and Mann-Whitney test was used for statistical analysis.

### **3.4.5 CD14 monocytes from AEIPF displayed a distinct profile consistent with M2 polarisation**

Patients meeting the criteria for acute exacerbation who were admitted to hospital for further management were analysed separately in order to gain insight into the possible perturbations occurring at the level of the monocyte during these events. All patients with AEIPF were taking corticosteroids, either orally or intravenously (section 3.4.1 Table 3-4).

In addition to increases in monocyte frequency and the proportion of classical monocytes seen in AEIPF (Figures 3-3c and 3-4), the expression of CD163 was upregulated in AEIPF compared to controls (Adj-p=0.015, Fig 3-6a). The MFI of CD64 was similar amongst AEIPF and control monocytes but increased in stable patients compared to controls (Adj-p=0.005, Fig 3-6b). The ratio of CD163/CD64 (representing the balance of M2/M1) was not significantly different in AEIPF monocytes compared to stable IPF and controls (Fig 3-6b-c). Expression of CD62L, a receptor associated with monocyte migration, was higher in AEIPF compared to stable patients (Adj-p=0.007, Fig 3.6d). No significant differences were seen in the expression of CCR7 (Fig 3.6e).

The expression of several representative M2 and M1 genes in AEIPF monocytes was markedly different from stable IPF and control monocytes and showed a pattern broadly consistent with M2 polarisation. In AEIPF, *IL-10* expression was increased alongside gene expression of *CD163* compared to controls (both Adj-p=0.003, Fig 3-7a and c). Expression of the IL-1 decoy receptor, *IL-1R2*, was also significantly up-regulated in AEIPF compared to both stable IPF and control monocytes (Adj-p=0.020 and <0.007 respectively, Fig 3-7d). Expression of *THSB1*, coding for thrombospondin 1, was increased in AEIPF compared to controls (p=0.021, Fig 3-7e). Interestingly, two genes associated with M2 responses, *TGM2* and *CD200R*, were decreased in AEIPF monocytes compared to controls (both Adj-p=0.008, Fig 3-7f and Table 3-5). M1-associated genes *TNF $\alpha$* , *FGL2* and *GBP1* were all downregulated in AEIPF monocytes

### Chapter 3: Monocyte phenotype in stable and acute exacerbations of IPF

in comparison to control monocytes (Adj p-values <0.003, 0.005 and 0.31 respectively, Fig 3-7g, j and k). *IL-6* expression was significantly lower in AEIPF compared to stable IPF (Adj p=0.022, Fig 3-7h). A downward trend was noted in *CXCL10* expression in AEIPF monocytes compared to control and stable IPF monocytes but statistical significance was not seen (Adj-p=0.132 and 0.481 respectively, Fig 3-7i).

### Chapter 3: Monocyte phenotype in stable and acute exacerbations of IPF

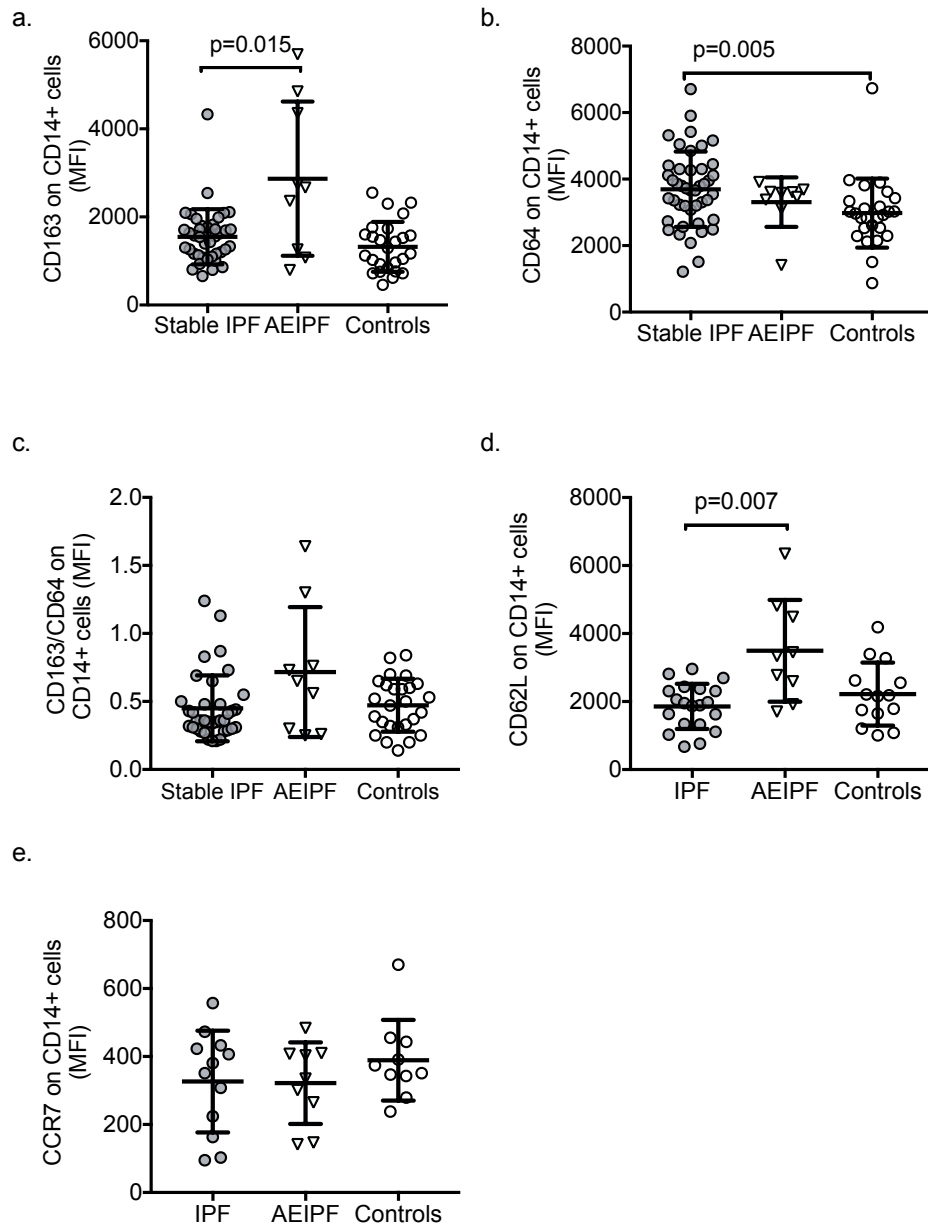
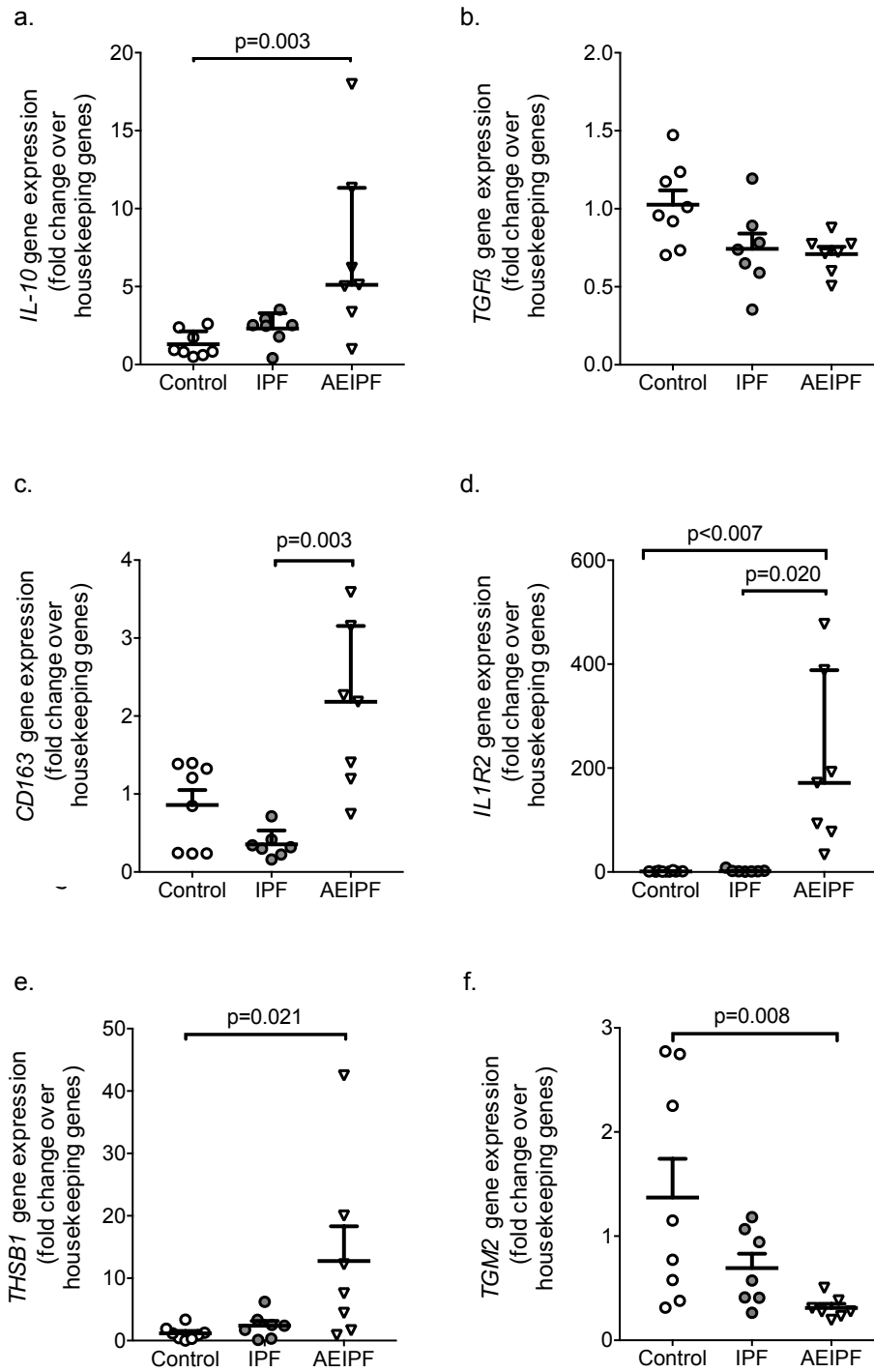


**Figure 3-6. The expression of receptors (MFI) associated with reparative (M2) and inflammatory (M1) phenotypes on monocytes from participants with stable IPF (IPF), AEIPF and controls.**

Monocytes were immunostained with mAb and flow cytometry was used to assess the expression (MFI) of 'M2' receptors CD163 and CD206 and 'M1' markers CD64, CD62L, CCR7 and CD86. Mean MFI(SD) are described here and illustrated on graphs. (a) The MFI of CD163 was significantly higher in AEIPF compared to controls but not stable IPF (AEIPF:2868(1751) vs HC: 1321(566.4) vs IPF:1550(625) AEIPF n=9, HC=26, IPF=40). (b) CD64 expression was not significantly different in AEIPF but was higher in stable IPF compared to controls (AEIPF:3308(743) vs HC:2979(1039) vs IPF:3695(1130) AEIPF n=44, HC=26, IPF=44). (c) The ratio of CD163/CD64 did not differ significantly between groups. (d) CD62L expression was increased in AEIPF compared to stable IPF but not controls (AEIPF: 3493(1497) vs HC:2219(927) vs IPF:1858(664) AEIPF n=9 HC=14, IPF=20). (e) CCR7 did not differ significantly between stable IPF, AEIPF and controls (AEIPF n=9, HC=10, IPF=12). D'Agostino and Pearson omnibus normality test and one-way ANOVA or Kruskal-Wallis test undertaken to assess the presence of significant differences between the three groups. Corrections for all multi-wise comparisons stated were performed using Dunn's method.



### Chapter 3: Monocyte phenotype in stable and acute exacerbations of IPF



## Chapter 3: Monocyte phenotype in stable and acute exacerbations of IPF

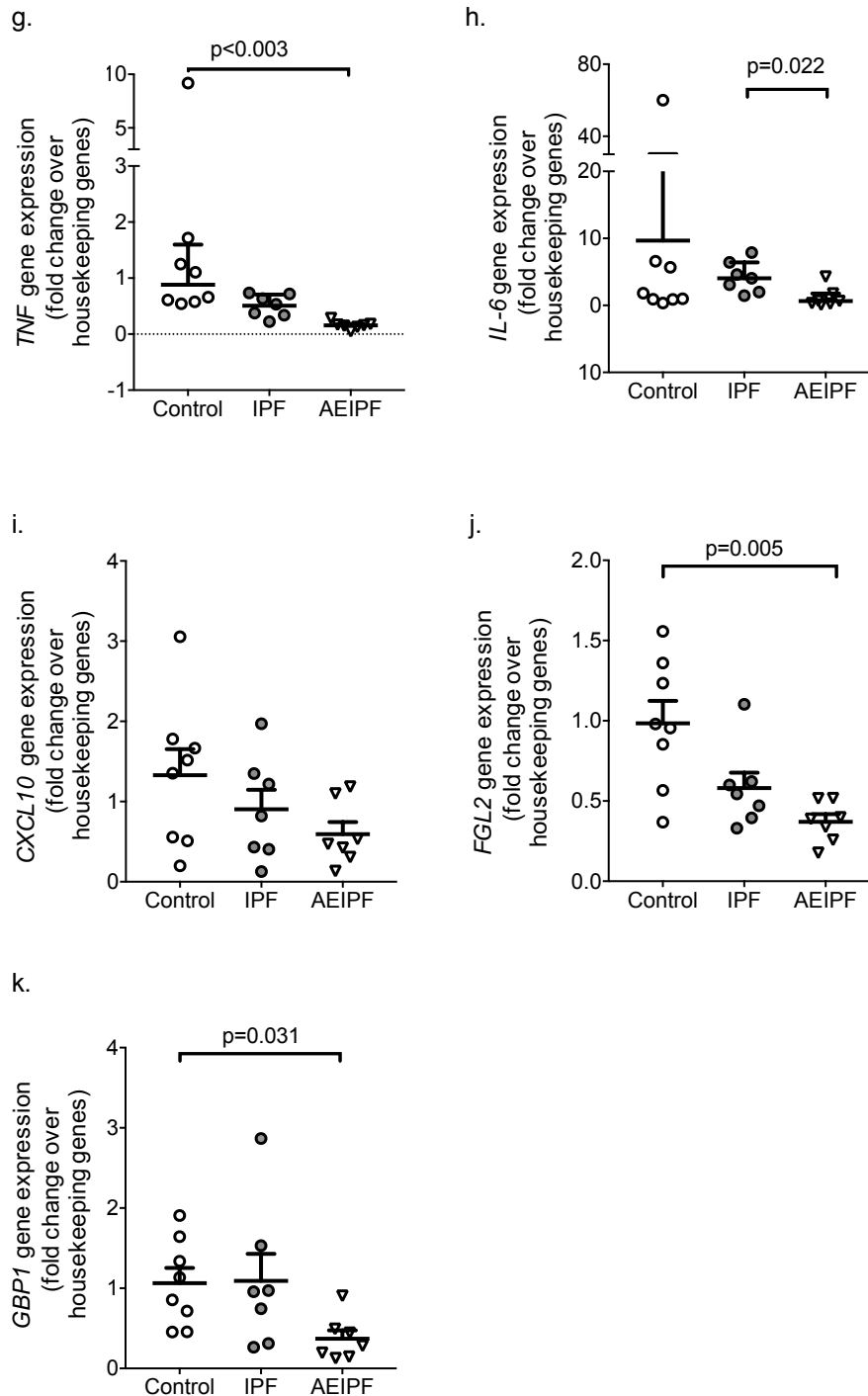


**Figure 3-7. Expression of genes associated with inflammatory (M1) and reparative (M2) functions in monocytes from controls, stable IPF and AEIPF.**

Monocytes were extracted by positive selection from freshly isolated PBMCs to examine the expression of inflammatory and reparative genes by qPCR. For normally distributed data, mean(SEM) are depicted in graphs. For non-parametric data, the median and interquartile range (IQR) are shown. (a-f) Genes associated with reparative/M2 phenotypes. (g-k) Genes associated with inflammatory/M1 phenotypes. The fold change over three housekeeping genes (*CYCLOPHILIN A*, *β2-MICROGLOBULIN* and *β-ACTIN*) was used to determine the relative expression of the genes of interest. (a) Gene expression of *IL-10* was

### Chapter 3: Monocyte phenotype in stable and acute exacerbations of IPF

increased in AEIPF compared to controls [7.14(2.16) vs 1.30(0.29)]. (b)  $TGF\beta$  expression did not differ significantly between groups. (c) *CD163* expression was increased in AEIPF compared to stable IPF [Mean(SEM) 2.08(0.39) vs 0.35(0.07)]. (d) *il1r2* was increased in AEIPF compared to stable IPF and controls [Median(IQR) 171.4(77.45-388.5) vs 1.52(1.17-2.17) vs 0.97(0.72-2.79)]. (e) *THSB1* was increased in AEIPF compared to controls [12.76(5.56) vs 1.16(0.38)]. (f) *TGM2* was decreased in AEIPF compared to controls [0.31(0.04) vs 1.37(0.37)]. (g) *TNFA* was lower in AEIPF compared to controls [0.16(0.13-0.18) vs 0.88(0.58-1.60)]. (h) *IL-6* was decreased in AEIPF compared to stable IPF [0.66(0.25-1.77) vs 4.06(1.99-6.41)]. (i) Significant differences were not seen in the expression of *CXCL10* between groups. (j) AEIPF showed a decrease in the expression of *FGL2* compared to controls [0.37(0.05) vs 0.98(0.15)]. (k) *GBP1* expression was lower in AEIPF compared to controls [0.37(0.10) vs 1.06(0.19)]. D'Agostino and Pearson omnibus normality test and Kruskal-Wallis test was undertaken to assess the presence of significant differences between the three groups. Corrections for all multi-wise comparisons stated were performed using Dunn's method. Controls n=8, Stable IPF n=7, AEIPF n=7.

### Chapter 3: Monocyte phenotype in stable and acute exacerbations of IPF

Association with in vitro polarisation	Gene	Protein transcript/role	Control Vs Stable IPF adj-p	Control Vs AEIPF adj-p	Stable IPF Vs AEIPF adj-p
<b>M2</b>	<i>TGF<math>\beta</math>1</i>	Pleiotropic profibrotic cytokine	0.167	0.065	>0.999
	<i>IL-10</i>	Immunomodulatory cytokine	0.501	<b>0.003</b>	0.192
<b>M2a (IL-4)</b>	<i>CD206</i>	Mannose scavenger receptor	<i>Low expression seen</i>		
	<i>CD200R1</i>	Glycoprotein receptor	0.454	<b>0.008</b>	0.383
	<i>PTGS2</i>	Prostaglandin-endoperoxide synthase	>0.999	0.141	0.071
	<i>TGM2</i>	Tissue transglutaminase	>0.999	<b>0.008</b>	0.119
<b>M2c (GC, IL10)</b>	<i>CD163</i>	Haemoglobin scavenger receptor	0.511	0.115	<b>0.003</b>
	<i>C1QA</i>	C1q (complement subcomponent)	0.302	0.142	>0.999
	<i>DSIPI</i>	TSC22 domain family, member 3	0.886	<b>0.030</b>	0.415
	<i>IDO1</i>	Indoleamine 2,3-dioxygenase 1	>0.999	0.286	0.698
	<i>THBS1</i>	Thrombospondin 1	0.893	<b>0.021</b>	0.325
<b>M1 (LPS, IFN<math>\gamma</math>)</b>	<i>TNF<math>\alpha</math></i>	Inflammatory cytokine	0.486	<b>&lt;0.003</b>	0.051
	<i>IL-6</i>	inflammatory cytokine	>0.999	0.193	<b>0.022</b>
	<i>CXCL10</i>	Chemokine	0.747	0.135	>0.999
	<i>FGL2</i>	Fibronogen-like protein 2	0.362	<b>0.005</b>	0.383
	<i>GBP1</i>	Guanylate binding protein 1	>0.999	<b>0.031</b>	0.097
<b>M1 and M2/ other</b>	<i>VEGF-A</i>	Angiogenesis growth factor	0.930	0.053	0.563
	<i>CCR2</i>	Receptor for CCL2 (MCP-1)	>0.999	>0.999	>0.999
	<i>IL1R2</i>	Decoy receptor	>0.999	<b>&lt;0.007</b>	<b>0.020</b>
	<i>CD14</i>	Co-receptor for TLR4	0.191	<b>0.020</b>	>0.999

**Table 3-5. List of genes analysed in freshly isolated monocytes from controls, stable IPF and AEIPF.** The fold change over three housekeeping genes (*CYCLOPHILIN A*,  *$\beta$ 2-MICROGLOBULIN* and  *$\beta$ -ACTIN*) was used to determine the relative expression of the genes of interest. Kruskal-Wallis test was undertaken to assess the presence of significant differences between the three groups. Corrections for all multi-wise comparisons stated were performed using Dunn's method. P values <0.05 taken to indicate statistical significance. Controls n=8, Stable IPF n=7, AEIPF n=7. Parentheses in first column indicate the types of stimulation used in vitro to induce up-regulation of the genes associated with M1 and M2 macrophages (GC- glucocorticoid, LPS-Lipopolysaccharide, IFN $\gamma$  - interferon-gamma).

### **3.4.6 Expression of M1/M2 genes differed in monocytes from patients with stable IPF compared to aged-matched healthy controls**

AEIPF patients enrolled within this study were treated with high-dose corticosteroids in order to dampen down inflammatory responses that may have precipitated their deterioration. Corticosteroids have been found to alter the phenotype of monocytes significantly [205, 220] and the comparison of AEIPF with stable IPF and control monocytes revealed large differences in the expression of inflammatory and reparative genes, which may have been confounded by steroid administration. The gene expression changes seen in the AEIPF monocytes may have overshadowed smaller differences existing between stable patients not on corticosteroids and aged-matched controls. Thus, the data was reanalysed with the exclusion of monocytes from patients with AEIPF.

Differences were noted between the two groups. Trends towards lower expression was seen in the inflammatory mediators *TNF $\alpha$*  and *CXCL10* in IPF monocytes ( $p=0.054$  and  $0.281$ , respectively, Fig 3.8a-b) whilst the anti-inflammatory cytokine *IL-10* showed a trend towards higher expression in stable IPF patients ( $p=0.050$ , Fig 3-8c). *FGL2*, coding for fibrinogen-like protein-2, was significantly lower in IPF monocytes compared to controls ( $p=0.038$ , Fig 3-8d). Interestingly, whilst the expression of the CD14 receptor was increased on the cell surface of IPF monocytes (Fig 3.3b), the gene expression of the same receptor was significantly lower compared to controls ( $p=0.017$ , Fig 3-8e). *CD163* was also decreased in stable patients compared to controls ( $p=0.035$ , Fig 3-8f). Fold changes in the gene expression of M1/M2 genes between stable IPF patients and controls are tabulated in Table 3-6.

## Chapter 3: Monocyte phenotype in stable and acute exacerbations of IPF

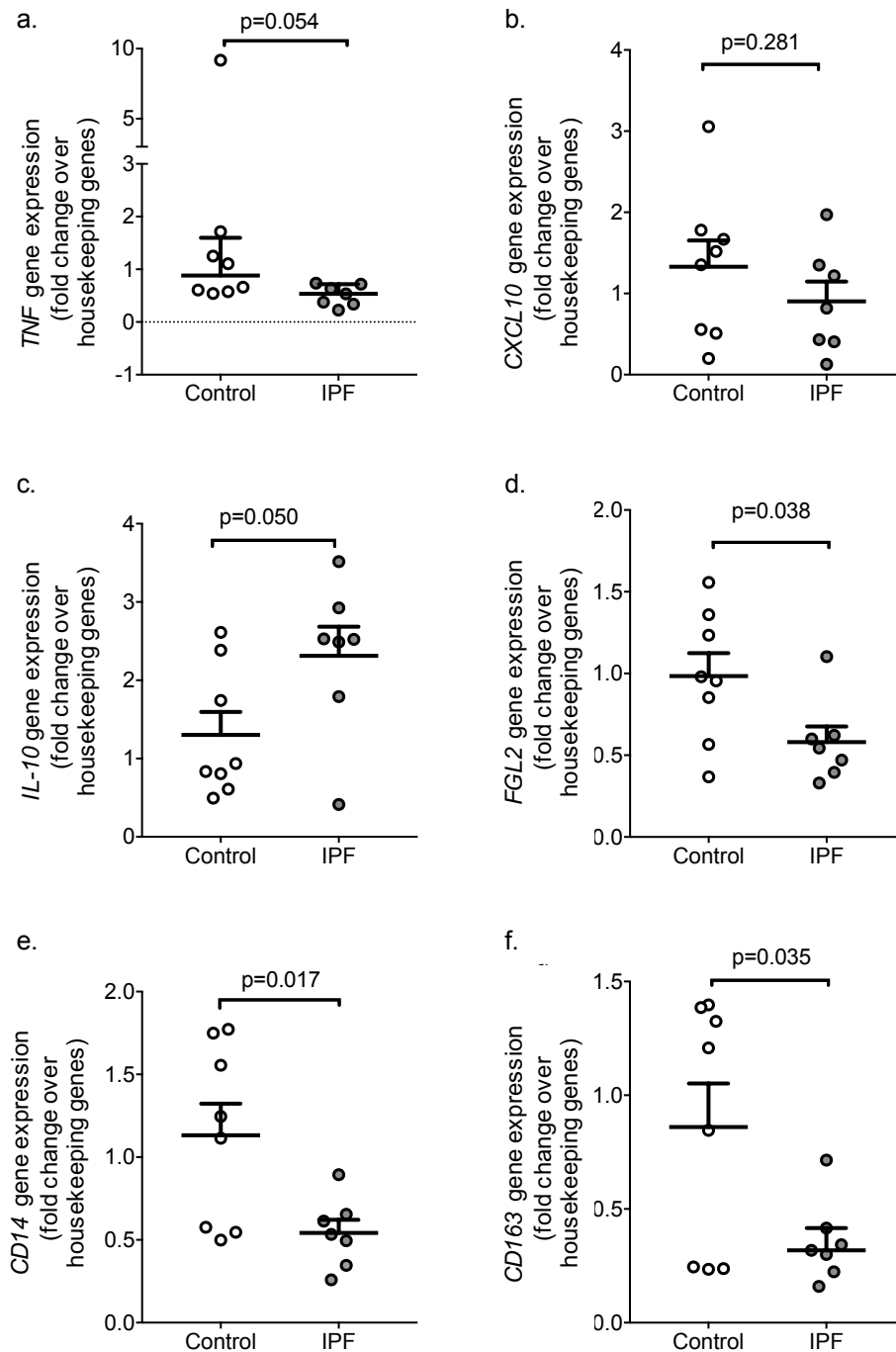


**Figure 3-8. The expression of M1/M2 genes in monocytes extracted from PBMCs in stable IPF patients and aged-matched controls.**

The fold change over three housekeeping genes (*CYCLOPHILIN A*, *β2-MICROGLOBULIN* and *β-ACTIN*) was used to determine the relative expression of the genes of interest. For normally distributed data, mean(SD) are depicted in graphs. For non-parametric data, the median and interquartile range are shown. (a-b) There is a downward trend in the expression of inflammatory mediators *tnfa* and *cxcl10* in monocytes from stable IPF compared to controls. (c) *IL-10* expression shows a trend towards increased expression in IPF monocytes compared to controls. (d-f) There is decreased expression of *FGL2*, *CD14* and *CD163* in IPF monocytes. Table 3-6 lists the mean fold gene expression(SD) and p-values for the full list of genes in stable IPF and controls.

### Chapter 3: Monocyte phenotype in stable and acute exacerbations of IPF

Gene	Protein transcript/role	Mean fold change (SEM)	Mean fold change (SEM)	Control Vs Stable IPF
		Stable IPF n=7	Controls n=8	P-value
<i>TGFβ1</i>	Pleiotropic profibrotic cytokine	0.74(0.10)	1.03 (0.09)	0.055
<i>CD14</i>	Co-receptor for TLR4	<b>0.54(0.08)</b>	<b>1.13(0.19)</b>	<b>0.018</b>
<i>IL-10</i>	Immunomodulatory cytokine	2.3(0.37)	1.3(0.29)	0.050
<i>CD206</i>	Mannose scavenger receptor	<i>Low expression seen</i>		
<i>CD200R1</i>	Glycoprotein receptor	0.51(0.10)	1.00(0.20)	0.062
<i>PTGS2</i>	Prostaglandin-endoperoxide synthase	1.31(0.27)	1.13(0.18)	0.612
<i>TGM2</i>	Tissue transglutaminase	0.69(0.14)	1.37(0.37)	0.131
<i>CD163</i>	Haemoglobin scavenger receptor	<b>0.35(0.07)</b>	<b>0.86(0.19)</b>	<b>0.035</b>
<i>C1QA</i>	C1q (complement subcomponent)	0.43(0.21)	0.89(0.20)	0.152
<i>DSIP1</i>	TSC22 domain family, member 3	0.81(0.12)	0.96(0.07)	0.288
<i>IDO1</i>	Indoleamine 2,3-dioxygenase 1	0.89(0.20)	0.97(0.15)	0.764
<i>THBS1</i>	Thrombospondin 1	2.37(1.78)	1.16(0.38)	0.231
<i>TNFα</i>	Inflammatory cytokine	0.51(0.07)	1.95(1.04)	0.054
<i>IL-6</i>	inflammatory cytokine	4.21(0.87)	9.66(7.25)	0.336
<i>CXCL10</i>	Chemokine	0.90(0.24)	1.33(0.32)	0.281
<i>FGL2</i>	Fibronogen-like protein 2	<b>0.58(0.10)</b>	<b>0.98(0.14)</b>	<b>0.038</b>
<i>GBP1</i>	Guanylate binding protein 1	1.09(0.34)	1.06(0.19)	0.779
<i>VEGF-A</i>	Angiogenesis growth factor	0.82(0.18)	1.15(0.19)	0.397
<i>CCR2</i>	Receptor for CCL2 (MCP-1)	1.19(0.76)	2.82(1.62)	0.401
<i>IL1R2</i>	Decoy receptor	2.53(1.00)	1.43(0.35)	0.232

**Table 3-6. Full list of genes analysed in freshly isolated monocytes extracted from PBMCs from aged-matched healthy controls and stable IPF patients not on steroid therapy.**

D'Agostino and Pearson omnibus normality test and Student t-test or Mann-Whitney test used for statistical analysis. P values <0.05 taken to indicate statistical significance. Controls n=8, Stable IPF n=7.

### **3.4.7 CD163 expression was down-regulated by LPS but retained following TLR7/8 stimulation**

To determine whether monocytes from IPF patients respond differently to viral and bacterial PAMPs compared to controls, Resiquimod (r848), a TLR7/8 agonist, and lipopolysaccharide (LPS), were used to stimulate monocytes within PBMCs. TLR7 and 8 are endosomal toll-like receptors that respond to single-stranded RNA present in viruses such as Coxsackie and Influenza. LPS is a constituent of gram negative bacterial cell walls and stimulates TLR4 pathways.

Expression of CD64 and CD163 (representing 'M1' and 'M2' responses) differed on monocytes stimulated with LPS and r848 although significant differences were not seen between control and IPF patients. The percentage of monocytes expressing CD163 and the MFI of CD163 were down-regulated by LPS in control, stable IPF and AEIPF monocytes compared to unstimulated cells (LPS vs unstimulated monocytes %CD163  $p=0.005$ ,  $<0.005$  and  $0.008$ ; MFI CD163  $p<0.009$ ,  $<0.007$  and  $0.014$  for controls, stable IPF and AEIPF respectively). CD163 expression however was not reduced on monocytes in response to stimulation by r848 in any of the groups (Fig 3-9a-b).

CD64 was expressed on all monocytes and therefore only the MFI was analysed. Comparing unstimulated monocytes within PBMCs to LPS-treated cells, monocytes from stable IPF patients upregulated expression of this receptor ( $p=0.044$ ). Significant differences in the expression of CD64 following LPS stimulation were not observed in control and AEIPF monocytes. r848 stimulation did not result in up-regulation of this receptor in any of the groups (Fig 3-9d).



### Chapter 3: Monocyte phenotype in stable and acute exacerbations of IPF

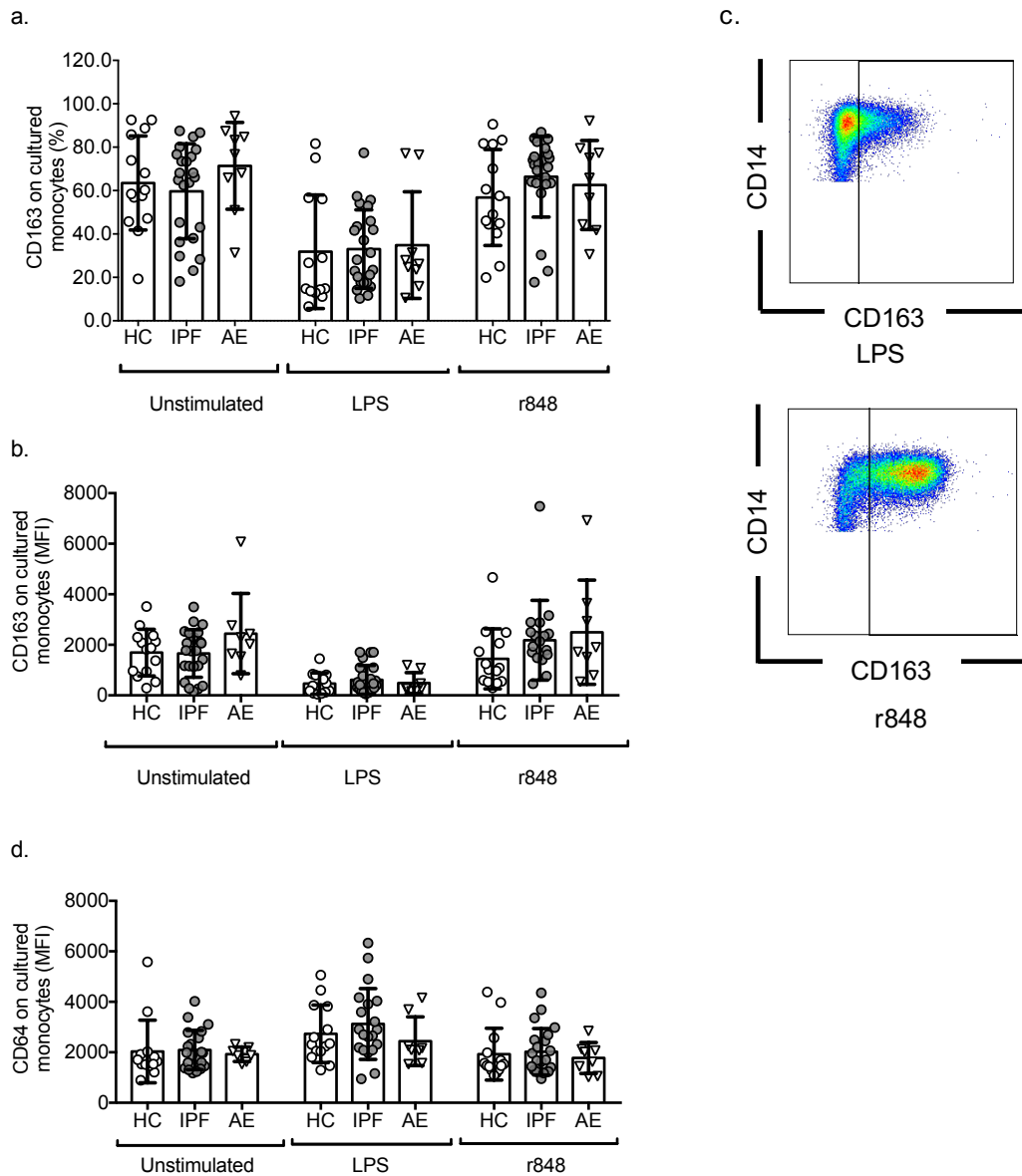


**Figure 3-9. The expression of CD163 and CD64 by control (HC), stable IPF (IPF) and AEIPF (AE) monocytes following stimulation with LPS and the TLR7/8 agonist, r848.**

PBMCs were cultured overnight with LPS, r848 or left unstimulated to assess monocyte responses to bacterial and viral PAMPs. LPS and the TLR7/8 agonist, r848, were used to determine whether IPF and control monocytes differed in the expression of CD163 (M2 marker) and CD64 (M1 marker) following stimulation. Mean(SD) are described here and illustrated on graphs. LPS downregulated the percentage and mean fluorescence intensity (MFI) of monocytes expressing CD163 in controls, IPF and AEIPF monocytes although CD163 was retained on monocytes following r848 stimulation. (a) Percentage of CD163 on unstimulated and stimulated monocytes [unstimulated vs LPS vs r848 mean %(SD) HC: 63.5(21.7) vs 31.8(26.2) vs 56.8(22.1) Adj-p=0.005 for unstimulated vs LPS, and Adj-p<0.999 for unstimulated vs r848; IPF: 59.7(21.9) vs 33.0(18.1) vs 66.4(18.6), Adj-p<0.005 for unstimulated vs LPS, Adj-p>0.999 for r848 vs unstimulated; AEIPF 71.4(20.0) vs 34.9(24.6) vs 62.6(20.5), Adj-p=0.008 for unstimulated vs LPS, Adj-p>0.999 for unstimulated vs r848]. (b) MFI CD163 on unstimulated and stimulated monocytes [unstimulated vs LPS vs r848 mean MFI(SD) HC: 1694(923) vs 466.8(422) vs 1446(1186) Adj-p<0.009 for unstimulated vs LPS, and Adj-p<0.999 for unstimulated vs r848; IPF: 1659(941.6) vs 615.8(570.4) vs 2182(1577), Adj-p<0.007 for unstimulated vs LPS, Adj-p>0.999 for r848 vs unstimulated; AEIPF: 2445(1589) vs 488(4122)

## Chapter 3: Monocyte phenotype in stable and acute exacerbations of IPF

vs 2498(2061), Adj-p=0.004 for unstimulated vs LPS, Adj-p>0.999 for unstimulated vs r848]. Statistically significant differences in expression were not seen between monocyte groups. (c) Representative FACS plots of CD163 expression on monocytes following LPS and r848 stimulation. (d) CD64 expression was increased on monocytes in response to LPS in IPF monocytes but not in response to r848. Significant differences in CD64 expression were not observed in control and AEIPF monocytes [unstimulated vs LPS vs r848 IPF: 2092(777) vs 3122(1402) vs 2020(921), unstimulated vs LPS Adj-p=0.044; HC: 2035(1241) vs 2733(1141) vs 1924(1028), unstimulated vs LPS Adj-p=0.111; AEIPF 1928(288) vs 2439(961) vs 1775(613), unstimulated vs LPS Adj-p= 0.304]. IPF=21 HC=13, AEIPF=7. D'Agostino and Pearson omnibus normality test and one-way ANOVA was undertaken to assess the presence of significant differences between groups. Corrections for all multi-wise comparisons stated were performed using Dunn's method.

### **3.4.8 IL-10 expression was attenuated in monocytes from patients with AEIPF in response to stimulation with LPS**

To determine whether the cytokine/chemokine response by monocytes to viral and bacterial PAMPs differed between IPF patients and controls, IL-10, MCP-1 and IL-6 expression were measured by flow cytometry.

Stimulation by LPS resulted in IL-10 expression by monocytes that was significantly attenuated in AEIPF compared to controls (Adj-p=0.005, Fig 3-10a). This contrasts with the gene expression data on freshly isolated monocytes, which showed that *IL-10* expression was higher in the AEIPF group (Fig 3-7a). Statistically significant differences in IL-10 expression in response to r848 stimulation were not observed between stable IPF, AEIPF and control monocytes.

There were no differences between stable IPF, AEIPF and control groups in monocyte expression of MCP-1 and IL-6 in response to LPS or r848 (Fig 3-10b-c). However, r848 induced significantly higher expression of MCP-1 compared to LPS in stable IPF, controls and AEIPF ( $p<0.001$ ;  $p<0.003$  and  $p=0.002$  respectively, Fig 3-10b). LPS and r848 induced a similar stimulatory effect on IL-6 expression in monocytes from stable IPF patients and controls (Fig 3-10c).

## Chapter 3: Monocyte phenotype in stable and acute exacerbations of IPF

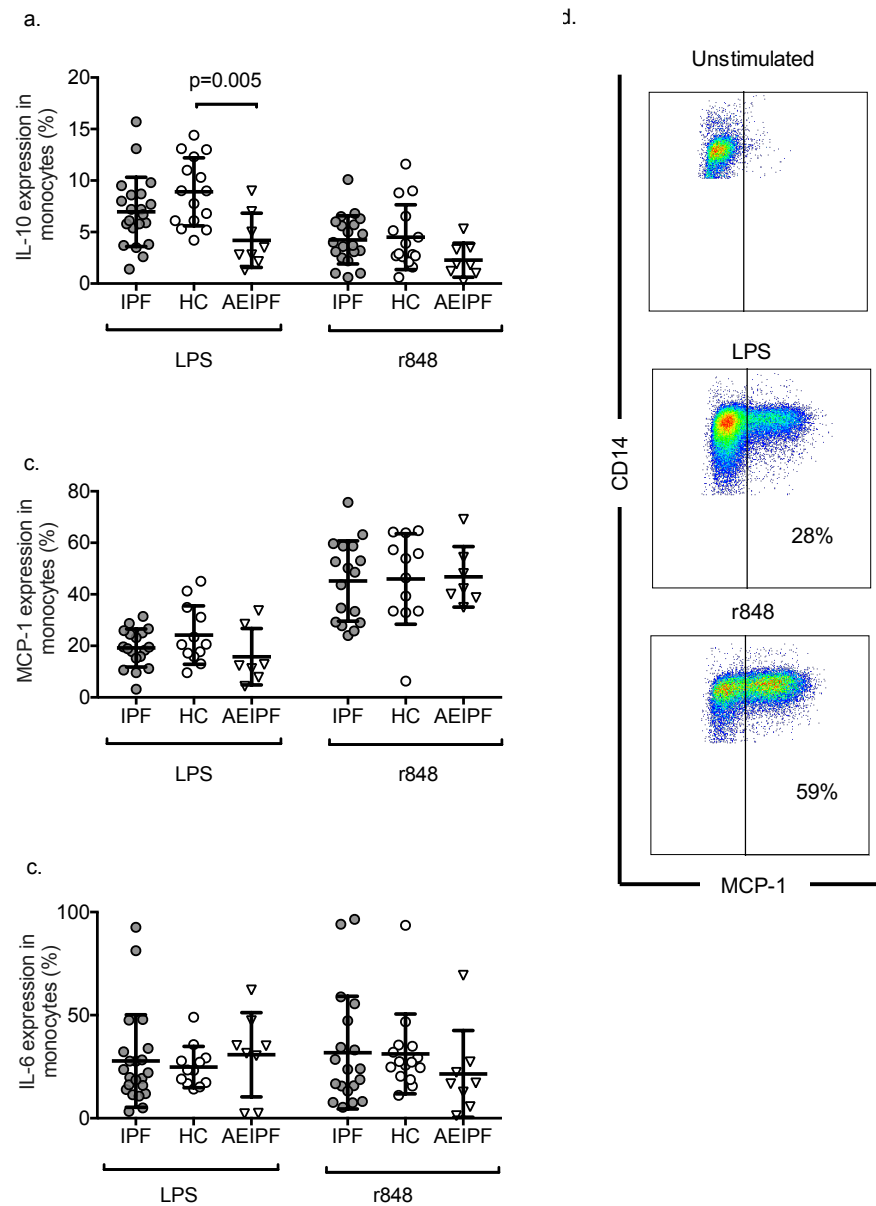


**Figure 3-10. Cytokine expression by monocytes from stable IPF patients (IPF), controls (HC) and those with acute exacerbations of IPF (AEIPF).**

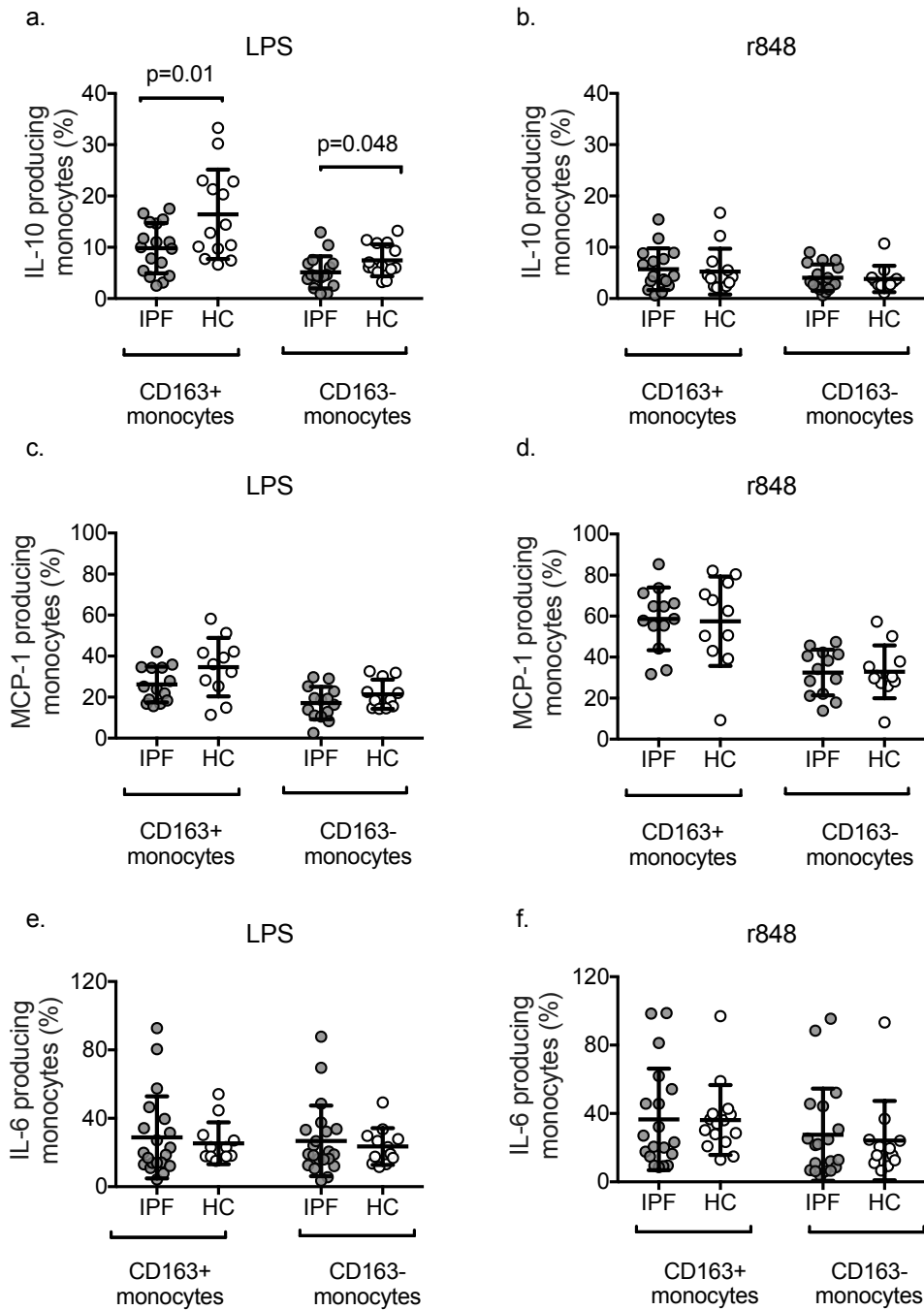
LPS and r848 were used to stimulate monocytes within PBMCs overnight and the expression of IL-10, IL-6 and MCP-1 was measured by flow cytometry. Unstimulated cells were used as a negative control to facilitate the gating strategy. Mean percentage (SD) are described here and illustrated on graphs. (a) Comparing monocytes from IPF, HC and AEIPF groups, the percentage of cells expressing IL-10 was lower in AEIPF compared to controls following stimulation with LPS [4.2%(2.6) vs 8.9%(3.3) n=8 and 15, One-way ANOVA]. (b) Comparing stable IPF, controls and AEIPF individually, MCP-1 expression was increased in all groups following stimulation by r848 compared to LPS [IPF 45.1%(15.6) vs 19.2%(7.4) n=17, p<0.001, HC: 46.0%(17.6) vs 24.2%(11.4) n=12, p<0.003; AEIPF 46.8%(11.8) vs 15.8%(10.9) n=7, p=0.002]. (c) IL-6 was upregulated by IPF, HC and AEIPF monocytes in response to LPS and r848 but differences were not seen between groups. (d) Representative FACs plots showing the gating strategy based on unstimulated cells to determine the proportion of monocytes expressing MCP-1 in response to r848 and LPS. Mann-Whitney test or one-way ANOVA (for multiple comparisons) were used for statistical analysis.

### **3.4.9 CD163+ monocytes showed enhanced cytokine/chemokine responses to LPS and r848 compared to their CD163- counterparts**

Following stimulation with LPS and r848, monocyte expression of CD163 differed significantly, with a reduction observed in LPS-treated cells (Fig 3-9 a-b). I was thus interested in determining whether the cytokine repertoire of monocytes expressing CD163 differed from monocytes lacking this receptor. Using the gating strategy depicted in Figure 3-3, monocytes were subdivided into those expressing CD163 and those negative for the receptor. Cytokine expression was measured in each by calculating the percentage of monocytes positive for IL-10, MCP-1 and IL-6 in stable IPF patients and controls.

In both IPF and controls, a higher percentage of CD163+ monocytes expressed IL-10 compared to CD163- monocytes in response to LPS. Significantly lower IL-10 expression was seen in CD163+ and CD163- subsets from stable IPF monocytes compared to controls ( $p=0.012$  and  $p=0.048$  for CD163+ and CD163- respectively, Fig 3-11a). The percentage of MCP-1 expressing monocytes was higher in the CD163+ compared to CD163- subset in both IPF and controls following LPS and r848 stimulation (for LPS both  $p<0.001$ , for r848  $p<0.001$  and  $p<0.004$  for IPF and controls, Fig 3-11c-d). r848, but not LPS, increased the percentage of IL-6 expression by CD163+ monocytes compared to CD163- monocytes in both IPF and control monocytes ( $p<0.001$  and  $p=0.005$  respectively, Fig 3-11e-f). The table in Figure 3-11i compares the expression of each of the cytokines in CD163+ and CD163- monocytes in response to r848 and LPS. The paired data shows that CD163+ monocytes generally express higher levels of IL-10, MCP-1 and IL-6 compared to CD163- cells in response to stimulation.

Chapter 3: Monocyte phenotype in stable and acute exacerbations of IPF



### Chapter 3: Monocyte phenotype in stable and acute exacerbations of IPF

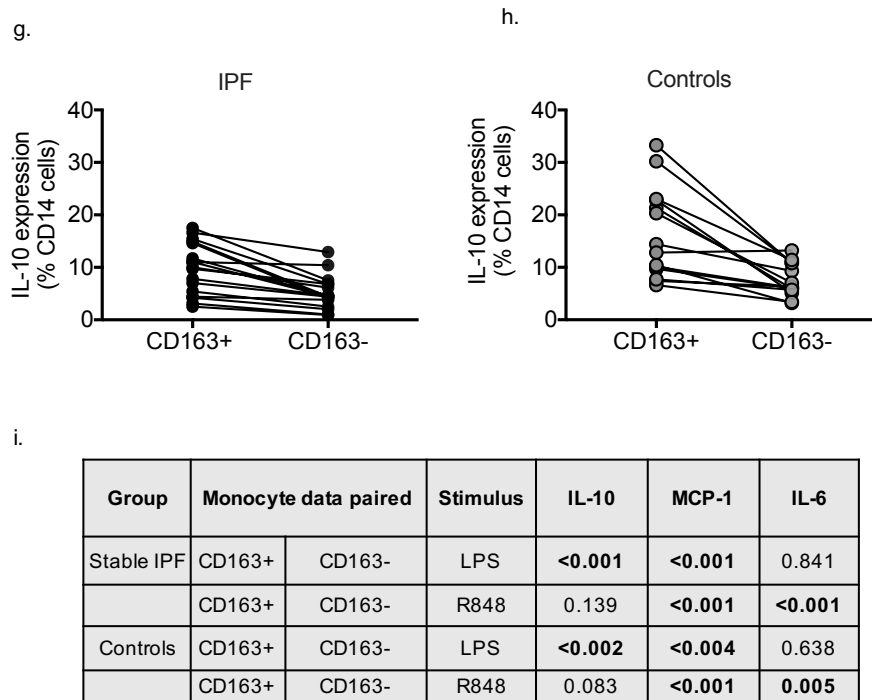


**Figure 3-11. Comparison of cytokine expression by CD163+ and CD163- monocytes in response to LPS and r848 stimulation in controls and stable IPF patients.**

Cytokine expression (indicated by % positive cells) was analysed in CD163+ and CD163- monocytes following overnight stimulation with LPS and r848 stimulation in controls (HC) and stable IPF (IPF) patients. Mean(SD) are described here and illustrated on graphs. (a) Following LPS stimulation, the percentage of monocytes expressing IL-10 was higher in CD163+ than in CD163- monocytes in both IPF and HC (paired data shown in g-h). IL-10 expression was lower in both CD163+ and CD163- monocytes from IPF patients compared to HC (CD163+ monocytes IPF vs HC: 9.81%(4.89) vs 16.43%(8.73) and CD163- monocytes IPF vs HC: 5.13%(3.13) vs 7.46%(3.11)  $p=0.012$  and  $0.048$  respectively. IPF  $n=17$  and HC=14, Student t-test). (b) No differences in IL-10 expression were noted in CD163+ and CD163- monocytes in response to r848 by IPF or HC monocytes. (c-d) The percentage of monocytes expressing MCP-1 was higher in CD163+ cells than CD163- monocytes in both IPF and HC following stimulation by LPS and r848 [CD163+ vs CD163- LPS: IPF 19.4%(28.4) vs 12.8%(20.8),  $p<0.001$ ; HC 34.6%(14.2) vs 21.4%(7.1)  $p<0.001$ , IPF  $n=17$  HC=14. CD163+ vs CD163- r848: IPF 49.9%(63.5) vs 27.5%(37.5)  $p<0.001$ ; HC 57.5%(21.8) vs 32.8%(12.9)  $p<0.004$ , IPF  $n=16$  HC=13, paired t-test] (e) IL-6 expression by CD163+ and CD163- monocytes following stimulation by LPS was not significantly different in either IPF or HCs. (f) In response to r848, a higher percentage of CD163+ monocytes produced IL-6 compared to CD163- monocytes in both IPF and HC (CD163+ vs CD163- r848: IPF 21.2%(32.2(27.9) vs 24.8%(4.8), HC 31.8%(12.1) vs 17.9%(8.6)  $p<0.001$  and  $0.005$  respectively IPF  $n=16$  HC=13). (g) Paired t-tests were performed on CD163+ monocytes and CD163- monocytes from IPF patients and (h) controls demonstrating that CD163+ monocytes express higher levels of IL-10 in response to LPS stimulation compared to CD163- monocytes. (i) Table summarising the p-values from paired CD163+ and CD163-monocyte data looking at the expression of IL-10, MCP-1 and IL-6 from stable IPF patients and controls in response to LPS and r848 (paired t-test/Wilcoxon test used). D'Agostino and Pearson omnibus normality test and Student t-test or Mann-Whitney test used for statistical analysis unless otherwise stated. P values  $<0.05$  taken to indicate statistical significance.

### 3.5 Discussion

Detailed characterisation of monocytes in the context of disease may be important. The prevailing paradigm that monocyte functionality is dictated by local signals has become questioned in recent years. Newer studies have provided evidence that monocytes may be primed early on during bone marrow (BM) development to perform specific functions following release into the periphery. Askenase *et al.* (2015). showed that early infection with *Toxoplasma gondii* prior to the onset of systemic inflammation resulted in transcriptional reprogramming of BM monocytes towards a regulatory phenotype [182]. The mechanism by which this occurred was through local IFN $\gamma$  release by activated NK cells within the BM. Studies looking at BCG responses have shown that childhood mortality from unrelated infections was reduced in vaccinated compared to unvaccinated children. This observation was linked to the epigenetic reprogramming of monocytes in response to vaccination resulting in long-term changes in function, a process referred to as 'Trained Immunity' [270]. Thus, variations in monocyte phenotype noted in humans may be partly the result of prior environmental exposures that modulate monocyte characteristics. Furthermore, specific types of exposures may result in reprogramming monocytes to perform particular functions that in response to further challenge may be detrimental, rather than beneficial, to the host. The data presented in this chapter has demonstrated differences in monocyte phenotype between healthy controls and IPF patients that may be of relevance to the pathogenesis of the disease.

In this study, monocytes were characterised in two ways. Initially, I examined monocyte phenotype according to the traditional classification system based on CD14 and CD16 expression. However, unlike autoimmune diseases such as SLE and RA [250, 253], differences in the monocyte subsets were not observed between stable IPF patients and controls. I then looked at markers associated with polarised macrophages within these subsets to determine if variations in receptor expression existed, and also to compare how receptors associated with inflammatory (M1) and reparative/regulatory (M2) macrophages related to the traditional subsets. The results showed differences in receptor expression on IPF monocytes but only partial concordance was seen when combining the two classification systems to define inflammatory and reparative/regulatory populations. The M1 marker CD64, for example, was most highly expressed on classical monocytes which are generally associated with inflammatory responses. The 'M2' marker CD163, however, was also expressed most intensely on the

### Chapter 3: Monocyte phenotype in stable and acute exacerbations of IPF

classical subset, whereas M1 markers CD86 and CCR7 were expressed at similar levels in all monocyte subgroups. There are several possible explanations for this observation. Firstly, the expression and function of these receptors may differ on monocytes compared to macrophages. CCR7 expression on monocytes, for example, may be up-regulated only by cells after they have entered the tissue [271], and CD163 expression may not in fact indicate an M2 bias. Indeed, it is possible that it may even be upregulated by certain inflammatory stimuli. CD163<sup>+</sup> monocytes were found to be a more 'activated' subset, producing higher levels of both inflammatory and immunoregulatory cytokines following stimulation (Section 3.4.9). Secondly, the traditional subsets in humans are less well defined compared to mice where Ly6C<sup>hi</sup> and Ly6C<sup>lo</sup> monocytes have fairly clear roles in response to injury and infection [272]. Thus, whilst the classical subset has been associated with inflammatory activities, this is not the universal consensus and elevation of non-classical monocyte levels during systemic inflammation [176] suggests that the spectrum of monocyte functionality is significantly more complex than can be defined by three subsets. Similarly, attempting to characterise *ex vivo* monocyte/macrophage populations according to *in vitro* polarised responses can be problematic, as cells within the periphery and in tissue integrate a variety of signals at any one time resulting in simultaneous expression of both 'M1' and 'M2' markers.

Despite the difficulties in characterising monocytes using these classification systems, the phenotypic differences in IPF monocytes are likely to be of relevance. Applying macrophage markers to monocytes from IPF patients did not identify cells with an M2 bias but rather showed up-regulation in the M1 marker CD64 (FcγRI). CD64 is elevated in autoimmune diseases such as RA and lupus [250, 251, 253] and one of the mechanisms by which CD64 exerts pathogenic responses is thought to be through its interaction with immune complexes that trigger a pro-inflammatory response. The release of cytokines such as MCP-1 and macrophage inflammatory protein-1 (MIP-1) following activation of the FcγRI receptor results in the recruitment and infiltration of monocytes and immune effector cells that then accentuate tissue damage [251]. Of interest, studies have reported high levels of immune complexes in the BALF of IPF patients, which correlated with the release of neutrophil chemoattractant by alveolar macrophages [273]. CD64 is also elevated in critically ill patients with systemic inflammatory response syndrome (SIRS) and the metabolic syndrome and is thus a marker closely associated with inflammatory responses [274, 275]. Interestingly, a study comparing monocyte profiles in patients with stable and progressive IPF (defined by a



### Chapter 3: Monocyte phenotype in stable and acute exacerbations of IPF

fall in functional vital capacity (FVC) >10%, transfer factor for carbon monoxide (TLCO) >15%, AEIPF or death) found that elevated percentages of CD64-expressing intermediate monocytes were associated with poor survival outcomes [259]. It is unknown whether the up-regulation of CD64 on monocytes occurs in response to disease processes, or whether monocytes highly expressing this receptor play a role in the pathogenesis of certain diseases themselves. It can be hypothesised that cumulative environmental exposures in susceptible individuals may lead to BM priming of monocyte precursors resulting in a phenotype that predisposes to the development of IPF. Subsequent disease-triggering events such as alveolar epithelial cell injury may then result in the homing of primed monocytes to sites of lung injury, which then potentiate rather than limit tissue damage, eventually leading to fibrosis.

Higher proportions of monocytes were noted in patients with stable IPF and AEIPF compared to controls. Patients with AEIPF were all administered high-dose corticosteroids (CS) within 14 days of sampling and 50% were on maintenance doses of prednisolone. Work investigating the effects of CS on monocytes demonstrated that cells treated with steroids and then exposed to the apoptosis-inducer staurosporine showed significant resistance to cell death compared to untreated cells. The anti-inflammatory profile of CS-treated monocytes is also associated with longevity [205] and in combination with reduced monocyte apoptosis, may explain the higher monocyte levels seen in AEIPF. Stress responses, such as those induced by strenuous exercise and myocardial ischaemia (and potentially AEIPF) [276, 277] can also rapidly increase monocyte levels. Animal studies have revealed the presence of monocyte reservoirs within the spleen that can be mobilised within minutes providing an explanation for rapid shifts in monocyte numbers during periods of physiological and pathological stress [276, 278]. The high monocyte levels in patients with stable disease are more difficult to explain but have also been observed in patients with systemic sclerosis-associated ILD (SSc-ILD) [279] and may be linked to the systemic release of soluble mediators from areas of active disease. Indeed, a study published in 1999 demonstrated elevated levels of the monocyte chemoattractant MCP-1 in the BAL of IPF patients [246], whilst a more recent study found elevated levels of the same chemokine were present in the serum of IPF patients with progressive disease [236]. The activation of lung macrophages in response to subclinical viral infection during AEIPF may also enhance production of MCP-1, as demonstrated in the *in vitro* r848 data herein (Section 3.4.8). This chemokine may then stimulate egress of monocytes from the bone marrow.

### Chapter 3: Monocyte phenotype in stable and acute exacerbations of IPF

Monocytes sampled from patients with acute exacerbations were significantly different to both controls and stable patients. Whilst strongly polarised responses are rarely seen *in vivo*, there are a few exceptions, such as the M2 macrophage bias seen in response to chronic parasitic infection in murine models [225, 226]. In this study, AEIPF monocytes showed a polarisation pattern consistent with 'M2c' macrophages. Elevated cell surface expression of CD163 was found, alongside gene transcripts that were high in *IL-10*, *IL1R2*, *THSB1* and *CD163*. This profile mirrors *in vitro* monocyte differentiation in the presence of corticosteroids [196, 205]. M2c responses are associated with immunoregulation, matrix deposition and tissue remodelling [126] and thus the polarisation characteristics of *ex-vivo* monocytes in this patient population may be of pathological significance. Indeed, there is evidence from other studies that AEIPF events represent an acceleration of the underlying disease process. Gene expression patterns from AEIPF lung explants were not indicative of superimposed inflammation but rather showed higher expression of genes that were noted to be up-regulated in stable disease, such as those related to AEC injury and proliferation [280]. Another study examining BAL fluid found elevated levels of M2 cytokines/chemokines including IL-1ra, MCP-1, CCL18 and CCL22 in both stable and AEIPF patients but levels were highest in those with exacerbations [240]. Interestingly, the graphical gene expression data (Fig 1-7g-k) revealed a trend towards decreased expression in stable IPF patients that sits part-way between controls and AEIPF. Thus, whilst corticosteroid administration may complicate the interpretation of the immunophenotyping data in patients with AEIPF, it may not provide the full explanation for the findings. Exogenous triggers, such as viral infection prior to the clinical onset of AEIPF, may also modulate the monocyte phenotype which could then contribute to the acceleration of the disease process. Alternatively, the polarised monocytes seen in AEIPF may be secondary phenomenon occurring in response to the injurious processes within the lung. CD163 in particular can be up-regulated during physiological responses to injury. Studies have shown that extracellular free haemoglobin is increased in inflammation, infection and trauma and acts as a DAMP, mediating the release of inflammatory cytokines and exerting a direct toxic effect on tissues. In response to this, haptoglobin, which binds strongly to haemoglobin, is increased, which may in turn result in the upregulation of CD163 on macrophages to facilitate clearance of haemoglobin-haptoglobin complexes. This process has been found to stimulate macrophage production of IL-10, which may in turn potentiate wound healing responses [281]. Regardless of the mechanisms involved in the polarisation of

### Chapter 3: Monocyte phenotype in stable and acute exacerbations of IPF

monocytes in AEIPF, an influx of M2 monocytes into the lung during these events may have detrimental consequences.

Differences in RNA expression were also observed between stable patients and controls. Whilst less dramatic than those seen in AEIPF monocytes, the findings are of interest as they provide evidence that IPF monocytes collectively differ from age-matched healthy controls. A trend towards lower *TNF $\alpha$*  and higher *IL-10* expression was observed, in keeping with 'M2' polarisation. In contrast, *FGL2*, which codes for fibrinogen-like protein-2, and *CD14* were significantly lower in IPF monocytes compared to controls. Martinez et al (2006) studied the gene expression of polarised macrophages in vitro and found that both *FGL2* and *CD14* were associated with M2 phenotypes and down-regulated by M1 stimuli. This again highlights the complexity and difficulty of attempting to categorise ex-vivo monocytes into defined populations based on in vitro polarisation. Discrepancies in RNA and phenotyping data are common and exist in the data presented in this chapter. The MFI of CD14 was increased in IPF monocytes yet the mean fold gene expression was lower compared to controls. Furthermore, in AEIPF monocytes, IL-10 cytokine expression was reduced in the flow analysis yet significantly upregulated in the monocyte RNA. With regard to IL-10, there may be several reasons for these differences. Firstly, it is likely that the response of cells within a plastic well to a purified TLR4 receptor agonist does not reflect in vivo responses. Secondly, the higher expression of *IL-10* RNA IN AEIPF by freshly isolated, unstimulated monocytes may indicate that IL-10 is already upregulated during exacerbations resulting in an impaired ability to mount a greater response following further stimulation. Lastly, the transcription of genes and the subsequent translation to activated proteins are not always directly proportionate.

IPF is characterised by progressive extracellular matrix deposition and it is postulated that external factors that cause tissue damage perpetuate the disease process and prevent tissue restoration. Respiratory tract infections by viruses are common and there is some evidence that they may act as co-factors in disease progression [64]. I was therefore interested in looking at the response of monocytes to ligands that activate TLRs involved in viral recognition. I postulated that the phenotypic and cytokine repertoire of monocytes in response to different TLR ligands would differ in IPF and this may have pathological consequences in vivo when monocytes encounter viruses within the lung. Phenotypic changes were noted following overnight incubation with LPS and r848 which did not differ significantly between patients and controls but did reveal some interesting findings. The most striking phenotypic change seen was a decrease in CD163

### Chapter 3: Monocyte phenotype in stable and acute exacerbations of IPF

expression on LPS treated monocytes in all groups. CD163 is defined as a M2 marker and therefore on initial consideration, lower expression was not unexpected in response to an M1-polarising agent. However, when comparing CD163+ and CD163- monocytes, expression of cytokines IL-6, MCP-1 and IL-10 were all higher in the CD163+ monocyte subset. There is a possible explanation for the seemingly contradictory finding that CD163 is simultaneously associated with 'M2' responses alongside enhanced inflammatory cytokine responses. A study by Fabrick *et al.* (2009) demonstrated that CD163, in addition to its role as a haemoglobin-haptoglobin scavenger receptor, also functions as a pattern recognition receptor (PRR), recognising both gram negative and gram positive bacterial components. Upon binding to LPS, CD163 is shed from the cell surface in a soluble form and thus serves to dampen down inflammatory responses induced in monocytes by LPS. Therefore, measurement of CD163 on the cell surface of the monocyte may not always provide information on its polarisation state [282]. Interestingly, and in contrast to the findings here, a study looking at monocytes from patients with SSc-ILD found higher expression of CD163 on the surface of SSc-ILD monocytes in response to LPS than controls [279]. The authors concluded that this related to an M2 bias, but may in fact represent the opposite. In keeping with the reported role of CD163 as a PRR for bacteria, r848 did not influence CD163 expression, which remained similar to unstimulated cells. Expression of MCP-1 however was far higher in response to r848 than LPS and given that this chemokine is a major chemoattractant for monocytes and stimulates BM egress of these cells, this finding may be of pathophysiological significance during viral encounters within the IPF lung.

This study has highlighted some of the difficulties in attempting to characterise monocytes based on macrophage polarisation markers. Whilst some receptors such as CD64 appear to represent inflammatory responses in both monocytes and macrophages and concur with the traditional monocyte subsets, other markers were less informative. CD206 was expressed at a very low level on monocytes, limiting its utility as a marker of pro-repair responses. CD163 was thus the sole marker used and due to its up-regulation in the presence of corticosteroids, interpretation of monocyte phenotype in AEIPF was limited. Thus, extending the repertoire of markers associated with 'M2'/reparative activity in this study may have provided additional phenotypic information. Furthermore, only three cytokines were included in the results as although fluorochrome-conjugated monoclonal antibodies to IL-4, IL-13 and IL-17A were used in preliminary studies, minimal expression was seen. This may have been due to the relatively low sensitivity

### Chapter 3: Monocyte phenotype in stable and acute exacerbations of IPF

of flow cytometry for cytokine detection and alternative techniques, such as ELISA, may have provided useful information regarding cytokine responses by monocytes from patients and controls. Whilst unlikely to be of significance, overnight stimulation may have up-regulated CD14 expression on PBMCs other than monocytes, such as on dendritic cells. All cells expressing CD14 (in the absence of CD15) were taken to represent monocytes, so the presence of other CD14 expressing cells may have slightly skewed the interpretation of the data.

The results presented here do not support the hypothesis that IPF monocytes are biased towards an M2/reparative phenotype, but differences in monocytes from IPF patients compared to aged-matched healthy controls have been identified. Monocyte levels are higher in IPF, expression of the M1 receptor CD64 is increased and genes *FGL2*, *CD14* and *CD163* are reduced. Monocytes from patients with AEIPF show a distinct phenotype which may have been moulded by processes linked to the pathophysiology of acute exacerbations although these are difficult to disentangle from corticosteroid administration. I have also demonstrated that monocytes respond differently to viral and bacterial PAMPs, which may be of pathophysiological significance during viral infection affecting the lungs of IPF patients. Despite being considered an 'M2' receptor in macrophages, work here found that monocytes expressing CD163 exhibited enhanced cytokine responses, suggesting that CD163 is associated with a more 'activated' phenotype in monocytes. How these observations relate to the disease processes occurring within the lung parenchyma has been hypothesised but further work is needed to shed light on the potential role monocytes may play in IPF and is the subject of the subsequent chapters.

## **4 Fibrotic burden, anti-fibrotic treatment and monocytes in IPF**

### **4.1 Introduction**

In the previous chapter I showed that monocyte levels were increased in IPF patients and expression of cell surface receptors, such as CD64, differed in comparison to healthy controls. In this chapter I examined the relationship between monocyte levels and phenotypic markers with indices of disease severity and anti-fibrotic treatment.

Determining the severity of disease in IPF can be problematic. Worsening breathlessness can signify progression of disease but this is often subjective and can be complicated by other co-morbidities. Commonly used physiological parameters include the forced vital capacity (FVC) and transfer factor for carbon monoxide (TLCO), although they do not always truly reflect disease extent. The FVC is broadly representative of lung volume and a fall in the value often indicates progression of the disease due to accumulating scar tissue contracting and shrinking the lung parenchyma [283]. The TLCO provides a measurement of the integrity of gas exchange units within the lung. Diseases affecting the interstitium (such as fibrosis) impair the ability of gases to transfer across the alveoli leading to a reduction in the value [284]. These measurements can be unreliable in the context of co-existent lung disease. Emphysema is present in up to a third of patients with IPF [11], and destruction of the alveoli results in permanent dilatation of the airspaces leading to air trapping which artificially elevates the FVC whilst disproportionately lowering the TLCO. The composite physiologic index (CPI), developed as a research tool [247], provides a value derived from a formula that attempts to overcome the confounding presence of co-existent airways disease by encompassing the FVC, TLCO alongside the FEV<sub>1</sub>, a value that is reduced in airways disease. This index was found to correlate well with radiological and histological extent of disease, but practical issues such as difficulty in performing lung function tests and poor patient technique can still result in inaccurate readings and overestimate disease severity.

An alternative way to measure disease severity is by calculating the amount of fibrotic change present on a high-resolution computed tomography scan (HRCT). There are

## Chapter 4: Fibrotic burden, anti-fibrotic treatment and monocytes in IPF

several published methods on how to do this but no universally adopted system [102, 103, 285-289]. Two approaches for evaluating a computed tomography scan (CT) have been used in IPF studies: a quantitative method using CT-derived indexes; or qualitative visual systems involving scoring disease within subsections of lung. The quantitative method was developed to reduce inter-observer variability and uses computer-generated indices to analyse lung parenchymal attenuation according to Hounsfield Units. A study looking at quantitative CT changes in IPF found that indices correlated moderately well with lung function parameters but when the same authors compared this system with visual CT scores and lung function values over time as tools to predict prognosis, the qualitative CT score was found to be most accurate in predicting mortality [285, 286]. Indeed, the majority of studies use a visual approach involving two or more radiologists who are usually blinded to the clinical data [102, 103, 286, 289-291].

Each individual study to date has adopted a different method to quantify and characterise disease. There does however appear to be a general consensus regarding the initial approach to scoring a HRCT which includes: the anatomical localisation of lung sections to be scored (6 in total), calculation of the area of abnormality to the nearest 5%; and incorporation of HRCT diagnostic criteria for IPF as stated in the ATS/ERS/JRS/ALAT IPF Guidelines [13] (section 1.1.3). Figure 4-1 depicts the typical fibrotic features seen on CT in a patient with IPF.

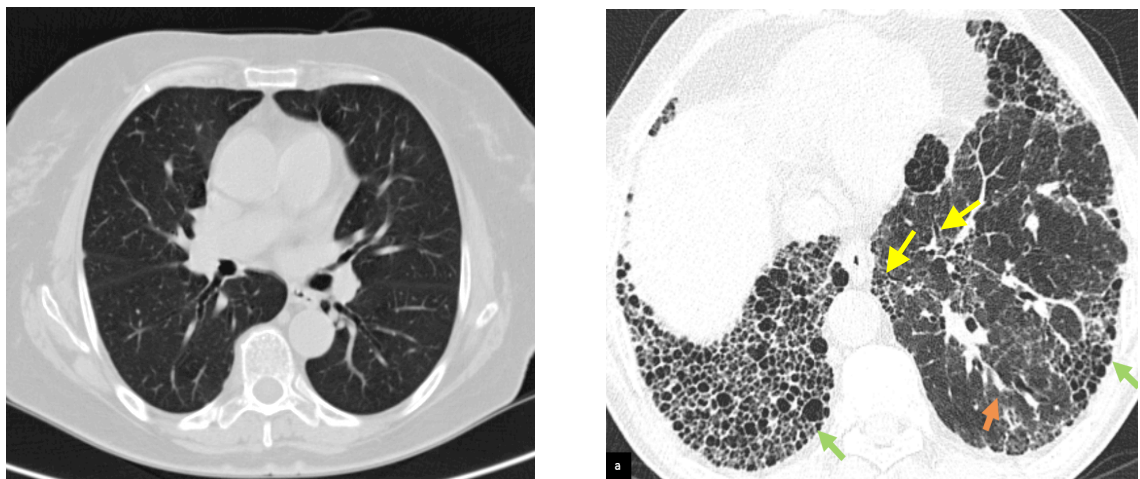


**Figure 4-1. Computed tomography (CT) images of a normal (left) and IPF lung (right).**

Green arrows demonstrate areas of honeycombing and the orange arrow shows an area of reticulation which signifies fine fibrosis. Yellow arrows point to dilated bronchi which are splinted open by the surrounding fibrotic parenchyma (traction bronchiectasis). Ground-glass changes (absent from this image) appear as areas of hazy opacification, which can signify inflammatory change but in the presence of traction bronchiectasis, usually indicates very fine fibrotic change.

## Chapter 4: Fibrotic burden, anti-fibrotic treatment and monocytes in IPF

The first aim of this study was thus to identify and optimise a CT scoring system that accurately reflected the extent of lung fibrosis in cases of IPF and provided an objective measure of disease severity that was not susceptible to the confounding factors associated with lung function parameters. Using this score, I then evaluated the relationship between monocyte levels and phenotype, with the extent of fibrosis.

The second aim of this study was to assess how anti-fibrotic treatment influenced monocyte characteristics. Almost 40% of patients within this part of the study were taking Pirfenidone at the time of blood sampling. Whilst its exact mechanism of action is unknown, Pirfenidone is thought to be pleiotropic in its activity targeting multiple fibrogenic pathways. Mouse models using bleomycin to induce lung fibrosis demonstrated a reduction of profibrotic cytokines including TGF $\beta$ , IL-1 $\beta$  and FGF, and a decrease in lung collagen content was measured following its administration [22]. Its effect on mononuclear phagocytes, however, is unknown. The second part of this study thus compares the immune characteristics of treatment naïve patients with those taking anti-fibrotic therapy to assess the potential modulating effects of Pirfenidone.

### 4.2 Hypothesis and aims

I hypothesised that monocytes from patients with IPF would exhibit distinct immune characteristics that were linked to disease extent and modulated by anti-fibrotic therapy.

To test this hypothesis, I undertook the following:

- iv. Identified and evaluated a CT-based fibrosis scoring system for IPF patients to quantify the extent of lung fibrosis and provide an objective measure of disease severity.
- v. Examined the relationship between monocyte levels and their phenotypic profile with the CT fibrosis score and other indirect indices of disease severity.
- vi. Compared the immunophenotype of monocytes from treatment naïve patients to those taking Pirfenidone.



## 4.3 Methods

### 4.3.1 Development of a computed tomography (CT) fibrosis score

For this study, a CT scoring system was devised following a review of the published literature. Whilst previous CT scores incorporated a large number radiological features into the overall score (one study looked at 22 components associated with interstitial lung disease [102]), only the principal features associated with a radiological diagnosis of IPF (i.e. those of usual interstitial pneumonia or UIP) were required in this study as all patients had a pre-existing diagnosis of the disease. The CT fibrosis score thus incorporated the HRCT diagnostic criteria for UIP as stated in the ATS/ERS/JRS/ALAT IPF Guidelines [13]. As the CT fibrosis score aimed to define the volume of fibrotic lung parenchyma, a detailed grading system was required and each fibrotic component within every section of lung was scored to the nearest 5%. In conjunction with two respiratory radiologists, the following method was used to determine the extent of fibrotic change in 40 patients with a definite or probable diagnosis of IPF:

- 1) The lungs were divided into upper, middle and lower zones. As per previous CT scoring systems, the zones were delineated by the tracheal carina defining the upper zone superiorly, the inferior pulmonary vein defining the boundary of the lower zone and the middle zone sitting in between. One standardised representative section of the CT scan was chosen per zone for scoring.
- 2) For each of the six zones, a representative section was selected and four radiological components associated with the diagnosis of UIP were quantified to the nearest 5%. These fibrotic features comprised: honeycombing, reticulation, ground glass associated with traction bronchiectasis, and traction bronchiectasis. Traction bronchiectasis was calculated by estimating the percentage of lung which contained dilated bronchi on each representative CT slice. Two components which did not support the criteria for UIP, those of ground glass change in isolation and areas of consolidation, were also measured for comparative purposes.
- 3) The Total CT Fibrosis Score (TFS) was then calculated by taking the sum score of the four fibrosis components (honeycombing, reticulation, traction

## Chapter 4: Fibrotic burden, anti-fibrotic treatment and monocytes in IPF

bronchiectasis and ground glass and traction) within the 6 zones and adding each together to reach a final score.

The CTs were scored by two interstitial lung disease (ILD)-specialist consultant radiologists, blinded to each other and the clinical data. Inter-observer reproducibility of these scores was assessed using the Pearson correlation test. A Bland-Altman analysis was performed to determine whether systematic deviation existed between the paired measurements. The mean of the scores from the two radiologists were then used for this study.

CT scans were taken within 12 months of blood sampling for monocyte profiling, except in two cases where there was an 18-month time difference as these patients had stable symptoms and static lung function findings (i.e. no evidence of disease progression).

### **4.3.2 Patient characteristics and monocyte profiling**

Patient data and samples collected for the initial characterisation of monocytes in Chapter 3 were used in this part of the study.

### **4.3.3 Lung function data collection and the composite physiologic index (CPI)**

Lung function tests (LFTs) were undertaken on the same day as blood sampling in all but 5 patients. In these cases, LFTs had been performed within three months of the appointment due to reasons of practicality. Two patients were unable to perform TLCO due to problems with technique. In instances of acute exacerbation, the most recent values obtained as an outpatient were recorded (all within a 12-month period of sampling). To obtain the composite physiologic index (CPI) [247], the following formula was used:

$$\text{CPI} = 91 - (0.65 \times \% \text{ predicted TLCO}) - (0.53 \times \% \text{FVC}) + (0.34 \times \% \text{ predicted FEV1})$$

## 4.4 Results

### 4.4.1 Patient characteristics

Table 4-1 shows the characteristics of patients involved in this part of the study. Patients have been subcategorised according to CPI to demonstrate the range of physiologically mild and severe disease. There was no relationship between patient age, sex and CPI although a higher CPI was associated with an increasing proportion of patients on anti-fibrotic agents. Only 11% of patients with stable disease had a CPI of greater than 60 whereas the mean CPI in the AEIPF group was 60.7.

Demographics	All patients	Stable IPF CPI <40	Stable IPF CPI 40-59	Stable IPF CPI 60+	Stable IPF CPI N/A	AEIPF
Number of samples	47	8	26	2	2	9
Number of patients with CT Fibrosis Score	31	5	14	1	2	9
% Male	81	87	80	85	50	78
Mean age	72.8	71.6 (64-78)	73.4 (57-80)	69 (65-74)	83 (79,87)	70.3 (52-80)
% Definite diagnosis	51	42	61	20	50	50
% Probable diagnosis	49	58	39	80	50	50
% on anti-fibrotics	41	25	39	100	0	56
Prednisolone/ Methylprednisolone (range)	4	0	3 (5-10 mg)	0	1 (5mg)	100 (15mg-1g)
Mean FVC (range)	71 (48-124)	88 (71-124)	70 (49-89)	63 (59-77)	60 (58-63)	61 (48-71)
Mean TLCO (range)	48 (18-90)	74 (57-90)	45 (31-61)	26 (25-27)	N/A	31 (18-46)
Mean FEV1 Range)	73 (40-107)	86 (70-107)	72 (40-99)	63 (59-77)	68 (63-74)	66 (45-86)
Mean CPI (range)	47 (15-6)	26 (15-37)	48 (40-59)	63 (62-63)	N/A	61 (52-67)

**Table 4-1. The demographics of patients involved in the characterisation of monocytes.**

The table includes patients sub-grouped according to CPI to give an indication of the proportions of patients with mild, moderate and severe disease. (CPI – Composite Physiologic Index; TLCO – Transfer Factor for Carbon Monoxide; FVC – Forced Vital Capacity, FEV1 - forced expiratory volume in 1 second).

#### **4.4.2 The Total CT Fibrosis Score (TFS) was highly reproducible between radiologists**

In order to determine the concordance in the fibrosis scores between the two radiologists, I examined the correlation in the percentages given by both assessors for the four components (namely, honeycombing, reticulation, traction bronchiectasis and ground glass opacification (GGO) with traction bronchiectasis [13]) alongside the TFS (the sum of all the scores).

Scores for all the fibrotic parameters were highly reproducible between the two radiologists (Fig 4-2), including the TFS. The Bland-Altman analysis undertaken on the TFS confirmed that no significant systemic deviation in the scores existed (Fig 4-2f). The TFS was used for further analyses.

## Chapter 4: Fibrotic burden, anti-fibrotic treatment and monocytes in IPF

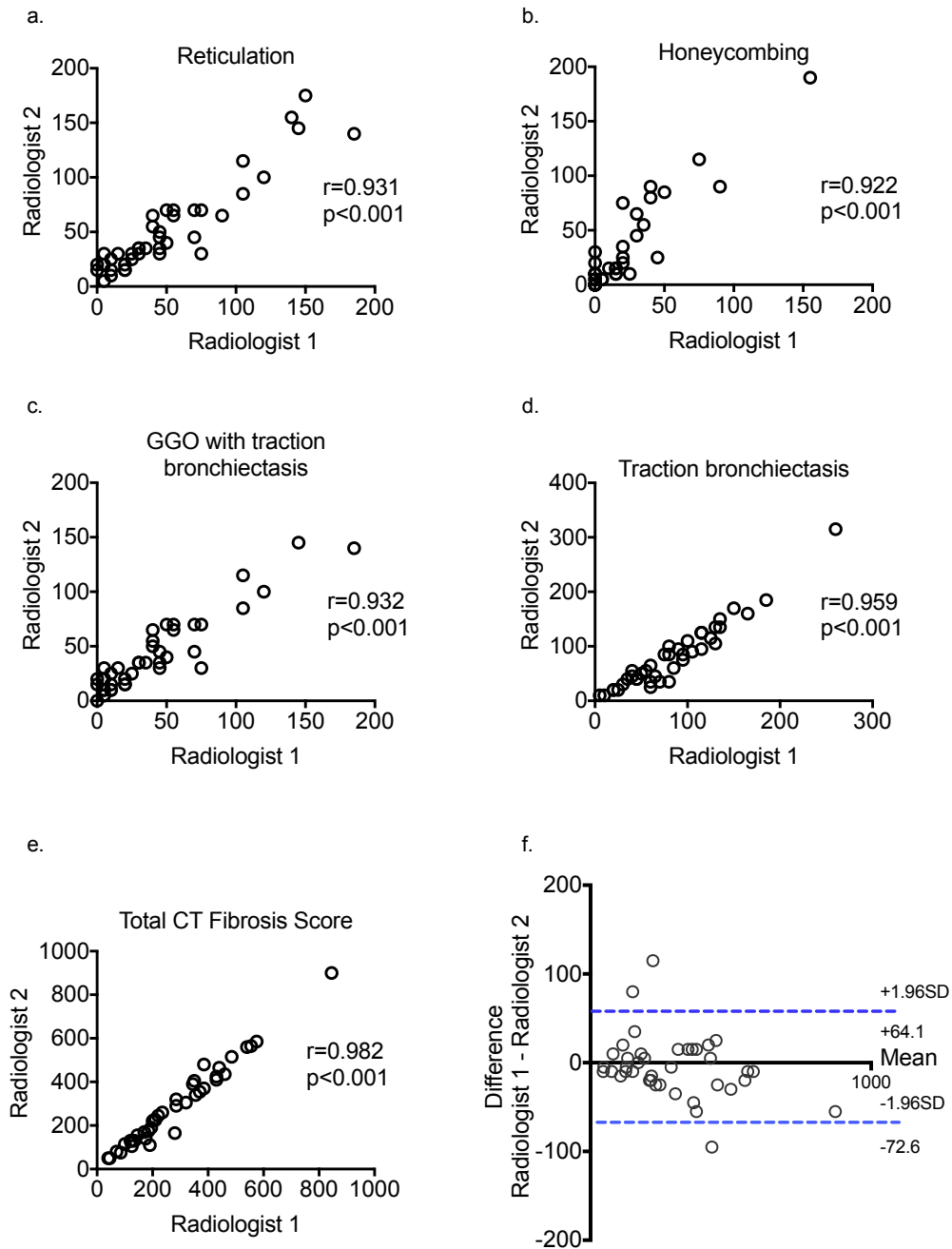


**Figure 4-2. Correlations in the scoring of fibrotic components on CT by two radiologists who were blinded to each other.**

Pearson correlation test used for a-e. Correlation in the scoring of: (a) reticulation (b) honeycombing (c) ground-glass opacification with traction bronchiectasis (d) traction bronchiectasis. (e) Correlation in the Total CT Fibrosis Score (TFS) which is the sum of these four components. (f) A Bland-Altman plot showing a lack of systemic deviation in the scoring of the Total CT Fibrosis Score by the two radiology assessors.

### 4.4.3 Validation of the TFS against lung function parameters CPI, FVC and TLCO

Disease severity in IPF is often estimated using lung function parameters but confounding factors such as coexistent lung disease and technical difficulties can make accurate interpretation difficult. The TFS should circumvent these issues and provide a direct method of measuring disease severity through the grading of amount of fibrotic tissue within the lung.

To evaluate how the TFS compares with lung function parameters, the CPI, TLCO and FVC from patients with stable disease were plotted against the TFS. Figure 1-3 shows that significant correlations were seen with all three of the lung function parameters, although the CPI most strongly correlated with the TFS ( $r=0.63$ ,  $p<0.001$ ) and the FVC was less closely associated ( $r=0.37$ ,  $p=0.03$ ). These results support the use of the TFS as a direct measure of disease severity (through grading of fibrotic extent) which is not subject to the confounding factors complicating lung function interpretation.

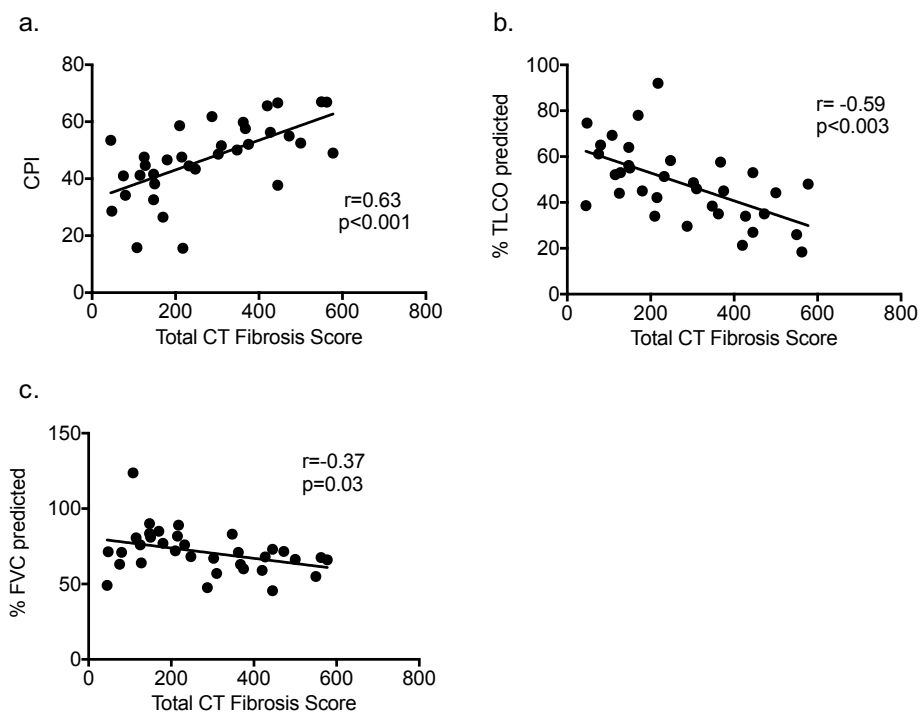


**Figure 4-3. Correlation between the Total CT Fibrosis Score and lung function parameters.** a) CPI b) TLCO and c) FVC. Pearson correlation test used.

#### **4.4.4 Monocyte levels correlated positively with the TFS but not with lung function parameters**

Using flow cytometry to identify monocyte populations, I questioned whether monocyte levels in IPF were associated with the extent of fibrosis using the TFS.

The TFS was compared to the percentage monocytes within peripheral blood mononuclear cells (PBMCs) in patients with stable disease. AEIPF were excluded from this analysis due to the possible confounding effects of corticosteroids on monocyte levels. Figure 4-4a demonstrates the strong correlation between the TFS and the proportion of monocytes ( $r=0.577$ ,  $p=0.006$ ) in patients with stable IPF. To determine which of the fibrotic components were most closely associated with monocyte levels, honeycombing, traction bronchiectasis, GGO with traction and reticulation were individually examined. Honeycombing and traction bronchiectasis were found to correlate significantly with monocyte percentage ( $r=0.520$ ,  $p=0.016$  and  $r=0.518$ ,  $p=0.016$  respectively, Fig 4-4b-c). The correlation values for ground glass change with traction bronchiectasis did not reach statistical significance ( $r=0.432$ ,  $p=0.0503$ , Fig 4-4d).

Chapter 4: Fibrotic burden, anti-fibrotic treatment and monocytes in IPF

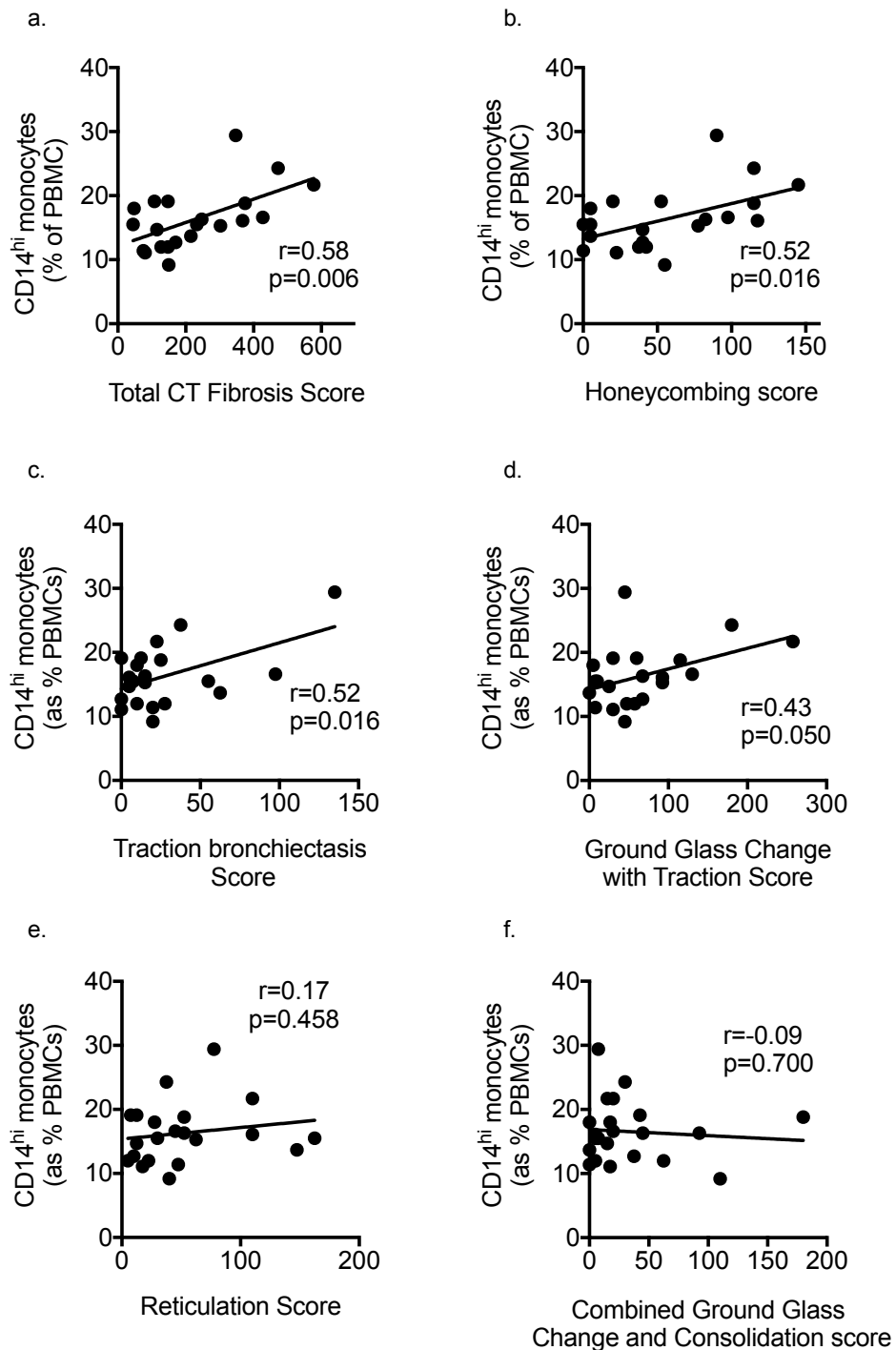


**Figure 4-4. The correlation of monocyte levels (represented as % of PBMCs) with the Total CT Fibrosis Score and the individual fibrotic components that make up the total score.**

Pearson correlation used for all analyses. The percentage of CD14<sup>+</sup> cells (monocytes) within PBMCs were correlated with: (a) The Total CT Fibrosis Score (b) Honeycombing (c) Traction bronchiectasis (d) Ground glass change with traction (e) Reticulation Score. n=21.



## Chapter 4: Fibrotic burden, anti-fibrotic treatment and monocytes in IPF

Given the correlation of the TFS with lung function parameters, I was interested in determining whether monocyte levels also correlated with these values. I thus compared the CPI, TLCO and FVC with monocyte percentage in stable IPF patients. In contrast to the TFS, no correlations were observed with any of the lung function parameters [CPI  $r=0.06$   $p=0.704$ ; TLCO  $r=-0.07$   $p=0.680$ ; FVC  $r=-0.07$   $p=0.675$  (Fig 4-5a-c)].

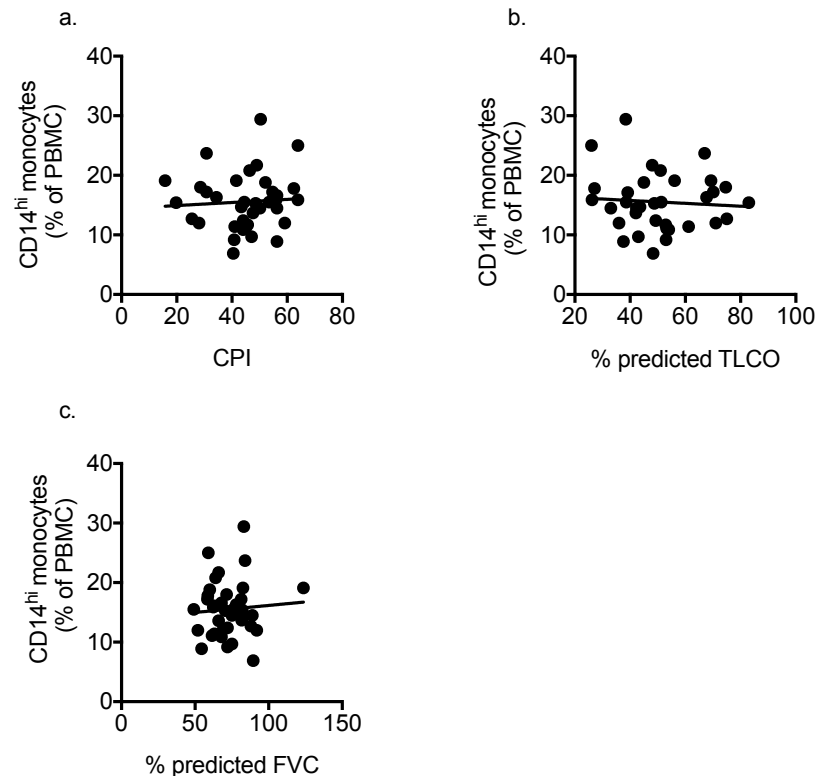


**Figure 4-5. The relationship of monocyte percentage (of PBMCs) and lung function values.**

Pearson correlation used for all analyses. (a) CPI (b) Percentage predicted TLCO (c) Percentage predicted FVC in stable IPF patients. (a) and (b)  $n=36$ , (c)  $n=38$ .

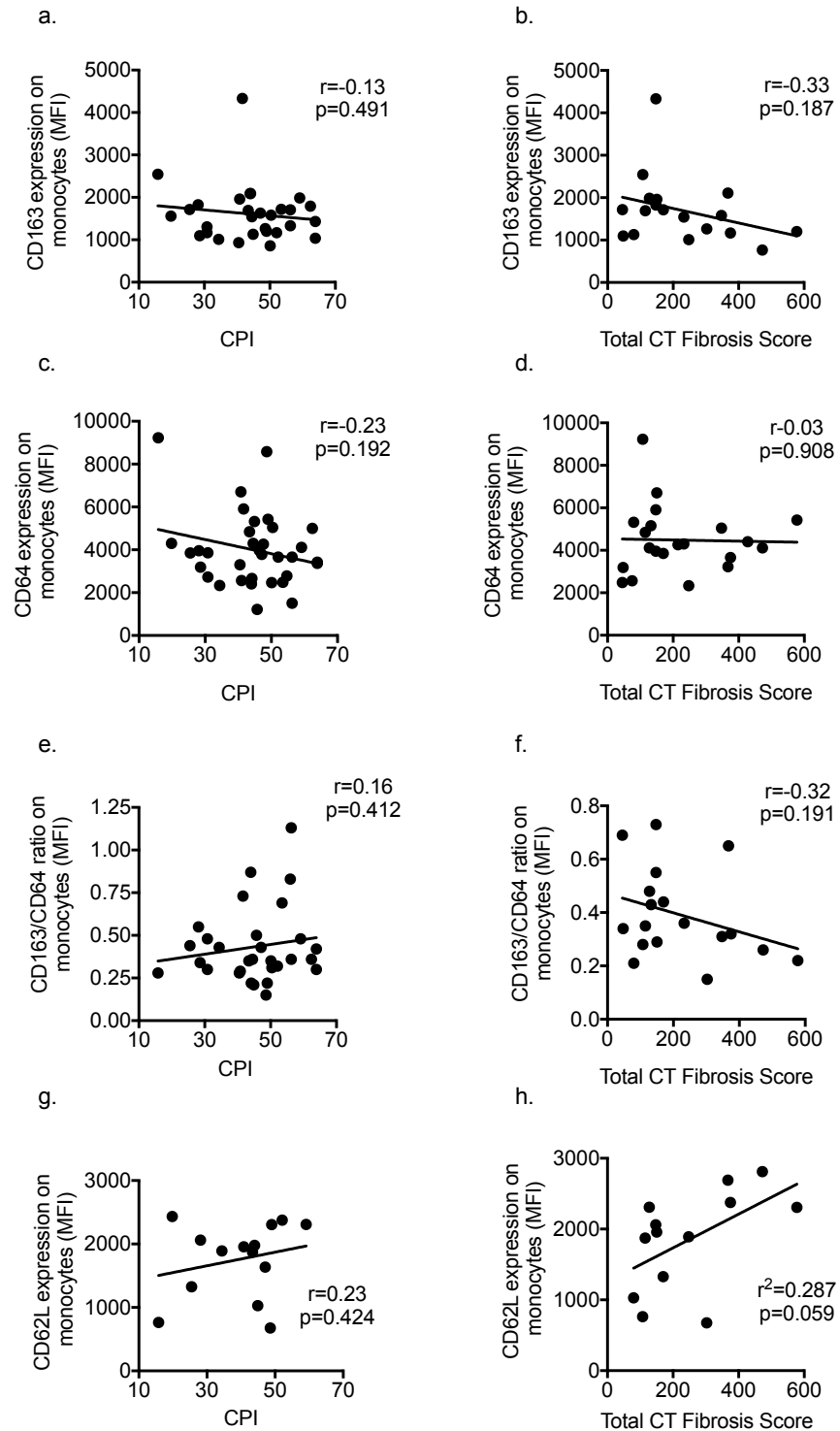
### 4.4.5 Cell surface markers CD64, CD163, CCR7, CD62L on monocytes and the CD163/CD64 ratio did not correlate significantly with the TFS or lung function indices

To examine whether there was an association between monocyte immunophenotype and indices of disease severity, correlations were undertaken comparing the expression (MFI) of CD62L, CCR7, CD163, CD64 and the CD163/CD64 ratio with the TFS and CPI in stable patients.

## Chapter 4: Fibrotic burden, anti-fibrotic treatment and monocytes in IPF

There was no statistical significance observed between any of the phenotypic markers and the TFS or CPI (Fig 4-6). CD62L however showed a trend towards higher expression in patients with a greater disease burden on CT. CCR7 was only measured on a small number of patients due to problems with the availability of antibody but shows a possible downward trend in patients with higher TFS scores (Fig 4-6j).

## Chapter 4: Fibrotic burden, anti-fibrotic treatment and monocytes in IPF



## Chapter 4: Fibrotic burden, anti-fibrotic treatment and monocytes in IPF

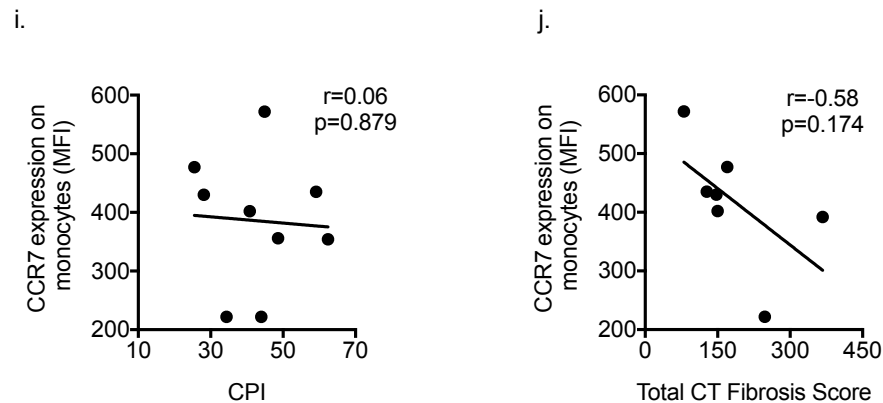


**Figure 4-6. Correlations between the CPI, Total CT Fibrosis Score (TFS) and cell surface receptors CD163, CD64, CD62L, CCR7 and the CD163/CD64 ratio to look at M2/M1 balance in different severities of disease.**

Pearson correlation used for all analyses. (a) The correlation between the MFI of CD163 and the CPI  $n=29$ . (b) The correlation between the MFI of CD163 and the TFS  $n=18$ . (c) CD64 versus CPI  $n=34$ . (d) CD64 versus the TFS  $n=21$ . (e) The M2/M1 ratio using CD163/CD64 correlated with the CPI  $n=30$  and (f) TFS  $n=18$ . (g) CD62L versus the CPI  $n=14$  and (h) TFS  $n=13$ . (i) CCR7 versus the CPI  $n=9$  and (j) TFS  $n=7$ .

### 4.4.6 Patients with AEIPF have a higher burden of lung fibrosis than patients with stable disease

Research into acute exacerbations of IPF has been hampered by inconsistencies used to define these events as well as differences in study design and reporting standards. Studies that have sought to identify risk factors for AEIPF have found that a lower FVC at baseline, the presence of pulmonary hypertension and patients who have never smoked are at higher risk of this complication [14-16, 24, 248, 292]. It is not known however whether more severe disease itself is a risk factor. I was therefore interested in determining whether patients who had AEIPF had greater disease burden on CT. The Total CT Fibrosis Score takes into account fibrosis components, but not ground-glass change and consolidation which are super-imposed changes seen during AEIPF. It was therefore used to determine whether extent of lung fibrosis (i.e. disease severity) was associated with AE events.

Patients with AEIPF who had CT scans undertaken within 2 months of blood sampling [mean time period: 14.8 days (range 0-60)] were compared to those with stable IPF. AEIPF patients had significantly higher fibrosis scores than stable patients ( $p<0.004$ , Fig 4-7a). Patients who had CT scans taken around the time of diagnosis of AEIPF [mean

## Chapter 4: Fibrotic burden, anti-fibrotic treatment and monocytes in IPF

difference in blood sampling from CT: 8.9 days (range 0-29)] had significantly higher scores of consolidation and ground glass change, in keeping with the diagnosis of AEIPF ( $p=0.001$ , Fig 4-7b).

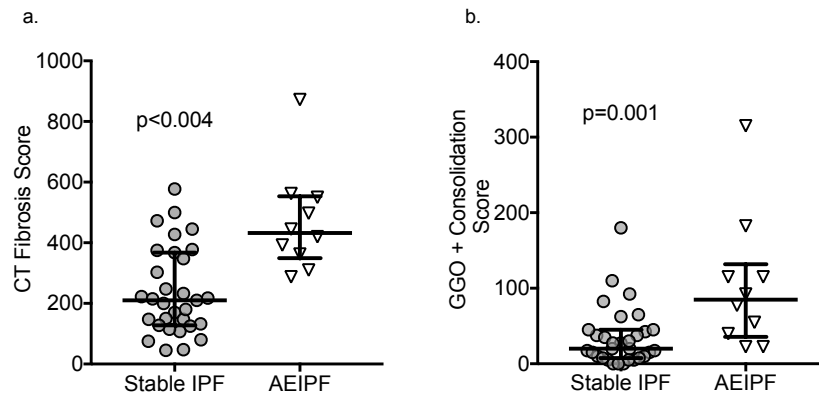


**Figure 4-7. Comparison of the Total CT Fibrosis Score and CT scores of ground-glass opacification (GGO) and consolidation in patients with stable disease and AEIPF.**

Median and interquartile range described here and depicted on graphs. (a) CT fibrosis score in stable patients and those with AEIPF: 210(127-367) vs 432(349-553) respectively. (b) CT scoring of GGO and consolidation in stable patients and those with AEIPF: 20.0(7.5-45) vs 85.0(35.6-131.9) respectively. Stable IPF and AEIPF  $n=31$  and  $10$ . Man Whitney test used for statistical analysis.

,

### 4.4.7 Pirfenidone attenuates CD64 expression on monocytes

Pirfenidone is a novel anti-fibrotic agent which attenuates the downstream effects of  $TGF\beta$ . It slows progression of the disease and recent data suggests a mortality benefit [19]. The mechanisms of its action have not been fully elicited but given its proven clinical efficacy, increasing numbers of patients are commenced on treatment. To evaluate its possible effect on monocyte phenotype, I compared patients taking Pirfenidone with treatment-naïve patients.

In the first instance, I compared the TFS and CPI between treated and untreated patients to determine whether potential differences in phenotypic markers could be due to disparities in disease severity (Fig 4-8 a-b). No significant differences were observed in Pirfenidone-treated and untreated patients. The percentage of monocytes within PBMCs were also similar between the two groups (4-8 c).

## Chapter 4: Fibrotic burden, anti-fibrotic treatment and monocytes in IPF

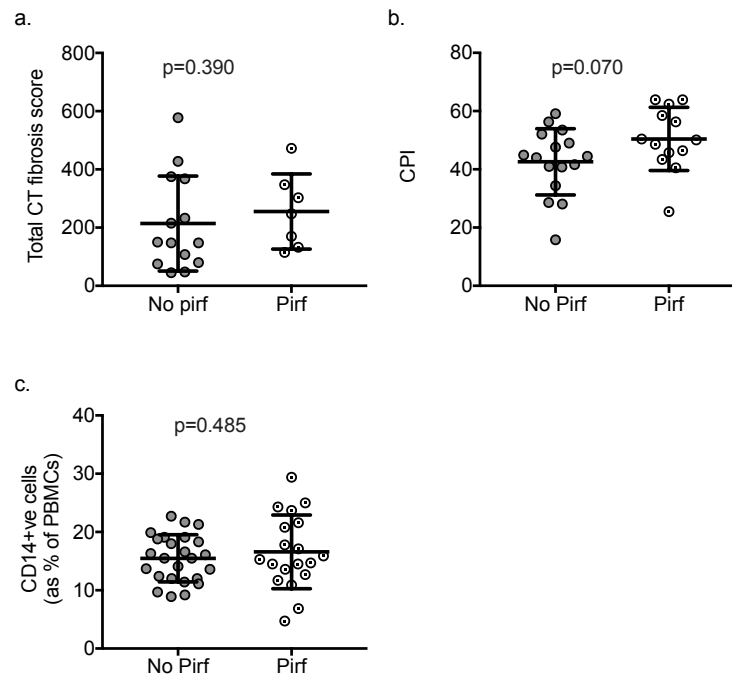


**Figure 4-8. The clinical parameters and monocyte percentages of patients off and on Pirfenidone (No Pirf/Pirf).**

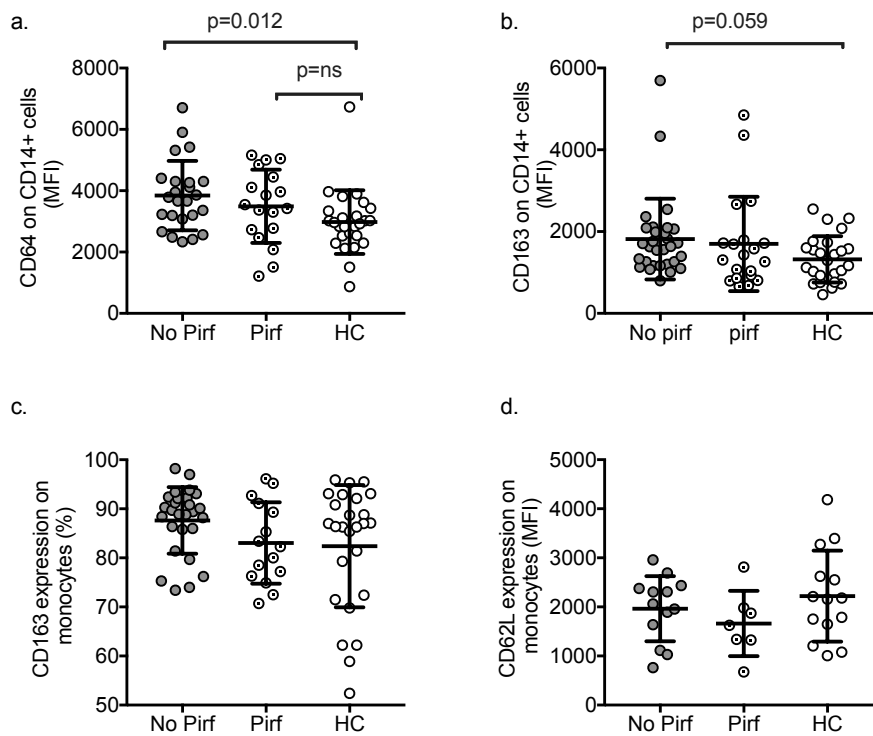
Mean(SD) depicted in graphs. (a) The total Fibrosis Score (b) the Composite Physiological Index (CPI) (c) and monocyte percentage within PBMCs. Student t test used for statistical analyses.  $P < 0.05$  taken to indicate statistical significance.

Comparisons of cell surface expression of CD64, CD163 and CD62L revealed one notable difference. CD64 expression (which is present on almost all monocytes and therefore only the MFI was compared) was lower in Pirfenidone treated patients compared to treatment-naïve patients (Adj-p=0.012 for treatment-naïve patients and controls, Adj-p=0.17 for Pirfenidone-treated IPF vs controls, Fig 4-9a). Thus, Pirfenidone appears to reduce CD64 expression on monocytes towards levels observed in aged-matched healthy controls. CD163 expression (MFI) on monocytes from treatment-naïve patients compared with treated patients and controls showed a trend towards higher expression but statistical significance was not reached (Adj-p=0.059 for treatment naïve IPF and controls, Fig 4-9b). CD62L, which is also expressed on almost all monocytes, did not show differences in the intensity of expression between groups (Fig 4-9d). CCR7 was not included in the analysis due to small sample size in the Pirfenidone group.

I next examined whether CD64 expression was associated with worsening disease in treatment-naïve patients in comparison to treated patients. As only 7 patients on

## Chapter 4: Fibrotic burden, anti-fibrotic treatment and monocytes in IPF

Pirfenidone had CT scoring undertaken, the CPI was used in preference. Examining the MFI of CD64 with the CPI revealed no significant correlations in either group although a downward trend in CD64 expression was observed in treatment-naïve patients with increasing CPI ( $r=-0.33$ ,  $p=0.140$ , Fig 4.9e) that was not seen in Pirfenidone-treated patients. There was no correlation between CD163 expression and CPI in treatment-naïve patients (Fig 4-9g-h).



## Chapter 4: Fibrotic burden, anti-fibrotic treatment and monocytes in IPF

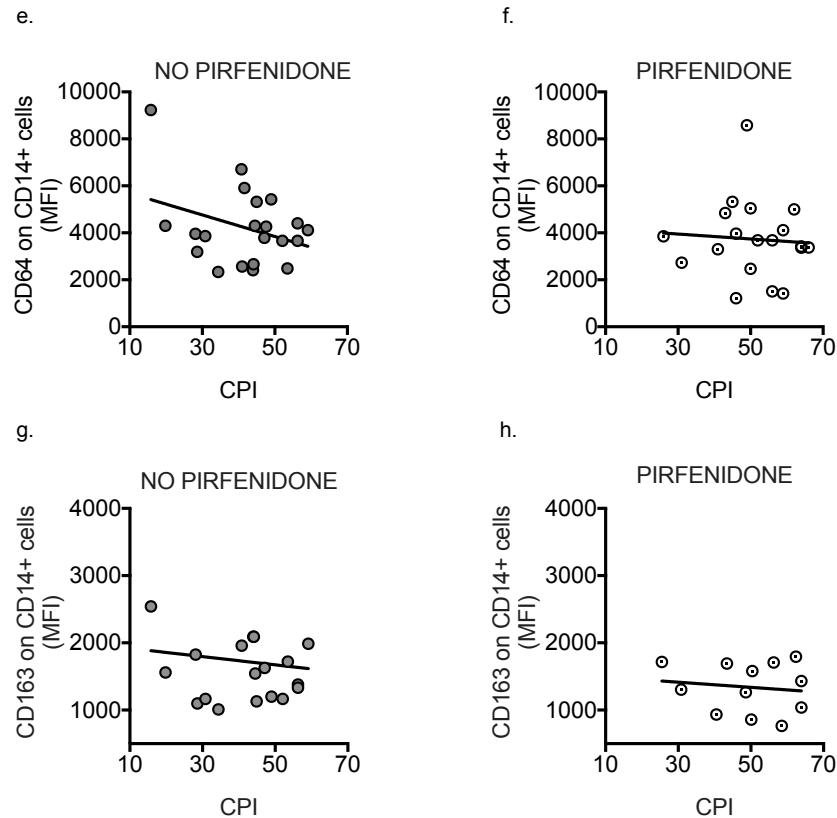


**Figure 4-9. Comparison of the expression of cell surface receptors CD163, CD64 and CD62L on monocytes from treatment-naïve patients (No Pirf), those on Pirfenidone (Pirf) and controls (HC).**

The MFI of CD64 and CD163 was plotted against the CPI to determine if disease severity in Pirfenidone treated and untreated patients correlated with the intensity of receptor expression. For figures a-d, SD(mean) is depicted in the graphs and quoted here. (a) The MFI of CD64 expression on monocytes from IPF patients not on Pirfenidone was significantly higher than in controls (Adj  $p=0.012$ ), whereas no significant difference was seen between Pirfenidone treated patients and controls (Adj  $p=0.170$ ). [SD(mean) No Pirf: 3841(1131) vs Pirf: 3492(1195) vs Controls: 2979(1039)  $n=24, 18$  and  $26$  respectively]. (b) The MFI of CD163 on monocytes from IPF patients on Pirfenidone showed a trend towards increased expression compared to controls (Adj  $p=0.059$ ). [No pirf: 1817(986.8) vs Pirf: 1698(1155) vs controls: 1321(566.4).  $n=28, 19$  and  $26$  respectively]. (c) The percentage of monocytes expressing CD163 from IPF patients not on Pirfenidone was similar to those on treatment and healthy controls. (d) CD62L expression between the three groups did not differ significantly. (e-f) Correlations between CD64 expression and CPI in patients not on treatment ( $r=-0.33$ ,  $p=0.140$ ) compared to those on Pirfenidone ( $r=-0.07$ ,  $p=0.782$ ). (g-h) Significant correlations were not seen between CD163 expression on monocytes and CPI in patients on and off Pirfenidone. For Figures a-d: Kruskal-Wallis or One-way ANOVA was used with Dunn's or Tukey's multiple comparison test. Pearson's correlation test was used for graphs e-h.



## 4.5 Discussion

This chapter has examined the association between the immunophenotype and levels of monocytes, with indices of disease severity and the use of anti-fibrotic therapy. Due to the difficulties in assessing severity of disease by use of lung function parameters, I assisted in the development of a CT fibrosis scoring system that specifically identifies the radiological components of fibrosis associated with usual interstitial pneumonia; the radiological pattern seen in IPF. This CT scoring system provides a direct measure of fibrotic extent and was found to correlate closely with monocyte levels. In addition, CD62L, a cellular adhesion molecule that facilitates monocyte migration and adhesion to the endothelium, showed a trend towards increased expression in patients with greater disease burden, supporting the hypothesis that as the disease progresses, monocytes are activated and recruited to the lung where they may potentiate collagen deposition. Monocyte immunophenotype from patients on Pirfenidone was found to differ from untreated patients, with CD64 expression reduced towards control levels. It is possible therefore that this drug directly or indirectly modulates monocyte phenotype and may be one of the mechanisms by which the drug slows progression of fibrosis.

The CT fibrosis score was developed to provide a direct measurement of fibrotic extent within the lung parenchyma. The low inter-observer variability in the CT scores and close correlation with lung function parameters provide evidence that TFS is a robust tool with which to assess disease severity. The finding therefore that monocyte levels were linked to the burden of fibrosis is likely to be of significance. Due to a lack of longitudinal data it is unclear whether high monocyte levels were present in a subset of patients from the outset of the disease and thus represent a risk factor for more rapid disease progression, or if circulating monocytes increase over the course of the disease as fibrosis progresses. This latter possibility fits well with the accepted pathogenesis of the disease. IPF is thought to arise from an aberrant healing response following alveolar epithelial cell (AEC) injury. Damage to AECs initiates a cascade of profibrotic pathways resulting in release of cytokines and chemokines that potentiate matrix deposition and inhibit resolution responses. Concentrations of MCP-1, a major monocyte chemoattractant, were found to be elevated in both the BAL and serum of IPF patients and thus monocytes may traffic to the lung along this chemotactic gradient [246]. IPF is characterised by temporal and spatial heterogeneity but as the disease progresses, the burden of chronic injury accumulates and this may proportionately increase the amount of monocyte

## Chapter 4: Fibrotic burden, anti-fibrotic treatment and monocytes in IPF

chemoattractants released, stimulating greater egress from the bone marrow. Repetitive lung damage depletes populations of resident macrophages and blood-borne precursors (monocytes) may subsequently occupy vacant niches within the lung and further exacerbate the deposition of fibrotic material. The expression of CD62L, which shows a trend towards higher expression on monocytes from patients with advanced disease, also supports this theory. CD62L is an important leucocyte homing receptor which enables cells such as monocytes and neutrophils to roll and adhere to the endothelium. In response to injury and inflammation, CD62L is upregulated on these cells and the endothelium simultaneously expresses a specific ligand that results in the adhesion of monocytes to the vessel wall prior to extravasation into tissue [293]. Interestingly, when examining the association of individual fibrotic components with monocyte levels, the closest correlation seen was with honeycombing whereas no correlation was observed with reticulation. The presence of honeycombing enables a diagnosis of 'definite' (rather than 'probable') IPF to be made, whereas reticulation is a feature of many interstitial lung diseases, raising the possibility that monocytes play a specific role in IPF that may not extend to other forms of fibrotic lung disease.

Whilst lung function values correlated well with TFS, they were not found to correlate with monocyte levels. This is likely to be because these parameters provide different information. The TFS gives a measure of pathological extent of disease, whereas lung function values provide a measure of physiological dysfunction. In addition to confounding factors such as co-existent disease, poor technique and variable reproducibility, the range of 'normal' lung function values span between 80-120%, so depending on the physiology of the individual, an FVC or TLCO of 70% can signify a loss of 10 to 42% of lung volume. Thus, whilst lung function parameters may provide a useful proxy measure of disease severity, the TFS provides a more reliable measure of extent of disease not affected by confounding issues.

In this study, the majority of CT scans undertaken in patients with AEIPF were performed early on following hospital admission. The CT fibrosis scores were higher in AEIPF patients, independent of super-imposed changes associated with these events. This most likely indicates that severe disease is a risk factor for exacerbation, which has been suggested by previous studies through surrogate markers such as the presence of pulmonary hypertension and a low FVC, but not noted with certainty. Indeed, Table 3-1 shows that patients with AEIPF had a higher mean CPI consolidating the TFS findings. There is also an alternative or additional explanation, which is that acute exacerbations

## Chapter 4: Fibrotic burden, anti-fibrotic treatment and monocytes in IPF

(AE) represent an acceleration of the underlying disease process and by the time the CT scans were undertaken, the increase in fibrotic burden had become visible and quantifiable. Two patients in the study had CT scans scored when their disease was stable and later during AEIPF. Despite only a 2 and 4-month period between scans, the CT fibrosis scores had increased from 472 to 497 and 302 to 392, respectively.

The previous chapter showed that CD64 was increased on monocytes from patients with stable IPF. This chapter has shown that this increase relates only to patients not on anti-fibrotic therapy. This mirrors the findings from other studies that demonstrated successful treatment of chronic inflammatory arthropathy resulted in restoration of CD64 expression to control levels [250, 253]. CD64 is an Fc receptor that activates inflammatory pathways following the binding of immune complexes (IC). These complexes result from antibodies binding to self-antigens which can then lodge in the microvasculature and cause tissue damage and inflammation. Successful treatment of autoimmune disease involves inhibiting autoantibody responses and thus the fall in CD64 expression observed after successful treatment may be a secondary phenomenon. IPF is not generally considered to be an autoimmune disease but autoantibodies and high levels of ICs in the BALF and serum have been identified in a significant proportion of patients [37, 143, 158, 294] suggesting a breakdown in immune tolerance may play a role in the disease [143]. Thus, Pirfenidone may be inhibiting processes that result in IC formation and by removing this stimulus, CD64 expression becomes lowered on monocytes. Alternatively, Pirfenidone may reduce CD64 expression directly through its recognised inhibitory effect on inflammatory processes. Pirfenidone may also modulate monocyte phenotype indirectly by attenuating the environmental cues (such as inhibiting TNF $\alpha$  production [295]) that promote 'M1' responses by monocytes).

The findings in this chapter support the hypothesis that monocytes play a role in the progression of IPF. The mechanism by which they influence fibrogenic processes is unknown however and larger studies, including longitudinal collection of data, would be useful in the first instance to further examine the relationship between monocytes and disease burden. If the findings presented here are consolidated, they may serve a clinical application. Whilst CT fibrosis scores provide a robust measure of disease burden and are likely to play a role in determining end-points in future IPF clinical trials [296], they are time-consuming to score and lack of radiologist expertise in many centres means that they are unlikely to become incorporated into clinical practice. Monocyte levels, alongside other proxy markers of disease severity, such as physiological parameters,

## Chapter 4: Fibrotic burden, anti-fibrotic treatment and monocytes in IPF

may thus assist in prognostication and the decision to commence treatment or monitor more closely. Furthermore, it would be of interest and clinical relevance to establish whether CD64 expression is attenuated on monocytes from all IPF patients on treatment or restricted to patients who respond well to therapy (i.e. demonstrate a slowing in disease progression). In a study by Matt et al. (2015) [250], CD64 expression was reduced only in rheumatoid patients who experienced a positive clinical response to treatment and a fall in inflammatory markers. If this finding is reproduced in the context of IPF, it may help to select out which patients are likely to benefit from long-term use of anti-fibrotic agents and lower the threshold for stopping treatment in those with side-effects.

## **5 Phenotypic and functional characteristics of monocyte-derived macrophages from IPF patients**

### **5.1 Introduction**

Within the lung, alveolar and interstitial macrophages represent two distinct populations [183, 297]. Research over recent years has demonstrated that alveolar macrophage populations become established during foetal and early post-natal development [194]. The origin of interstitial macrophages is less clearly understood, with evidence existing to support both a haematopoietic and embryonic origin [188, 189, 269, 298]. These tissue-based macrophage populations facilitate lung homeostasis but during lung injury cell numbers become diminished [188, 189]. Monocytes play a vital role in orchestrating reparative responses and are present throughout all stages of the wound healing process. In cases of chronic injury or repeated infection, there is evidence that monocyte-derived-macrophages (MDMs) replenish vacant lung niches and can, over time, contribute to the macrophage population [193, 269]. Furthermore, studies have found that depleting peripheral monocytes in a model of murine lung fibrosis reduced fibrosis severity [25, 193].

In the previous two chapters I showed that monocyte levels were increased in IPF patients and this correlated with fibrotic burden. Phenotypic differences in IPF monocytes, such as the elevated expression of CD64 and CD14, were also observed. Monocytes from patients with acute exacerbations of IPF (AEIPF), who were taking high dose corticosteroids, also showed high expression of CD163. It is unknown however how these differences translate as IPF and healthy control monocytes differentiate into macrophages. This question is important since IPF is a tissue-specific disease and the influence of monocytes on fibrogenic processes is likely to be exerted predominantly following extravasation and differentiation within the lung parenchyma. Of significance, a recent study by Misharin et al. found that the ontogeny of murine macrophages differed in the context of lung fibrosis with monocyte-derived-macrophages representing a substantial proportion of the total population [193]. Leading investigators in IPF propose that chronic or repetitive injury exacerbates and may even drive fibrogenic processes. Such injurious stimuli, alongside the replacement of healthy tissue with fibrotic material, may deplete resident macrophages and result in a compensatory rise in macrophages

## Chapter 5: Phenotypic and functional characteristics of MDMs from IPF patients

derived from monocyte precursors. The functional and cytokine repertoire of these blood-derived cells has been found to differ from embryonically-derived macrophages and depending on their characteristics, may either enhance or inhibit matrix deposition [193, 299, 300].

The focus of this chapter was therefore to characterise monocytes following *ex-vivo* differentiation into macrophages. I was interested in determining whether IPF MDMs differed from healthy controls and whether these differences resembled macrophage phenotypes associated with reparative and profibrotic activities. To evaluate this, I looked at markers associated with defined macrophage populations identified predominantly through *in vitro* work. Using 'M1' and 'M2' as a framework, I studied the expression of cell surface markers associated with polarised phenotypes. I then compared the expression of key genes differentially expressed by macrophage populations associated with early (inflammatory) and late (reparative) stages of wound repair (Figure 5-1). To determine whether phenotypic changes observed may be related to factors within the serum, I measured the concentration of M-CSF to see if endogenous production of this growth factor differed between IPF patients and controls. To investigate whether MDMs from patients and controls exhibited functional differences that may have pathophysiological relevance *in vivo*, I looked at the generation of reactive oxygen species in response to stimulation and the release of IL-1 $\beta$  following activation of the NLRP3 inflammasome. Lastly, to determine the impact of steroid administration on monocytes, I examined at the phenotype of MDMs following both *in vivo* and *in vitro* exposure to corticosteroids.

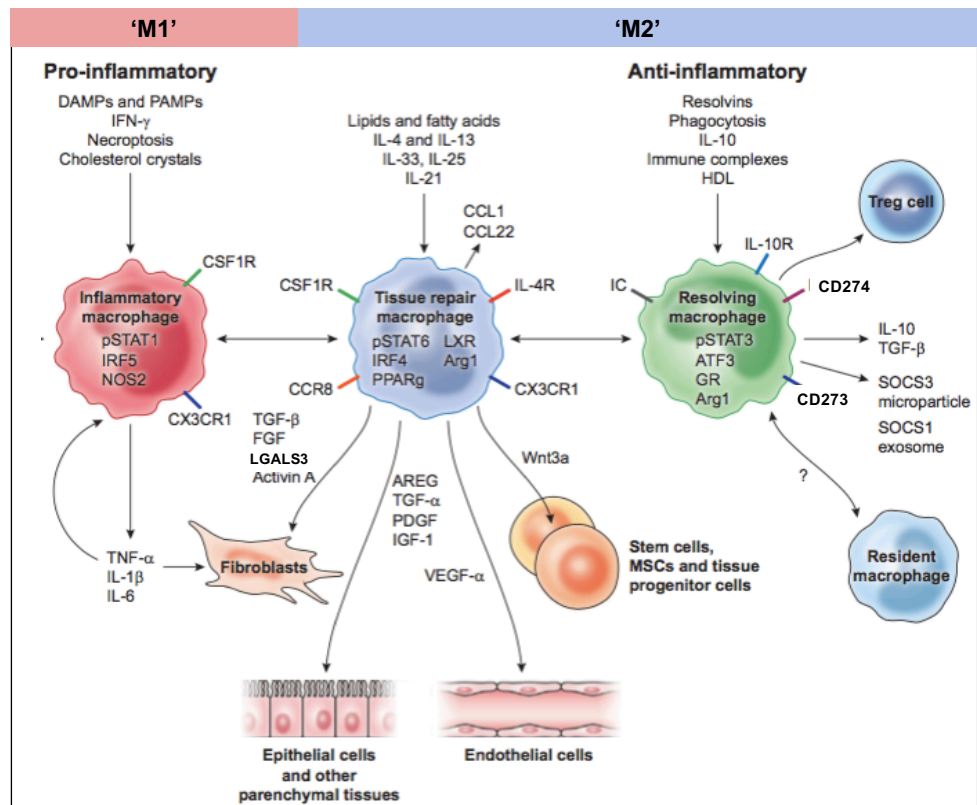


**Figure 5-1. The major macrophage phenotypes associated with inflammatory (M1) and reparative/resolution (M2) processes.**

Phenotype and function are modulated by external triggers including DAMPs, PAMPs, cytokines and other soluble factors. Transcription factors, cytosolic and cell surface proteins plus cytokines/chemokines associated with inflammatory (M1) and reparative/resolution (M2) responses are depicted in this diagram. Adapted from T Wynn 'Macrophages in Tissue Repair, Regeneration and Fibrosis' (2016) *Immunity* [126].

## 5.2 Hypothesis and aims

I hypothesised that monocytes from IPF patients differentiate into macrophages with pro-repair characteristics. To explore this, I performed the following:

1. Examined the differentiation and phenotypic characteristics of monocyte-derived macrophages from IPF patients compared with age-matched healthy controls.
2. Compared the phenotype of MDMs from patients on corticosteroids to those not on treatment in order to determine how steroid use influences monocyte to macrophage differentiation.

## Chapter 5: Phenotypic and functional characteristics of MDMs from IPF patients

3. Compared the apoptotic index of cultured monocytes during the process of macrophage differentiation in controls and IPF patients.
4. Analysed RNA expression of key genes associated with inflammatory and reparative macrophage functions.
5. Measured M-CSF to determine if soluble factors within the serum may be influencing patterns of differentiation.
6. Examined the ability of MDMs from IPF patients and controls to release reactive oxygen species (ROS) and IL-1 $\beta$  in response to stimulation.

### 5.3 Methods

#### 5.3.1 Participant samples

Samples were collected from April 2015 to August 2016. Patient samples were acquired during specialist ILD clinics or during in-patient stays. Age and sex-matched healthy volunteers were recruited from orthopaedic pre-assessment clinics or the University and screened for the presence of co-existent inflammatory conditions and lung disease. Only ex-smokers or non-smokers were included in the study.

Further details are documented in section 2.1.

#### 5.3.2 Generation of monocyte-derived macrophages (MDMs)

PBMCs were extracted using the Ficoll gradient-sedimentation method (section 2.3.2) and monocytes isolated through positive selection using CD14 microbeads (section 2.3.4). Isolated monocytes were suspended at a concentration of  $1 \times 10^6$ /ml in X-vivo (Lonza) and supplemented with 10% autologous serum. 50ng/ml of M-CSF was added on day 0 only and cells were plated onto either 6 well low-adherence plates. Media was replenished on day 4 and cells were harvested on day 7 (section 2.3.5).



### 5.3.3 Dexamethasone assay

Monocytes from controls and IPF were isolated and prepared as described above. Participant samples were plated in duplicate and media containing Dexamethasone was added to one plate on day 0 and day 3. A stock solution of Dexamethasone (Sigma D4902) was prepared by dissolving 1mg Dexamethasone in 1ml of ethanol. Further dilutions were made using sterile media to obtain a final 100uM concentration. Cells were then harvested on day 7 and stained with flouochrome conjugated antibodies (mAbs) for flow cytometric analysis. Dexamethasone-treated MDMs and non-treated cells from the same donor were directly compared.

### 5.3.4 Flow cytometry and gating strategy

MDMs were plated into 96 well plates at a concentration of  $1 \times 10^5$ /well, incubated with a viability dye followed by surface staining using mAbs and fixed. Cells were then permeabilised with Saponin buffer (Table 2-1, section 2.3.1) and stained with the intracellular macrophage marker CD68 for 30 minutes. Cells were then washed twice in Saponin buffer, once in FACs buffer and finally resuspended in fixative for flow cytometric analysis (section 2.4).

The gating strategy depicted in Figure 5.2 was used to determine the percentage of cells positive for the receptor of interest. A singlet gate was first applied using FSC-H/FSC-A followed by the gating out of non-viable cells (typically around 10%). Isotype controls were used to establish the gating for the positive population and the gate was then applied to the test sample. Due to the high proportion of MDMs expressing the majority of receptors analysed, the geometric mean fluorescence intensity (MFI) was used to determine the relative intensity of expression by the MDMs.

Apoptosis assays were undertaken on monocytes at day 1, 3 and 5 using annexin V and 7AAD. For experiments investigating preferential apoptosis of monocytes expressing CD64 and CD163, cells were harvested on day 1 and first incubated with mAbs against these receptors prior to annexin V and 7AAD staining (section 2.7).

## Chapter 5: Phenotypic and functional characteristics of MDMs from IPF patients

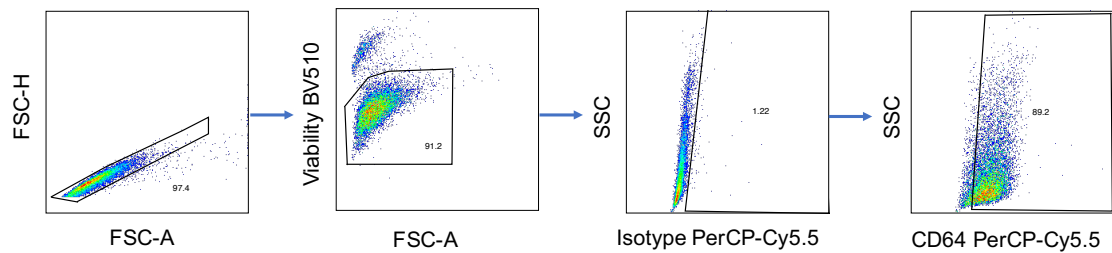


**Figure 5-2. Gating strategy for MDM phenotyping.**

From left to right: Singlet gate; live cells; isotype control used to determine gating of positive population; test sample with gate applied to determine percentage of cells positive for the protein of interest.

### 5.3.5 ELISA for M-CSF

Serum collected from study participants was heat inactivated at 56°C and frozen at -20°C. Serum samples for ELISA were then thawed and M-CSF was measured using a quantitative sandwich ELISA (R&D Systems). See section 2.6 for further details.

### 5.3.6 Functional assays

**Reactive oxygen species (ROS) generation** by MDMs was assessed using the compound CM-H2DCFDA (Molecular Probes).  $1 \times 10^5$  MDMs were plated onto a 96 well plate and incubated in PBS and 5µM of the compound for 30 minutes at 37°C. Cells were then washed and oxidative stress induced by the addition of 0.03% hydrogen peroxide for 1 hour. Viability dye was then added for 10 minutes before samples were placed on ice for immediate acquisition on the flow cytometer (section 2.5.2).

**Inflammasome assay:** IL-1β release resulting from inflammasome activation was assessed using LPS as a priming signal and Nigericin as a second signal (section 2.5.3).  $1 \times 10^5$  MDMs were plated onto a 96 well plate and incubated overnight for 16 hours in R10 and 0.1µg/ml LPS. 1µg/ml of Nigericin was then added to control and test wells for 30 minutes to activate the NLRP3 inflammasome to release IL-1β. The supernatant was then removed and frozen at -20C. A quantitative sandwich ELISA for IL-1β (R&D Systems) was used to quantify the amount of IL-1β released (section 2.6.1).

### 5.3.7 RNA extraction and qPCR

To consolidate the MDM phenotypic findings, RNA was extracted from day 7 MDMs. qPCR using SYBR® Green was undertaken to compare the expression of reparative and inflammatory genes in 6 control and 8 IPF MDM samples (section 2.9). Fold change was calculated using three housekeeping genes,  $\beta$ 2 microglobulin,  $\beta$ -actin and cyclophilin A. Details of genes analysed are listed in Table 2-6 and 2-9 (section 2.10).

## 5.4 Results

### 5.4.1 Participant demographics

Patients enrolled into this part of the study are listed in Table 5-1. All had a definite or probable diagnosis of IPF. For phenotyping studies, patients on prednisolone with stable disease and AEIPF were included for comparative purposes but analysed separately. For all other studies, including RNA extraction, patients on prednisolone were excluded although 29% were on anti-fibrotic therapy. Controls were similarly matched in age although a higher proportion of females were enrolled (32% versus 15%).

Demographics	All IPF	Stable IPF not on Prednisolone	Stable IPF on Prednisolone	AEIPF	Controls
Sample number	25	17	4	4	19
% Male	85	78	100	75	68
Mean age (range)	69.9 (45-87)	72.8 (63-87)	58.2 (45-78)	67.7 (67-69)	64.9 (49-86)
% Definite diagnosis	48	57	0	75	N/A
% on Anti-fibrotics (number) N=Nintedanib P=Pirfenidone	44 (11) N=0 P=11	29 (5)	50 (2)	50 (2)	N/A
Dose of Prednisolone/ Methylprednisolone (range)	-	N/A	20.7 mg (10-40mg)	147mg (20-500mg)	N/A

**Table 5-1. Demographic details of patients and controls participating in MDM phenotyping.**

Stable patients not on corticosteroids were analysed separately from patients on prednisolone with stable disease and those with AEIPF (N/A information not applicable or unavailable).

## Chapter 5: Phenotypic and functional characteristics of MDMs from IPF patients

Table 5-2 shows the characteristics of patients involved in functional assays and gene expression analysis.

Demographics	ROS		Inflammasome		RNA	
	IPF	Controls	IPF	Controls	IPF	Controls
Sample number	9	7	13	11	8	6
% Male	100	86	69	64	87	83
Mean age (range)	71.8 (57-82)	66.9 (57-73)	74.7 (62-87)	68.8 (58-84)	72.2 (66-79)	65.2 (51-71)
% Definite diagnosis	78	NA	46	NA	13	NA
% on anti-fibrotics N=Nintedanib P=Pirfenidone	78 (N=1 P=6)	NA	38 (N=2 P=3)	NA	37 (N=2, P=1)	NA

**Table 5-2. Demographic details of patients and controls participating in MDM functional assays and RNA analysis.**

A variable proportion of patients were taking Nintedanib (N) or Pirfenidone (P) at the time of blood sampling.

### 5.4.2 CD14 expression was down-regulated and CD68 up-regulated during the differentiation of monocytes to macrophages in culture

During the one week culture period, I observed that monocytes from both IPF patients and healthy controls undergo distinct morphological changes. When monocytes were first isolated from PBMCs they were small and spherical in appearance. After 24 hours, many could be seen adhering to the base of the well, often in clusters as depicted in Figure 5-3a. Over 7 days, they enlarged in size and appeared more granular and irregular in outline. By day 7, they had formed complex dendritic processes which often extended between cells. The photomicrographs below illustrate the morphological changes that occurred during the process of monocyte to macrophage differentiation.

As monocytes started to acquire the morphological characteristics of macrophages, CD14, a membrane receptor that distinguishes monocytes from other mononuclear cells, was down-regulated. CD68, an intracellular lysosomal scavenger receptor and macrophage marker, was correspondingly up-regulated. This is demonstrated in Fig 5-3

## Chapter 5: Phenotypic and functional characteristics of MDMs from IPF patients

which shows the percentage of monocytes from healthy volunteers expressing CD14 falling over 7 days as they matured into macrophages and started to up-regulate expression of CD68.

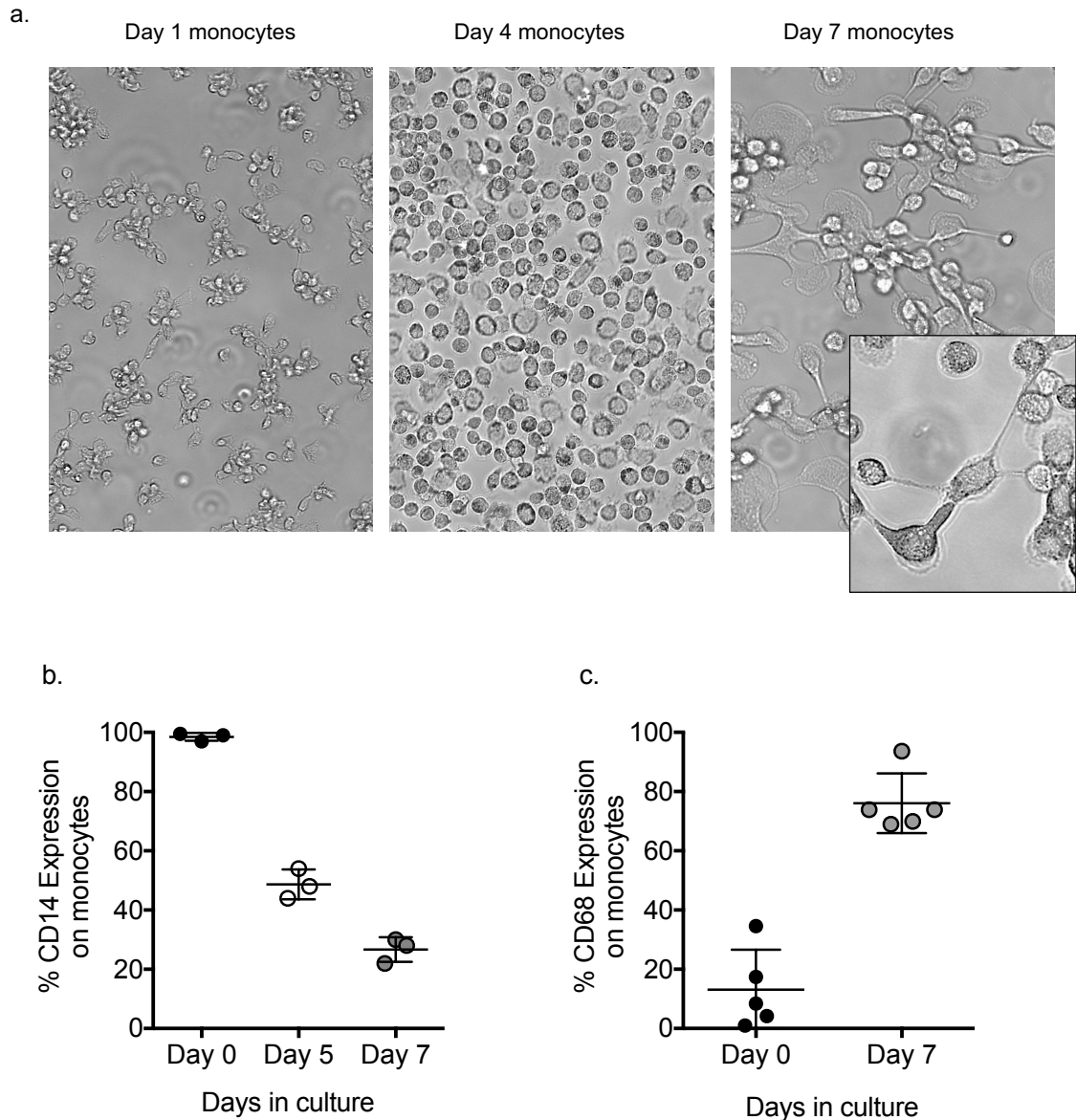


**Figure 5-3. Monocytes change morphologically and phenotypically as they differentiate into macrophages.**

Positively selected monocytes from healthy controls were immunostained for CD14 and CD68 or cultured in duplicate to determine the expression of these receptors on day 5 (CD14 only) and 7. (a) photomicrograph images of monocytes in culture on day 1, 4 and 7. Insert shows close up image of the dendritic processes extending from one cell to another. (b) Using flow cytometry, CD14 expression on monocytes from healthy volunteers was found to be down-regulated as cells differentiate in culture over a 7-day period. (c) The percentage of monocytes expressing CD68 was low in freshly isolated monocytes but by day 7 the majority of cells expressed this intracellular receptor. CD14 n=3, CD68 n=5. SD(mean) illustrated in graphs.

### 5.4.3 Monocytes from IPF patients showed evidence of delayed differentiation in ex vivo culture

To assess the differentiation of monocytes to macrophages, cells were stained on day 7 with the monocyte marker CD14 and macrophage marker CD68.

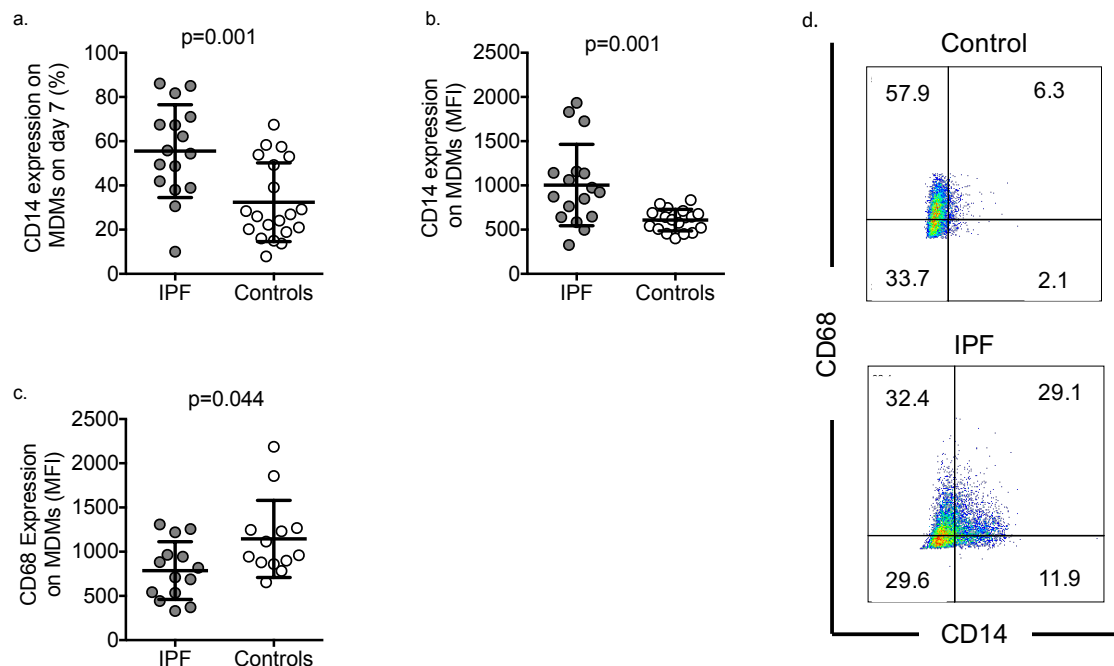


**Figure 5-4. Expression of the monocyte marker CD14 and the macrophage marker CD68 on day 7 monocyte-derived macrophages (MDMs) from stable IPF patients and controls.**

Positively selected monocytes were cultured for 7 days in autologous serum then stained with mAb for flow cytometric analysis. SD(mean) quoted here and depicted in the graphs. (a-b) The percentage and mean fluorescent intensity (MFI) of CD14 expression on MDMs from IPF patients was significantly higher compared to MDMs from age-matched controls [57%(21) vs 32%(18) and MFI 1004(460) vs 608(122) n=17 and 19]. (c) The MFI of CD68 on day 7 MDMs was lower in IPF patients compared to controls [786(327) vs 1144(436) n=14 and 13]. (d) Representative FACS plots of day 7 MDMs from a control and IPF patient (gating based on exclusion of doublets, dead cells and use of isotype controls for CD14 and CD68). Pearson-D-Agostino normality test and Student t-test or Mann-Whitney test used.  $P<0.05$  taken to indicate statistical significance.

In concordance with preliminary experiments described above, I found that CD14 was down-regulated and CD68 expression up-regulated in both patient and control groups after 7 days in culture. Differences however were noted between the two groups with the percentage of MDMs that still expressed CD14 and the mean fluorescence intensity

## Chapter 5: Phenotypic and functional characteristics of MDMs from IPF patients

(MFI) of CD14 significantly higher in the IPF group compared to controls ( $p$ -values both 0.001, Fig 5-4a-b). Correspondingly, the MFI of CD68 was lower in the IPF group ( $p=0.044$ , Fig 5-4c) suggesting that MDMs from IPF patients are less well differentiated than healthy controls and continue to possess a more monocyte-like phenotype after 7 days.

### **5.4.4 Monocytes from IPF patients differentiated into phenotypically distinct MDMs**

To determine if monocytes from IPF patients differentiated into macrophages with reparative (M2) or inflammatory phenotypes (M1), day 7 MDMs from patients and controls were immunostained using antibodies against receptors associated with M1/M2 macrophage characteristics.

CD64 and CD86 were used as M1 markers. CD86 is upregulated on MDMs in response to LPS, IFN $\gamma$  and TNF $\alpha$  in vitro [196] and was used as replacement for CCR7 as this receptor was found to be down-regulated as monocytes differentiated into macrophages during optimisation experiments, as demonstrated in Figure 5-5.

CD163 and CD200R were chosen as M2 markers. CD200R is a cell surface glycoprotein up-regulated by macrophages following in vitro exposure to IL-4 [209] and was used as an alternative to CD206, which had showed similar levels of expression in both control and IPF monocytes.

I found that CD64 and CD86 were significantly downregulated on the cell surface of MDMs in IPF patients compared to controls ( $p=0.005$  and  $<0.002$  for CD64 and CD86 respectively, Fig 5-6 a-b). The expression of M2 receptors, CD163 and CD200R were not significantly different in IPF patients compared to controls (Fig 5-6c-d).

Chapter 5: Phenotypic and functional characteristics of MDMs from IPF patients

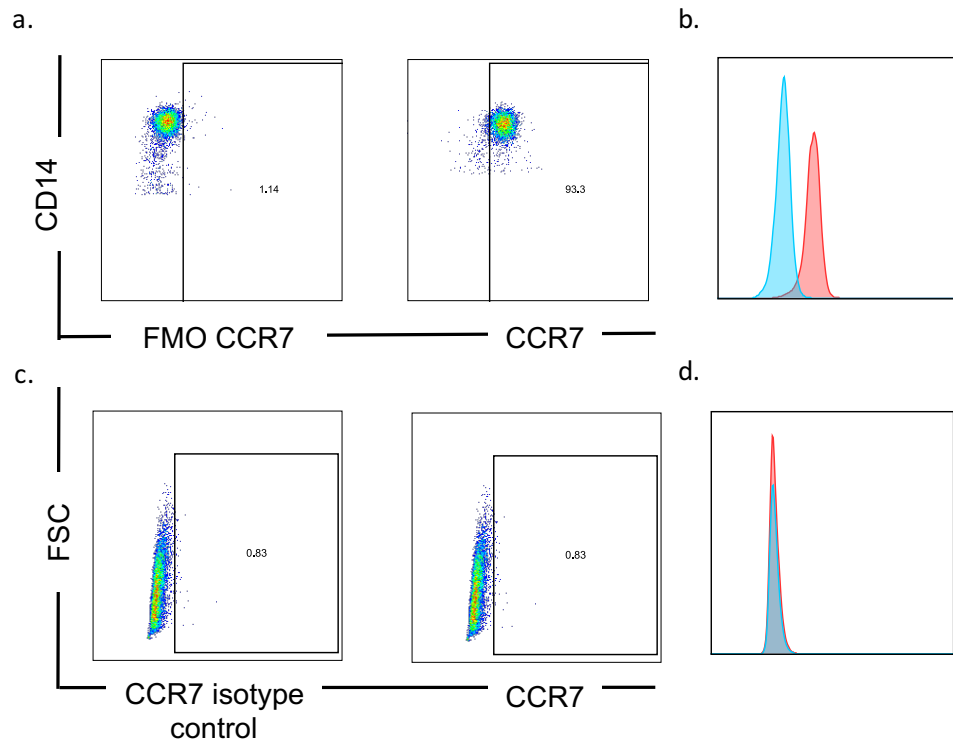


**Figure 5-5. Expression of CCR7 on human monocytes and following differentiation into macrophages.**

(a) Expression of CCR7 on CD14<sup>+</sup> monocytes with gating based on fluorescence-minus one (FMO) samples. (b) Histogram demonstrating expression of CCR7 on monocytes (red) compared to the FMO (blue). (c) FACS plot of MDMs stained with an isotype control for CCR7 (left) and CCR7 (right) demonstrating the absence of staining. (d) Histogram illustrating that the isotype control for CCR7 (blue) and mAb against CCR7 (red) are the same. (data based on analysis of 6 control and 6 IPF monocytes and MDMs).



## Chapter 5: Phenotypic and functional characteristics of MDMs from IPF patients

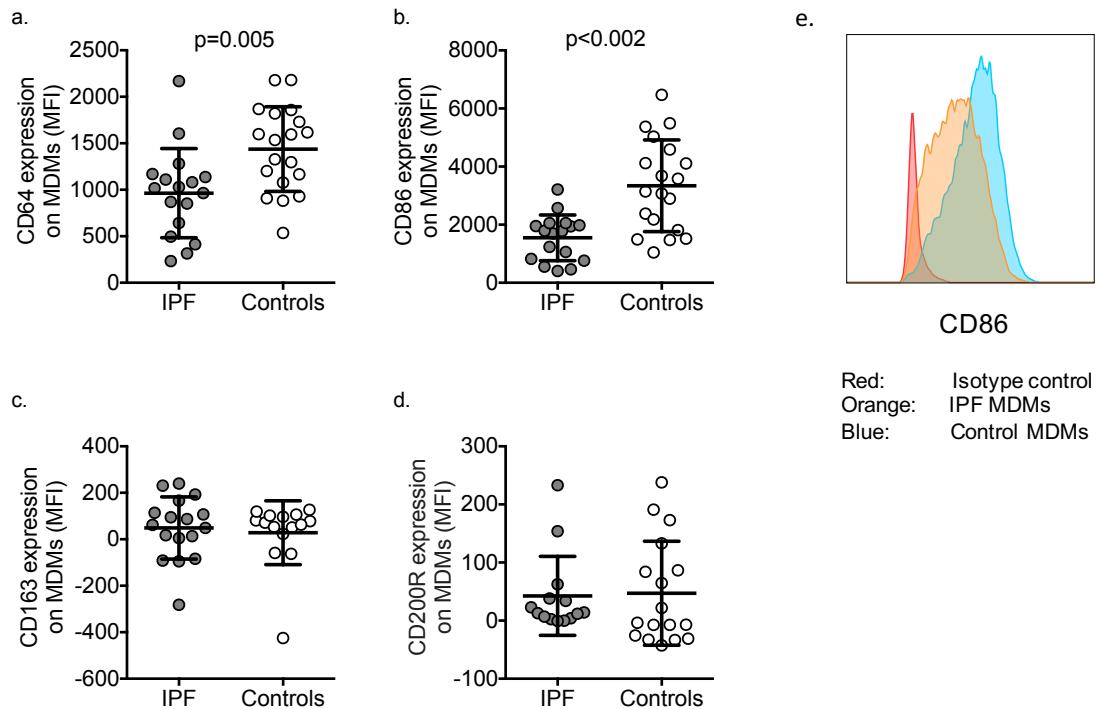


**Figure 5-6. The expression of cell surface receptors associated with inflammatory ('M1') and reparative ('M2') macrophage phenotypes on MDMs from stable IPF patients and age-matched controls.**

Monocytes were positively selected from PBMCs and differentiated in autologous serum for 7 days. Cells were immunostained for flow cytometric analysis. Mean(SD) are described here and illustrated on graphs. (a-b) The expression of 'M1' receptors CD64 and CD86 were lower on MDMs from IPF patients compared to controls [MFI CD64: 963(480) vs 1437(455) and MFI CD86: 1549(787) vs 3340(1577) n=17 and 19]. (c-d) MFI of 'M2' markers CD163 and CD200R on MDMs from controls and IPF patients were similar. (e) A representative histogram demonstrating the MFI of CD86 in MDMs from a control (blue) and IPF patient (orange) compared to the isotype control (red). Pearson-D-Agostino normality test and Student t-test or Mann-Whitney test used for statistical analysis.  $P < 0.05$  taken to indicate statistical significance.

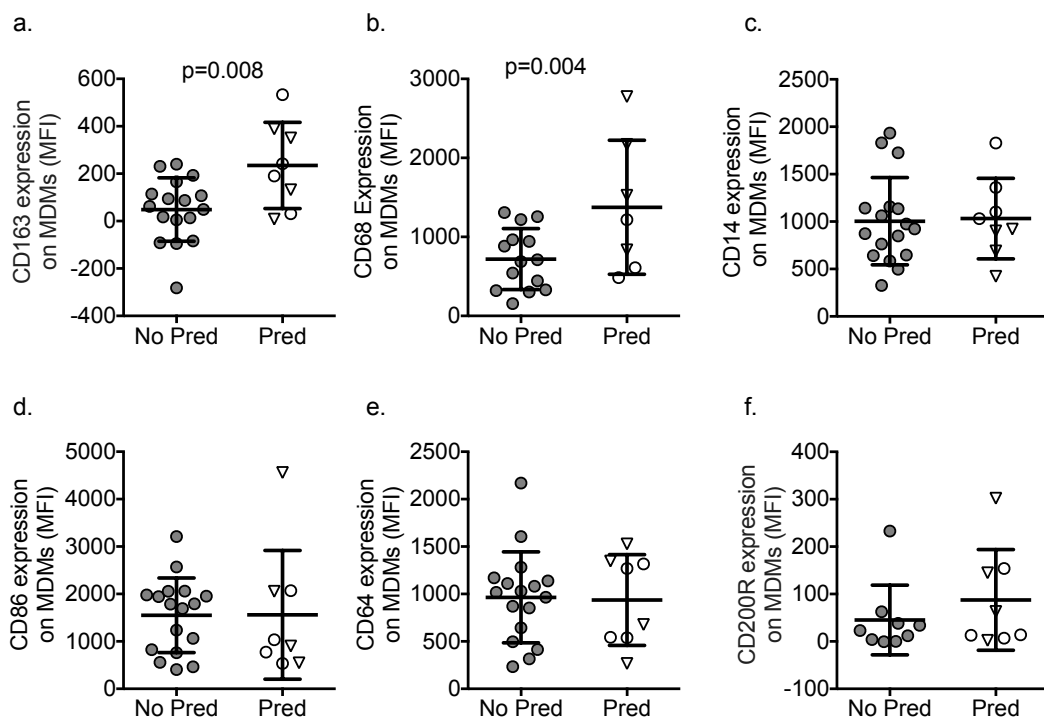
### 5.4.5 MDMs from AEIPF and stable patients on Prednisolone showed up-regulation of CD163 after 7 days' ex vivo culture

Monocytes from patients with acute exacerbations showed phenotypic changes that differed from both stable IPF patients and healthy controls. The receptor and gene expression findings were consistent with M2c polarisation with high CD163, *IL-10*, *DSIPI*, *THBS1* and low *TNF $\alpha$* . In vitro, this phenotype can be induced by IL-10, TGF $\beta$  and glucocorticoids [196, 198, 205, 301]. M2 MDMs polarised in this way are associated with reparative and immune-regulatory activities [126, 196, 205] (section 1.3.4, Fig 1-10).

## Chapter 5: Phenotypic and functional characteristics of MDMs from IPF patients

I was therefore interested in determining whether phenotypic characteristics associated with corticosteroid (CS) exposure persisted after monocytes obtained from Prednisolone-treated patients (both stable and AEIPF) were differentiated into MDMs ex-vivo. Monocytes were also differentiated in the presence of Dexamethasone (Dex), a CS with a similar molecular structure and pharmacodynamics to Prednisolone [302]. This was undertaken to determine whether the phenotypic changes mirrored those seen in Prednisolone-treated patients.

Patients treated with Prednisolone (Pred) showed up-regulation of CD163 expression compared to those not on treatment (No Pred) ( $p=0.008$ , Fig 5-7a). The macrophage marker CD68 was also upregulated in the Pred group ( $p=0.004$ , Fig 5-7b) although CD14 expression remained similar between groups (Fig 5-7c). AEIPF patients are depicted in Figure 5-7 as clear triangles to determine whether monocytes from patients with acute exacerbations exhibited a different phenotypic profile to stable patients on Prednisolone. Expression of CD163 was similar in both stable and AEIPF groups on Prednisolone although a possible trend towards lower CD14 expression and higher CD68 in the AEIPF group compared to stable Prednisolone-treated patients can be seen. AEIPF patients were receiving the highest doses of Prednisolone (Table 5-1). No significant differences in the expression of CD86, CD14, CD64 or CD200R were observed between patient groups ( $p$ -values 0.982, 0.885, 0.892 and 0.370, respectively).



## Chapter 5: Phenotypic and functional characteristics of MDMs from IPF patients

### **Figure 5-7. Intensity of receptor expression (MFI) on MDMs from IPF patients not on prednisolone (No Pred) compared to those on prednisolone treatment (Pred).**

Monocytes from IPF patients (including AEIPF on steroid therapy) were differentiated in autologous serum for 7 days and immunophenotyped using flow cytometry to compare the potential impact of in vivo corticosteroids on phenotype following ex vivo culture. Mean(SD) are described here and illustrated on graphs. (a) The MFI of CD163 was higher in MDMs derived from IPF patients on Prednisolone compared to those not on treatment [235(182) vs 49(134) n=17 and 8]. (b) CD68 expression was higher in MDMs from Pred patients compared to No Pred patients (1375(848) vs 719(385) n=6 and 14]. No significant differences were seen in the expression of (c) CD14, (d) CD86, (e) CD64 and (f) CD200R in MDMs from No Pred and Pred patients. Clear circles – stable IPF on Prednisolone; clear triangles – AEIPF on prednisolone. Pearson-D-Agostino normality test and Student t-test or Mann-Whitney test used.  $P < 0.05$  taken to indicate statistical significance.

I then examined the morphological and phenotypic characteristics of monocytes differentiated in the absence or presence of Dex. As the aim of the experiment was to determine the effects of Dex on monocyte differentiation, both control and IPF monocytes were used. Figure 5-8 shows the combined data from both groups after Dex treatment, which were similar between IPF and controls (p-values not significant, graphs differentiate IPF and control samples by black or grey circles, respectively). CD206 was used in preference to CD200R as this receptor is associated with M2c polarisation [198, 199, 301].

MDMs differentiated with Dex (Dex+) had different morphological appearances to MDMs differentiated without Dex (Dex-). Dex+ cells retained a circular shape and appeared smaller than untreated MDMs, aggregating in clusters loosely or non-adherent to the base of the well (Fig 5-8a). I found that Dex+ cells had lower expression of the M1 receptor CD64 ( $p=0.006$ , Fig 1-8a) and higher expression of M2 receptors CD206 and CD163 ( $p=0.008$  and  $p < 0.006$  respectively, Fig 5-8d-e). CD14 was also more highly expressed on Dex+ monocytes ( $p=0.011$ , Fig 5-8f). CD86 expression was not significantly different on MDMs following Dex exposure ( $p=0.093$ , Fig 5-8c).

## Chapter 5: Phenotypic and functional characteristics of MDMs from IPF patients

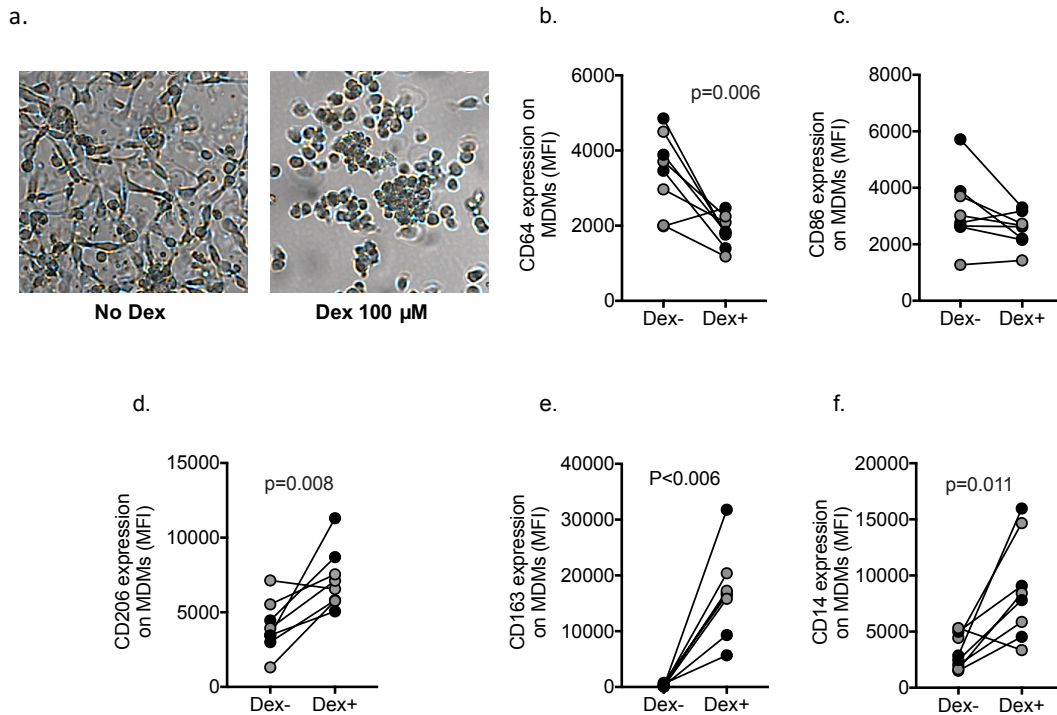


**Figure 5-8. Morphological appearances and expression of M1 and M2 receptors on day 7 MDMs differentiated in the absence (Dex-) and presence of Dexamethasone (Dex+).**

Monocytes from IPF and HCs were cultured in duplicate wells with one well containing media supplemented with 100  $\mu$ M of Dex. Cells were harvested on day 7 for immunostaining with mAb and flow cytometric analysis. (a) Morphological appearances under light microscopy of MDMs cultured with and without Dexamethasone. (b) Expression of the M1 receptor CD64 was down-regulated on MDMs following Dex exposure [Dex+ 1850(425) vs Dex- 3422(1054)]. (c) CD86 expression was not significantly different following Dex exposure [Dex+ 2536(603) vs Dex- 3203(1289),  $p=0.093$ ]. (d-e) Expression of M2 receptors CD206 and CD163 were significantly up-regulated following Dex [CD206: Dex+ 7230(2006) vs Dex- 4040(1738) and CD163: Dex+ 16695(7729) vs Dex- 355(240)]. (f) CD14 expression was increased following exposure to Dex [Dex+ 8713(4526) vs Dex- 3163(1536)].  $n=8$ . SD(mean) quoted in text and illustrated on graphs. Grey circles – healthy controls; black circles – IPF patients. Pearson and D'Agostino normality test and paired t-tests used for all comparisons.

### 5.4.6 CD64<sup>+</sup> monocytes exhibit preferential apoptosis in IPF patients

Expression of CD64 on freshly isolated monocytes from IPF patients was increased compared to age-matched controls (Section 3.4.7 and 3.4.8). Day 7 MDMs from IPF patients however showed lower expression of CD64 compared to controls (Fig 5-9a-d). This finding suggests that IPF monocytes either differentially down-regulate this receptor during the process of MDM differentiation or that IPF monocytes with high CD64 expression undergo preferential apoptosis.

## Chapter 5: Phenotypic and functional characteristics of MDMs from IPF patients

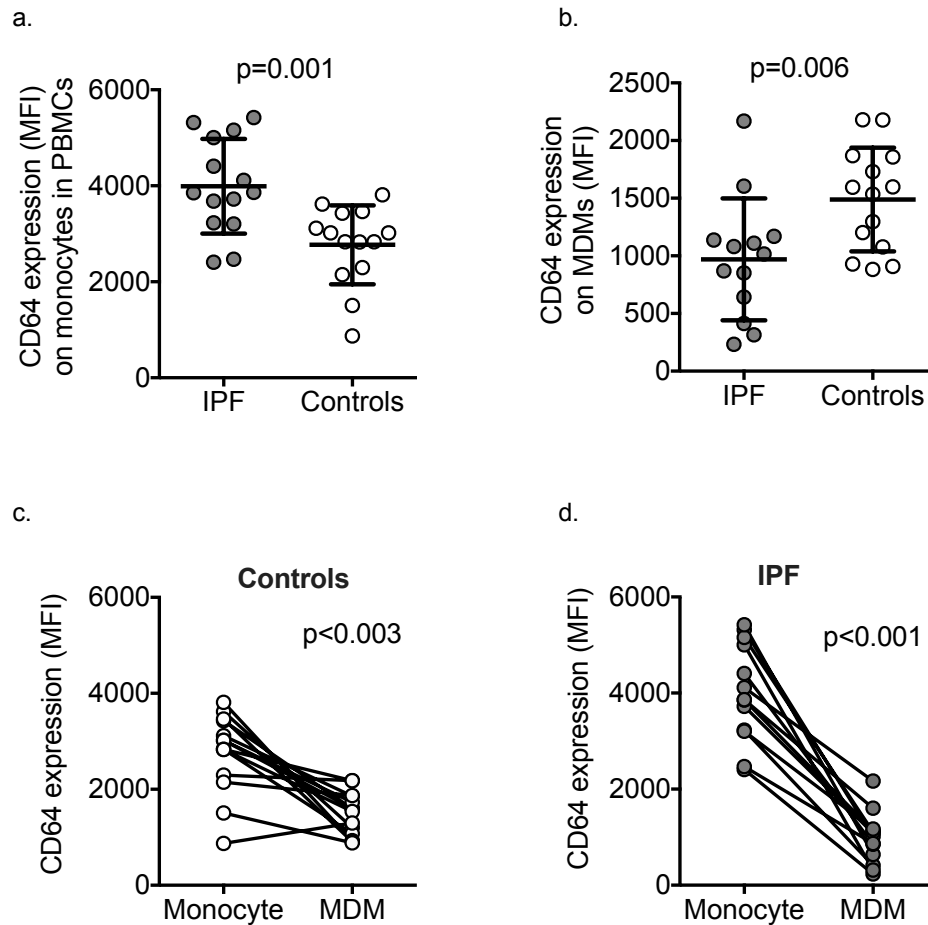


**Figure 5-9. The expression of CD64 on monocytes and day 7 MDMs from IPF and control participants.** Expression of CD64 was measured on freshly isolated monocytes within PBMCs and following monocyte isolation and culture over 7 days. (a) CD64 expression on monocytes within PBMCs was significantly higher in IPF patients compared to controls [3990(985) vs 2771(822)]. (b) Following differentiation to MDMs, CD64 expression was lower in IPF patients compared to controls [970(529) vs 1489(449)]. Expression (MFI) of CD64 on monocytes was directly compared to expression on MDMs from the same donor. (c-d) Paired data showing that CD64 expression falls as monocytes differentiate into MDMs but a greater reduction in expression was seen in the IPF group. For a-b, Mann-Whitney test was used and SD(mean) quoted in text and illustrated on graphs. For c-d, the paired t-test was used. n=14 and 14.

To firstly investigate the hypothesis that an increased proportion of IPF monocytes undergo apoptosis during *ex vivo* differentiation, monocyte apoptosis was initially assessed on day 1, 3 and 5 (Fig 5-10). Monocytes undergoing apoptosis were identified by Annexin V staining. Those additionally positive for 7AAD indicated cells in the later stages of apoptosis and therefore Annexin V +/-7AAD staining was included in analysis. I found that the majority of apoptosis occurred on day 1, with a far smaller proportion of monocytes staining positive for Annexin V on day 3 and day 5. Day 1 was therefore

## Chapter 5: Phenotypic and functional characteristics of MDMs from IPF patients

selected for subsequent analysis. The extent of apoptosis was found to be similar between controls and patients.

To next determine whether monocytes expressing CD64 from IPF patients undergo preferential apoptosis, I immunostained cells with mAbs to CD64 and CD163. CD163 was included to represent cell populations with a reparative (M2) phenotype. The extent of apoptosis was then analysed on monocytes positive for CD64 and negative for CD163 (CD64<sup>+</sup>CD163<sup>-</sup> monocytes), and cells that were dual positive for both receptors (CD64<sup>+</sup>CD163<sup>+</sup>) as the population of CD163<sup>+</sup>CD64<sup>-</sup> monocytes was not large enough for separate analysis.

Whilst the overall proportion of monocytes undergoing apoptosis did not differ between IPF and controls, I found that the proportion of CD64<sup>+</sup>CD163<sup>-</sup> monocytes from IPF patients undergoing apoptosis on day 1 was significantly higher than control monocytes [mean%(SD) 30(20) vs 14(4) n=13 and 12, p=0.009 Student t-test (Fig 5-11b)]. There were no statistically significant differences in the extent of apoptosis seen in CD64<sup>+</sup>CD163<sup>+</sup> monocytes although a possible trend towards less apoptosis occurring in this subset was observed in the IPF cohort (Fig 5-11c).

## Chapter 5: Phenotypic and functional characteristics of MDMs from IPF patients

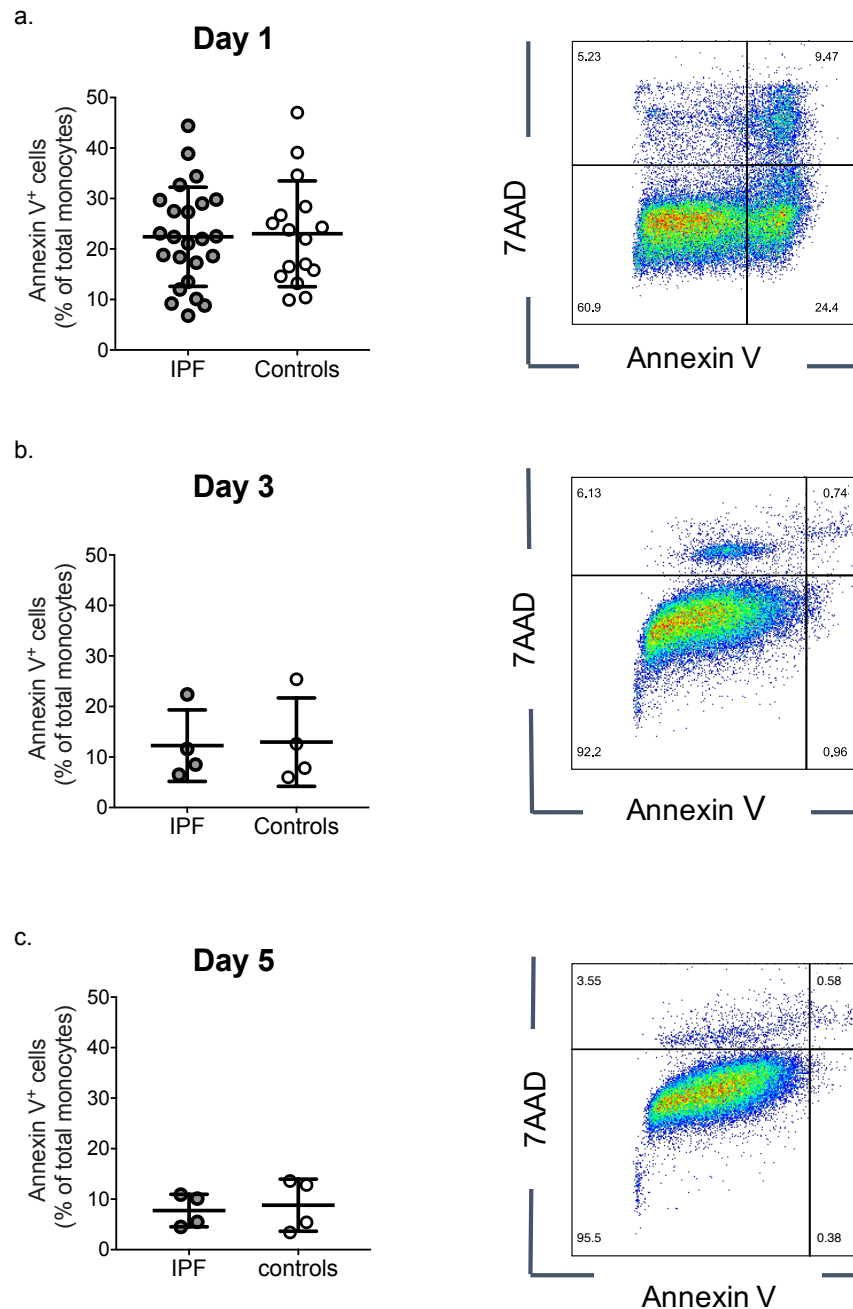


**Figure 5-10. The proportion of apoptotic monocytes (Annexin V<sup>+</sup> +/-7AAD) within the total monocyte population on days 1, 3 and 5 of culture.**

Monocytes were isolated from PBMCs using positive selection and cultured in autologous serum. After harvesting monocytes on day 1, 3 or 5, cells were stained with the apoptosis marker Annexin V and the cell viability marker 7-AAD for flow cytometry. Included in the analysis are cells staining for Annexin V only (early apoptosis) and cells positive for both Annexin V and 7AAD (late apoptosis). Mean(SD) are described here and illustrated on graphs. (a) The highest percentage of monocytes positive for annexin V were seen on day 1 compared to day 3 and 5 and no differences were seen between controls and IPF monocytes (controls: 23.0%(10.5) vs IPF 22.4%(9.8),  $p=0.856$ ,  $n=16$  and  $24$ , Student t-test). (b-c) On day 3 and 5, only a small proportion of cells were positive for Annexin V and no differences were seen between controls and IPF monocytes. Representative FACS plots at each time point depicted on the right.

## Chapter 5: Phenotypic and functional characteristics of MDMs from IPF patients

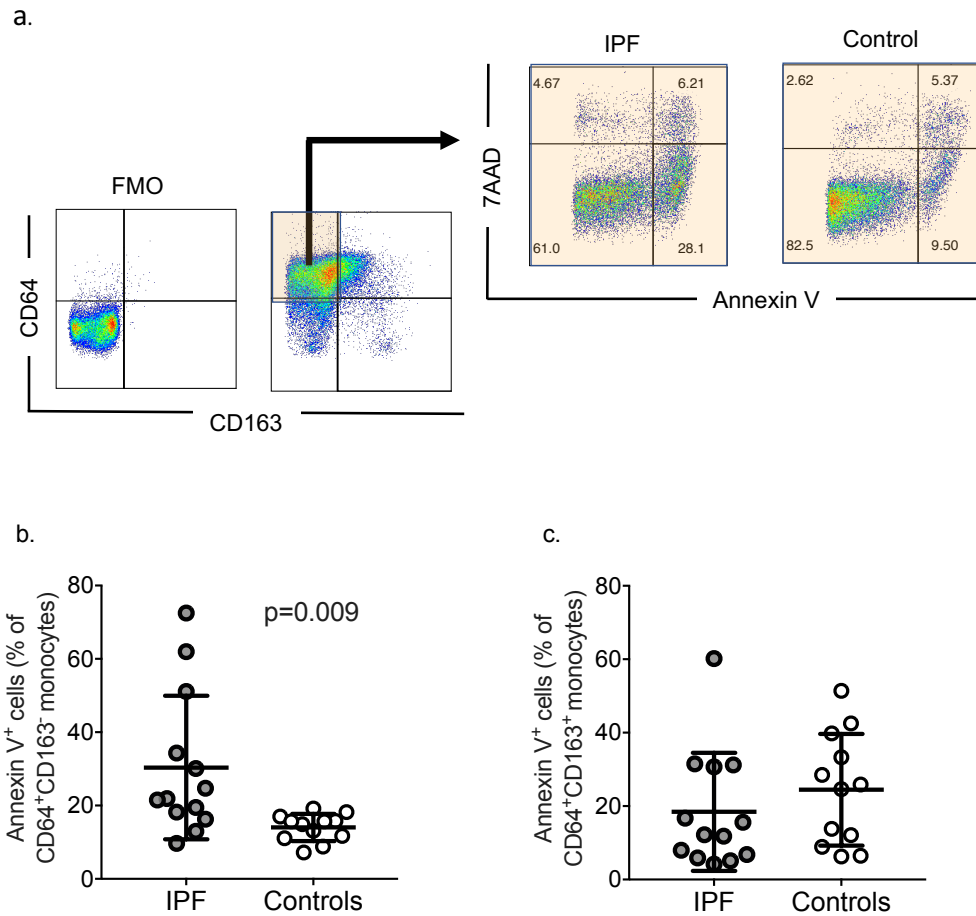


**Figure 5-11. Percentage of CD64<sup>+</sup>CD163<sup>-</sup> and CD64<sup>+</sup>CD163<sup>+</sup> monocytes in apoptosis on day 1 ex vivo culture.**

(a) Representative FACS plots demonstrating the gating of CD64 and CD163 (based on FMOs) and an example of the proportion of CD64<sup>+</sup>CD163<sup>-</sup> monocytes staining for annexin V (AV) in a control and IPF patient. Mean(SD) are described here and illustrated on graphs. (b) The proportion of CD64<sup>+</sup>CD163<sup>-</sup> monocytes undergoing apoptosis (% Annexin V<sup>+</sup> +/- 7AAD) from IPF patients was higher than in control participants [30%(20) vs 14%(4)] (c) The proportion of CD64<sup>+</sup>CD163<sup>+</sup> monocytes undergoing apoptosis did not differ significantly between IPF patients and controls (18.5%(16.1) vs 24.5%(15.2). IPF n=13, controls=12. Student t-test used.

### 5.4.7 RNA expression of key inflammatory and reparative genes differs significantly between IPF and control MDMs

Over recent years, research has been undertaken to characterise monocytes and macrophages involved in the different phases of tissue repair and regeneration. Following injury, monocytes/macrophages orchestrate a highly co-ordinated sequence



## Chapter 5: Phenotypic and functional characteristics of MDMs from IPF patients

of cellular events to enable the restoration of healthy tissue. Aberrations in the function or number of monocytes and macrophages have been linked to both fibrogenesis and delayed wound healing [126, 229, 254, 303]. Indeed, models of lung and liver fibrosis have shown that depleting monocytes/macrophages at different stages after injury can either hasten or delay the clearance of fibrotic tissue [25, 235, 304]. Macrophages with distinct phenotypic and functional characteristics have been identified at different phases of the healing process, with the initial presence of inflammatory monocytes/macrophages followed by populations which assist with matrix deposition, tissue remodelling and resolution responses. It remains unclear whether monocytes/macrophages undergo a phenotypic switch during the evolution of repair or if distinct populations are sequentially recruited to the site of injury. Evidence for the later was demonstrated in a murine model of cardiac ischaemia where the authors identified early recruitment of inflammatory (Ly6-C<sup>hi</sup>) monocytes to the site of injury corresponding to the presence of macrophages expressing IL-6 and TNF $\alpha$ , followed by the subsequent infiltration of reparative (Ly6C<sup>lo</sup>) monocytes after three days [234].

Decreased expression of M1 receptors CD64 and CD86 were noted on IPF MDMs, suggesting that the phenotype of these cells may be less inflammatory than MDMs from healthy age-matched controls. Given the established role MDMs play in tissue repair and fibrosis, I was interested in establishing whether other phenotypic differences existed between the two groups. In particular, I wanted to determine whether MDMs from IPF patients exhibited the characteristics of macrophages involved in the later, reparative (M2) stages of repair. To investigate this, I selected genes associated with macrophage phenotypes involved in inflammatory, wound healing and resolution responses, as defined by the current literature and summarised in Figure 5-1 and Table 5-3 [126, 196, 199].

Figure 5-12 demonstrates the expression of cytokines and soluble factors in relation to three housekeeping genes in IPF and control MDMs. I found a significant increase in the expression of the inflammatory cytokine *TNF $\alpha$*  in IPF MDMs compared to controls ( $p=0.013$ , Fig 5-12a). AREG (amphiregulin) is an Epidermal Growth Factor (EGF)-like molecule implicated in tissue repair, immune regulation [305] and more recently in certain inflammatory responses [305]. Gene expression of *AREG* was higher in IPF MDMs compared to controls ( $p=0.029$ , Fig 5-12d). Trends towards higher expression of *IL-1 $\beta$*  and *IL-6* were seen in IPF MDMs ( $p$ -values 0.108 and 0.181 respectively, Fig 5-12b-c) alongside downward trends in the expression of *IL-10*, *VEGF-A* and *COX-2* ( $p$ -140

## Chapter 5: Phenotypic and functional characteristics of MDMs from IPF patients

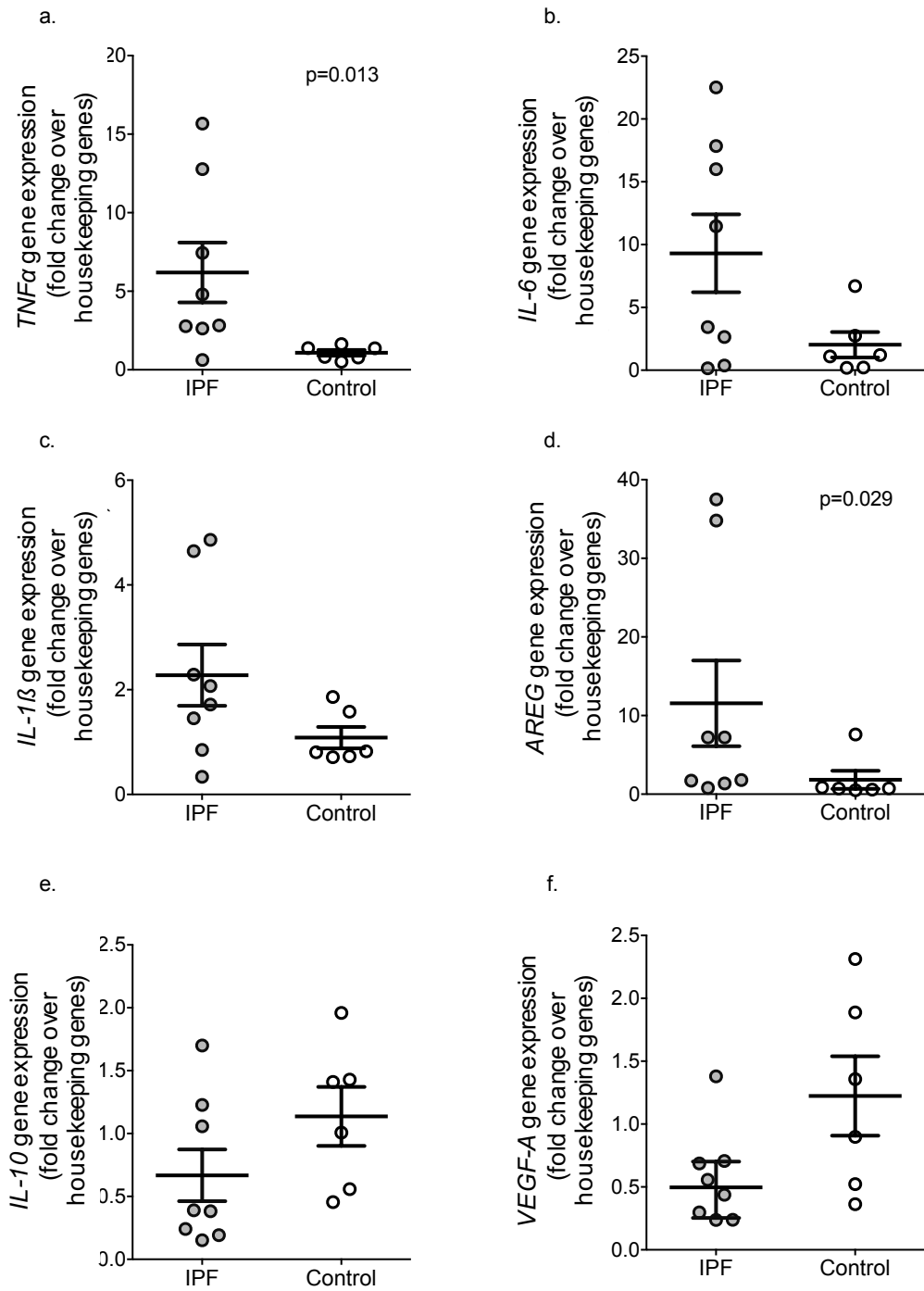
values 0.108, 0.108 and 0.117, respectively, Fig 5-12e, f, h). In contrast to studies comparing alveolar macrophage production of CCL-18 in IPF patients and controls [39, 41], gene expression of this chemokine did not differ between the two groups (Fig 1-12h). *LGALS3*, coding for the protein Galectin-3, a binding protein with diverse activities that has been implicated in lung fibrosis and found to be highly expressed in AMs from IPF patients [306], was correspondingly up-regulated in IPF MDMs compared to controls ( $p=0.007$ , Fig 5-12i). *INHA* is a gene that codes for inhibin-alpha subunit, a preproprotein that is proteolytically cleaved to generate multiple peptide products. These proteins are involved in the regulation of numerous cellular processes, including proliferation and apoptosis [307]. IPF MDMs showed a trend towards increased expression of *INHA* compared to controls. ( $p=0.082$ , Fig 5-12j).

Transcription factors and nuclear receptors associated with inflammatory, reparative and immunomodulatory pathways were analysed. *STAT1*, a transcription factor linked to inflammatory responses, was up-regulated in IPF MDMs compared to controls ( $p=0.008$ , Fig 5-13a). In association with this, M2-associated genes were also more highly expressed by IPF MDMs, including nuclear receptors *GR* (coding for the Glucocorticoid Receptor), *PPAR $\gamma$* , and the transcription factor *IRF4* ( $p$ -values 0.029, 0.016, 0.043 respectively, Fig 5-13 d-f). 'M2' Transcription factors *STAT6* and *ATF3* also showed a trend towards higher expression in IPF MDMs compared to controls ( $p$ -values 0.092, and 0.086, respectively, Fig 5-13c and g).

*CD14* mRNA levels were reduced in IPF MDMs compared to controls ( $p=0.020$ , Fig 5-14a) and no difference was seen in *CD64* expression ( $p=0.295$ , Fig 5-14b). These findings were in contrast to the protein expression of these receptors where CD14 was noted to be increased and CD64 decreased on the cell surface of IPF MDMs compared to controls (Fig 5-3). Expression of *CSF1-R*, coding for the CSF-1 Receptor and associated with both M1 and M2 responses, was reduced in IPF MDMs compared to controls ( $p=0.037$ , Fig 5-14c). *CD274* expression was increased in IPF MDMs ( $p=0.024$ , Fig 5-14d) but *CD273* expression was not significantly different (Fig 5-14e). IPF MDMS exhibited a trend towards increased expression of *IL-4R*, which codes for the IL-4 Receptor ( $p=0.108$ , Fig 5-14f).

The full set of genes analysed are listed in Table 5-3.

## Chapter 5: Phenotypic and functional characteristics of MDMs from IPF patients



## Chapter 5: Phenotypic and functional characteristics of MDMs from IPF patients

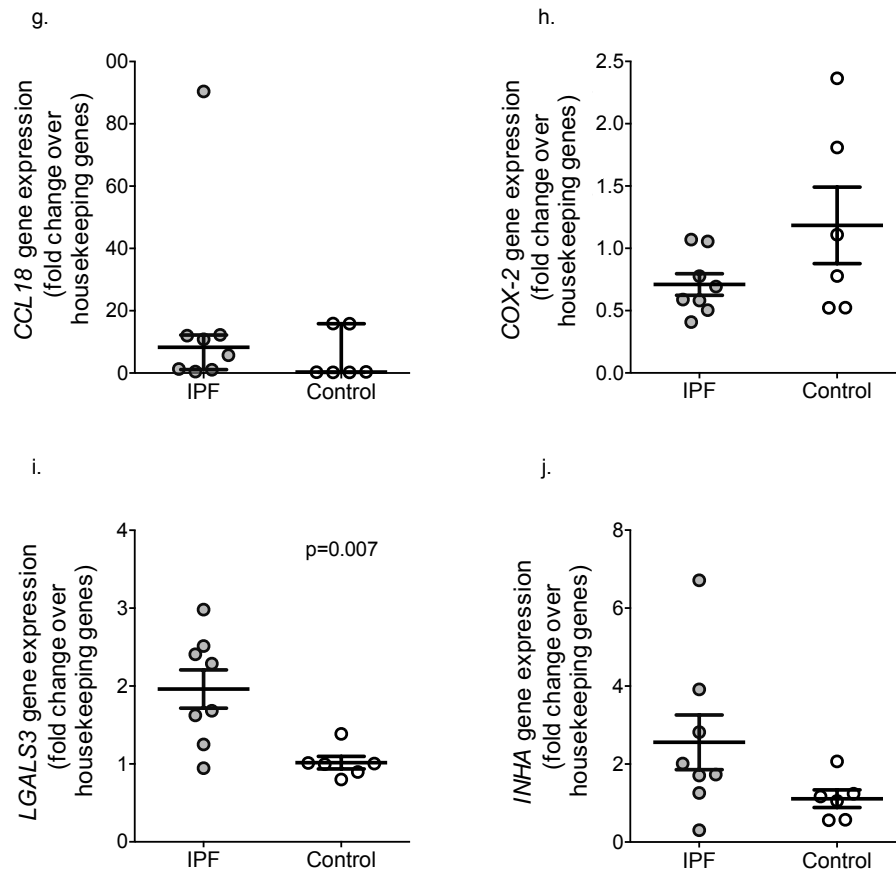
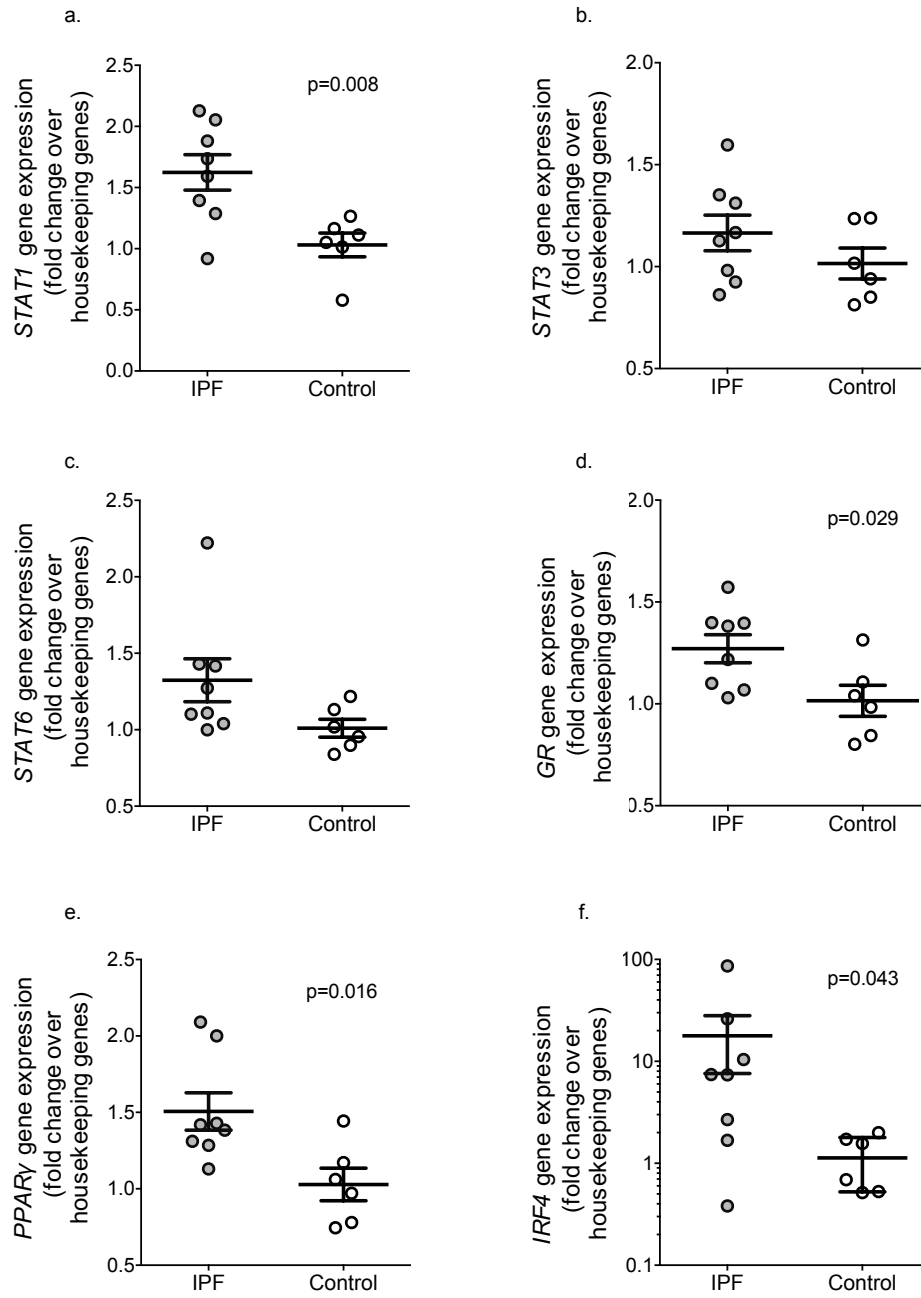


**Figure 5-12. Gene expression of soluble factors and proteins in IPF and control MDMs.**

qPCR was undertaken on day 7 MDMs to determine the gene expression of factors associated with inflammatory, reparative and immunomodulatory responses. The fold change over three housekeeping genes (*CYCLOPHILIN A*,  *$\beta$ 2-MICROGLOBULIN* and  *$\beta$ -ACTIN*) was used to determine the relative expression of the genes of interest. For normally distributed data, mean(SEM) are depicted in graphs. For non-parametric data, the median and interquartile range are shown. (a) *TNF $\alpha$*  was higher in IPF MDMs. (b) *IL-6* and (c) *IL-1 $\beta$*  expression were not significantly increased in IPF MDMs compared to controls ( $p=0.108$  and  $0.181$  respectively). (d) *AREG* expression was higher in IPF MDMs compared to controls. Expression of (e) *IL-10* and (f) *VEGF-A* did not differ significantly in IPF MDMs compared to controls ( $p$ -values both  $0.108$ ). (g) *CCL18* expression was similar between IPF and control MDMs (h) *COX-2* did not differ significantly between groups ( $p=0.117$ ). (i). *LGALS3* expression was higher in IPF MDMs compared to controls. (j) *INHA* expression showed an increased trend in IPF MDMs ( $p=0.082$ ). Mann-Whitney or Student t-test were used to compare data sets.  $p<0.05$  taken to indicate statistical significance. IPF  $n=8$ , controls  $n=6$ . Full gene list and further details are provided in Table 5-3.

## Chapter 5: Phenotypic and functional characteristics of MDMs from IPF patients



## Chapter 5: Phenotypic and functional characteristics of MDMs from IPF patients

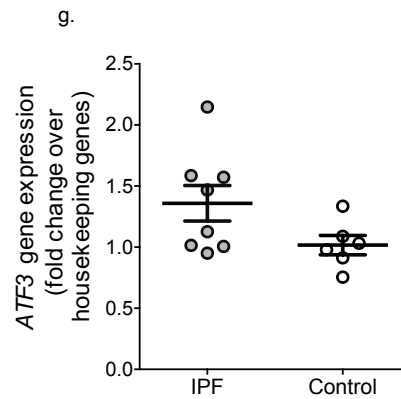


**Figure 5-13. Gene expression of transcription factors and nuclear receptors in IPF and control MDMs.**

qPCR was undertaken on day 7 MDMs to determine the relative gene expression of transcription factors associated with 'M1' signalling and reparative/immunomodulatory 'M2' signalling responses. The fold change over three housekeeping genes was used (*CYCLOPHILIN A*,  *$\beta$ 2-MICROGLOBULIN* and  *$\beta$ -ACTIN*). For normally distributed data, mean(SEM) are depicted in graphs. For non-parametric data, the median and interquartile range are shown. (a) *STAT1* expression was higher in IPF MDMs compared to controls (b) *STAT3* expression did not differ significantly between groups. (c) A trend towards increased expression of *STAT6* was seen in IPF MDMs ( $p=0.098$ ). Significant increases in the expression of genes associated with 'M2' responses were seen in IPF MDMs compared to controls: (d) *GR* (e) *PPAR $\gamma$*  (f) *IRF4* expression was up-regulated in IPF MDMs compared to controls. (g) A trend towards increased expression of *ATF3* was seen in IPF MDMs ( $p=0.086$ ). Mann-Whitney or Student t-test were used to compare data sets.  $p<0.05$  taken to indicate statistical significance. IPF  $n=8$ , controls  $n=6$ . Full gene list and further details are provided in Table 5-3.

## Chapter 5: Phenotypic and functional characteristics of MDMs from IPF patients

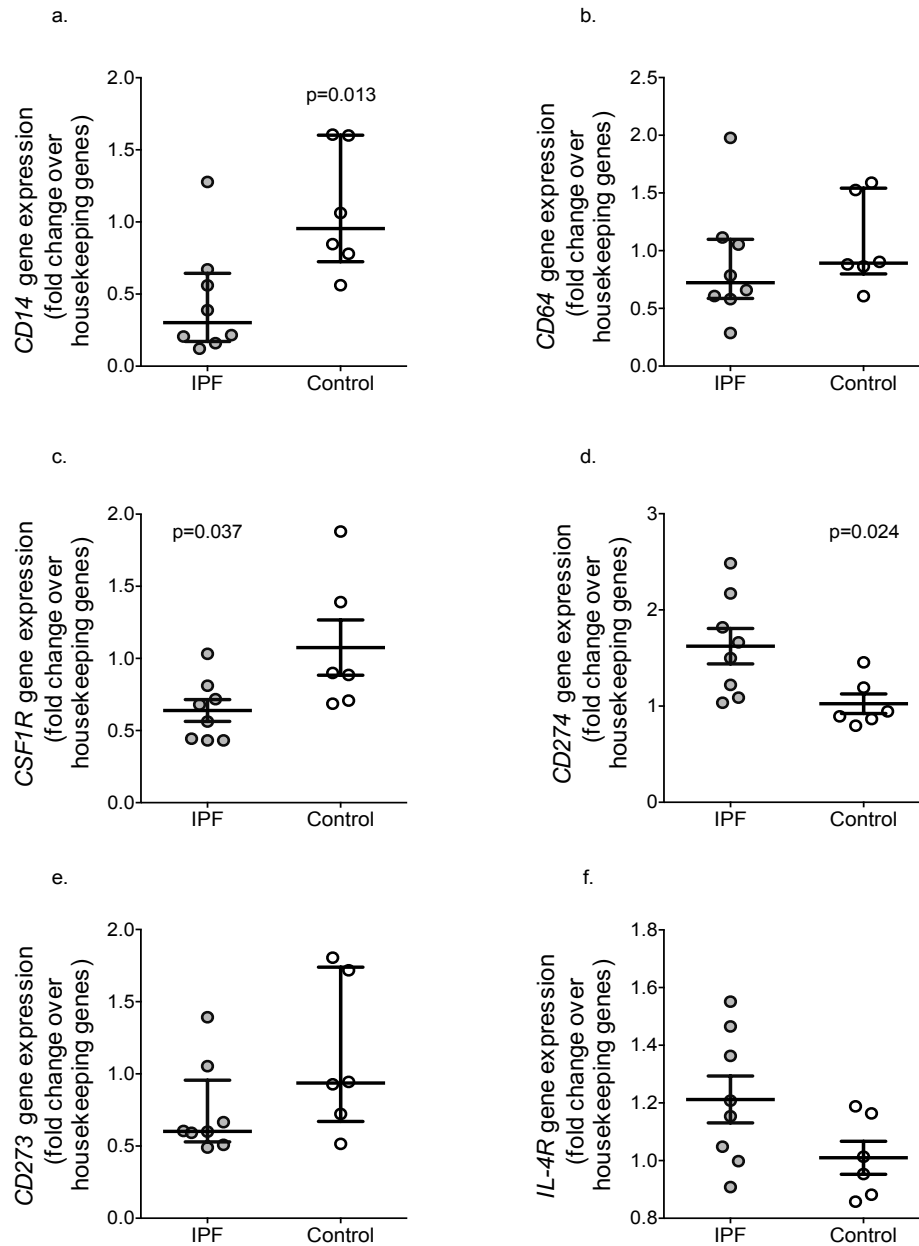


**Figure 5-14. Gene expression of cell surface receptors in IPF and control MDMs.**

qPCR was undertaken on day 7 MDMs to determine the relative gene expression of cell surface receptors associated with inflammatory ('M1') and reparative/immune-modulatory ('M2') responses. The fold change over three housekeeping genes was used (*CYCLOPHILIN A*, *β2-MICROGLOBULIN* and *β-ACTIN*). For normally distributed data, mean(SEM) are depicted in graphs. For non-parametric data, the median and interquartile range are shown. (a) *CD14* expression was lower in IPF MDMs compared to controls. (b) *CD64* expression was similar between IPF and control MDMs. (c) *csf1r* expression was decreased in IPF MDMs compared to controls. (d) Expression of *CD274* was higher in IPF MDMs. (e) *CD273* expression not differ between the two groups. (f) *IL-4R* expression was not significantly increased in IPF MDMs compared to controls (p=0.108). Mann-Whitney or Student t-test were used to compare data sets. p<0.05 taken to indicate statistical significance. IPF n=8, controls n=6. Full gene list analysed and further details are provided in Table 5-3.

## Chapter 5: Phenotypic and functional characteristics of MDMs from IPF patients

Category	Gene	Protein transcript	Description	Mean fold change (SEM)	Mean fold change (SEM)	Median fold change (IQR)	Median fold change (IQR)	P-value
				HC	IPF	HC	IPF	
Pro-inflammatory	<i>TNF<math>\alpha</math></i>	Tumour necrosis Factor alpha (TNF $\alpha$ )	Cytokine	<b>1.08 (0.44)</b>	<b>6.19 (5.39)</b>	<b>1.09 (0.71-1.45)</b>	<b>3.81 (2.66-11.44)</b>	<b>0.013</b>
	<i>IL-1<math>\beta</math></i>	Interleukin-1 beta (IL-1 $\beta$ )	Cytokine	1.08 (0.50)	2.28 (1.65)	0.81 (0.72-1.65)	1.89 (1.00-4.06)	0.108
	<i>IL-6</i>	Interleukin-6 (IL-6)	Cytokine	2.03 (2.47)	9.3 (8.78)	1.15 (0.21-3.73)	7.45 (0.94-17.39)	0.181
	<i>COX-2</i>	Cyclooxygenase-2 (COX-2)	Enzyme	1.18 (0.75)	0.71 (0.24)	0.94 (0.52-1.94)	0.64 (0.52-0.98)	0.117
	<i>CD64</i>	CD64	Receptor	1.06 (0.40)	0.88 (0.52)	0.89 (0.80-1.54)	0.72 (0.59-1.10)	0.295
	<i>HLA-DR</i>	HLA-DR	Receptor	1.13 (0.62)	1.18 (0.57)	0.88 (0.66-1.78)	1.08 (0.65-1.79)	0.950
	<i>STAT1</i>	<b>Signal Transducer And Activator Of Transcription 1 (STAT1)</b>	Transcription factor	<b>1.03 (0.24)</b>	<b>1.62 (0.41)</b>	<b>1.08 (0.90-1.19)</b>	<b>1.66 (1.31-2.01)</b>	<b>0.008</b>
	<i>IDO1</i>	indoleamine 2,3-dioxygenase 1 (IDO1)	Enzyme	1.04 (0.32)	16.7 (26.63)	0.92 (0.78-1.33)	6.21 (0.95-25.41)	0.142
	<i>IRF5</i>	Interferon Regulatory Factor 5 (IRF5)	Transcription factor	1.03 (0.26)	1.22 (0.28)	0.94 (0.85-1.19)	0.82 (0.95-1.46)	0.207
Reparative	<i>VEGF-A</i>	Vascular Endothelial Growth Factor (VEGF-A)	Growth factor	1.22 (0.77)	0.57 (0.38)	1.13 (0.48-1.99)	0.50 (0.25-0.70)	0.108
	<i>IGF-1</i>	Insulin-like Growth Factor-1 (IGF-1)	Growth factor	4.34 (5.60)	0.24 (0.19)	1.49 (0.09-11.14)	0.18 (0.11-0.40)	0.282
	<i>AREG</i>	<b>AREG/ amphiregulin</b>	Growth factor	<b>1.83 (2.82)</b>	<b>11.55 (15.41)</b>	<b>0.73 (0.55-2.54)</b>	<b>4.51 (1.45-27.91)</b>	<b>0.029</b>
	<i>TGF<math>\beta</math></i>	Transforming Growth Factor beta (TGF $\beta$ )	Growth factor	1.01 (0.17)	0.92 (0.16)	0.97 (0.87-1.12)	0.87 (0.87-0.98)	0.142
	<i>CCL18</i>	Chemokine CCL18	Chemokine	5.46 (8.1)	16.75 (30.18)	0.32 (0.20-15.85)	8.27 (1.10-12.20)	0.228
	<i>CCL22</i>	Chemokine CCL22	Chemokine	1.18 (0.64)	1.51 (1.10)	1.11 (0.64-1.83)	1.21 (0.77-1.79)	0.852
	<i>CD206</i>	CD206	Receptor	1.13 (0.69)	1.38 (0.85)	0.84 (0.70-1.61)	1.28 (0.62-2.30)	0.662
	<i>CD209</i>	CD209	Receptor	1.10 (0.51)	1.55 (1.32)	0.97 (0.65-1.63)	1.39 (0.49-1.90)	0.662
	<i>IL-4R</i>	IL-4 Receptor (IL-4R)	Receptor	1.01 (0.14)	1.21 (0.23)	0.98 (0.88-1.17)	1.18 (1.01-1.44)	0.108
	<i>STAT3</i>	Signal Transducer And Activator Of Transcription 3 (STAT3)	Transcription factor	1.02 (1.21)	1.16 (1.37)	0.98 (0.84-1.24)	1.15 (0.94-1.34)	0.239
	<i>STAT6</i>	Signal Transducer And Activator Of Transcription 6 (STAT6)	Transcription factor	1.01 (0.14)	1.32 (0.40)	0.99 (0.88-1.15)	1.19 (1.05-1.43)	0.092
	<i>IRF4</i>	<b>Interferon Regulatory Factor 4 (IRF4)</b>	Transcription factor	<b>1.17 (0.67)</b>	<b>17.82 (28.88)</b>	<b>1.13 (0.52-1.79)</b>	<b>7.41 (1.93-22.23)</b>	<b>0.043</b>
	<i>PPAR<math>\gamma</math></i>	<b>Peroxisome Proliferator-activated Receptor-gamma (PPAR<math>\gamma</math>)</b>	Nuclear Receptor	<b>1.03 (0.26)</b>	<b>1.51 (0.35)</b>	<b>1.02 (0.77-1.24)</b>	<b>1.40 (1.29-1.86)</b>	<b>0.016</b>
	<i>LGALS3</i>	<b>Galectin-3 (LGALS3)</b>	Binding protein	<b>1.02 (0.20)</b>	<b>1.96 (0.69)</b>	<b>1.00 (0.87-1.11)</b>	<b>1.98 (1.34-2.49)</b>	<b>0.007</b>
	<i>INHHA</i>	Inhibin alpha subunit (INHHA)	Proprotein	1.11 (0.55)	2.56 (2.00)	1.11 (0.57-1.45)	1.87 (1.37-3.64)	0.082
Anti-inflammatory / Immunomodulatory	<i>IL-10</i>	Interleukin -10 (IL-10)	Cytokine	1.14 (0.57)	0.67 (0.58)	1.21 (0.53-1.56)	0.39 (0.20-1.18)	0.108
	<i>CD163</i>	CD163	Receptor	1.68 (1.82)	0.83 (0.83)	1.05 (0.34-2.98)	0.64 (0.17-1.22)	0.228
	<i>CD273/PDL-2</i>	CD273/Programmed cell death ligand 2 (PDL2)	Receptor	1.10 (0.53)	0.74 (0.32)	0.94 (0.67-1.74)	0.60 (0.53-0.96)	0.142
	<i>CD274/PDL-1</i>	<b>CD274/Programmed cell death ligand 1 (PDL1)</b>	Receptor	<b>1.02 (0.25)</b>	<b>1.62 (0.52)</b>	<b>0.92 (0.85-1.26)</b>	<b>1.58 (1.12-2.08)</b>	<b>0.024</b>
	<i>IL-10R<math>\beta</math></i>	IL-10 Receptor beta (IL-10R $\beta$ )	Receptor	1.03 (0.27)	0.91 (0.15)	0.95 (0.89-1.16)	0.94 (0.79-1.02)	0.340
	<i>GR/NR3C1</i>	<b>Glucocorticoid Receptor (GR)/Nuclear Receptor Subfamily 3 Group C Member 1 (NR3C1)</b>	Nuclear receptor	<b>1.01 (0.19)</b>	<b>1.27 (0.19)</b>	<b>1.01 (0.83-1.16)</b>	<b>1.3 (1.08-1.40)</b>	<b>0.029</b>
	<i>ATF3</i>	Activating Transcription Factor 3 (ATF3)	Transcription factor	1.02 (0.19)	1.36 (0.41)	1.00 (0.87-1.15)	1.30 (1.01-1.58)	0.086
Inflammatory and reparative or other	<i>CD14</i>	<b>CD14</b>	Receptor	<b>1.08 (0.44)</b>	<b>0.45 (0.39)</b>	<b>0.95 (0.72-1.60)</b>	<b>0.30 (0.17-0.64)</b>	<b>0.013</b>
	<i>CSF1-R</i>	<b>Colony stimulating Factor-1 Receptor (CSF1-R)</b>	Receptor	<b>1.07 (0.47)</b>	<b>0.64 (0.21)</b>	<b>0.89 (0.70-1.51)</b>	<b>0.43 (0.43-0.79)</b>	<b>0.037</b>

**Table 5-3. The full list of genes analysed on day 7 MDMs from IPF patients and aged-matched healthy controls (HC).**

Genes are grouped according to their association with inflammatory ('M1') and reparative/anti-inflammatory and immunomodulatory ('M2') responses. Mean and median fold change were calculated in relation to housekeeping genes, *cyclophilin a*,  $\beta$ 2-microglobulin and  $\beta$ -actin. D'Agostino Pearson normality test was used to determine distribution of data and Student t-test or Mann-Whitney test used to compare groups. P-value <0.05 was taken to indicate statistical significance and these results are highlighted in bold. SEM- standard error of the mean, IQR- interquartile range, CD- Cluster of differentiation. IPF n=8, controls=6



#### 5.4.8 M-CSF was increased in the serum of IPF patients

IPF Macrophages derived from monocytes cultured in autologous serum exhibited distinct phenotypic differences compared to age-matched controls. Expression of inflammatory receptors, CD64 and CD86, was down-regulated whereas CD14 remained elevated following differentiation. Gene expression data showed distinct differences in the fold change of reparative/immunomodulatory and inflammatory genes. Whilst preferential apoptosis of inflammatory monocytes may provide a partial explanation for these findings, I questioned whether serum factors may also influence the pattern of monocyte differentiation.

M-CSF is a growth factor important for the survival and differentiation of monocytes. In addition, in vitro studies have demonstrated that it can polarise monocytes towards an 'M2' phenotype [196, 210, 308]. Patients with IPF were found to have elevated M-CSF in the BALF and M-CSF knock-out mice were protected from bleomycin-induced lung fibrosis [309]. To determine whether M-CSF was also elevated in the serum of IPF patients, I used an ELISA assay to analyse the concentration of this growth factor in the serum of stable patients and controls.

The results confirmed that the concentration of M-CSF was significantly higher in the serum of IPF patients compared to healthy controls ( $p < 0.001$ , Fig 5-15).

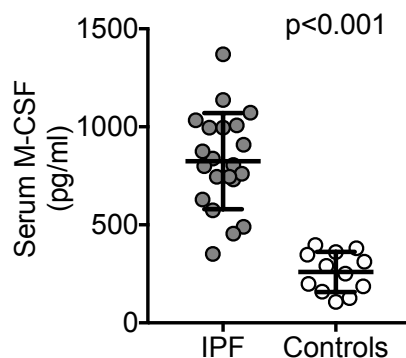


**Figure 5-15. The concentration of M-CSF in serum from IPF patients was significantly higher than healthy controls.**

An ELISA-based assay was undertaken on heat-inactivated serum samples from stable IPF patients and healthy controls to determine the concentration of M-CSF. Mean(SD) illustrated in graph. [Mean concentration (pg/ml) (SD) 824.8(245) vs 259.8(102.6) n=21 and 12 for IPF and controls respectively], Student t-test used.

#### **5.4.9 The production of reactive oxygen species (ROS) is impaired in IPF MDMs compared to controls**

I found that the phenotypic characteristics of IPF MDMs differed significantly from MDMs derived from healthy, age-matched controls in both protein and RNA expression. To assess whether these phenotypic differences translated to functional differences, I looked at the ability of MDMs to generate reactive oxygen species in response to oxidative stress induced by hydrogen peroxide. Given that ROS production is associated with inflammatory rather than reparative macrophage activity, I hypothesised that generation of ROS would be lower in IPF MDMs. Of interest, however, a study published in 1991 using a luminol-dependant chemiluminescence assay to assess ROS generation, found that alveolar macrophages (AMs) isolated from IPF patients produced greater ROS. This was attributed to AMs possessing a more 'monocyte-like' phenotype due to decreased differentiation of monocyte-derived-macrophages [310].

ROS activity in this experiment was measured using the oxidative stress indicator CM-H2DCFDA, which is retained in the cell following passive diffusion. MDMs were then stimulated by hydrogen peroxide resulting in the generation of ROS and oxidation of CM-H2DCFDA. This process of oxidation yields a fluorescent adduct that can be measured by flow cytometric analysis.

In contrast to the study on AMs, I found that MDMs from IPF patients produced significantly less ROS in response to oxidative stress compared to healthy controls. Baseline levels of ROS, measured by the percentage of MDMs positive for the dye and the MFI of CM-H2DCFDA on live cells, were similar between the two groups. Following incubation with 0.03% H<sub>2</sub>O<sub>2</sub> for 60 minutes, however, distinct differences in ROS production were observed. Less ROS was generated by IPF MDMs compared to controls ( $p=0.032$  and  $p=0.011$  for the percentage and MFI respectively, Fig 5-16c and d).

## Chapter 5: Phenotypic and functional characteristics of MDMs from IPF patients

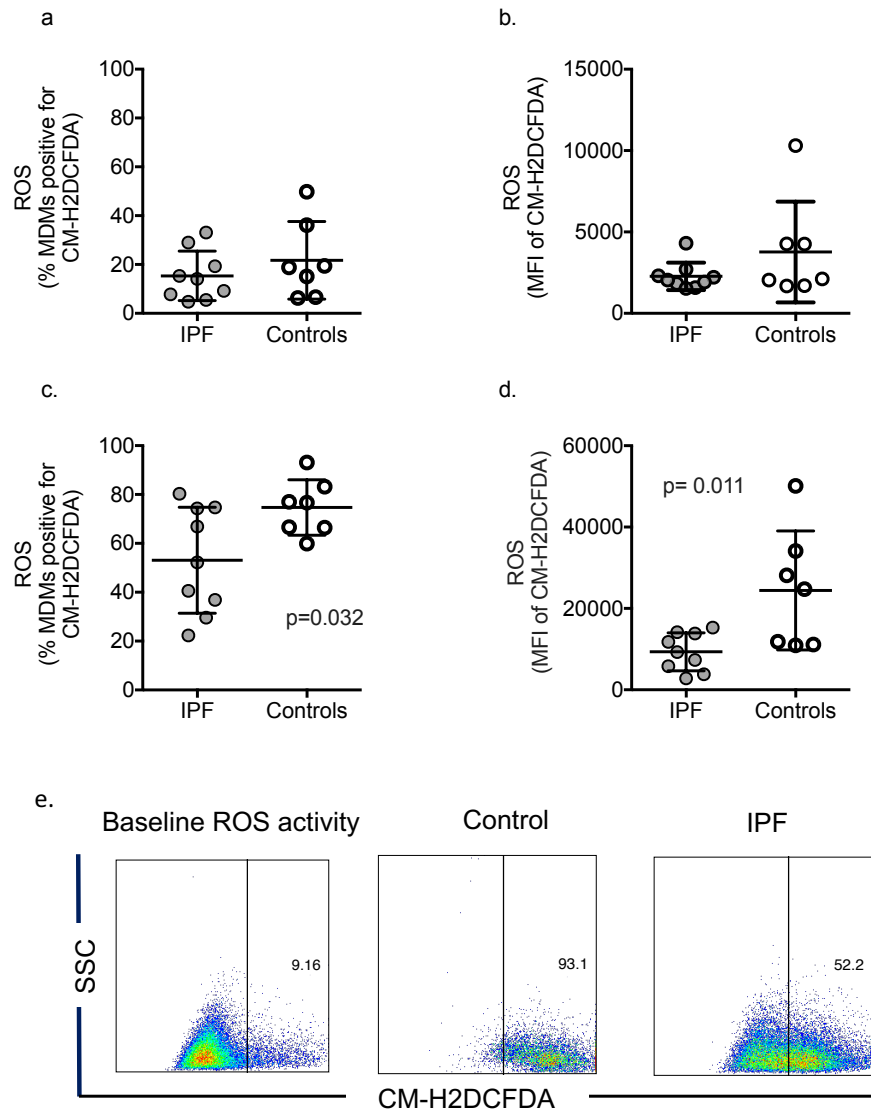


**Figure 5-16. Assay comparing ROS generation by IPF and control MDMs following stimulation with hydrogen peroxide (H<sub>2</sub>O<sub>2</sub>).**

MDMs were incubated for 1 hour with the oxidative stress indicator CM-H2DCFDA, then stimulated with 0.03% H<sub>2</sub>O<sub>2</sub> to induce oxidative stress. ROS generation resulted in the oxidation and fluorescence of CM-H2DCFDA enabling the comparative measurement of ROS within cells using flow cytometry. Mean(SD) quoted here and illustrated on graphs. Baseline ROS production in IPF and control MDMs was similar, as indicated by: (a) the percentage and (b) the MFI of cells fluorescing following incubation with CM-H2DCFDA (without H<sub>2</sub>O<sub>2</sub>). ROS production following stimulation with 0.03% H<sub>2</sub>O<sub>2</sub> for one hour was lower in IPF MDMs compared to controls, indicated by: (c) percentage of positive cells [53%(22) vs 75%(11)] and (d) MFI of CM-H2DCFDA in all live cells [(24426(14644) vs 9348(4665)]. n=9 and 7, D'Agostino Pearson normality test and Student t-test used. (e) FACs plots gated on live cells, showing unstimulated MDMs (baseline ROS activity) and following stimulation with H<sub>2</sub>O<sub>2</sub> in a control and IPF patient. (ROS - reactive oxygen species; SSC - side-scatter).

#### 5.4.10 IL-1 $\beta$ secretion in response to inflammasome activation does not differ between IPF and control MDMs

IL-1 $\beta$  is an inflammatory cytokine predominantly released by macrophages following activation of pattern-recognition receptors (PRRs). Sustained release of IL-1 $\beta$  potentiates fibrogenic pathways through up-regulation of growth factors and cytokines such as PDGF and TGF $\beta$  [98, 109, 113]. Studies have found an increase in IL-1 $\beta$  in BALF and lung tissue from IPF patients and mRNA levels were elevated in AMs [98, 113]. A trend towards increased *IL-1 $\beta$*  mRNA expression was noted in IPF MDMs ( $p=0.189$ , Fig 5-12c), and given that MDMs are likely to contribute to the lung macrophage population in the context of fibrosis [193], I was interested in determining whether IL-1 $\beta$  secretion was enhanced in IPF MDMs following stimulation.

Release of active IL-1 $\beta$  requires cleavage of the precursor protein pro-IL-1 $\beta$  which is mediated by the enzyme caspase-1. Caspase-1 is activated following assembly of a multimeric protein complex termed the NLRP3 inflammasome. Activation of NLRP3 usually requires two forms of stimuli. The first is necessary to 'prime' the cell resulting in increased cellular expression of NLRP3 and pro-IL-1 $\beta$ , and the second stimulus leads to assembly of NLRP3 and activation of caspase-1 which then cleaves pro-IL-1 $\beta$  to its active form [111, 311, 312]. In this experiment, LPS was used as a priming signal followed by Nigericin, a toxin that induces a fall in intracellular potassium levels resulting in a second signal that triggers caspase-1 activation (Fig 5-17) [312, 313]. The concentration of active IL-1 $\beta$  was then measured in the supernatant of MDMs via ELISA.

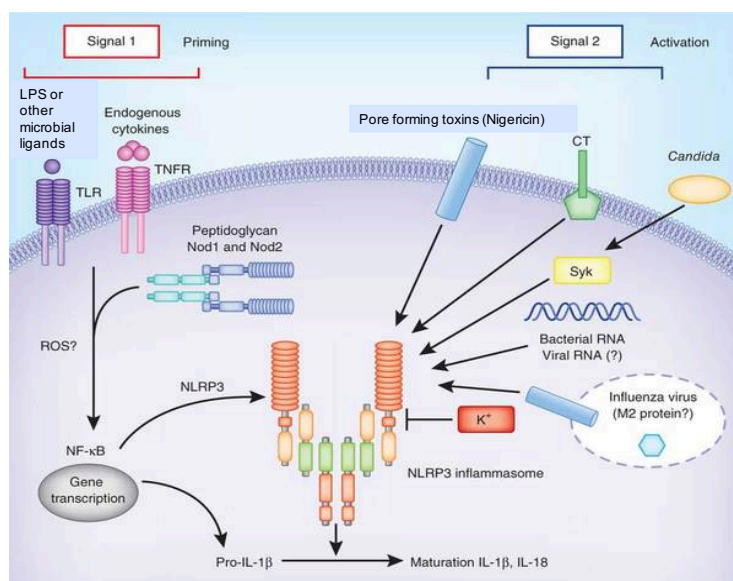


**Figure 5-17. Activation of the NLRP3 inflammasome triggers release of IL-1 $\beta$ .**

Assembly of the NLRP3 inflammasome usually requires both priming (Signal 1) and activation stimuli (Signal 2). Signal 1 includes Toll-like receptor ligands such as LPS which increase cellular expression of NLRP3 and pro-IL-1 $\beta$ . The second signal includes DAMPs and PAMPs and results in activation of the NLRP3 inflammasome which cleaves pro-caspase-1. Caspase-1 then converts pro-IL-1 $\beta$  to active IL-1 $\beta$ . Adapted from Franchi *et al.* [312].

## Chapter 5: Phenotypic and functional characteristics of MDMs from IPF patients

Figure 5-18 shows the concentration of IL-1 $\beta$  secreted by day 7 MDMs after priming with LPS overnight followed by Nigericin. Active IL-1 $\beta$  was not produced in significant concentration by unstimulated cells or those stimulated by Nigericin alone although LPS evoked IL-1 $\beta$  release in this in vitro experiment. Both stimuli in combination elicited the highest production of IL-1 $\beta$ , as measured by ELISA (Fig 5.18a). A difference in the concentration of IL-1 $\beta$  secreted by MDMs was not found between patients and controls.

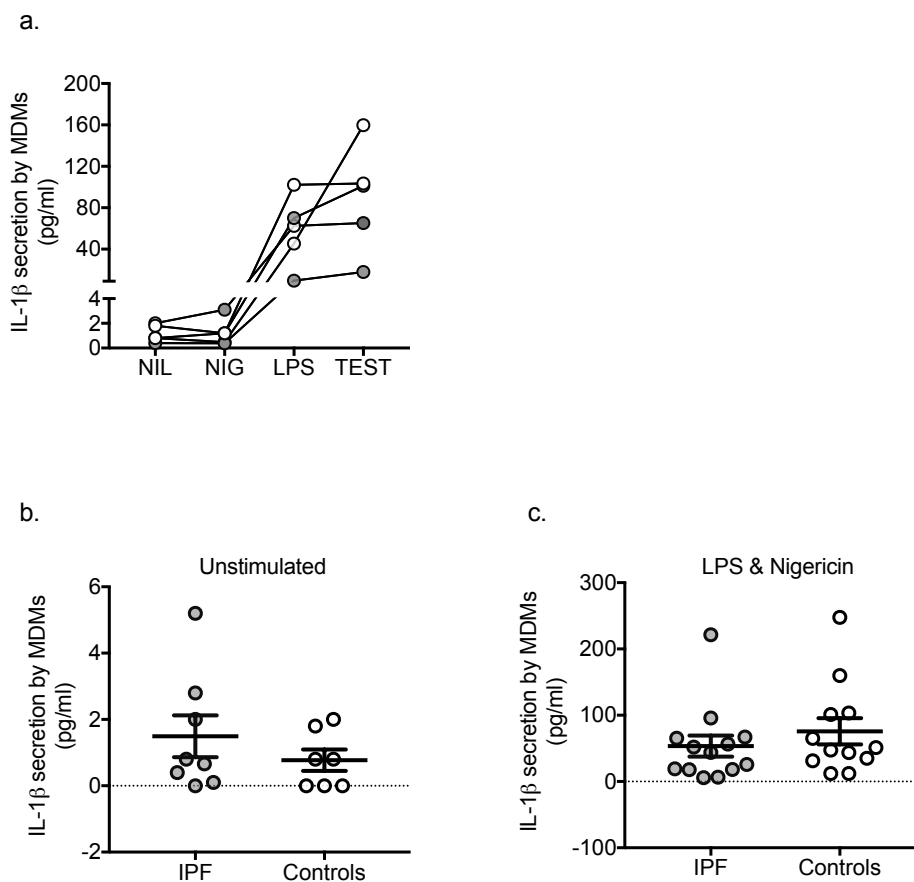


**Figure 5-18. IL-1 $\beta$  secretion following activation of the NLRP3 inflammasome in MDMs.**

The concentration of IL-1 $\beta$  released by IPF and control MDMs was measured in the supernatant by ELISA after priming cells with LPS (1:10000) for 16h followed activation by Nigericin (1:1000) for 30 minutes. SD(mean) illustrated in graphs. (a) The concentration of IL-1 $\beta$  from MDMs left unstimulated (NIL), stimulated with Nigericin (NIG) or LPS (LPS) alone and in combination (TEST). IPF and control MDMs were analysed together n=5 grey circles - IPF, clear circles - controls. (b) Baseline IL-1 $\beta$  secretion by unstimulated MDMs was minimal in both IPF and control MDMs. (c). IL-1 $\beta$  was produced by MDMs in response to LPS and Nigericin but differences in the concentration were not observed between IPF and controls ( $p=0.398$ , IPF n=8, controls n=7, Mann-Whitney test).

## 5.5 Discussion

Circulating monocytes from treatment-naïve patients showed subtle phenotypic differences, but given that IPF is a disease exclusively affecting the lung parenchyma, defining the characteristics of monocytes as they differentiate into tissue-based macrophages is of relevance. Simulating monocyte maturation in culture over 7 days using autologous serum revealed that IPF MDMs followed a differentiation pathway that was divergent and distinct from healthy controls. The data has demonstrated marked differences in the phenotype and function of IPF MDMs, providing evidence that monocytes from IPF patients may exert differential effects following differentiation in vivo. The high concentration of M-CSF within the serum of IPF patients and the preferential apoptosis of inflammatory monocytes are likely to be contributing factors to the differences observed.

The first clear phenotypic difference in IPF MDMs is the higher intensity and proportion of cells expressing CD14. As demonstrated in Figure 5-3, monocyte to macrophage differentiation is associated with down-regulation of this receptor and up-regulation of the lysosomal scavenger receptor CD68. The relative expression of these receptors can be used to distinguish monocyte and macrophage populations respectively and this pattern is demonstrated within the control arm of the study. The retention of CD14 on day 7 IPF MDMs coupled with a reduction in CD68 suggests that monocytes show delayed maturation to macrophages and potentially possess a more monocyte-like phenotype following tissue entry in vivo. There are other possibilities for the retention of CD14 however, which are perhaps less likely but worthy of consideration, particularly as CD14 was also more highly expressed on monocytes from IPF patients. CD14 is a pattern recognition receptor that can recognise a number of ligands including apoptotic cells, fungi and bacterial cell components [314]. It is most recognised for its role as the LPS co-receptor where in conjunction with TLR4, it mediates a signalling pathway resulting in production of TNF $\alpha$  and other pro-inflammatory cytokines [315]. Transgenic mice over-expressing CD14 show a hypersensitive response to LPS and develop endotoxin shock, whereas mice lacking CD14 show blunted inflammatory responses to LPS challenge [316, 317]. Expression of CD14 was also found to be increased on monocytes in patients with active vasculitis and correlated with autoantibody levels, leading the authors to speculate that CD14 may be a marker of monocyte activation [318]. Thus, it is possible that its elevated expression indicates that monocytes from IPF

## Chapter 5: Phenotypic and functional characteristics of MDMs from IPF patients

patients differentiate into macrophages that are more 'activated' than controls and primed to respond to challenge by PAMPs and DAMPs. The gene expression data is partially in keeping with this suggestion, showing up-regulation in both *TNF $\alpha$* , and *STAT1*. In conflict to this hypothesis however, was my finding that Dexamethasone (an 'M2c' polarising agent, section 1.3.4) increased CD14 expression. Furthermore, two published studies reported that CD14 was up-regulated following the differentiation of monocytes to MDMs using the M2-polarising agents IL-4 and M-CSF [197, 308]. In addition, this hypothesis cannot explain several other findings presented in this chapter including the down-regulation of 'inflammatory' receptors CD64 and CD86 on the cell surface of IPF MDMs and the blunted production of ROS in response to stimulation.

The reduced expression of ROS by IPF MDMs contrasts with a study that found ROS generation was higher in IPF alveolar macrophages that were derived from BAL fluid [310]. The discrepancies in the findings may relate to the different techniques used to measure ROS, the cell type involved (including the potential for contamination of AMs by neutrophils and presence of tissue-resident macrophage populations) and the use of anti-fibrotic treatment by patients in this arm of the study (6 out of the 8 patients were on treatment). The findings in my work may also relate to the preferential apoptosis of inflammatory monocytes (CD64<sup>+</sup>CD163<sup>-</sup>) occurring early on in the process of monocyte to macrophage differentiation. Monocytes from IPF patients expressed high levels of CD64, a marker associated with inflammatory and activated cells but a significantly higher proportion of these cells were noted to be undergoing programmed cell death on day 1. By day 7, IPF MDMs expressed lower CD64, supporting the hypothesis that the dominant population of monocyte-derived-macrophages in IPF become skewed towards a non-inflammatory phenotype.

The gene expression findings reveal a number of interesting and distinct differences between controls and IPF MDMs but do not enable the categorisation of these cells into defined populations described in the literature. Polarisation of macrophages towards 'M2' by stimulation of receptors such as IL-10R and IL-4R initiates downstream signalling pathways resulting in the phosphorylation of transcription factors STAT3 and STAT6 and up-regulation of other molecules such as PPAR $\gamma$  and IRF4 that mediate cellular responses involved in immunomodulatory and reparative activities. They are also documented to inhibit STAT1 signalling pathways involved in inflammatory responses to type 1 interferons and PAMPs [216]. As demonstrated in Figure 5-13, whilst the majority of genes up-regulated in IPF MDMs were those associated with broad 'M2' functions,

## Chapter 5: Phenotypic and functional characteristics of MDMs from IPF patients

increased expression of *STAT1* and its major product of activation, *TNF $\alpha$* , are somewhat contradictory and once again highlight the complexity of delineating macrophage phenotypes. Clearly, the framework of M1 and M2 is inadequate to describe the MDM characteristics reported here and it is likely that several subpopulations exist in both groups, complicating interpretation. Assessing the 'balance' of M2 and M1 genes may therefore be a more practical method of predicting the functionality of these cell populations from phenotypic and gene expression data, and overall IPF MDMs appear to more closely resemble macrophages involved in the later stages of repair. This stated, a greater proportion of genes examined in my work were associated with reparative and immunomodulatory functions and thus broadening the panel of genes associated with inflammation would be required to confirm this assertion. The genes up-regulated and down-regulated in IPF MDMs are depicted in the diagram below (Fig 5-19) and can be compared to those described diagrammatically by Wynn (5-20) to depict macrophages involved in inflammatory, reparative and resolution responses [126].

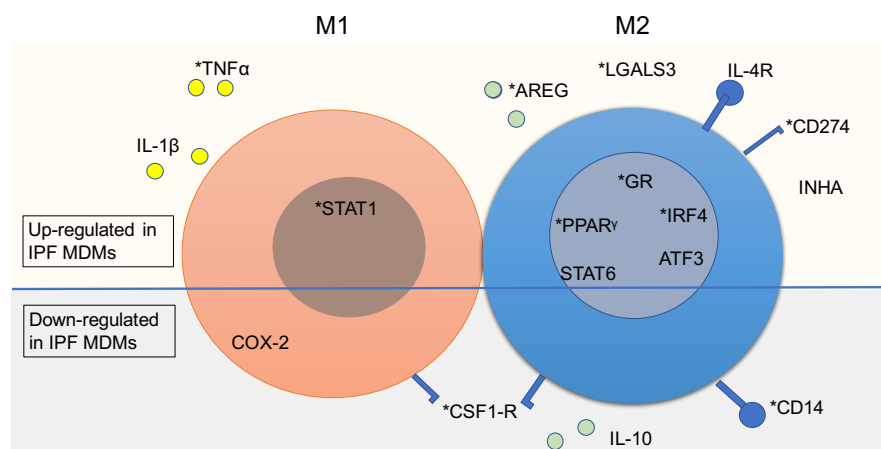


**Figure 5-19. Diagrammatic representation of the main genes up-regulated and down-regulated in IPF MDMs compared to controls.**

Asterisk indicates differences with a p-value < 0.05, all other genes indicate differences of p < 0.12. Fold change over three housekeeping genes was used (cyclophilin A,  $\beta$ 2-microglobulin and  $\beta$ -actin).



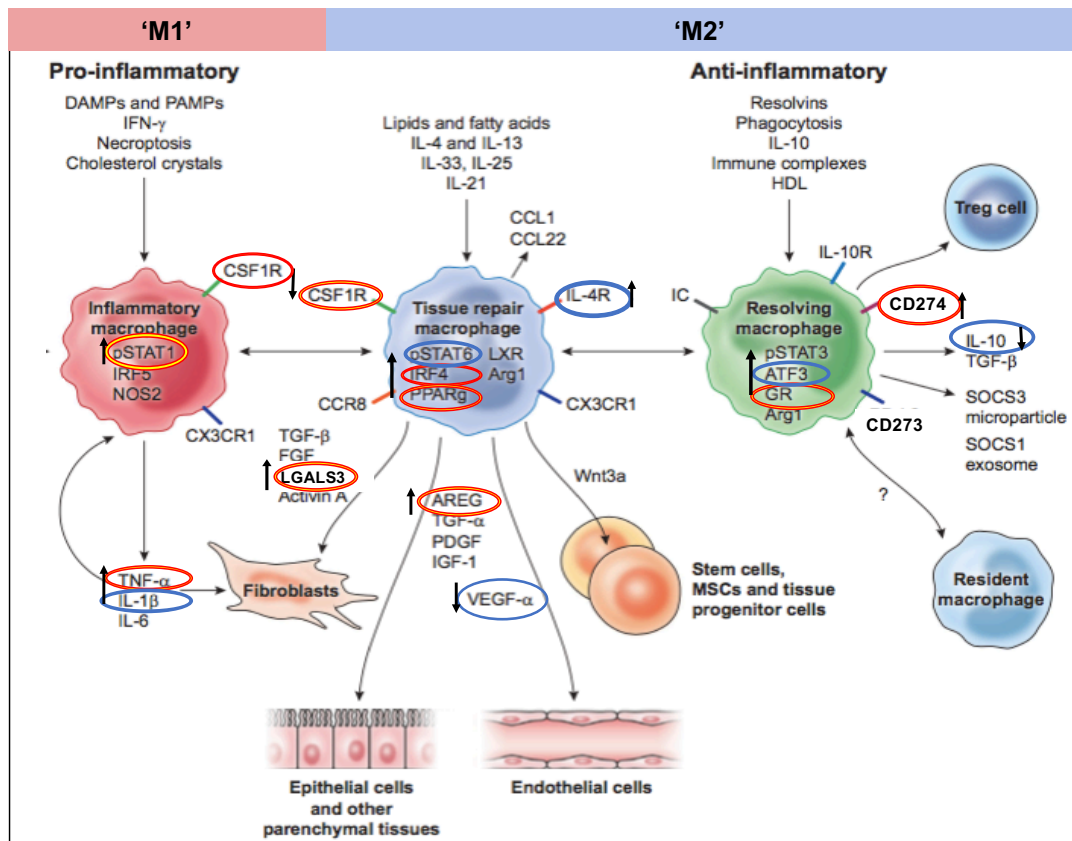


**Figure 5-20. The major macrophage phenotypes associated with inflammatory and reparative/resolution activities.**

Phenotype and function are modulated by external triggers including DAMPs, PAMPs, cytokines and other soluble factors. Transcription factors, cytosolic and cell surface proteins plus cytokines/chemokines associated with inflammatory (M1) and reparative/resolution (M2) responses are depicted in this diagram. Genes significantly up-regulated in IPF MDMs are circled in red/yellow ( $p < 0.05$ ) with trends towards increased expression circled in blue ( $p < 0.12$ ). Adapted from T Wynn [126].

Over-expression of *AREG* and *LGALS3* by IPF MDMs may be of particular interest. *AREG* is an epidermal growth factor receptor ligand that is induced by TGF $\beta$  and implicated in tissue repair and lung fibrosis. *AREG* directly increases fibroblast activation and proliferation in vitro, whilst in vivo work has found that inhibiting *AREG* attenuated fibrosis following bleomycin injury. Of relevance, a study investigating the cellular source of *AREG* in bleomycin-treated mice found that it was predominantly expressed by bone-marrow derived CD11c $^+$  cells. Depleting these cells reduced collagen deposition whilst adoptive transfer of CD11c $^+$  cells into mice following bleomycin intensified tissue fibrosis [319, 320]. Whilst CD11c $^+$  defines dendritic cells, they share a common myeloid lineage with monocyte-derived-macrophages thus raising the possibility that both cell

## Chapter 5: Phenotypic and functional characteristics of MDMs from IPF patients

populations may potentiate fibrogenesis through high *AREG* expression. Galectin-3 is the protein product of *LGALS3*. It is  $\beta$ -galactoside-binding protein implicated in diverse physiological processes, including the development of liver cirrhosis and lung fibrosis in bleomycin mouse models [321]. A study to investigate its potential role in IPF examined BAL fluid from participants with fibrotic lung disease including IPF, non-fibrotic lung diseases and healthy controls. The researchers found a high concentration of the protein in those with lung fibrosis only and expression of *LGALS3* was increased in IPF alveolar macrophages compared to controls [306]. In vitro work by the same authors demonstrated that *LGALS3* expression was induced by TNF $\alpha$  and TNF $\alpha$  itself was up-regulated by Galectin-3. I found that TNF $\alpha$  was also more highly expressed in IPF MDMs, suggesting that a possible autocrine or paracrine feedback loop may be driving the expression of both.

Monocytes isolated from PBMCs continue to show the characteristic hallmarks of corticosteroid (CS) exposure following macrophage differentiation a full week after the dose was last taken by the patient. The haemoglobin-haptoglobin scavenger receptor, CD163, up-regulated by corticosteroids [196, 220], remains higher in the Prednisolone-treated group even in MDMs from patients on lower doses of Prednisolone. Interestingly, the expression of CD68, a marker associated with macrophage differentiation was also increased, suggesting that Prednisolone may influence macrophage maturation. Phenotypic differences between AEIPF and those with stable disease on Prednisolone cannot be identified, suggesting that steroids either 'mimic' the phenotype of monocytes in AEIPF, or far more likely, exert a dominant modulatory influence that supersedes any subtle changes induced by mediators released during exacerbations of disease.

MDMs differentiated in the presence of Dexamethasone had a distinct morphology and its administration resulted in up-regulation of M2 receptors CD163 and CD206 alongside lower expression of the M1 receptor CD64. Interestingly, CD86 did not change significantly following treatment, questioning its utility as an 'M1' marker. Unlike the in vivo Prednisolone data, CD14 expression was also increased by Dexamethasone, which may be related to the higher concentration used in these experiments. There thus exists a partial similarity in the phenotype induced by Dexamethasone in vitro compared to that observed in vivo from patients on Prednisolone. Prednisolone has a half-life of between 2-4 hours in vivo but the bioactivity of the drug is estimated to be significantly longer [302]. Thus, it is probable that the MDMs from steroid-treated patients were cultured in serum still containing the drug (or its bioactive metabolites). Interestingly, research

## Chapter 5: Phenotypic and functional characteristics of MDMs from IPF patients

investigating gene expression in MDMs following in vitro steroid exposure has identified the up-regulation of genes also observed in the non-steroid IPF group [205, 322]. These include the glucocorticoid receptor (*GR*), *PPAR $\gamma$* , *IRF4* and *CD274*, alongside *STAT3*, *STAT6* and *IL-4R* genes, which showed an increased trend in expression.

Differences seen in the MDM phenotype of patients not taking steroids may be partially attributable to the high concentration of M-CSF present in the serum of IPF patients. Whilst the single dose of recombinant M-CSF given on Day 0 of monocyte culture was higher than the amount of M-CSF within the serum, it is possible that the additional contribution of autologous M-CSF was sufficient to skew the differentiation characteristics of IPF monocytes. Given that M-CSF is produced by a variety of cells, including monocytes and MDMs, higher production by those from IPF patients may have resulted in autocrine and paracrine stimulation. M-CSF is thought to 'prime' cells towards an M2 phenotype but depending on the contribution of other soluble factors, may promote the differentiation of cells with mixed inflammatory and reparative characteristics [207, 209, 210, 309]. To understand the potential contribution of other mediators, a comprehensive analysis of the serum looking at a range of cytokines and chemokines would be required.

This chapter has characterised MDMs from IPF and control participants. In order to do this, experiments were undertaken to identify and define macrophage populations according to inflammatory and reparative descriptions. As discussed above, the M1/M2 paradigm is a simplistic framework that can be useful when ascribing defined phenotypic features to possible in vivo functions. As demonstrated here however, this categorisation system is often unable to accommodate the complexity and plasticity of macrophages, which frequently exhibit characteristics of both. Furthermore, in vivo animal models demonstrate that sustained inflammatory cytokine release can eventually result in fibrotic endpoints indicating that 'M1' responses can lead to 'M2' consequences under certain circumstances. Thus, IPF MDMs evade textbook definition, which is not unexpected and does not subtract from the key finding of this chapter, which is that monocytes from IPF patients differentiate into phenotypically and functionally distinct macrophages. Furthermore, the increased *STAT1* and *TNF $\alpha$*  expression alongside up-regulation of 'M2' genes, combined with a decrease in 'M1' surface markers and poor ROS generation is not out of keeping with published findings that show evidence of mixed reparative/inflammatory responses occurring in IPF. Alveolar macrophages, for example, have been shown to exhibit phenotypic characteristics of 'M2' with high CD206

## Chapter 5: Phenotypic and functional characteristics of MDMs from IPF patients

and CD163 expression [25, 39, 268] alongside increased expression of inflammatory cytokines TNF $\alpha$  and IL-1 $\beta$ , and higher ROS generation [98, 104, 310].

Lineage tracing in mice has revealed that pulmonary fibrosis induced by bleomycin results in an influx of monocytes that contribute significantly to the lung macrophage pool. Weeks after injury, these cell populations were phenotypically distinct and depleting monocytes in the lung through necroptosis ameliorated fibrosis [193]. This study thus provides evidence that MDMs actively participate in matrix deposition in mouse models of lung fibrosis. Whilst pathogenic processes in bleomycin-induced injury cannot be directly extrapolated to IPF, there are likely to be similarities in the mechanisms at play. In support of this work, studies examining BAL cells found macrophage populations in IPF patients more closely resembled monocytes in morphology and differentiation markers [310, 323]. Thus, if monocyte-derived macrophages represent a significant proportion of the total lung macrophage population in IPF, then the phenotypic changes between IPF and control MDMs highlighted in this chapter may be of significance.

The reasons for these differences in phenotype are unknown but the findings here suggest that high serum levels of M-CSF and selective apoptosis of inflammatory monocytes play a role. Additional soluble factors within the serum of IPF patients may also be contributing factors. Alternatively (or in addition), recent work has demonstrated that epigenetic modifications of BM precursor cells can occur following certain stimuli (such as immunisation with BCG) [270], and it is thus possible that in IPF certain environmental exposures result in partial pre-programming of monocyte precursors, which subsequently influences their differentiation profiles. Whilst the conditions used to generate macrophages in this study are remote from the pathways taken by monocytes in vivo, the differences seen in MDMs from IPF patients may reflect an increased propensity to potentiate fibrosis and it is conceivable that the differentiation patterns of monocytes represent a risk factor for development of lung fibrosis. To determine whether MDMs from IPF patients differentially influence fibrogenic endpoints is the subject of the next chapter.

## 6 The influence of MDMs on fibrogenic end-points

### 6.1 Introduction

The previous chapters have highlighted differences in the phenotypic and functional characteristics of monocytes and MDMs from IPF patients compared with aged-matched healthy controls. It is unknown however whether the characteristics identified in IPF MDMs translate to differences in the capacity of these cells to modulate fibrogenic processes. This chapter therefore explores the influence of MDMs on fibroblast proliferation and activation, and examines how MDMs may impact on the process of epithelial-mesenchymal-transition (EMT).

In health, fibroblasts are quiescent with minimal metabolic activity, maintaining the architecture of the tissue in which they reside. Following injury however, they become 'activated', defined by high proliferative ability, a change in morphology from spindle to stellate shape and secretion of extracellular matrix (ECM) [134]. They also secrete cytokines such as PDGF, VEGF, TGF $\beta$ , HGF, FGF as well as inflammatory mediators such as IL-6, MCP-1, TNF and IFN $\gamma$  [80, 135, 324]. Activated fibroblasts, termed myofibroblasts, exert traction forces which contract the edges of a wound together and are identifiable by the expression of alpha-smooth muscle actin ( $\alpha$ SMA) [325]. In normal wound healing, fibroblasts acquire a reversibly activated phenotype to enable the formation of granulation tissue through construction of an ECM scaffold and recruitment of circulating and resident cells that repair and replenish denuded areas. Subsequently, this tissue is remodelled leading to the restoration of healthy tissue and fibroblasts undergo apoptosis or reprogramming back to a senescent state. In cases of chronic injury however, fibroblasts may become irreversibly activated, which can eventually result in tissue fibrosis. Such fibroblasts have been described as fibrosis-associated fibroblasts (FAFs) [324, 326]. In cancer, fibroblasts close to the tumour can also acquire a state of permanent activation resulting in alteration of the surrounding stroma and the secretion of soluble mediators that can either assist or inhibit local tumour spread and metastases [324]. Indeed, cancer-associated fibroblasts (CAFs) share many similarities with fibroblasts associated with fibrogenic responses such as those seen in IPF [324, 327, 328]. Here, fibroblasts demonstrate a pathological phenotype characterised by uncontrolled proliferation, matrix deposition and increased ability to invade the matrix [329, 330].

## Chapter 6: The influence of MDMs on fibrogenic endpoints

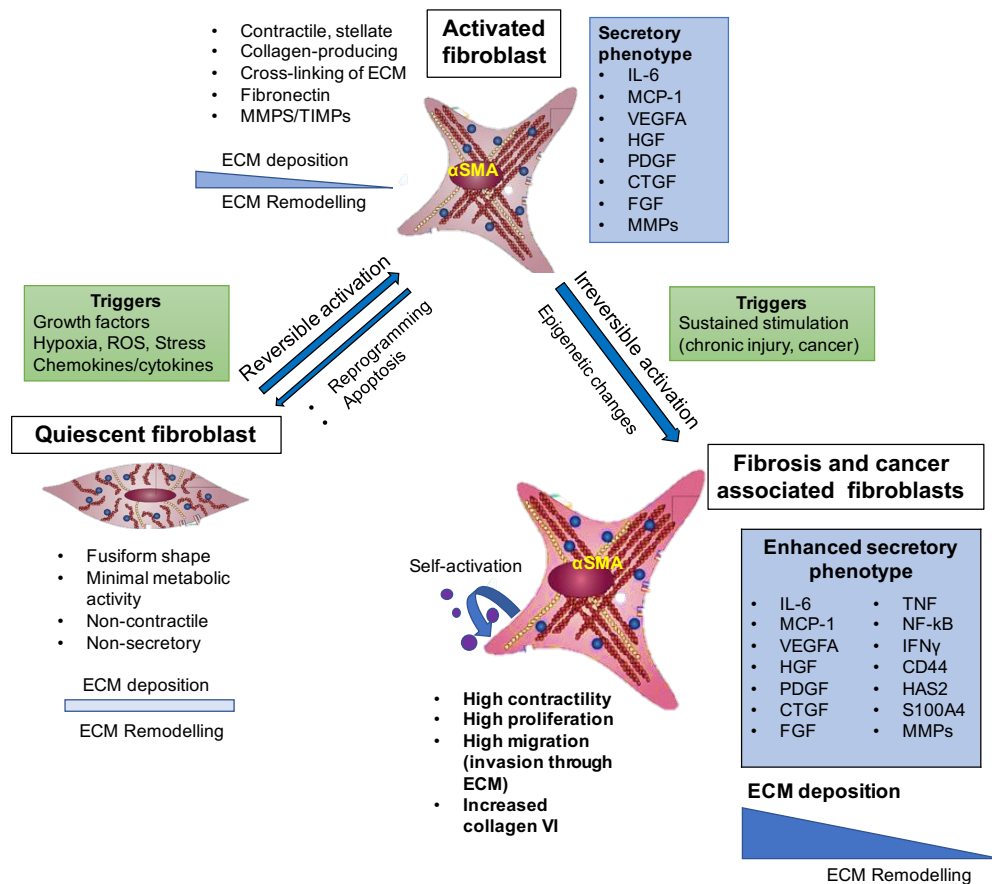


**Figure 6-1. Fibroblast activity during tissue homeostasis and following injury and disease states.**

During tissue homeostasis, fibroblasts exist in a senescent state and support the tissue architecture. Activation of fibroblasts induced by injury, stress and soluble mediators (growth factors, chemokines and cytokines) can result in the proliferation and activation of fibroblasts into secretory cells with contractile properties. Activated fibroblasts, termed myfibroblasts (usually identified through  $\alpha$ SMA expression), produce large quantities of ECM alongside soluble factors that assist in further recruitment and activation of fibroblasts and facilitate the process of chemotaxis (MCP-1, IL-6), angiogenesis (VEGF-A, PDGF) and tissue remodelling (MMPs and TIMPs). Successful repair is associated with fibroblast apoptosis or reprogramming back to a quiescent state. Sustained stimulation and chronic injury however can induce epigenetic changes resulting in permanent activation of fibroblasts with an enhanced secretory profile resulting in excessive ECM deposition and the development of fibrosis. *ECM extracellular matrix; ROS reactive oxygen species; MMPs metalloproteinases; TIMPs tissue inhibitors of metalloproteinases;  $\alpha$ SMA alpha-smooth muscle actin; VEGFA vascular endothelial growth factor; PDGF platelet-derived growth factor; MCP-1 monocyte chemoattractant protein-1; HGF- hepatocyte growth factor; FGF fibroblast growth factor; CTGF connective tissue derived growth factor; TNF tumour necrosis factor; IFN $\gamma$  interferon gamma; HAS2 hyaluronan synthase 2.*

Abnormalities in apoptotic pathways, Wnt signalling and autophagy are thought to contribute to the prolonged survival of IPF fibroblasts, whilst epigenetic changes have been linked to irreversibly activated phenotypes [137, 138, 330, 331]. Aberrant activation

## Chapter 6: The influence of MDMs on fibrogenic endpoints

of fibroblasts is likely to result from a number of causes, not least through stimulation induced by chronic or repetitive injury [332]. The deposition of stiffened matrix by fibroblasts was also found to enhance their activation in a positive feedback loop [44], alongside sustained autocrine and paracrine activation [324]. Factors such as TGF $\beta$ -1, PDGF, IL-1 $\beta$ , IL-6 and IL-13 produced by neighbouring and infiltrating cells such as macrophages, monocytes and lymphocytes can also contribute to fibroblast activation [126, 135] (Fig 6-1).

Activated fibroblasts synthesise all components of the extracellular matrix. The ECM is comprised of structural proteins (collagens), adhesive proteins such as fibronectin which bind cells to the protein, and ground substance; a gelatinous medium through which cells can migrate. In the human lung, type I collagen is the most prevalent, with smaller proportions of type III and V present [333, 334]. In health, type VI collagen is restricted predominantly to the bronchioles and arterioles within the lung but a study looking at its distribution in cases of pulmonary fibrosis found high expression within areas of scar formation on biopsy samples [47]. Fibroblasts also assist in the maintenance and degradation of ECM through the production of matrix degrading enzymes and their inhibitors (metalloproteinases, or MMPs, and tissue-inhibitors of metalloproteinases, TIMPS) [135]. In addition to degrading matrix, MMPs cleave cytokines, chemokines and growth factors into bioactive mediators and dysregulated expression of these enzymes has been linked to IPF pathogenesis [57].

In IPF, fibroblasts are postulated to derive from three sources. Local recruitment and proliferation of lung fibroblasts are likely to be the major contributors to the fibroblast pool, but the process of epithelial-mesenchymal-transition (EMT) may also play a role in the expansion of fibroblast populations. Studies have demonstrated that epithelial markers are down-regulated and mesenchymal markers such as fibronectin and  $\alpha$ SMA are expressed in epithelial cells at the sites of active lesions in IPF [92, 142, 335]. Fibroblasts may also be produced by bone marrow derived precursor cells called fibrocytes, although the contribution that these cells play in the process of fibrogenesis is debated [87, 336].

Immune cells modulate fibroblast phenotype through release of soluble factors and macrophages play key roles in the activation and termination of fibroblast responses in the process of repair [126]. I was therefore interested in determining whether monocyte-derived macrophages (MDMs) from IPF patients influenced markers of fibroblast

## Chapter 6: The influence of MDMs on fibrogenic endpoints

activation and proliferation, and whether these responses differed from MDMs derived from age-matched controls. The close association demonstrated between CAFs and FAFs, and the recognised involvement of macrophages with polarized 'M2' characteristics in tumour and fibrosis progression (termed tumour-associated macrophages or TAMs) [80, 126, 200, 213, 337-340], led me to question whether IPF MDMs may modulate fibroblasts towards these activated phenotypes. To this end, I looked at the expression of genes associated with FAFs and CAFs in fibroblasts co-cultured with IPF and control MDMs. Lastly, I investigated whether MDMs from patients and controls differentially influenced the process of EMT alongside its regression (mesenchymal-epithelial transition).

### 6.2 Hypothesis and aims

I hypothesised that MDMs from IPF patients would potentiate fibrogenic processes by increasing fibroblast proliferation and/or differentiation and enhance the process of EMT. To address this hypothesis, I performed the following:

- i. Co-cultured primary human lung fibroblasts with MDMs from control and IPF participants and measured markers of fibroblast proliferation and differentiation.
- ii. Examined the expression of genes associated with activated fibroblast phenotypes following transwell co-culture with MDMs from controls and IPF patients.
- iii. Measured epithelial and mesenchymal markers associated with EMT on a type II alveolar epithelial cell line (A549) following co-culture with IPF and control MDMs. The reversal of EMT, termed mesenchymal-epithelial transition (MET), was also studied following EMT induction by TGF $\beta$  and subsequent co-culture with MDMs from control and IPF patients.



## **6.3 Methods**

### **6.3.1 Participant samples**

Samples were collected from April 2016 to March 2017. Patient samples were acquired during specialist ILD clinics. Aged-matched healthy controls were recruited from orthopaedic pre-assessment clinics or the University. Further details of eligibility and exclusion criteria are documented in section 2.1.

### **6.3.2 Generation of human lung fibroblasts**

Human lung fibroblasts (ELF) were derived from explanted pneumonectomy samples (section 2.11.1). Fibroblasts were used at passage 2-7 and cultured in D10 (Table 2-1, section 2.3.1). Fibroblasts were stained with violet proliferation dye (VPD) (section 2.11.2) and  $5 \times 10^4$  were plated onto 12 well plates for each experiment.

### **6.3.3 Generation of monocyte-derived macrophages**

Monocyte derived macrophages were generated as described in section 2.3.5. Briefly, following positive selection using CD14 microbeads (Miltenyi), cells were cultured on 24 well low-adherence plates in X-vivo (Lonza) and 10% heat-inactivated autologous serum and 50ng/ml M-CSF (added on day 0 only). Media was replenished on day 4 and MDMs were used for co-culturing experiments on day 6.

### **6.3.4 Preparation of A549 cells for use in EMT and MET experiments**

The human type II alveolar epithelial cell line, A549, was used for EMT experiments at low-passage (4-6). Cells were cultured in R10 (Table 2-1, section 2.3.1). Prior to assays, A549 cells were stained with the cell tracer VPD (section 2.11.2). For EMT experiments,  $1.25 \times 10^4$  cells were seeded into 12 well plates for 72h prior to the addition of MDMs.

## Chapter 6: The influence of MDMs on fibrogenic endpoints

To determine whether MDMs could reverse the process of EMT (i.e. induce MET) after it had occurred, EMT was first induced in A549 cells by TGF $\beta$ 1. The optimal dose of TGF $\beta$  required to induce EMT was determined during optimisation experiments. As the process of EMT was found to be associated with lower cell proliferation, twice the number of cells ( $2.5 \times 10^4$ ) were seeded into 12 well plates and cells were cultured for 72h in the presence of 5ng/ml of TGF $\beta$ . Morphological appearances of EMT (spindle shaped morphology of cells and decreased cell-cell contact) were confirmed prior to the addition of MDMs (section 2.12).

### 6.3.5 Co-culture experiments

Media from wells containing fibroblasts or A549 cells was replaced with fresh media containing a lower percentage of FCS (2.5%) due to concerns that soluble factors within FCS may confound the results (studies have found variable concentrations of growth factors present in FCS that could potentially influence the process of fibroblast activation or EMT directly [341, 342]).

$2 \times 10^5$  MDMs were used for experiments. The ratio of MDMs to ELF and A549 cells was based on the population doubling time determined through optimisation experiments and/or specifications from the supplier (ATCC® for A549 cells). Therefore, for MDM and fibroblast experiments, a ratio of 4:1 was used; for EMT experiments using highly proliferative A549 cells a ratio of 16:1 was used; and for MET experiments in which A549 cells showed reduced proliferation, I used a ratio of 8:1. MDMs were added either directly to the culture wells containing ELF or A549 cells or onto a 0.4 $\mu$ m pore transwell insert (Corning).

Direct fibroblast-MDMs co-cultures were harvested after 72h and A549-MDM assays after 96h (following optimisation experiments). In transwell experiments, the same time frame was used but the upper insert containing MDMs was discarded. Trypsin-EDTA was used to detach the cells, which were then washed in media and transferred to 96 well plates for flouochrome-conjugated antibody staining.

## Chapter 6: The influence of MDMs on fibrogenic endpoints

### 6.3.6 Flow cytometry, gating strategy and analysis

Surface staining using a fluorescently-conjugated monoclonal antibody (mAb) to HLA-DR was used to identify MDMs as this receptor was not found to be expressed on A549 cells or ELF. Fibroblasts and A549 cells were pre-labelled with the cell tracer VPD. To study the effect MDMs have on the process of EMT, a mAb to E-cadherin was used. This epithelial cellular adhesion molecule is highly expressed on the surface of epithelial cells but down-regulated during mesenchymal transition [92]. Cells were then fixed and permeabilised with saponin buffer to enable intracellular staining. A mAb to fibronectin was then added. This intracellular adhesion protein is expressed predominantly by fibroblasts but up-regulated in epithelial cells during EMT [92]. To assess the influence of MDMs on fibroblast activation/differentiation, I used a mAb to  $\alpha$ SMA which is contractile protein expressed by myofibroblasts but not by quiescent fibroblasts [80, 135, 325].

Both MDM-fibroblast and MDM-A549 co-culture experiments were analysed in the same way. Doublet cells were removed from analysis using FSC-H and FSC-A, and dead cells were gated out. Fibroblasts and A549 cells were differentiated from MDMs by plotting VPD against HLA-DR. VPD-positive cells were selected and isotype controls or FMOs were used to establish the gating of positive cell populations (Fig 6-2).

VPD is a cell tracer that binds covalently to free amines on the surface and inside the cell and is stable over 8-10 generations. During cell division, daughter cells receive half the cellular material and thus the concentration of VPD falls proportionately with each successive generation [343]. VPD in these experiments did not provide a direct measure of cellular proliferation but was used as a comparative value. By measuring the mean fluorescent intensity (MFI) of the total population of VPD-treated cells and comparing it to the control value (fibroblasts/A549 cells cultured without MDMs), it was possible to determine whether the addition of MDMs increased or decreased proliferation in the target population (the lower the value, the greater the proliferation). To ensure consistency and comparability, control wells were included with every experiment and the ratio of the MFI of VPD from MDM-treated cells was divided by the VPD MFI from cells cultured alone (the control).

## Chapter 6: The influence of MDMs on fibrogenic endpoints

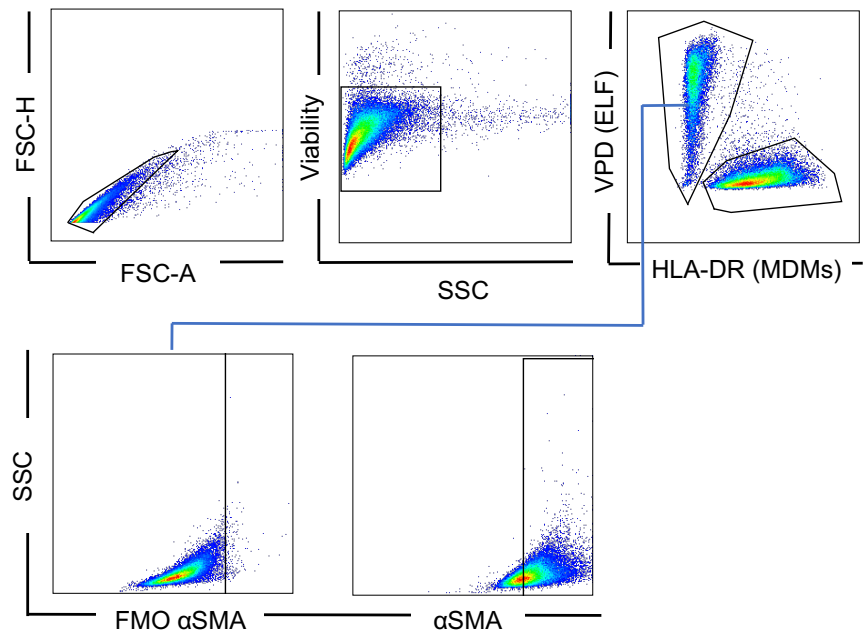


**Figure 6-2. Gating strategy for fibroblast (ELF) analysis following co-culture with MDMs.**

From left to right: Singlet gate; exclusion of dead cells; fibroblasts identified following labelling with VPD (cell tracer) and MDMs immunostained with HLA-DR; Fibroblast gate isolated from analysis with a plot showing the FMO for  $\alpha$ SMA (left bottom) used to determine the positive staining for the test sample (right bottom).

### 6.3.7 RNA extraction and qPCR

To determine whether MDMs influenced fibroblast gene expression, RNA was extracted from ELF cells following transwell co-culture. Fibroblasts were seeded onto 12 well plates and MDMs placed onto an upper 0.4  $\mu$ m transwell insert. After 72 hours, the inserts and media were removed and 500 $\mu$ l RLT was added to the wells containing adherent fibroblasts to aid cell disruption. The cell lysate was then removed and frozen at -80°C for RNA extraction (detailed in section 2.11.2 and 2.9). qPCR using SYBR® Green was undertaken to examine the expression of genes from fibroblasts cultured in isolation (n=10) compared to fibroblasts co-cultured with 10 control and 18 IPF MDM samples. Fold change was calculated using three housekeeping genes,  $\beta$ 2 microglobulin,  $\beta$ -actin and cyclophilin A. Details of genes analysed are listed in Table 2-7 and 2-8 (section 2.10).

## 6.4 Results

### 6.4.1 Participant demographics

Demographics	Fibroblast Co-cultures		EMT studies		RNA	
	IPF	Controls	IPF	Controls	IPF	Controls
Sample number	16	9	12	9	18	10
% Male	88	56	92	56	83	60
Mean age (range)	74 66-83(6)	66 (57-72)	76 (62-82)	66 (57-72)	75 (62-83)	68 (52-78)
% Definite diagnosis	56	N/A	50	N/A	44	N/A
% on Anti-fibrotics (number) N=Nintedanib P=Pirfenidone	50 (8) N=4 P=4	N/A	25 (3) N=1 P=2	N/A	33 (6) N=2 P=4	N/A

**Table 6-1. Demographics of IPF patients and healthy controls involved in fibroblast and EMT experiments. N=nintedanib; P=Pirfenidone; N/A – data not applicable to healthy controls.**

### 6.4.2 MDMs decrease $\alpha$ SMA expression in primary lung fibroblasts

Following injury, fibroblasts are activated and transform into myofibroblasts which are the key effector cells in the process of repair and fibrogenesis. These cells are most commonly identified by the expression of  $\alpha$ SMA, a cytoskeletal contractile protein [344]. Numerous factors induce their differentiation/activation, including cytokines such as TGF $\beta$ , TNF $\alpha$  and IL-13 [80], and I was therefore interested in determining whether MDMs could also influence the differentiation of fibroblasts. To test the hypothesis that IPF MDMs induce myofibroblast differentiation, I undertook co-culturing experiments using MDMs from IPF patients and controls and measured the expression of  $\alpha$ SMA on fibroblasts via flow cytometry and immunofluorescence (IF) microscopy.

To ensure that fibroblasts could be differentiated to myofibroblasts during in vitro experiments, I first cultured primary human lung fibroblasts (ELF) in the presence of TGF $\beta$ 1 given on day 0, 3 and 5. I found that expression of  $\alpha$ SMA on ELF was increased following 5ng/ml TGF $\beta$ 1 and increased further with 10ng/ml compared to cells not exposed to TGF $\beta$ 1 (Fig 6-3a). These findings were confirmed on IF which demonstrated

## Chapter 6: The influence of MDMs on fibrogenic endpoints

expression of the cytoskeletal protein in fibroblasts cultured in the presence of TGF $\beta$  but minimal expression in unstimulated cells (Fig 6-3b).

To assess the influence of MDMs on  $\alpha$ SMA expression, ELF and MDMs were co-cultured directly for 72h. In contrast to my hypothesis, MDMs from IPF patients (ELF<sup>IPF</sup>) and controls (ELF<sup>HC</sup>) resulted in the down-regulation of  $\alpha$ SMA compared to ELF cultured alone ( $p=0.001$  and  $0.010$  for ELF<sup>IPF</sup> and ELF<sup>HC</sup> respectively, Fig 6-3c).

To determine whether this phenomenon was related to direct cell contact by MDMs or due to the release of soluble mediators, the experiment was repeated using a transwell system of co-culture where fibroblasts were seeded onto the bottom of the well and MDMs onto the upper insert. Similar trends to the direct co-culture method were observed although statistically significant differences were not seen in  $\alpha$ SMA expression in fibroblasts cultured alone or with MDMs from IPF patients and controls ( $p=0.099$  and  $p=0.102$  for ELF<sup>IPF</sup> and ELF<sup>HC</sup> respectively Fig 6-3d). To determine whether the reduction in  $\alpha$ SMA expression was proportionate to the number of MDMs present, fibroblasts were co-cultured with differing ratios of MDMs (1:1, 2:1, 4:1 and 8:1). Increasing the number of MDMs appeared to be associated with lower expression of  $\alpha$ SMA (Fig 6-3e).

## Chapter 6: The influence of MDMs on fibrogenic endpoints

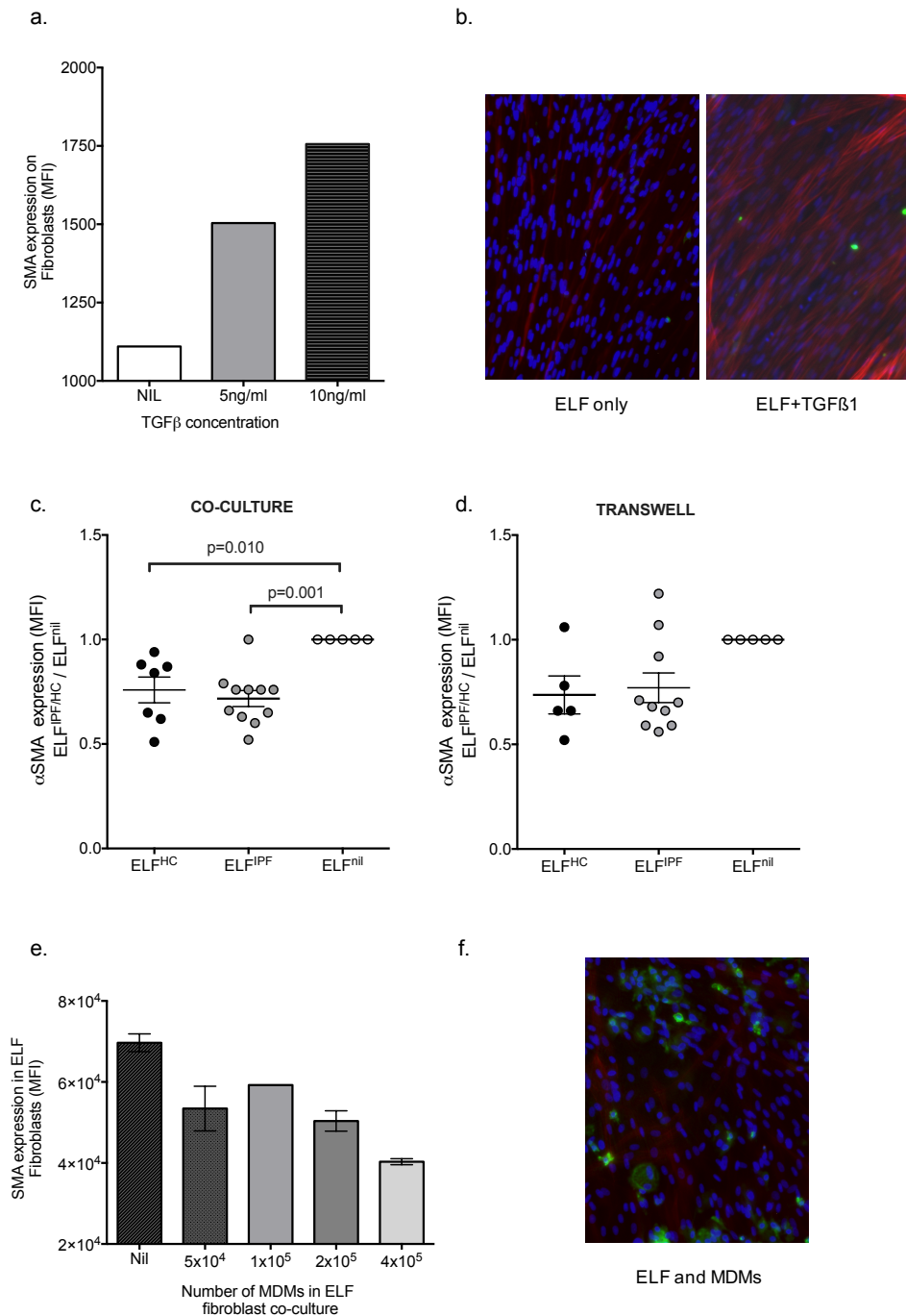


**Figure 6-3. The influence of TGFβ1 and MDMs on the expression of αSMA by primary human lung fibroblasts (ELF).**

ELF were incubated with 5-10ng/ml TGFβ or MDMs for 72 hours. ELF cells were then fixed, permeabilised and immunostained with a mAb to αSMA for flow cytometric analysis or immunofluorescence (IF). MDMs were identified using mAb to HLA-DR and excluded from analyses. ELF cultured alone (ELF<sup>nil</sup>) were included in every experiment as a control and to standardise the results which are displayed as the ratio of αSMA MFI in ELF<sup>IPF/HC</sup> / ELF<sup>nil</sup> in (c-d). (a) TGFβ increased αSMA expression (MFI) in a dose dependent manner (n=1 for each group). (b) IF images demonstrating high expression of αSMA in TGFβ-treated fibroblasts (red αSMA, blue DAPI). (c) MDMs down-regulated expression of αSMA in ELF following direct co-culture although differences were not observed between IPF and HC MDMs (ELF<sup>IPF</sup> and ELF<sup>HC</sup>). [Mean ratio of co-

## Chapter 6: The influence of MDMs on fibrogenic endpoints

cultured ELF over ELF<sup>nil</sup> (SEM): ELF<sup>IPF</sup> 0.72(0.04); ELF<sup>HC</sup> 0.76(0.06) n=11 and 7]. (d) A statistically significant decrease in  $\alpha$ SMA expression was not seen in ELF<sup>IPF</sup> or ELF<sup>HC</sup> cultured via a transwell system compared to ELF<sup>nil</sup> [ELF<sup>IPF</sup>/ELF<sup>nil</sup> 0.77(0.07); ELF<sup>HC</sup>/ELF<sup>nil</sup> 0.74(0.09), n=5 and 10]. (e) The expression of  $\alpha$ SMA by ELF decreased with increasing concentrations of MDMs in co-culture (nil n=2, 5x10<sup>4</sup> n=3, 1x10<sup>5</sup> n=1, 2x10<sup>5</sup> n=3, 4x10<sup>5</sup> n=2). (f) IF image of ELF and MDM co-culture after 72h showing an absence of  $\alpha$ SMA staining (green-MDMs, blue-DAPI,  $\alpha$ SMA-red). For (c) and (d) one-way ANOVA used with Tukey's multiple comparisons test for statistical analysis.

### 6.4.3 MDMs increase fibroblast proliferation

Whilst  $\alpha$ SMA expression was reduced in fibroblasts following MDM co-culture, I noted a higher density of fibroblasts when cultured with MDMs compared to those cultured in isolation (Fig 1-4a). This suggested that MDMs increase fibroblast proliferation and to explore this further, fibroblasts were labelled with a cell tracer (VPD) prior to co-culture. This tracer provides an indication of proliferation, with the intensity of its expression (the MFI) reducing with successive cell divisions.

VPD-labelled fibroblasts (ELF) were incubated in the same well as MDMs for 72h. Using flow cytometry to distinguish ELF from MDM populations, the expression of VPD (MFI) was then measured on the isolated ELF population. ELF cultured in the presence of MDMs showed a significant fall in VPD compared to ELF<sup>nil</sup> indicating that MDMs increased fibroblast proliferation (p=0.035 and 0.013 for ELF<sup>IPF</sup> and ELF<sup>HC</sup>, respectively, Fig 6-4b).

To determine whether this was a direct effect by MDMs or mediated by soluble factors, the experiment was repeated using a transwell with fibroblasts seeded at the bottom of the well and MDMs on the upper insert. In this experiment, ELF that had been cultured with MDMs showed a trend towards lower expression of VPD compared to ELF<sup>nil</sup> but this was not statistically significant (p=0.053 and 0.452 ELF<sup>IPF</sup> and ELF<sup>HC</sup> vs ELF<sup>nil</sup>, respectively, Fig 6-4c). Differences were not seen between ELF cultured with IPF MDMs and control MDMs in either experiment.



## Chapter 6: The influence of MDMs on fibrogenic endpoints

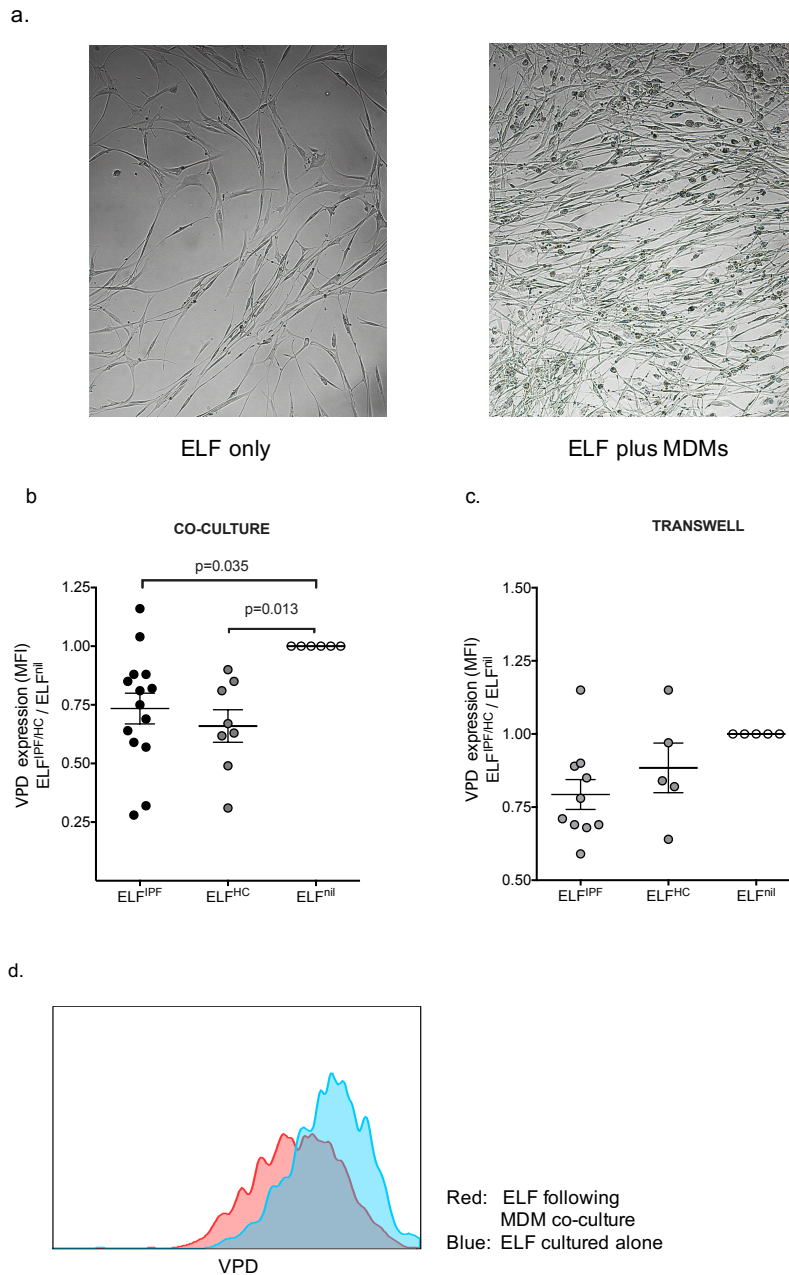


**Figure 6-4. The influence of MDMs on fibroblast proliferation using the cell tracer VPD (violet proliferation dye) as a comparative measure.**

ELF were labelled with VPD then co-cultured with MDMs directly or via a transwell system for 72h. Flow cytometry was used to identify ELF populations and calculate the intensity of VPD expression using the mean fluorescence intensity (MFI). ELF<sup>nil</sup> were included in every experiment as a control and to standardise the results which are displayed as the ratio of VPD MFI in ELF<sup>IPF/HC</sup> / ELF<sup>nil</sup>. (a) Microscopic appearances of fibroblasts (ELF) cultured in isolation (left) and with IPF MDMs (right). (b) VPD expression was lower in ELF<sup>IPF</sup> and ELF<sup>HC</sup> than ELF<sup>nil</sup> [ratio of VPD MFI of ELF<sup>IPF/HC</sup> over ELF<sup>nil</sup> (SEM): ELF<sup>IPF</sup> 0.73(0.06); ELF<sup>HC</sup> 0.66(0.07) n=14 and 8]. (c) A statistically significant fall in VPD expression was not seen in transwell co-cultures compared to ELF cultured in isolation [ELF<sup>IPF</sup> 0.79(0.05); ELF<sup>HC</sup> 0.88(0.08) n=10 and 5]. One-way ANOVA with Tukey's multiple comparisons test used for statistical analysis. (d) A histogram of VPD in ELF cultured alone (blue) and following culture with IPF MDMs (red).

#### 6.4.4 MDMs induce the expression of fibroblast genes associated with an activated phenotype

Studies have found that fibroblasts from IPF patients produce more ECM and possess an invasive phenotype similar to that seen in cancer. In addition, they release higher concentrations of soluble factors that act in an autocrine and paracrine manner to enable their sustained activation and survival [135, 138, 328, 330, 334]. Given that MDMs increased fibroblast proliferation, I hypothesised that they may influence other aspects of fibroblast biology and was interested in determining whether MDMs induce changes at the gene expression level. In particular, I wanted to determine whether IPF MDMs influenced the development of an activated phenotype associated with FAFs and CAFs (Fig 6-1). Genes reported to be up-regulated in these activated and invasive fibroblast phenotypes were examined and are listed in Table 6-2.

Following transwell co-culture with MDMs, fibroblasts were harvested and processed for qPCR. The first sets of genes I examined related to the expression of soluble factors associated with fibroblast activation. ELF co-cultured with IPF MDMs (ELF<sup>IPF</sup>) expressed higher levels of *IL-6* compared to ELF cultured alone (ELF<sup>nil</sup>). A trend towards higher expression of *IL-6* in ELF co-cultured with control MDMs (ELF<sup>HC</sup>) was also seen but did not reach statistical significance (Adj-p=0.035 and 0.072 for ELF<sup>IPF</sup> and ELF<sup>HC</sup> vs ELF<sup>nil</sup> respectively, Fig 6-5a). Expression of *MCP-1* was also higher in ELF<sup>IPF</sup> and ELF<sup>HC</sup> compared to ELF<sup>nil</sup> (Adj-p=0.013 and 0.004 for ELF<sup>IPF</sup> and ELF<sup>HC</sup> vs ELF<sup>nil</sup> respectively, Fig 6-5b). Conversely, expression of *CTGF* was down-regulated in ELF<sup>IPF</sup> and ELF<sup>HC</sup> compared to ELF<sup>nil</sup> (Adj-p<0.001 for both ELF<sup>IPF</sup> and ELF<sup>HC</sup> vs ELF<sup>nil</sup>, Fig 6-5c). Expression of other growth factors and cytokines were not significantly different between groups.

Gene expression of *COL1A1*, *COL3A1*, *COL5A1* and *COL6A1* (coding for pro-collagen I, III, V and VI respectively) and other extracellular components were examined. ELF<sup>IPF</sup> and ELF<sup>HC</sup> showed increased expression of *COL6A1* compared to ELF<sup>nil</sup> (both p=0.023, Fig 6-6a). *HAS2* which codes for hyaluronan synthase 2, was significantly higher in ELF co-cultured with both control and IPF MDMs than ELF<sup>nil</sup> (Adj-p=0.032 and 0.010 for ELF<sup>IPF</sup> and ELF<sup>HC</sup>, respectively. Fig 6-6e).

## Chapter 6: The influence of MDMs on fibrogenic endpoints

The full list of genes analysed and their association with fibrogenesis are tabulated in Table 6-2.

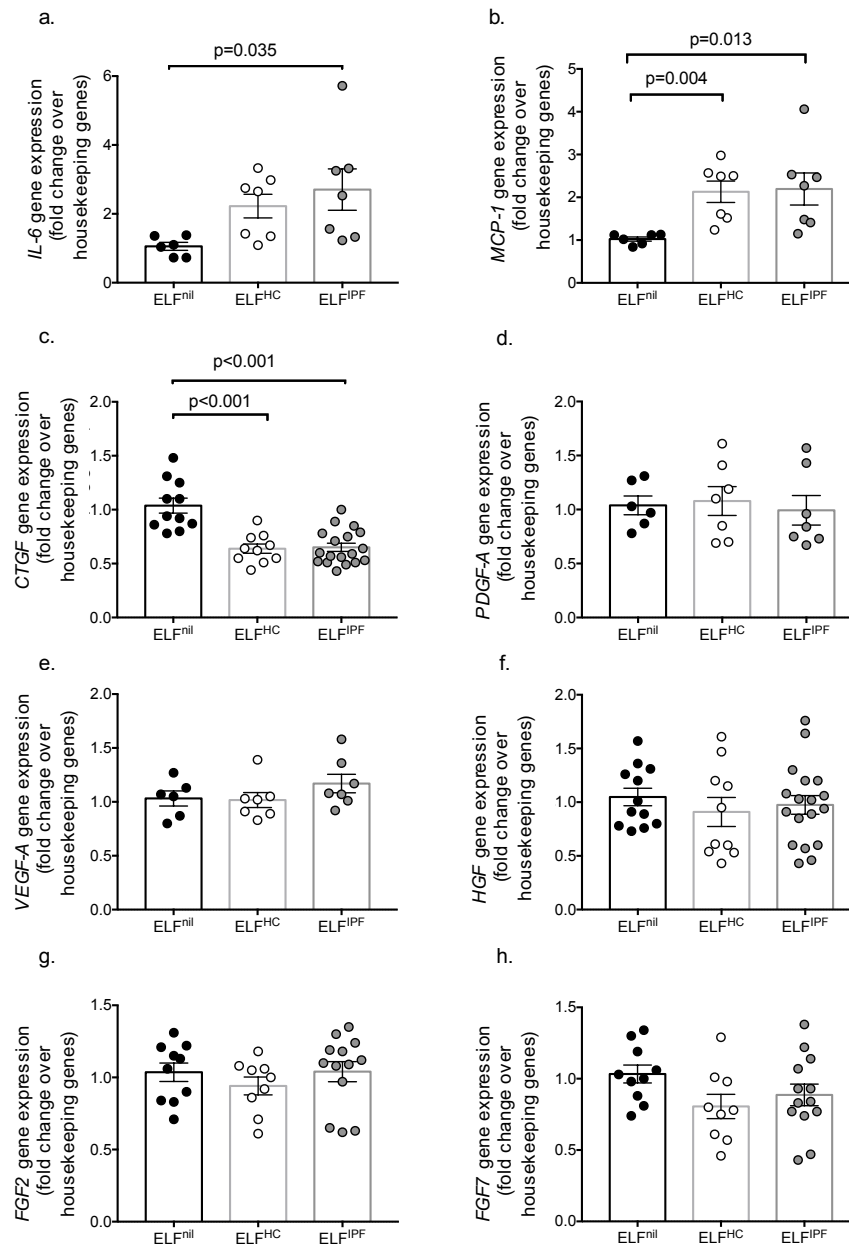


**Figure 6-5. Gene expression of cytokines, chemokines and growth factors associated with activated fibroblast phenotypes in fibroblasts cultured alone (ELF<sup>nil</sup>), with IPF MDMs (ELF<sup>IPF</sup>) or control MDMs (ELF<sup>HC</sup>) for 72 hours via a transwell.**

Mean fold change(SEM) illustrated on graphs and quoted below. (a) Gene expression of *IL-6* was higher in ELF<sup>IPF</sup> compared to ELF<sup>nil</sup> [ELF<sup>IPF</sup> 2.71(0.60), ELF<sup>HC</sup> 2.22(0.34), ELF<sup>nil</sup> 1.06(0.12); n=7, 7 and 6]. (b) Expression of the chemokine *MCP-1* was increased in ELF<sup>IPF</sup> and ELF<sup>HC</sup> compared to ELF<sup>nil</sup> [ELF<sup>IPF</sup> 2.20(0.37), ELF<sup>HC</sup> 2.13(0.25) ELF<sup>nil</sup> 1.02(0.05); n=7, 7 and 6]. (c) Expression of *CTGF* was lower in ELF<sup>IPF</sup> and ELF<sup>HC</sup> compared to ELF<sup>nil</sup> [ELF<sup>IPF</sup> 0.65(0.04), ELF<sup>HC</sup> 0.64(0.04) ELF<sup>nil</sup> 1.04(0.23); n= 18, 10 and 11]. (d-f) Expression of growth factors *VEGF-A*, *PDGF-A* and *HGF* did not differ between groups. The mean(SD) illustrated in the graphs are quoted below. (g-h) IPF and HC MDMs did not influence the expression of

## Chapter 6: The influence of MDMs on fibrogenic endpoints

fibroblast growth factors *FGF2* and *FGF7*. The fold change over three housekeeping genes (*CYCLOPHILIN A*,  *$\beta$ 2-MICROGLOBULIN* and  *$\beta$ -ACTIN*) was used to determine the relative expression of the genes of interest. One-way ANOVA or Kruskal-Wallis test with Dunn's multiple comparisons test used for statistical analysis. Adjusted p-values are fully tabulated in Table 6-2.

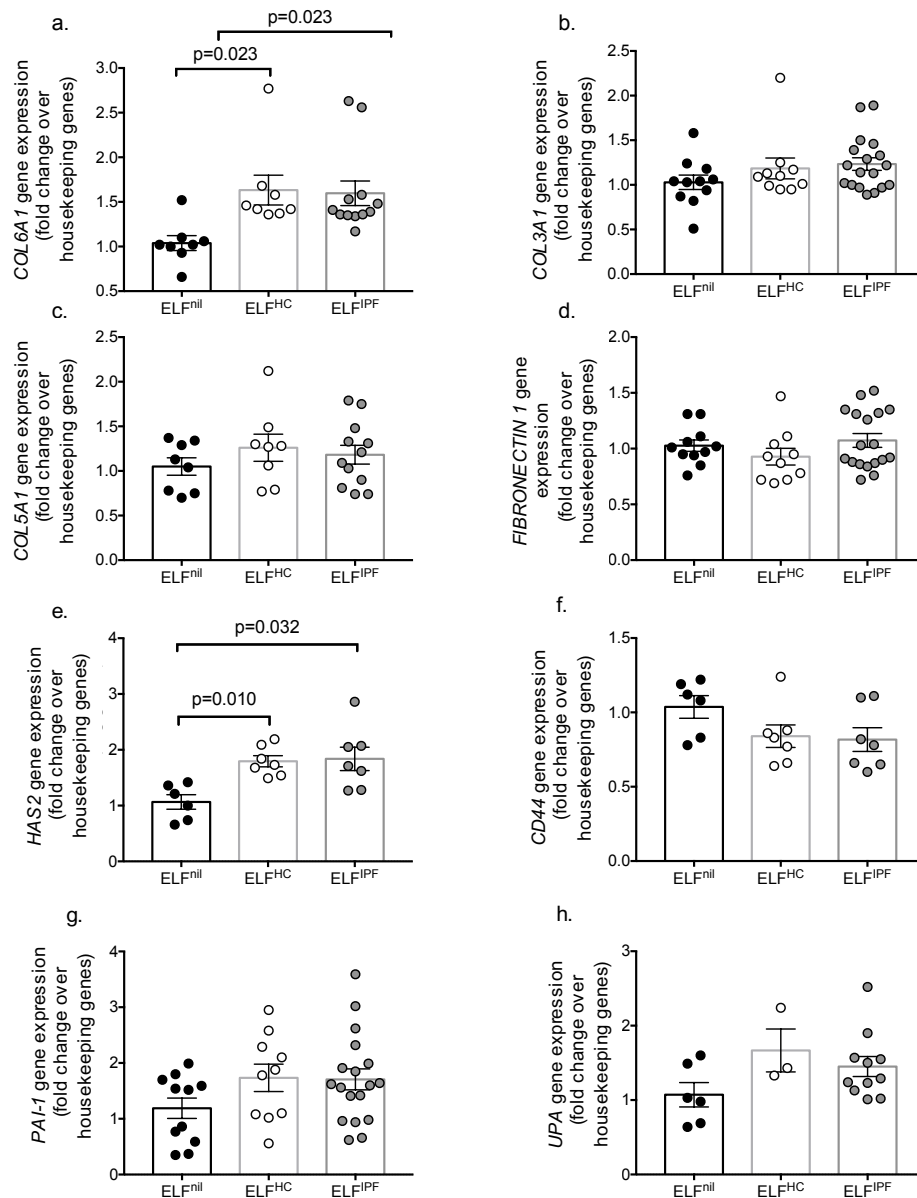


**Figure 6-6. The expression of ECM genes and genes associated and activated/invasive fibroblast phenotypes in fibroblasts cultured alone (ELF<sup>nil</sup>), with IPF MDMs (ELF<sup>IPF</sup>) or control MDMs (ELF<sup>HC</sup>) for 72 hours via a transwell.**

The mean fold change(SEM) illustrated in the graphs are quoted below. (a) Expression of *COLL6A1* was higher in ELF<sup>IPF</sup> and ELF<sup>HC</sup> compared to ELF<sup>nil</sup> [ELF<sup>IPF</sup> 1.60(0.14), ELF<sup>HC</sup> 1.63(0.17), ELF<sup>nil</sup> 1.04(0.08); n=12, 8 and 8]. Differences were not seen in the expression of (b) *COLL3A1* (c) *COLL5A1* or (d) *FIBRONECTIN*. (e) Expression of *HAS2* was higher in ELF<sup>IPF</sup> and ELF<sup>HC</sup> compared to ELF<sup>nil</sup> [ELF<sup>IPF</sup> 1.84(0.21), ELF<sup>HC</sup> 1.79(0.10), ELF<sup>nil</sup> 1.06(0.13); n=7, 7 and 6]. (f) *CD44* (g) *PAI-1* and (h) *UPA* did not differ significantly between groups. The fold change over three housekeeping genes (*CYCLOPHILIN A*,  *$\beta$ 2-MICROGLOBULIN*

## Chapter 6: The influence of MDMs on fibrogenic endpoints

and  $\beta$ -ACTIN) was used to determine the relative expression of the genes of interest. One-way ANOVA or Kruskal-Wallis test with Dunn's method for multiple comparisons were used for all stated statistics. Adjusted p-values are fully tabulated in Table 6-2.

Fibroblast feature	Gene	Protein transcript	Association with fibrogenesis	ELF <sup>HC</sup> Vs ELF <sup>IPF</sup> (Adj-p)	ELF <sup>HC</sup> Vs ELF <sup>nil</sup> (Adj-p)	ELF <sup>IPF</sup> Vs ELF <sup>nil</sup> (Adj-p)
<b>Growth factors</b>	<i>FGF2</i>	FGF2 - Fibroblast growth factor 2	Angiogenesis	>0.999	0.638	0.395
	<i>FGF7</i>	FGF7 - Fibroblast growth factor 7	Cell growth/ invasion	>0.999	0.138	0.520
	<i>PDGF-A</i>	PDGF - Platelet-derived growth factor alpha	Angiogenesis	>0.999	>0.999	>0.999
	<i>VEGF-A</i>	VEGF - Vascular endothelial growth factor alpha	Angiogenesis	0.311	>0.999	0.851
	<i>CTGF</i>	CTGF - Connective tissue growth factor	Fibroblast activation [37]	0.852	<b>&lt;0.001</b>	<b>&lt;0.001</b>
	<i>HGF</i>	HGF - Hepatocyte growth factor	Epithelial and endothelial cell survival, fibroblast quiescence [38]	>0.999	0.989	>0.999
	<i>IGF-1</i>	IGF-1 - Insulin-like growth factor-1		Minimal expression noted		
<b>Cytokines and chemokines</b>	<i>IL-6</i>	IL-6 Interleukin 6	Fibroblast activation and proliferation [39]	>0.999	0.072	<b>0.035</b>
	<i>MCP-1 (CCL2)</i>	MCP1- Monocyte chemoattractant protein-1	Fibroblast activation [40-43]	>0.999	<b>0.004</b>	<b>0.013</b>
	<i>TGFB1</i>	TGF $\beta$ 1 Transforming growth factor beta 1	Fibroblast activation	0.996	0.869	>0.999
<b>ECM components</b>	<i>COL1A1</i>	Collagen type I $\alpha$ 1 chain	Structural protein	>0.999	>0.999	>0.999
	<i>COL3A1</i>	Collagen type III $\alpha$ 1 chain	Structural protein	>0.999	>0.999	0.322
	<i>COL5A1</i>	Collagen type V $\alpha$ 1 chain	Structural protein	0.885	0.489	0.709
	<i>COL6A1</i>	Collagen type VI $\alpha$ 1 chain	Structural protein Increased in IPF lung [19]	0.854	<b>0.023</b>	<b>0.023</b>
	<i>FIBRONECTIN1</i>	Fibronectin	Adhesive ECM protein	0.475	0.619	>0.999
	<i>MMP2</i>	MMP2 - Metalloproteinase 2	ECM remodeling	>0.999	0.718	>0.999
	<i>MMP9</i>	MMP9 - Metalloproteinase 9	ECM remodeling	Minimal expression noted		
	<i>MMP11</i>	MMP11 - Metalloproteinase 11	ECM remodeling	>0.999	0.607	>0.999
	<i>PAI-1</i>	Plasminogen activator inhibitor type 1	ECM remodeling (inhibits ECM degradation) [44]	>0.999	0.224	0.273
	<i>UPA</i>	Urokinase-type plasminogen activator	ECM remodeling [44]	>0.999	0.283	0.414
	<i>TGM2</i>	TGM2 - Transglutaminase 2	ECM formation [45]	>0.999	>0.999	>0.999
	<i>TIMP1</i>	TIMP-1 Tissue inhibitor of metalloproteinase 1	ECM remodeling	>0.999	>0.999	>0.999
<b>Invasion</b>	<i>S100A4</i>	S100 calcium binding protein A4	Tissue invasion	>0.999	>0.999	0.745
	<i>HAS2</i>	Hyaluronan synthase 2	Tissue invasion [9]	>0.999	<b>0.001</b>	<b>0.032</b>
	<i>CD44</i>	CD44 - Cognate receptor for hyaluronan	Adhesion molecule, role in tissue invasion [9]	>0.999	0.480	0.162

**Table 6-2. Genes analysed in primary human fibroblasts (ELF) following transwell co-culture with IPF and control MDMs (ELF<sup>IPF</sup> and ELF<sup>HC</sup>) compared to fibroblasts cultured in isolation (ELF<sup>nil</sup>).** One-way ANOVA or Kruskal-Wallis test with corrections for all multi-wise comparisons were performed using Dunn's method. P<0.05 taken to indicate statistical significance. Adj-P= adjusted p-value.

## Chapter 6: The influence of MDMs on fibrogenic endpoints

### 6.4.5 Optimisation of an A549 cell-based EMT assay

The process of EMT, by which epithelial cells gain characteristics of mesenchymal cells, has been described in various models of fibrosis and may contribute to the fibroblast pool in interstitial lung diseases such as IPF [51, 332, 345]. The process of EMT involves a down-regulation of adhesion molecules such as E-cadherin resulting in loss of cell-cell contact and apical-basal polarity and up-regulation of markers associated with mesenchymal cells such as fibronectin, N-cadherin and vimentin. To determine whether MDMs influence the process of EMT, co-culture experiments using a biologically relevant cell line (A549) were undertaken. A549 is commonly used to study the process of EMT [346-348] and derived from type 2 AECs, which is the cell type implicated in the initiation of IPF

Optimisation experiments on different batches of A549 cells were carried out to ensure that baseline epithelial markers were present. A549 cells were also stimulated with TGF $\beta$  to ensure EMT could be induced in culture. Under light microscopy, TGF $\beta$ -treated A549 cells demonstrated loss of cell-cell contact and acquired a spindle-shaped appearance after 72h (Fig 6-7a). This also corresponded to a decrease in E-cadherin expression and an upregulation of fibronectin (Fig 6-7b-c) suggesting that TGF $\beta$ -induced EMT had taken place. Low-passage A549 cells showed high E-cadherin expression and low fibronectin expression (Fig 6-7b-c) but E-cadherin was down-regulated in high-passage A549 cells and N-cadherin, a marker of mesenchymal cells, was highly expressed (Fig 6-7d). The seeding density of A549 cells also affected the expression of E-cadherin, with higher cell concentrations leading to loss of E-cadherin following 96h in culture (Fig 6-7e). Low-passage A549 cells were thus used for all experiments and a seeding density that was not associated with significant loss of E-cadherin was selected for EMT experiments ( $1.25 \times 10^4$ ).

## Chapter 6: The influence of MDMs on fibrogenic endpoints

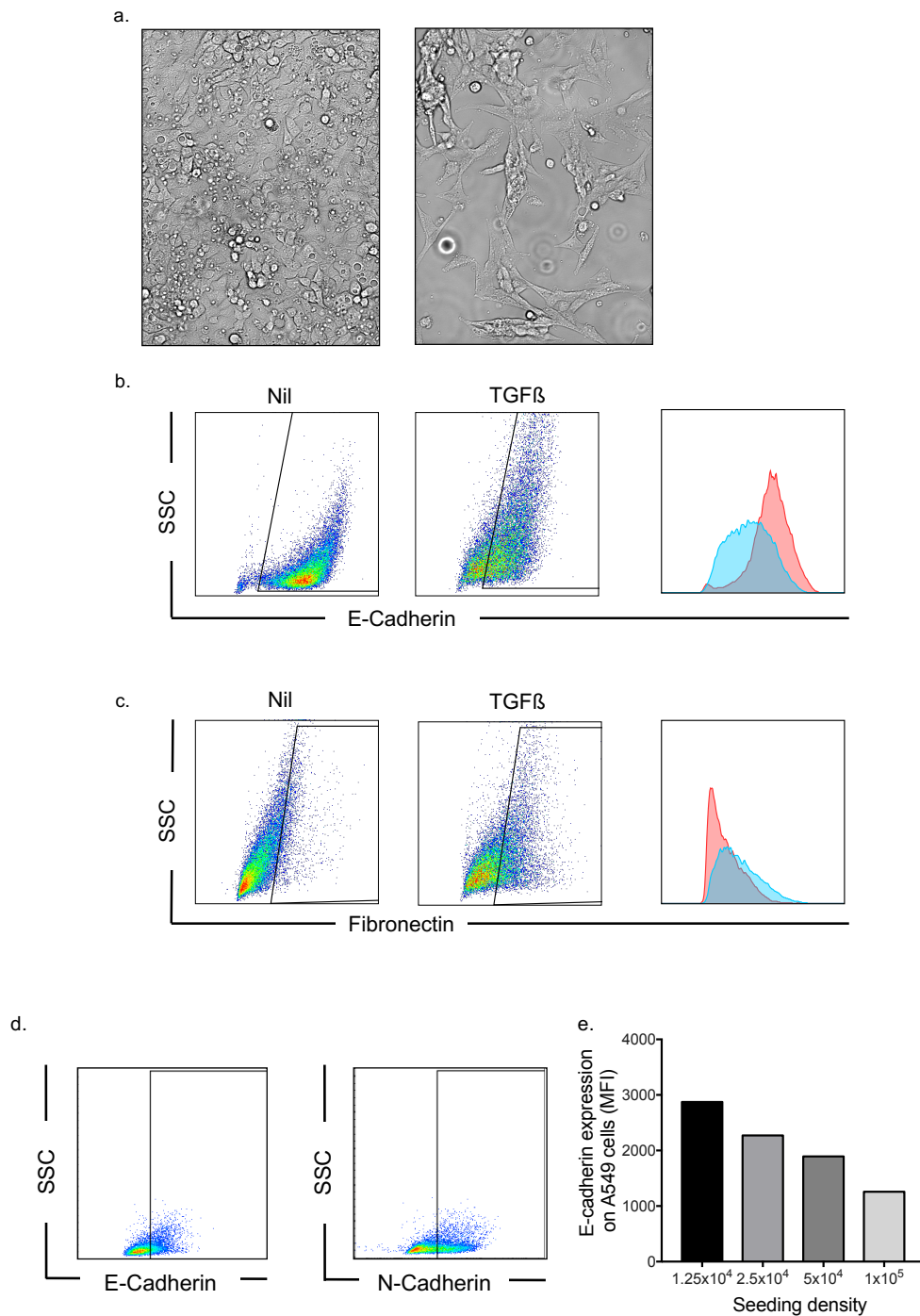


**Figure 6-7. The morphological appearance and expression of EMT markers in A549 cells cultured in the absence and presence of TGFβ.**

Light microscopy images of A549 cells cultured to confluence without TGFβ (left) and with 5ng/ml TGFβ after 72h (right). (b) FACS plots showing expression of E-cadherin by low-passage A549 cells following culture with and without TGFβ and a representative histogram (c) FACS plots showing expression of fibronectin by low-passage A549 cells following culture with and without TGFβ and a representative histogram (red: no TGFβ, blue: A549 following TGFβ). (d) The expression of E-cadherin and N-cadherin in high-passage A549 cells (e) The influence of initial seeding density of A549 into 12-well plates cells on E-cadherin expression following 96h culture.

#### 6.4.6 MDMs inhibit the loss of E-cadherin on A549 cells

Soluble mediators including TGF $\beta$  and TNF $\alpha$  induce the process of EMT [92, 349]. MDMs from IPF patients were found to be phenotypically and functionally distinct from age-matched controls and the gene expression of TNF $\alpha$  was high in MDMs from IPF patients. I was therefore interested in determining whether MDMs modify the process of EMT and if MDMs from IPF patients exert effects that differ from control MDMs. E-cadherin was used as an epithelial marker whilst fibronectin was selected as a mesenchymal marker. N-cadherin and  $\alpha$ SMA were also used in these experiments but staining was not seen so the results have not been included in the presentation of data.

To firstly determine the contribution of soluble mediators released by MDMs on A549 cells, a transwell co-culture system was used. E-cadherin, an adhesion molecule that mediates cell-cell contact, became down-regulated during the process of EMT. Surprisingly, A549 cells exposed to control and IPF MDMs (A549<sup>HC</sup> and A549<sup>IPF</sup>) via the transwell were found to retain expression of this marker following 96h of culture compared to A549 cells cultured alone which down-regulated E-cadherin ( $p=0.009$  and  $0.003$  for A549<sup>IPF</sup> and A549<sup>HC</sup>, respectively, Fig 1-8a). This was not related to an increase in cellular proliferation by A549 cells cultured without MDMs. VPD, which provides a marker of proliferation (the MFI decreasing with successive cell divisions) was significantly lower in A549<sup>IPF</sup> and A549<sup>HC</sup> cells ( $p<0.001$  and  $<0.005$ , respectively, Fig 1-8c), suggesting that soluble mediators released by MDMs stimulate more rapid proliferation. Fibronectin expression, a marker of mesenchymal cells, did not change significantly following transwell culture with MDMs (Fig 6-8b). No differences were seen between A549<sup>HC</sup> and A549<sup>IPF</sup> for EMT or proliferative markers.

To next determine whether direct cell-cell contact between MDMs and A549 cells influenced the expression of EMT markers differently, cells were co-cultured together within the well for 96 hours. Fibronectin expression did not differ significantly between groups. Trends towards retained E-cadherin expression were seen in MDM-cultured A549 cells but statistical differences were not observed (Fig 6-9a-b). VPD expression on A549 was significantly lower in A549<sup>IPF</sup> and A549<sup>HC</sup> indicating that MDMs increase A549 proliferation ( $p=0.004$  and  $0.005$  for A549<sup>IPF</sup> and A549<sup>HC</sup>, respectively, Fig 6-9c). No differences were observed between A549<sup>IPF</sup> and A549<sup>HC</sup> cells.



## Chapter 6: The influence of MDMs on fibrogenic endpoints

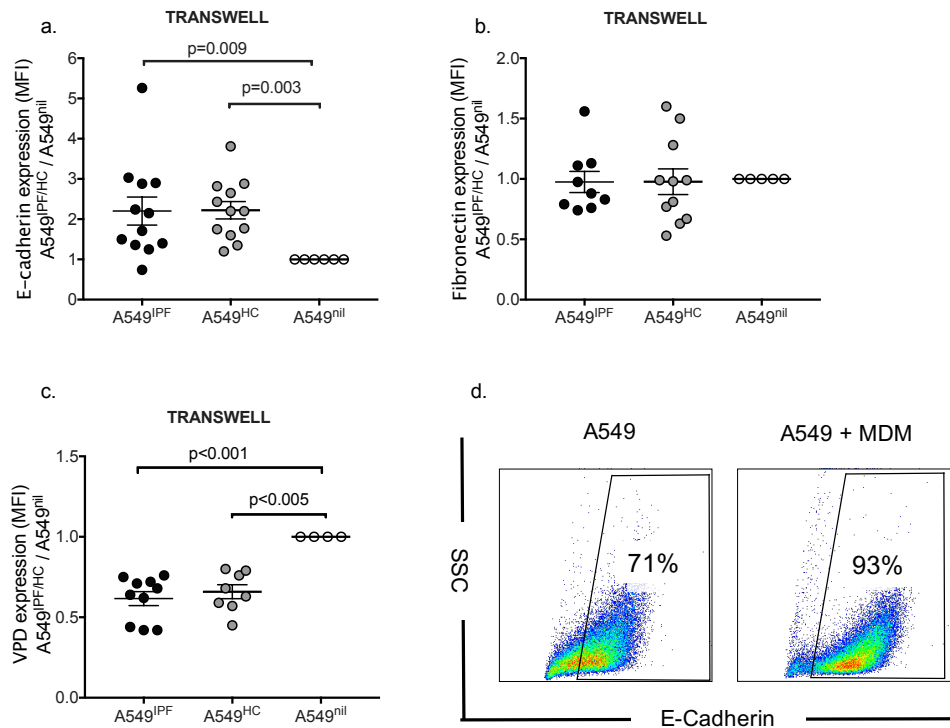


**Figure 6-8. The influence of IPF and control MDMs on E-cadherin and fibronectin expression (MFI) in A549 cells.**

A549 cells were labelled with the cell tracer VPD and then co-cultured with MDMs using a transwell for 96h. A549 were immunostained for E-cadherin and fibronectin and analysed using flow cytometry. VPD was used as a comparative indicator of cellular proliferation. A549 cultured in isolation (A549<sup>nil</sup>) were included in every experiment as a control and to standardise the results which depict the MFI as a ratio (A549<sup>IPF/HC</sup> / A549<sup>nil</sup>). (a) E-cadherin expression on A549 cells co-cultured with IPF MDMs (A549<sup>IPF</sup>) and healthy control MDMs (A549<sup>HC</sup>) was increased in comparison to A549<sup>nil</sup> [ratio of E-cadherin MFI A549<sup>IPF/HC</sup> over A549<sup>nil</sup> (SEM): A549<sup>IPF</sup> 2.2(0.35) and A549<sup>HC</sup> 2.2(0.22); n=12 and 12]. (b) Fibronectin expression on A549<sup>IPF</sup> and A549<sup>HC</sup> was similar to A549<sup>nil</sup>. (c) VPD expression on A549<sup>IPF</sup> and A549<sup>HC</sup> was lower than A549<sup>nil</sup> [A549<sup>IPF</sup>/A549<sup>nil</sup> 0.62(0.04) and A549<sup>HC</sup>/A549<sup>nil</sup> 0.66(0.04); n=10 and 8]. (d) FACs plot showing the percentage of A549 cells expressing E-cadherin following culture in isolation (left) and with MDMs (right). One way ANOVA with Tukey's test for multiple comparisons used for (a) and Kruskal-Wallis with Dunn's method for multiple comparisons used for (c).

## Chapter 6: The influence of MDMs on fibrogenic endpoints

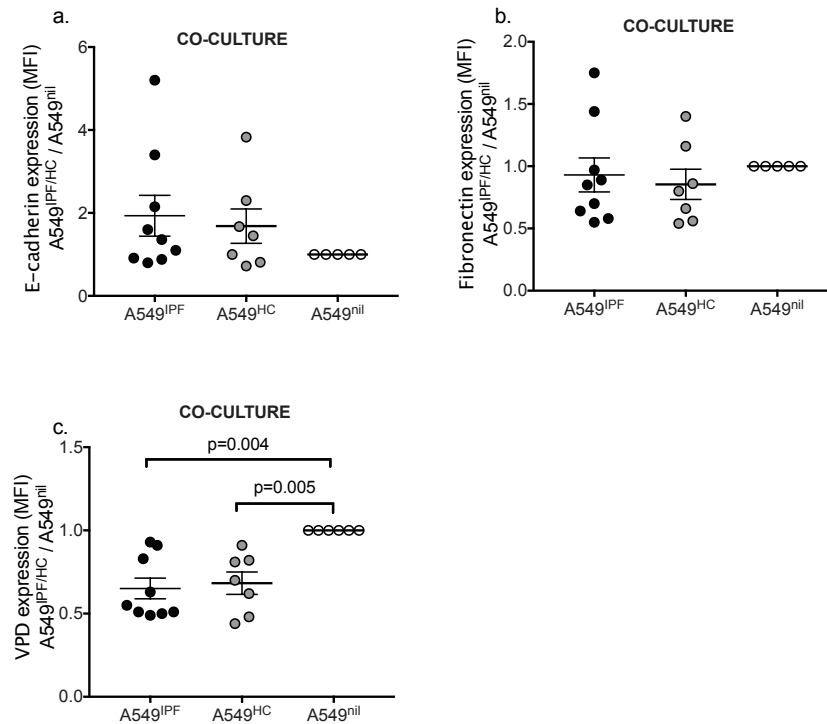


**Figure 6-9. The influence of IPF and control MDMs on E-cadherin and fibronectin expression (MFI) in A549 cells following direct co-culture.**

A549 cells were labelled with the cell tracer VPD and then directly co-cultured with MDMs for 96h. A549 were immunostained for E-cadherin and fibronectin and analysed using flow cytometry. VPD was used as a comparative indicator of cellular proliferation. A549<sup>nil</sup> were included in every experiment as a control and to standardise the results which depict the MFI as a ratio (A549<sup>IPF/HC</sup> / A549<sup>nil</sup>). (a) E-cadherin expression did not differ significantly between MDM-co-cultured A549 cells (A549<sup>IPF</sup> and A549<sup>HC</sup>) compared to A549<sup>nil</sup> in direct co-culture. (b) Fibronectin expression on A549<sup>IPF</sup> and A549<sup>HC</sup> was similar to A549<sup>nil</sup> in direct co-culture (c) VPD expression was significantly lower in A549<sup>IPF</sup> and A549<sup>HC</sup> compared to A549<sup>nil</sup> [A549<sup>IPF</sup>/A549<sup>nil</sup> 0.65(0.06) and A549<sup>HC</sup>/A549<sup>nil</sup> 0.67(0.07); n=9 and 7]. One way ANOVA with Tukey's test for multiple comparisons used for statistical analysis.

### 6.4.7 MDMs potentiate mesenchymal-epithelial transition (MET) in A549 cells

To explore the possibility that MDMs from IPF patients may be defective at inhibiting fibrogenic processes in the context of EMT, MDMs from control and IPF patients were added to A549 cells that had already undergone EMT to see whether the reversal of this process could be induced (MET). EMT was induced by TGF $\beta$  and confirmed by morphological appearances on microscopy (Fig 6-7a).

A549 cells cultured with TGF $\beta$  alone showed a decrease in E-cadherin expression, in keeping with the process of EMT. VPD expression was also higher in A549<sup>nil</sup>, indicating

## Chapter 6: The influence of MDMs on fibrogenic endpoints

that transdifferentiation during EMT is associated with decreased proliferation. To examine the influence of soluble factors released from MDMs on MET, a transwell system was used. A549<sup>HC</sup> showed higher E-cadherin expression compared to A549<sup>nil</sup> with a similar trend seen in A549<sup>IPF</sup> that did not reach statistical significance ( $p=0.034$  and  $0.071$  for A549<sup>HC</sup>/A549<sup>nil</sup> and A549<sup>IPF</sup>/A549<sup>nil</sup>, respectively, Fig 6-10a). When the mean MFI of E-cadherin expression on A549<sup>IPF</sup> and A549<sup>HC</sup> cells pre-exposed to TGF $\beta$  was calculated for each experiment and compared to the mean MFI of A549<sup>nil</sup> not exposed to TGF $\beta$  per experiment, expression was similar. This suggests that MDMs partially reverse the effect of TGF $\beta$  treatment (Fig 6-10b). Similarly, VPD expression was decreased in A549<sup>IPF</sup> and A549<sup>HC</sup> cells ( $p=0.005$  and  $0.001$  for A549<sup>IPF</sup> and A549<sup>HC</sup>, respectively, Fig 6-10c) and the mean MFI for each experiment comparable to A549<sup>nil</sup> without pretreatment with TGF $\beta$  (Fig 6-10d). Fibronectin expression was not affected by MDM exposure (Fig 6-10e). Differences between A549<sup>IPF</sup> and A549<sup>HC</sup> cells were not observed.

Direct co-culture of MDMs with A549 cells pre-treated with TGF $\beta$  to induce EMT showed similar results to the transwell experiments with a decrease in VPD expression on A549 cells cultured with MDMs ( $p=0.001$  and  $<0.008$  for A549<sup>IPF</sup> and A549<sup>HC</sup> respectively, Fig 6-11a). Although there was a trend towards increased E-cadherin expression in MDM-cultured A549 cells, this was not statistically significant and no differences were seen in fibronectin expression (Fig 6-11b-c). Differences were not observed between A549<sup>IPF</sup> and A549<sup>HC</sup> cells.

## Chapter 6: The influence of MDMs on fibrogenic endpoints

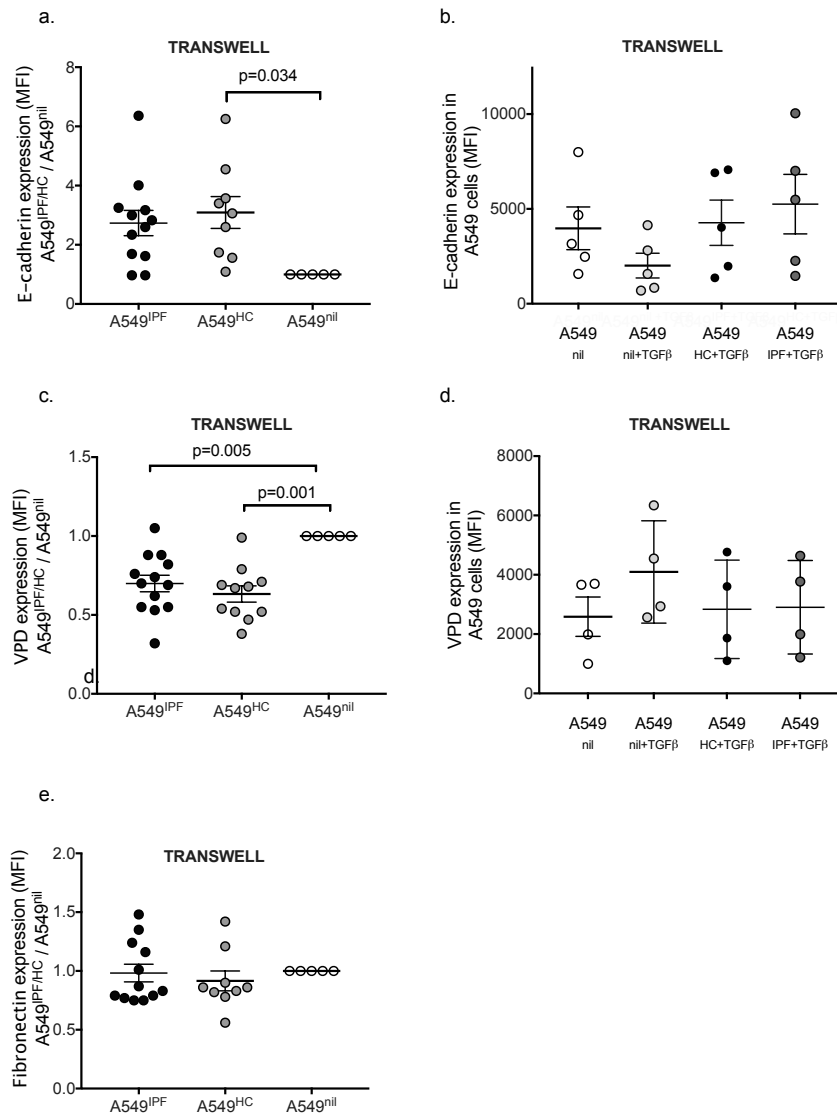


**Figure 6-10. The influence of MDMs on mesenchymal-epithelial transition (MET) in A549 cells following indirect co-culture.**

A549 cells were labelled with the cell tracer VPD then treated with TGF $\beta$  to induce EMT. A549 were subsequently co-cultured with IPF or control MDMs using a transwell for 96h. A549 cells were immunostained with mAbs to E-cadherin and fibronectin and analysed using flow cytometry. VPD was used as a comparative indicator of cellular proliferation. A549<sup>nil</sup> were included in every experiment as a control and to standardise the results which depict the MFI as a ratio (A549<sup>IPF/HC</sup> / A549<sup>nil</sup>). (a) E-cadherin expression was significantly higher in A549<sup>HC</sup> compared to A549<sup>nil</sup> [A549<sup>IPF/HC</sup> / A549<sup>nil</sup> (SEM): A549<sup>IPF</sup> 2.73(0.43) and A549<sup>HC</sup> 3.10(0.54); n=12 and 9]. (b) MDMs show a trend towards increasing E-cadherin expression in TGF $\beta$  exposed A549 cells. The graph shows the mean MFI of E-cadherin per experiment on A549<sup>nil</sup>, A549<sup>nil</sup>+TGF $\beta$  and A549<sup>HC</sup>+TGF $\beta$  and A549<sup>IPF</sup>+TGF $\beta$ . (c) VPD expression is reduced in A549<sup>IPF</sup> and A549<sup>HC</sup> compared to A549<sup>nil</sup> [A549<sup>IPF</sup>/A549<sup>nil</sup> 0.70(0.05) and A549<sup>HC</sup>/A549<sup>nil</sup> 0.63(0.05); n=13 and 11]. (d) TGF $\beta$ -treated A549 cells demonstrate high VPD expression but the addition of MDMs results in a trend towards decreased VPD expression to levels similar to A549 cultured without TGF $\beta$ . The graph shows the mean MFI of VPD per experiment in A549<sup>nil</sup>, A549<sup>nil</sup>+TGF $\beta$  and A549<sup>HC</sup>+TGF $\beta$  and A549<sup>IPF</sup>+TGF $\beta$ . (e) MDMs do not influence the expression of fibronectin by A549 cells. One way ANOVA with Tukey's test for multiple comparisons used for statistical analysis (not applied to b and d).

## Chapter 6: The influence of MDMs on fibrogenic endpoints

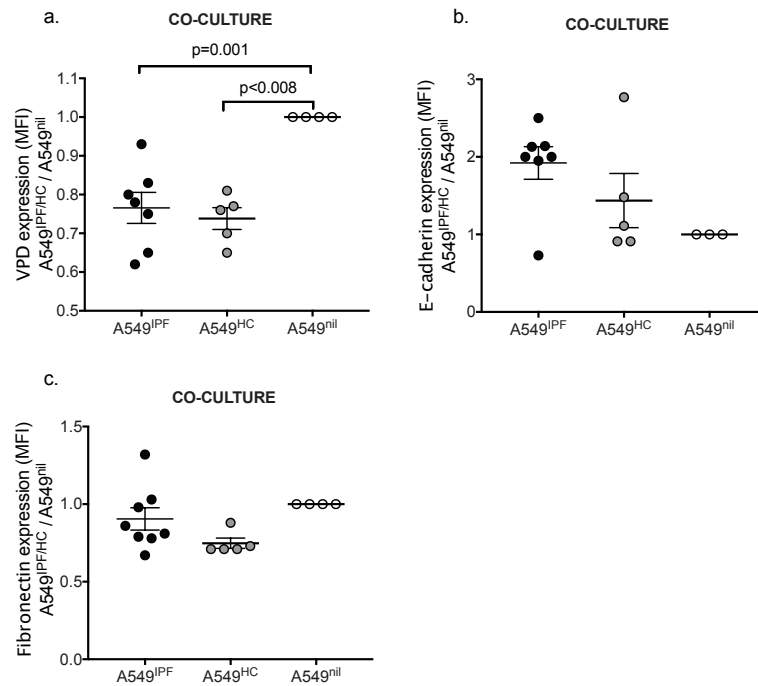


**Figure 6-11. The influence of MDMs on mesenchymal-epithelial transition (MET) in A549 cells following direct co-culture.**

The expression of VPD, E-cadherin and fibronectin (MFI) was measured in A549 cells pre-treated with TGF $\beta$  then co-cultured directly with IPF or control MDMs for 96h. A549<sup>nil</sup> were included in every experiment as a control and to standardise the results which depict the MFI as a ratio (A549<sup>IPF/HC</sup> / A549<sup>nil</sup>). (a) VPD expression on A549<sup>IPF</sup> and A549<sup>HC</sup> was lower than A549<sup>nil</sup> [ratio of VPD MFI on A549<sup>IPF/HC</sup>/A549<sup>nil</sup> (SEM): A549<sup>IPF</sup> 0.77(0.04) and A549<sup>HC</sup> 0.74(0.03); n=7 and 5]. (b) MDMs did not significantly influence the expression of E-cadherin or (c) fibronectin in A549 cells. One way ANOVA with Tukey's test for multiple comparisons used for statistical analysis.

## 6.5 Discussion

This chapter has highlighted how MDMs modulate the characteristics of fibroblasts in culture. MDMs were noted to increase the proliferation of explanted human lung fibroblasts (ELF), upregulate ELF expression of *HAS2*, a gene associated with invasive fibroblast phenotypes, and increase *COL6A1* expression, a gene coding for collagen VI which is present within fibrotic lung lesions [47, 330]. Furthermore, MDMs increased fibroblast expression of inflammatory mediators *IL-6* and *MCP-1*. Interestingly, MDMs simultaneously down-regulated  $\alpha$ SMA alongside gene expression of the profibrotic mediator *CTGF*, and inhibited the process of EMT in an epithelial cell line. Whilst differences were not observed between IPF and control MDMs, the findings identified here may be of relevance given mounting evidence that MDMs replenish resident

## Chapter 6: The influence of MDMs on fibrogenic endpoints

macrophages following lung injury [193]. Expansion of monocyte-derived macrophage populations within the lung may contribute to the proliferation and sustained activation of fibroblasts resulting in interstitial fibrosis.

There are several findings presented in this chapter that support the hypothesis that MDMs potentiate the development of fibrosis-associated fibroblast (FAF) phenotypes. Firstly, there was a significant increase in fibroblast proliferation in ELF cultured with MDMs compared to those cultured in isolation. Whilst the transwell experiments did not reach statistical significance for fibroblast proliferation, the trends observed suggest that MDMs influence proliferation predominantly through the release of soluble factors. Secondly, MDMs up-regulated fibroblast expression of *HAS2*, a gene that encodes hyaluronan synthase 2, an enzyme involved in the synthesis of hyaluronan (HA). HA is a glycosaminoglycan that accumulates in fibrotic tissue and its overexpression by cancer cells has been linked to invasive capacity and metastasis [350-352]. To investigate whether *has2* expression may be linked to FAFs, Li et al. generated transgenic mice that over-expressed *has2* in fibroblasts [330]. Following bleomycin injury, mice developed severe and sustained lung fibrosis and accumulated HA within the lung interstitium. Fibroblasts isolated from these mice demonstrated a superior ability to invade through matrigel; an artificial matrix simulating the basement membrane. Of greater relevance, fibroblasts from IPF patients also showed marked capacity to invade through matrigel compared to ELF from healthy tissue. Cells that traversed the matrix were found to highly express *HAS2*, and the use of small interfering RNA (siRNA) to knock down the gene inhibited the capacity of fibroblasts to invade [330]. The observation that macrophages increase fibroblast proliferation and may enhance invasive capacity has been reported in a murine model. Using a co-culture system of fibroblasts and peritoneal macrophages to compare bioactive wound dressings, the investigators found that in the presence of macrophages, fibroblasts proliferated more rapidly and exhibited greater invasion into the hydrogel dressing. Analysis of the supernatant revealed elevated levels of IL-6, MCP-1, GM-CSF, TNFR and IL-13 from co-cultures compared to fibroblasts and macrophages cultured in isolation [353].

Thirdly, in concordance with the study discussed above [353], the gene expression of mediators *IL-6* and *MCP-1* were increased in fibroblasts cultured with MDMs. In this setting, if transcription is proportionate to translation, enhanced release of these inflammatory mediators by fibroblasts may perpetuate fibrosis. IL-6 is important in acute phase responses but has also been implicated in the development of fibrosis [115, 116].

## Chapter 6: The influence of MDMs on fibrogenic endpoints

In a murine model of peritonitis, recurrent episodes of inflammation induced by a microbial-derived stimulus resulted in the development of peritoneal fibrosis that was dependent on IL-6 [354]. The cellular source of IL-6 was not investigated but a study examining dermal fibroblasts from fibrotic areas in systemic sclerosis patients found expression of IL-6 was more than 30-fold higher than in fibroblasts from non-affected areas [119]. Furthermore, IL-6 has been demonstrated to mediate the differentiation of fibroblasts to myofibroblasts in vitro [355] and blocking the *trans* signalling pathway of IL-6 attenuated pulmonary fibrosis in a bleomycin model [100]. In concordance with my work, a study looking at fibroblast co-culture with human monocytes and a macrophage cell line also found that mononuclear phagocytes increased fibroblast gene expression of *IL-6*. The authors found that IL-6 mediated the upregulation of MMP-1, a metalloproteinase noted to be increased in IPF lungs [57, 117]. Chapter 3 showed that control and IPF monocytes highly expressed IL-6 following stimulation by LPS and unstimulated IPF MDMs on day 7 showed a trend towards higher IL-6 gene expression (5.4.7 Fig 5-12b). Thus, IL-6 from both fibroblasts and MDMs may potentiate fibroblast proliferation and activation in an autocrine and paracrine positive feedback loop.

MCP-1 has also been implicated in fibrosis and found to be elevated in the serum, BAL and alveolar epithelium of IPF patients [246, 309, 356]. One study found that levels of MCP-1 in BALF correlated with a poor prognosis in patients with the disease [245]. Like IL-6, MCP-1 is important in both inflammatory and fibrogenic processes. It can increase fibroblast proliferation, angiogenesis and myofibroblast differentiation [357, 358]. One study compared the effect of MCP-1 on fibroblasts isolated from IPF lungs with fibroblasts from non-fibrotic lung samples. The authors found that IPF fibroblasts demonstrated a 'fibrogenic' phenotype at baseline with high gene expression of  *$\alpha$ SMA*, *COL1A1* and *COL3A1* alongside increased *TGF $\beta$ 1*, *TGF $\beta$ R1* AND *TGF $\beta$ R2*. IPF fibroblasts were highly responsive to MCP-1, with expression of the same profibrotic genes at higher magnitude. In contrast, normal lung fibroblasts were relatively unresponsive to the chemokine [359]. Thus, the finding that MCP-1 expression by fibroblasts is induced by MDMs may be of significance in the IPF lung where recruited MDMs may further augment pro-fibrogenic fibroblast phenotypes.

Lastly, MDMs increased gene expression of *COL6A1* by fibroblasts. Type I and III collagens are the major collagens present in healthy lung tissue. In this study, MDMs had no effect on gene expression of *COL1A1* or *COL3A1*. Fibroblast expression of *COL6A1* however was significantly up-regulated by both IPF and control MDMs. The

## Chapter 6: The influence of MDMs on fibrogenic endpoints

protein product of *COL6A1*, collagen VI, is resistant to degradation by metalloproteinases and in normal lung is restricted to the walls of the bronchioles and pulmonary vessels. A study looking at fibrotic lung samples used a combination of in-situ hybridisation and immunohistochemistry to identify the distribution of collagen VI which was noted to be highly expressed within areas of active fibrosis and localised to  $\alpha$ SMA-expressing fibroblasts [47]. This supports the hypothesis that MDMs exert a pro-fibrogenic influence on fibroblasts and high concentrations of monocytes recruited into the lung may actively enhance fibroblast production of collagen VI.

The results presented here however are not straightforward and contradictions appear to exist. In particular,  $\alpha$ SMA expression, a hallmark of myofibroblast differentiation, was down-regulated in fibroblasts co-cultured with MDMs. Furthermore, there appeared to be a 'dose response' with higher numbers of MDMs decreasing fibroblast  $\alpha$ SMA expression proportionately. Whilst this could indicate that MDMs exert an inhibitory effect on fibrogenesis, this may be a misinterpretation due to the influence they had on proliferation. Following injury, fibroblasts have been demonstrated to assume a migratory, then proliferative and finally a profibrotic phenotype [50]. A study looking at early and late fibrotic lesions in lung tissue from IPF patients, found that early fibrotic change was associated with fibroblast up-regulation of basic fibroblast growth factor and telomerase, mediators associated with proliferative responses [60]. Late fibrotic lesions however, with areas of honeycombing present, identified fibroblasts with high  $\alpha$ SMA and low telomerase expression. This suggests that fibroblast proliferation may be important in the initiation of early fibrotic lesions, with myofibroblast differentiation occurring at a later stage leading to ECM deposition and maturation of fibrotic tissue [61]. Differentiation to a myofibroblast phenotype was also associated with a reduced proliferative capacity during in vitro experiments [360]. I carried out fibroblast assays at 72 hours and this time point may reflect a period of fibroblast 'activation', indicated by high proliferation and elevated expression of secretory mediators. Subsequently, 'activated' fibroblasts may up-regulate  $\alpha$ SMA expression as they differentiate into myofibroblasts (i.e. activation may precede differentiation). Extended co-culture experiments may have demonstrated this finding but were not undertaken due to concerns I had regarding the viability of cells in prolonged culture. MDMs were also found to decrease the gene expression of a major profibrotic mediator *CTGF*. *CTGF* is a matricellular protein with four binding domains and the ability to modulate multiple molecular pathways. The exact mechanisms by which *CTGF* mediates cellular



## Chapter 6: The influence of MDMs on fibrogenic endpoints

processes are incompletely understood but relate to its interaction with other molecules. CTGF can associate with a range of proteins including growth factors IGF, TGF $\beta$  and VEGF, alongside matrix proteins such as fibronectin and heparin sulfate. CTGF can thus influence a diversity of cellular processes including cellular migration, angiogenesis and fibroblast activation and differentiation. In my work, MDMs appeared to inhibit CTGF expression by fibroblasts at 72 hours, possibly providing an additional explanation for the lower expression of  $\alpha$ SMA found in co-cultured fibroblasts.

Low-passage A549 cells from the same stock were used for all assays and initial experiments demonstrated the presence of baseline epithelial characteristics. Cells were cuboidal in morphology, expressed high E-cadherin on the cell surface, and did not express the mesenchymal marker fibronectin. Over a 5-day period, A549 cells cultured in isolation down-regulated E-cadherin and increased expression of the intracellular protein fibronectin. High-passage A549 also showed low E-cadherin expression and high expression of the mesenchymal marker N-cadherin. This suggests that cellular overcrowding and/or multiple cell divisions alters the phenotypic characteristics of A549 from epithelial to mesenchymal i.e. induces the process of EMT. It is possible that the oncogenic properties of A549 cells enabled the down-regulation of the cellular adhesion protein E-cadherin in order to continue proliferating after a monolayer within the culture well had been established. Thus, increasing the seeding density resulted in earlier cellular confluence, down-regulation of E-cadherin and subsequent disorganised overgrowth. MDMs appeared to inhibit the process of EMT in A549 with retention of E-cadherin following co-culture. Interestingly however, the mechanism by which this occurred was not related to inhibition of cellular proliferation by MDMs, which was in fact enhanced, thus indicating that proliferation is not always linked to E-cadherin down-regulation in A549 cells. Inhibition of EMT by macrophages has been previously noted in other in vitro studies. A study using the epithelial cell line LA-4 to study EMT found that the addition of conditioned media from RAW 264.7 macrophages exposed to apoptotic cells, inhibited TGF $\beta$ -induced EMT. The authors attributed this finding to the release of hepatocyte growth factor and prostaglandins E2 and D2 produced by macrophages in response to a phenotypic switch induced by efferocytosis [361, 362]. Whilst analysis of the supernatant was not undertaken in my work, it is possible that similar factors induced by the efferocytosis of apoptotic MDMs by viable MDMs resulted in the inhibition of EMT in co-cultured A549 cells.

## Chapter 6: The influence of MDMs on fibrogenic endpoints

MDMs also appeared to positively influence the process of MET (demonstrated by increased E-cadherin expression on A549 cells) after EMT was induced by TGF $\beta$ . A549 cells cultured in the presence of TGF $\beta$  developed spindle morphology and phenotypic markers of mesenchymal cells and on microscopy, proliferation appeared to be inhibited, suggesting that TGF $\beta$  induced a state of 'semi-terminal' differentiation. The addition of MDMs however partially reversed this, with higher cell numbers observed within the culture wells and lower VPD expression (indicating higher proliferation) in A549 co-cultured with MDMs. Explanations for these observations were not explored but the proliferative capacity of monocytes and macrophages has been long recognised. A study published in 1977 demonstrated that peritoneal macrophages from guinea pigs induced neovascularisation in the normally avascular cornea of animals of the same species [363]. Adoptive transfer of bone marrow-derived macrophages into rats with anti-glomerular basement membrane disease led to an accumulation of macrophages at the disease site and mesangial cellular proliferation [364]. Furthermore, an in vitro study found that macrophages polarised to an 'M2' phenotype (using CD163 as a marker) following exposure to cigarette smoke increased A549 proliferation on co-culture [365]. Smokers in my study were excluded, but it is possible that by day 12, inflammatory ('M1') macrophages had undergone apoptosis resulting in a preponderance of longer lived 'M2' cells which released mediators that induced proliferation.

Control and IPF MDMs did not appear to differ in their ability to influence fibrogenic endpoints and it is possible that the co-culture of allogenic cells per se, resulted in modulating fibroblast responses. However, it also remains plausible that IPF and control MDMs do exert some differential effects on fibroblast phenotype/EMT but that the experimental conditions used in my work were too simplistic to detect subtle differences. Monocytes were cultured in autologous serum and factors within the serum are likely to have influenced their differentiation characteristics. To study the effect of MDMs on ELF/A549, co-culture experiments were performed using fresh media containing foetal calf serum, which, in combination with a relatively large volume of fresh media (1ml), may have diluted out differences in the production of soluble factors by IPF and control MDMs. Furthermore, the release of cytokines, growth factors and chemokines from proliferating fibroblasts and A549 cells may have modulated MDMs and the influences of these factors superseded the phenotypic changes of MDMs noted on day 7. Lastly, the single time point chosen to harvest fibroblasts for analysis provided a 'snapshot' view that may have differed during earlier or later time frames.

## Chapter 6: The influence of MDMs on fibrogenic endpoints

Whilst differences in fibrogenic end-points were not observed in the experiments I performed, MDMs as a collective population significantly increased proliferation and modulated the phenotype of both fibroblasts and A549 cells. In the context of lung injury, monocytes infiltrating the lung may differentiate into MDMs that enhance fibroblast proliferation, activation and invasion. Recent *in vivo* work supports this assertion. A radionuclide probe that labelled cysteine cathepsins (proteases present in high concentration within the lysosomes of monocytes), was injected into mice. Mice were then subjected to bleomycin and the deposition of the nuclear probe within the tissue was analysed. Non-invasive imaging revealed that the probe signal within the lungs increased during the evolution of the fibrotic response. Subsequent histological staining of lung tissue demonstrated co-localisation of the probe within macrophages, indicating a monocytic origin. [366].

Monocyte-derived-macrophages within the lung may potentiate fibrogenic processes regardless of phenotype, but given that IPF MDMs exhibited phenotypic characteristics distinct from age-matched controls, I hypothesised that functional differences may exist that affect fibrogenic processes indirectly. In the last chapter I therefore explore phagocytosis, a key function of macrophages that is essential for the maintenance of tissue homeostasis and the restoration of healthy tissue after injury.

## **7 Phagocytosis and neutrophil efferocytosis by monocyte-derived macrophages in IPF**

### **7.1 Introduction**

Phagocytosis, the process of engulfing and ingesting microorganisms, foreign particles, cells and their components, is a major function of macrophages, from which their name is derived (Greek: makros=large phagein=to eat). The consumption of aged and redundant cells by macrophages (termed efferocytosis) is essential for the maintenance of tissue homeostasis, controls the inflammatory response, and facilitates the restoration of healthy tissue following injury [367]. Studies have suggested that macrophages may even help control the accumulation of collagen within wounds through the phagocytosis of redundant extracellular material laid down during earlier stages of healing [368, 369].

In previous chapters, I demonstrated that IPF monocytes and MDMs were phenotypically distinct from age-matched controls. Preferential apoptosis of inflammatory monocytes was noted and day 7 MDMs showed a reduction in 'M1' markers CD64 and CD86, in conjunction with attenuated ROS generation. The analysis of key genes associated with inflammatory and reparative macrophages showed that the balance of genes up-regulated in IPF MDMs favoured repair over inflammation. Phenotypic changes however did not convincingly translate into differences in fibrogenic endpoints and the effects on EMT, fibroblast activation and proliferation were similar between control and IPF MDMs. I therefore questioned whether other aspects of macrophage function differed that could have pathophysiological relevance. In this chapter, I examined whether the ability of IPF MDMs to undertake phagocytosis and efferocytosis differed from controls. I reasoned that defects in these processes may contribute to the cycle of chronic injury that predisposes to aberrant repair.

The process of efferocytosis by macrophages is thought to be fundamental to limiting inflammatory responses and initiating tissue repair [370]. Studies have demonstrated that impaired clearance of inflammatory cells such as neutrophils can result in these cells undergoing secondary necrosis leading to the release of toxic mediators that may amplify tissue injury [371, 372]. Following efferocytosis, a phenotypic shift in macrophages occurs leading to enhanced production of reparative and immunomodulatory cytokines such as TGF $\beta$ , IL-10, hepatocyte growth factor (HGF) and vascular endothelial growth

## Chapter 7: Phagocytosis and neutrophil efferocytosis by MDMs in IPF

factor (VEGF) [370]. A study by Fadok *et al.* showed that uptake of apoptotic cells by MDMs profoundly inhibited the release of TNF $\alpha$  in response to LPS stimulation whilst augmenting TGF $\beta$  production [373]. A further *in vivo* study found that a single intratracheal injection of apoptotic cells into mice with bleomycin-induced lung injury resulted in decreased inflammation and attenuation of fibrotic responses. This was associated with enhanced HGF production by alveolar macrophages [374].

Defective efferocytosis has been observed in a number of lung diseases including COPD, asthma and cystic fibrosis [375]. In a murine model, efferocytosis was inhibited by blocking phosphatidylserine (a major 'eat-me signal') on the surface of apoptotic cells. Emphysema subsequently developed which was attributed to the failure of macrophages to undergo a phenotypic switch. Macrophages isolated from the BALF expressed high levels of matrix metalloproteinases (MMPs), MMP-2 and MMP-12, enzymes which degrade interstitial collagen [376]. A small study looking at the efferocytosis of aged neutrophils by alveolar macrophages found that those isolated from IPF patients had a lower phagocytic index than AMs isolated from non-fibrotic lung disease patients [237]. There are no published studies to date examining the ability of monocyte-derived-macrophages to undertake phagocytosis or efferocytosis in patients with fibrotic lung disease. Given the recent evidence that MDMs are likely to contribute to the lung macrophage population in the context of pulmonary fibrosis [193], the capacity of MDMs to perform these processes may have important implications in controlling the extent of epithelial alveolar cell (AEC) damage that occurs during infection or in the presence of excessive numbers of inflammatory cells. Defective efferocytosis in MDMs may also inhibit the functional evolution of these cells from potentiating matrix deposition during early repair to aiding in the termination of these processes after repair is complete [367, 370-373, 377].

### 7.2 Hypothesis and aims

I hypothesised that phagocytosis and efferocytosis would be impaired in IPF MDMs in comparison to aged-matched healthy controls and defects in these processes may contribute to the pathogenesis of the disease.

To address this I undertook the following:

## Chapter 7: Phagocytosis and neutrophil efferocytosis by MDMs in IPF

- i. Investigated whether phagocytosis differed in control and IPF MDMs by measuring the phagocytic uptake of *E. coli* bioparticles.
- ii. Isolated neutrophils for an assay comparing the ability of MDMs from IPF patients and controls to undertake efferocytosis.
- iii. Compared the expression of key genes associated with efferocytosis and phagocytosis in control and IPF MDMs.

### 7.3 Methods

#### 7.3.1 Participant samples

Samples were collected from September 2016 to April 2017. Patient samples were acquired during specialist ILD clinics or during in-patient stays. Age and sex-matched healthy volunteers were recruited from orthopaedic pre-assessment clinics or the University and screened for the presence of co-existent inflammatory conditions and lung disease. Only non-smokers were included in the study.

Further details including inclusion/exclusion criteria and ethical approval are documented in Chapter 2.1.

#### 7.3.2 Sample processing

Monocyte derived macrophages were generated as described in section 2.3.5. Briefly, following positive selection using CD14 microbeads (Miltenyi), cells were cultured on 24 well low-adherence plates in X-vivo (Lonza) and 10% heat-inactivated autologous serum and 50ng/ml M-CSF (added on day 0 only). Media was replenished on day 4 and MDMs were used for phagocytosis/efferocytosis experiments on day 7.

### 7.3.3 Phagocytosis

Phagocytosis was assessed using two methods (section 2.5.1 for details). Firstly, carboxylate-modified polystyrene latex yellow-green beads (Sigma) were incubated with  $1 \times 10^5$  cells for 2 hours at 37°C. A ratio of 30 beads per cell was selected following optimisation experiments. Samples were then acquired by flow cytometry and analysed to assess the proportion of cells that had taken up the beads. Cytochalasin D was used as a negative control. The pHrodo® assay (Molecular Probes) was also employed to assess phagocytic ability. Green E. coli bioparticles conjugated to a pH-sensitive fluorophore were diluted in PBS and incubated with  $1 \times 10^5$  MDMs within a 96 well plate for 30 minutes at 37°C. A viability dye was used to enable the exclusion of non-viable cells and samples placed on ice and acquired immediately on the LSRII flow cytometer.

### 7.3.4 Neutrophil isolation

To determine the optimal method of isolating neutrophils, three techniques were tested.

**Neutrophil isolation using the Ficoll density method:** 10ml of whole blood was mixed with an equal volume of R10 and layered over 15ml of Lymphoprep™ (Axis-Shield). Samples were centrifuged at 2000rpm for 20 minutes without a break enabling separation of the different cellular layers. PBMCs were removed from the upper interface layer using a Pasteur pipette and discarded. The lower portion of the Ficoll layer, containing the majority of the neutrophils, was then pipetted out and placed into a separate Falcon tube. 15ml of red cell lysis buffer was then added for 5 minutes followed by 25ml of R10. The sample was centrifuged and the supernatant removed. The red cell lysis buffer step was repeated once more and the cells then counted and suspended in R10.

**Neutrophil positive selection:** Neutrophils were isolated according to the manufacturer's protocol (Miltenyi Biotec). In brief, 10ml of whole blood was collected and divided into 2 Falcon tubes. 45ml of red cell lysis buffer was added to each tube for 5 minutes. Tubes were then centrifuged and the supernatant removed. The red cell lysis buffer step was repeated once more, and cells were then washed in MACs buffer, counted and resuspended in MACs buffer at a concentration of  $10^7/80\mu\text{l}$  cells as per the manufacturer's protocol. 20 $\mu\text{l}$  of anti-CD15 microbeads (Miltenyi Biotec) per  $10^7$  cells

## Chapter 7: Phagocytosis and neutrophil efferocytosis by MDMs in IPF

was added to the Falcon tube and incubated for 15 minutes at 4°C. 10ml of MACs buffer was then added and the tube centrifuged to pellet the cells. Cells were resuspended in 500µl of MACs buffer and passed through an LS column for positive selection. Finally, cells were counted, washed and suspended in R10.

**Neutrophil negative selection:** Neutrophils were isolated from whole blood using the MACSxpress® isolation kit (Miltenyi Biotec). The separation was carried out according to the manufacturer's instructions. 8ml of blood was placed into a 15ml Falcon tube and incubated for 5 minutes with a vial of reconstituted Neutrophil Isolation Cocktail on a tube rotator running at 12rpm. The isolation cocktail magnetically labels components of whole blood with the exception of neutrophils. The Falcon tube was then transferred to a magnet (MACSxpress® Separator) for 15 minutes where the magnetically labelled cells adhere to the wall of the tube whilst the erythrocytes and platelets aggregate at the bottom. The supernatant, containing the unlabelled neutrophils, was then transferred to a new Falcon tube using a Pasteur pipette and red cell lysis buffer was added to remove any contaminating red cells. Purity of neutrophils was assessed via flow cytometry.

Purity of neutrophils obtained using each method was assessed using flouochrome-conjugated antibodies to CD3, CD19, CD14, CD16 and CD15.

Negative selection of neutrophils using the MACSxpress® isolation kit was found to be the best method for isolating neutrophils and used in the experimental protocol (see section 1.4.2).

### 7.3.5 Neutrophil preparation

Neutrophils from two healthy donors were used for all efferocytosis experiments. Following isolation, neutrophils were washed in PBS and stained with the cell tracer Far Red (Molecular Probes) at a concentration of 1µl/ml for 10 minutes. Cells were then washed, resuspended in R10, and placed in an incubator at 37°C for 18h prior to use in the efferocytosis assay. To assess the extent of neutrophil apoptosis, an aliquot of neutrophils was stained at the time of the assay for Annexin V and 7AAD (Chapter 2.9). Cells were counted prior to the assay and suspended in R10 in a concentration of  $2 \times 10^6$ /ml.



### **7.3.6 MDM preparation**

Day 6 MDMs were transferred from culture plates to mini Falcon tubes and washed in PBS. The cell tracer Violet Proliferation Dye (VPD, Molecular Probes), was added to the cell pellets, after the supernatant was removed, at a concentration of 1 $\mu$ M and cells resuspended thoroughly to ensure a single cell suspension was achieved. The mini-Falcon tubes were then placed in a water bath set at 37°C for an incubation period of 10 minutes. R10 was then added to the tubes to quench the dye and cells washed twice in R10. MDMs were counted using an automated cell counter and suspended in R10 at a concentration of 10<sup>6</sup>/ml.

### **7.3.7 Efferocytosis assay**

Flat bottomed 96 well plates were used for the efferocytosis assay and 100 $\mu$ l of cell solution (10<sup>5</sup> MDMs) was added to each well. For each participant sample, two wells were required; one for the test and another to serve as a negative control to facilitate the gating of the positive population for subsequent flow cytometric analysis. The negative control was achieved using Cytochalasin D, added at a concentration of 30nM for 30 minutes prior to the addition of neutrophils. Aged neutrophils (between 18-20 hours' post venesection) were added to MDMs at a ratio of 2:1. Cells were incubated at 37°C for 2 hours then fixed with stabilising fixative. Cells were acquired via flow cytometry (LSRII). Figure 7-1 depicts the steps used in this experiment.

## Chapter 7: Phagocytosis and neutrophil efferocytosis by MDMs in IPF

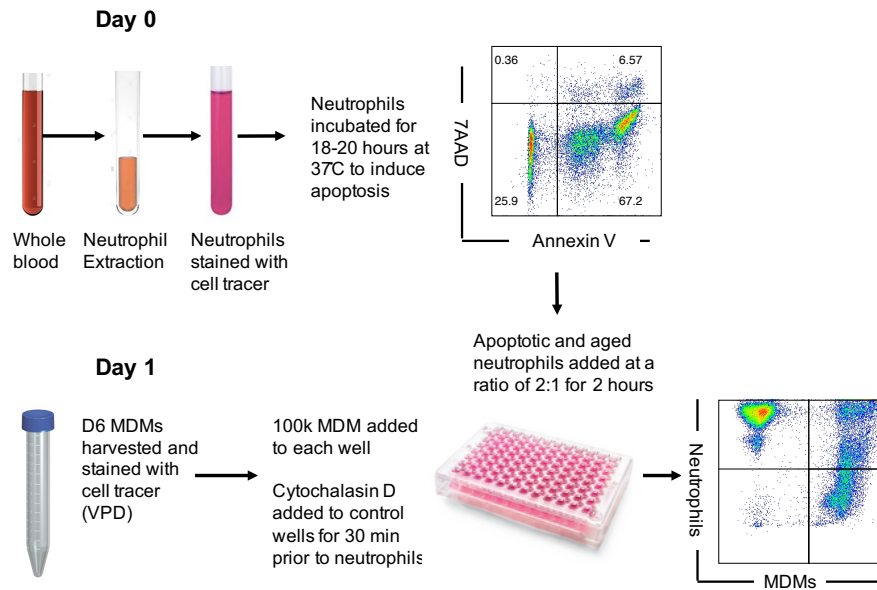


**Figure 7-1. Graphical representation of the experimental protocol used for neutrophil efferocytosis assay.**

### 7.3.8 Gating strategy

Cell populations positive for both tracer dyes were taken to be indicative of neutrophil efferocytosis by MDMs. Samples pre-treated with cytochalasin D were used to define the two cell populations and aid in the gating of the double positive population. MDMs were then gated on to determine the percentage of MDMs taking up neutrophils, as indicated in Figure 7-2.

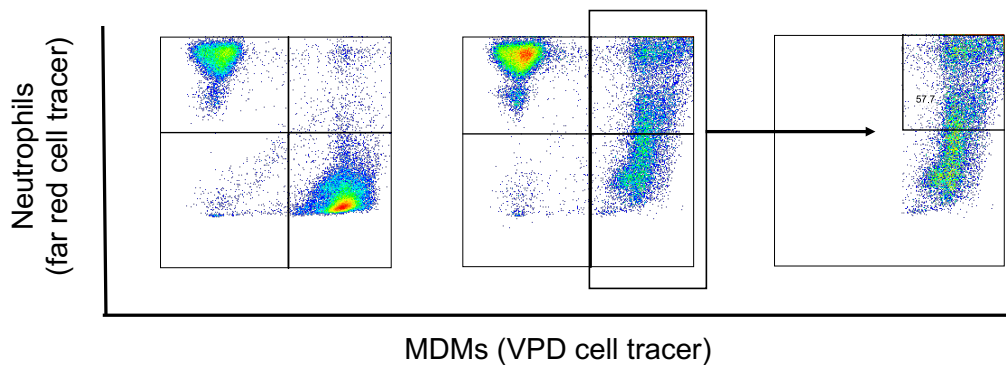


**Figure 7-2. Gating strategy used for neutrophil efferocytosis assay.**

MDMs were labelled with cell tracer VPD (excitation/emission spectrum equivalent to BV421) and neutrophils with far red cell tracer (APC equivalent) prior to the assay. From left to right: Cytochalasin D treated sample was used to define position of cell populations; test sample following incubation of aged/apoptotic neutrophils with MDMs for 2 hours; the MDM positive population was then gated on to determine the percentage of MDMs that have taken up neutrophils.

### 7.3.9 RNA extraction and qPCR

To complement the phagocytosis data and determine whether the expression of genes involved in phagocytosis are differentially expressed in patients and controls, RNA was extracted from 8 IPF MDMs and 6 age-matched controls and qPCR undertaken using SYBR® green (section 2.9-10). Fold change was calculated using three housekeeping genes, *β2 microglobulin*, *β-actin* and *cyclophilin A*. The genes analysed are detailed in section 2.10, Table 2-8 and 2-9).

## 7.4 Results

### 7.4.1 Participant demographics

Demographics	Neutrophil Efferocytosis		pHRodo® Monocyte-MDM Phagocytosis		RNA	
	IPF	Controls	IPF	Controls	IPF	Controls
Sample number	17	15	6	6	8	6
% Male	88	66	66	66	87	83
Mean age (range)	76 (66-85)	65.6 (57-75)	76.7 (69-86)	72.8 (57-80)	72.2 (66-79)	65.2 (51-71)
% Definite diagnosis	40	N/A	50	N/A	13%	NA
% on Anti-fibrotics (number) N=Nintedanib P=Pirfenidone	46 (6) N=2 P=4	N/A	50 (3) N=2 P=1	N/A	37 (3) N=2 P=1	NA

**Table 7-1. Demographic details of IPF patients and controls sampled for the efferocytosis and phagocytosis assays and the expression of phagocytic genes.**

N=nintedanib; P=Pirfenidone; N/A – data not applicable to healthy controls.

### 7.4.2 MDMs from IPF patients showed evidence of impaired phagocytosis

Phagocytosis is an essential process in host defence and a major function of macrophages is to engulf and destroy invading pathogens following tissue injury [378, 379]. Phagocytosis is also important in the maintenance of tissue homeostasis and in

## Chapter 7: Phagocytosis and neutrophil efferocytosis by MDMs in IPF

the lung, macrophages play a role in regulating the turnover of ECM through the phagocytosis of collagen [367, 377, 380]. To determine whether the ability of MDMs to undertake the process of phagocytosis differed between IPF and healthy controls, I undertook two assays.

Phagocytosis by day 7 MDMs was assessed initially by utilising fluorescent latex beads and examining the proportion of cells positive for beads via flow cytometry. Figure 7-3a shows the percentage of cells positive for fluorescent beads and there appears to be no difference in phagocytic ability between patient and control MDMs. Whilst the ratio of beads to cells and the incubation period were optimised, due to concerns that beads may be non-specifically binding to the surface of cells, Cytochalasin D was used as a negative control. This compound inhibits actin cytoskeleton realignment in phagocytic cells thereby preventing cells from encapsulating and internalising particulate and cellular matter [381]. The use of cytochalasin D in this assay revealed that a variable and often high proportion of beads that appeared to have been phagocytosed were stuck on the surface of cells inhibited with the compound, making meaningful interpretation of phagocytosis impossible (Fig 7-3c).

## Chapter 7: Phagocytosis and neutrophil efferocytosis by MDMs in IPF

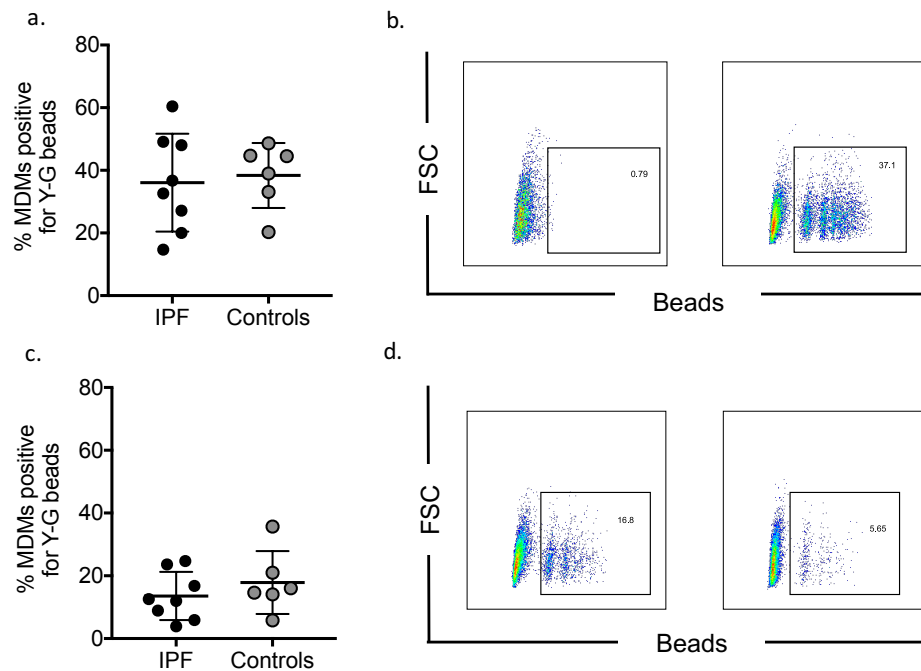


**Figure 7-3. Phagocytosis assay utilising fluorescent latex beads and effect of the phagocytosis inhibitor Cytochalasin D on apparent bead uptake.**

(a) The percentage of MDMs positive for beads after a 2-hour incubation period in stable IPF patients compared to controls. (b) Representative FACS plots demonstrating appearance of control cells (without beads) on the left and the gating of MDMs taking up the beads (right). (c) Percentage of MDMs appearing to have internalised beads following Cytochalasin D administration. (d) FACS plots demonstrating the variability in bead-positive cells after inhibition with Cytochalasin D in two different samples. (*Y-G yellow-green beads; FSC forward scatter*).

The pHrodo® assay was thus employed which utilises a pH-sensitive fluorochrome that only emits light within the acidic environment of the lysosome after it has been taken up by the phagocyte (Fig 7-4a). Inhibiting these cells with Cytochalasin D resulted in an almost complete absence of fluorescence enabling accurate interpretation of phagocytic uptake in test samples. The assay demonstrated that the phagocytic ability of MDMs derived from IPF patients was impaired compared to age-matched healthy controls ( $p=0.013$ , Fig 7-4b).

## Chapter 7: Phagocytosis and neutrophil efferocytosis by MDMs in IPF

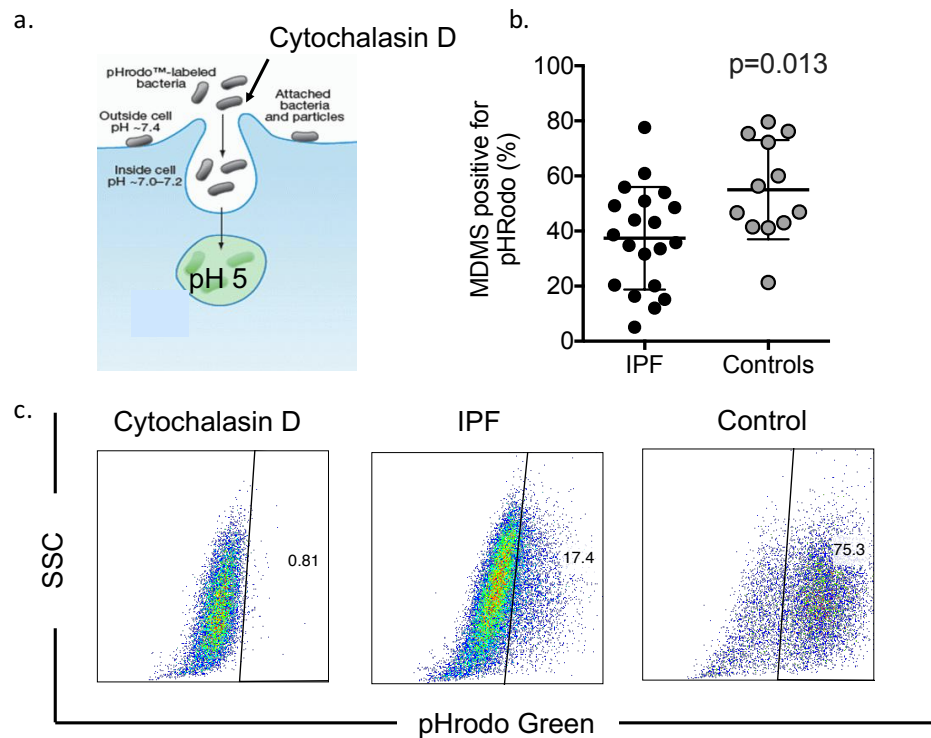


**Figure 7-4. Phagocytosis using the pHrodo® assay.**

Phagocytic ability by IPF and control MDMs was tested using the pHrodo® bioparticles assay. SD(mean) described here and depicted in graph. (a) Pictorial representation of how bacterial bioparticles conjugated to a pH-sensitive fluorescent dye fluoresce at acidic pH such as within the lysosome. Cytochalasin D prevents phagocytosis by inhibiting realignment of the actin cytoskeleton required for encapsulation of the bioparticle. (b) Percentage of MDMs taking up *E coli* bioparticles was decreased in IPF MDMs compared to controls [% (SD): 37(19) vs 55(18) n=20 and 12, Student t-test]. (c) FACS plots from left to right: Cytochalasin D resulted in inhibition of phagocytosis; FACS plot of MDMs from an IPF patient and a healthy control demonstrating decreased phagocytic uptake by IPF MDMs.

### 7.4.3 Defective phagocytosis in IPF was linked to macrophage differentiation and not observed in monocytes

Phagocytosis to *E coli* bioparticles was impaired in IPF MDMs harvested on day 7 compared to MDMs from age-matched controls. In chapter 4 I found that clear phenotypic differences existed between MDMs from controls and IPF patients, which were not apparent in monocytes. I was therefore interested in determining whether functional differences, such as the ability to undertake phagocytosis, was an inherent defect in IPF monocytes or acquired during the process of monocyte to macrophage

## Chapter 7: Phagocytosis and neutrophil efferocytosis by MDMs in IPF

differentiation. To determine this, the phagocytic ability of monocytes from aged-matched controls and IPF participants was assessed on day 1, 3 and 7.

Comparison of the phagocytic uptake of *E coli* bioparticles in 6 IPF and 6 healthy control monocytes over 7 days did not show significant differences between the two groups, which may be attributable to the small sample size. However, day 1 IPF monocytes showed a trend towards enhanced phagocytosis compared to controls (Fig 7-5a). Interestingly, the process of monocyte to macrophage differentiation appeared to affect the ability of IPF monocytes to phagocytose and by day 7, MDMs from IPF patients showed a trend towards decreased phagocytic ability compared to control MDMs (Fig 7-5b-c).

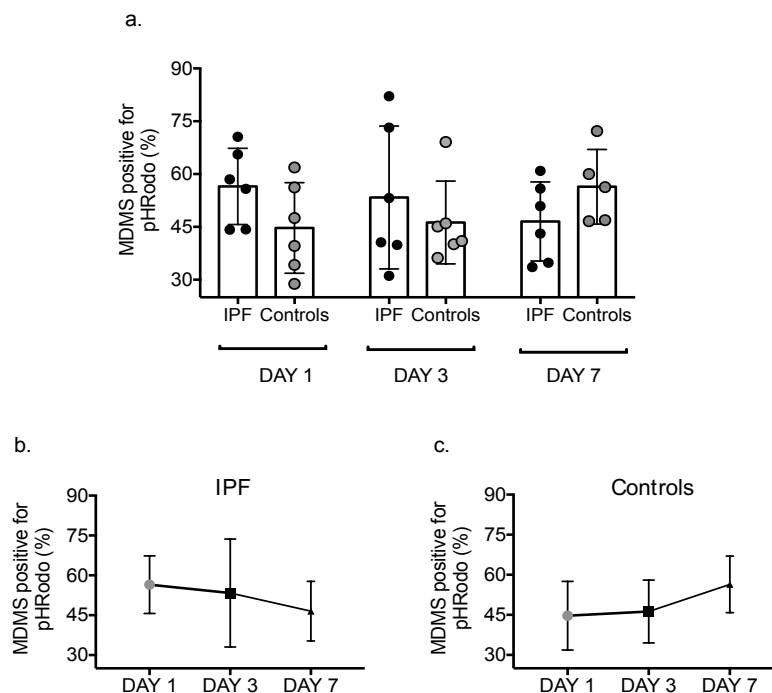


**Figure 7-5. Phagocytic ability of monocytes from IPF patients and healthy age-matched controls as they differentiate into macrophages over 7 days.**

The pHrodo® assay was used to assess phagocytosis by IPF and control MDMs at different time points during their differentiation process. MDMs were incubated with *E. coli* bioparticles, washed, then stained with viability dye and acquired via flow cytometry. (a) The percentage of monocytes/MDMs positive for fluorescent *E. coli* bioparticles (pHRodo) on day 1, 3 and 7. (b-c) The phagocytic ability of monocytes and MDMs over the three time points in IPF patients (b) and healthy controls (c). IPF n=6 controls=6. p=n.s.

#### 7.4.4 Neutrophil isolation using negative selection was the preferred method for the efferocytosis assay

To determine whether efferocytosis was also impaired in IPF MDMs, I assessed the ability of macrophages to efferocytose aged neutrophils. To undertake this assay, I first optimised the isolation procedure for neutrophils and three methods were tested as described in 7.3.4. Table 7-2 documents the purity of the populations obtained, assessed via flow cytometry looking at the proportion of CD15+CD16+ cells within a panel that encompassed CD3 (T cells), CD19 (B cells) and CD14 (monocytes).

The highest purity of neutrophils was achieved from positive selection using CD15 microbeads. Due to concerns that the magnetic beads labelling neutrophils may stimulate the process of efferocytosis and confound the results, the efferocytosis assay was tested with CD15-bead labelled neutrophils and found to be significantly higher in both controls and IPF patients compared to other methods ( $p < 0.001$ , Fig 7-6). This method was therefore not used subsequently and due to the reasonable purity obtained using the MACSxpress kit (>96%), this technique was adopted for all the efferocytosis assays reported in this study. Figure 7.7 illustrates the gating strategy used to assess the purity of neutrophil following negative selection.

Neutrophil isolation method	Purity (%)	Issues
Ficoll density method	88	Low purity
Positive selection (CD15 microbeads)	99.6	Beads on neutrophils may stimulate phagocytic pathways
Negative selection (MACSxpress <sup>®</sup> kit)	96.4	- -

Table 7-2. Neutrophil purity and issues with three different methods of isolation.



## Chapter 7: Phagocytosis and neutrophil efferocytosis by MDMs in IPF

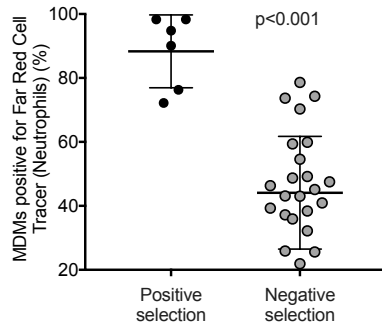


**Figure 7-6.** The percentage of MDMs participating in efferocytosis using neutrophils isolated with CD15 microbeads (positive selection) compared to those isolated with the MACSexpress® kit (negative selection). MDMs involved in efferocytosis were calculated by measuring the proportion of MDMs positive for the Far-Red cell tracer used to label neutrophils. Cumulative data is shown which includes both controls and IPF patients in both groups. Positive selection n=6, negative selection n=26.

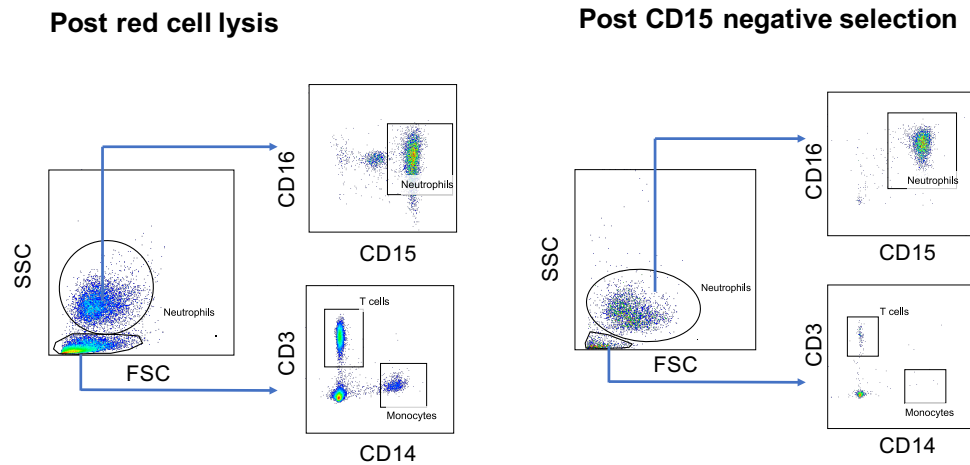


**Figure 7-7.** FACS plots demonstrating the purity of the neutrophils following isolation using the MACSexpress® neutrophil isolation kit.

Left: SSC/FSC plot of blood post red-cell lysis to show the relative proportion of neutrophils (large circle) and mononuclear cells (oval) which were then gated on to determine the proportion of T cells (CD3), monocytes (CD14) and B cells (CD19 – not shown). Right: post negative selection, the same gating strategy is used and the proportion of remaining T cells and monocytes of the total cell population is less than 4% (Table 7-2).

## Chapter 7: Phagocytosis and neutrophil efferocytosis by MDMs in IPF

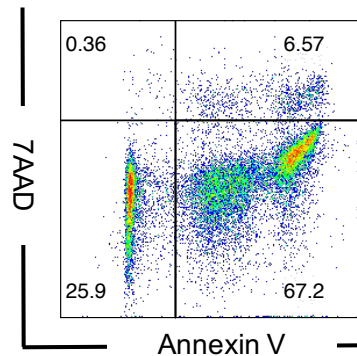


**Figure 7-8. The proportion of neutrophils that had undergone cell death or were in the process of apoptosis 18h post isolation was assessed via flow cytometry.**

The FACs plot shows the percentage of cells in apoptosis (indicated by positive staining for annexin V+/-7AAD).

### 7.4.5 Efferocytosis was impaired in MDMs from IPF patients

The removal of aged and dying cells through phagocytosis (efferocytosis) by macrophages is essential for maintaining tissue homeostasis. Phagocytosis was found to be reduced in IPF MDMs and I therefore questioned whether efferocytosis of aged neutrophils by IPF monocyte-derived macrophages would also be impaired compared to age-matched healthy controls.

Figure 7-8 shows the proportion of neutrophils staining positive for annexin V and 7AAD and indicated that the majority of neutrophils used for the assays were in the process of apoptosis or had undergone cell death (60-70% on each occasion). MDMs were labelled with VPD and the percentage of these cells engaged in efferocytosis was determined by measuring the proportion of MDMs that stained dual-positive for the far-red cell tracer dye used to label neutrophils following isolation (Fig 7-2 for gating strategy). MDMs from IPF patients had reduced ability to efferocytose aged neutrophils compared to controls ( $p=0.031$ , Fig 7-9).

## Chapter 7: Phagocytosis and neutrophil efferocytosis by MDMs in IPF

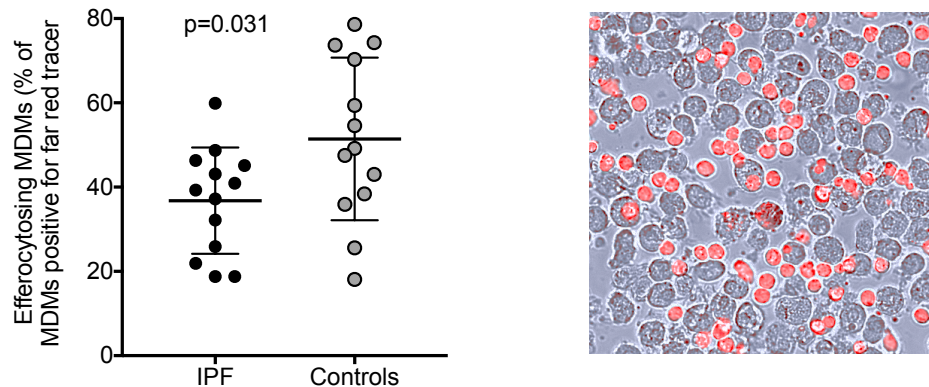


**Figure 7-9. The proportion of MDMs phagocytosing neutrophils in IPF and age-matched controls.**

Left: Neutrophils were labelled with far red cell tracer and efferocytosis was measured by calculating the percentage of MDMs positive for the cell tracer. Mean(SD) described here and illustrated on the graph. A lower percentage of IPF MDMs participated in efferocytosis compared to control MDMs [36.8%(12.6) vs 51.4%(19.3) n= 13 for both groups, Student t-test]. Right: Immunofluorescence image of MDMs (grey) and neutrophils (red) taken during the efferocytosis assay.

### 7.4.6 The expression of genes involved in phagocytosis was decreased in IPF MDMs

I found that both efferocytosis and phagocytosis were impaired in IPF MDMs compared to aged-matched controls. The engulfment of cellular and particulate matter is mediated by binding to specific scavenger receptors. Scavenger receptors represent a diverse group of transmembrane and soluble receptors that recognise a wide range of ligands including modified self-proteins and conserved motifs on microbial structures [344]. CD36, MSR1, MARCO and MerTK have been identified as key receptors in the uptake of apoptotic cells and pathogen-associated-molecular patterns (PAMPs). Studies inhibiting the activity of CD36 and MerTK resulted in an accumulation of apoptotic cells and the development of autoimmune pathology [382, 383]. MARCO and macrophage scavenger receptor-1 (MSR1 or SR-A1) are type A scavenger receptors that function as pattern recognition receptors (PRR) involved in the uptake and internalisation of bacteria and DAMPs. In the airways, these receptors are involved in clearance of airborne pathogens and inhaled particulates [384, 385]. Given the reduced phagocytic and efferocytic ability of IPF MDMs, I was interested in determining whether this may be linked to reductions in the expression of scavenger receptors that mediate this process.

## Chapter 7: Phagocytosis and neutrophil efferocytosis by MDMs in IPF

There was lower gene expression of the scavenger receptor *MSR1* ( $p=0.001$ , Fig 7-10a). Significant differences in the expression of *MARCO*, *CD36* and *MERTK* were not observed although there was a trend towards lower expression of *CD36* and *MERTK* by IPF MDMs ( $p=0.108$  and  $p=0.196$ , Fig 7-10c-d respectively).

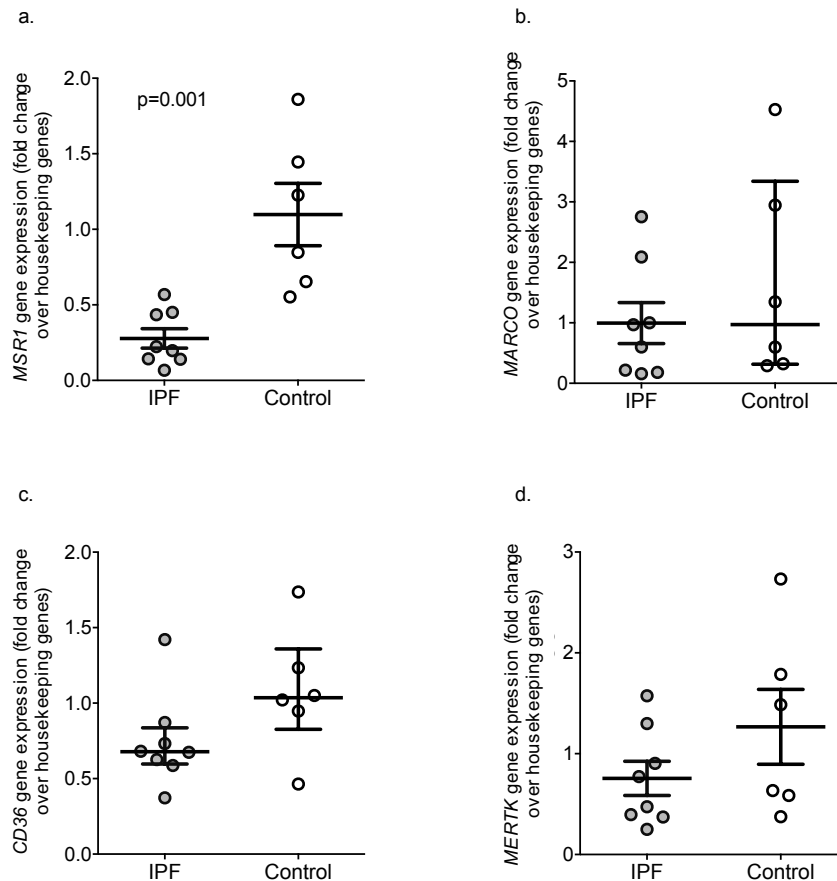


**Figure 7-10. The gene expression of key scavenger receptors and *MERTK* in IPF and control MDMs.** Monocytes from IPF and control participants were cultured for 7 days in autologous serum and then processed for qPCR to determine the expression of genes involved in phagocytic pathways. The fold change over three housekeeping genes (*CYCLOPHILIN A*,  *$\beta$ 2-MICROGLOBULIN* and  *$\beta$ -ACTIN*) was used to determine the relative expression of the genes of interest. For normally distributed data, mean(SEM) are depicted in graphs. For non-parametric data, the median and interquartile range are shown. (a) The expression of *MSR1* was significantly lower in IPF MDMs compared to controls [0.06(0.08) vs 1.98(2.26), Student t-test] (b) Expression of *MARCO* did not differ between IPF and control MDMs [0.68(0.60-0.84) vs 1.04(0.83-1.36);  $p=0.414$ , Mann-Whitney test]. (c) *cd36* showed a non-significant trend towards lower expression in IPF MDMs compared to control MDMs [0.78(0.19-1.82) vs 0.97(0.31-3.34);  $p=0.108$ , Mann-Whitney test]. (d) *MERTK* expression was not significantly different between IPF and control MDMs [0.76(0.17) vs 1.27(0.37);  $p=0.196$ , Student t-test].  $p<0.05$  taken to indicate statistical significance. IPF MDMs  $n=8$  and control MDMs  $n=6$ .

## 7.5 Discussion

In this chapter I found that both phagocytosis and efferocytosis were impaired in day 7 MDMs derived from IPF patients, in comparison to MDMs from age-matched healthy controls. If these defects reflect *in vivo* functionality, the consequences may be of pathological significance and contribute to the development and progression of lung fibrosis.

Phagocytosis of invading pathogens by lung macrophages is an essential process in counteracting systemic infection and characterises the innate response during the early stages of microbial encounter [229]. Animal models of lung fibrosis have demonstrated that monocyte-derived-macrophages contribute substantially to the lung macrophage pool [193, 269]. Therefore, the finding that IPF MDMs exhibit defective phagocytosis of *E coli* bioparticles may reflect impaired ability of MDMs to clear pathogenic organisms within the IPF lung. Furthermore, chronic tissue damage combined with treatments that suppress immune function in IPF may predispose to the presence of pathogenic and opportunistic species causing subclinical or recurrent infection. Whilst a causal relationship between infection and disease pathogenesis has not been established, viruses and bacteria within the lower respiratory tract can cause alveolar epithelial cell injury, which may indirectly trigger or perpetuate profibrotic pathways [386]. Indeed, studies have found evidence of viruses in a high proportion of lung biopsies obtained from IPF patients [387-389]. More relevant to the findings here, a study by Molyneux *et al.* reported an elevated bacterial burden within BALF from IPF patients, which was found to correlate inversely with functional vital capacity (FVC) and increased risk of mortality [63]. Another study isolated *Pneumocystis jirovecii* (an opportunistic fungus that can cause severe pneumonia in immunocompromised patients) from 38% patients with IPF [390]. The initial host response to this fungus is mediated by alveolar macrophages through recognition of pathogen-associated molecular patterns (PAMPs) by pattern recognition receptors (PRRs), including toll-like receptors (TLR) 4 and 2 [391, 392]. The binding of fungal components triggers activation of the cell, leading to phagocytosis and the release of pro-inflammatory cytokines. Intracellular killing is then mediated predominantly through the generation of reactive oxygen species [393], which in addition to phagocytosis, was found to be attenuated in IPF MDMs (5.4.8). These findings could thus partly explain the increased incidence of infectious organisms identified in patients with IPF.

## Chapter 7: Phagocytosis and neutrophil efferocytosis by MDMs in IPF

As highlighted previously, phagocytosis in this chapter was assessed using *E coli* bioparticles. These particles contain lipopolysaccharide, a PAMP that stimulates phagocytosis through activation of TLR4 [256]. Numerous scavenger receptors and PRRs exist which recognise specific molecular motifs on damage-associated molecular patterns and PAMPs [344], and thus the phagocytic defect to *E coli* bioparticles by IPF MDMs may not extend to other substrates. Investigating whether IPF MDMs exhibit a more global defect in phagocytosis however may be of relevance as regulation of collagen turnover has been demonstrated to be partly mediated by macrophages through small-particle phagocytosis (termed endocytosis) [367, 380]. In a study investigating the cellular uptake of collagen, mice engineered to express GFP within macrophages were given intradermal injections of fluorescent type I collagen. Immunofluorescence imaging subsequently revealed that the majority of macrophages had internalised this collagen into lysosomal components after 24 hours [377]. Thus, a reduction in collagen turnover due to defects in its removal through phagocytosis may contribute to the gradual accumulation of collagen-rich matrix seen in IPF.

In the same study, the authors reported that 'M2' macrophages were the predominant population involved in collagen endocytosis supporting the theory that these macrophage populations are superior at phagocytosis. In chapter 5, I found the M1/M2 polarisation system inadequate to define healthy control and IPF MDMs, but assessing the characteristics of these cells together (as determined through the combined analysis of gene expression, cell surface receptor expression and ROS generation), there appeared to be an overall balance of features suggestive of a reparative rather than an inflammatory phenotype. Thus, the phagocytosis findings presented here were perhaps out of keeping with the phenotypic findings. I therefore questioned whether this may be related to the cellular characteristics present in IPF MDMs at the specific time point the assay was undertaken (on day 7). To explore this, and to establish whether monocytes from IPF patients also showed defective phagocytosis, the experiment was repeated at two different time points during monocyte-macrophage differentiation. Interestingly, monocytes from IPF patients followed an opposite trend to that observed in controls. Day 1 monocytes exhibited high phagocytic ability but by day 7, this capacity had reduced. In contrast, phagocytosis increased during the course of monocyte-macrophage differentiation in healthy controls. One explanation for this finding is the differential apoptosis of specific monocyte populations that occurred during the in vitro differentiation of IPF monocytes (5.4.6). A high proportion of CD64<sup>+</sup>CD163<sup>-</sup> monocytes underwent

## Chapter 7: Phagocytosis and neutrophil efferocytosis by MDMs in IPF

apoptosis in IPF patients suggesting that cells with enhanced phagocytic capacity may lack longevity in the IPF population. Another possibility is that highly phagocytic monocytes from IPF patients efferocytose other monocytes undergoing apoptosis whilst in culture. By day 7, the phenotype and function of these cells may be altered by this process and in their 'post phagocytic' state lose the ability to undertake further efferocytosis as efficiently. Whilst the experiment would need to be repeated at different time intervals with apoptotic cells, this could partially explain the phenotypic differences found between control and IPF MDMs.

Cells isolated through bronchoalveolar lavage reflect the cellular milieu within the alveolar space and smaller bronchi [394]. The preponderance of neutrophils within the BALF of IPF patients is a well-recognised finding and has been attributed to increased levels of neutrophil chemoattractants that are present within the lavage fluid of IPF patients [368, 369]. In one study, alveolar macrophages themselves were found to express high levels of the cytokine IL-8, which stimulates the chemotaxis and activation of neutrophils [395]. An additional explanation for their predominance may be that neutrophils persist within the alveoli due to defective efferocytosis by macrophages. Indeed, the impaired efferocytosis by MDMs demonstrated in this chapter consolidates the work undertaken by Morimoto *et al.* who showed that efferocytosis by AMs from 8 IPF patients was decreased, alongside a proportionate increase in the numbers of apoptotic bodies counted [254]. Thus, whilst the reduction in efferocytosis by IPF MDMs was modest compared to controls, a collective defect in this function may have far reaching consequences if excessive numbers of neutrophils enter the lung and exceed the efferocytic capacity of macrophages.

Impaired neutrophil efferocytosis may potentiate fibrogenesis by more than one mechanism. Decreased capacity to clear excess numbers of aging neutrophils can result in the process of secondary necrosis, leading to the release of toxic mediators by dying neutrophils. This may exacerbate alveolar epithelial cell injury [371, 372, 375]. Neutrophils may also directly promote fibrosis and a recent study has demonstrated that a serine protease derived from neutrophils induces both fibroblast proliferation and myofibroblast differentiation in a TGF $\beta$ -independent manner [396]. As highlighted in the introduction, it has been found that the process of efferocytosis itself may limit the inflammatory response and enhance resolution of repair, by inducing a phenotypic switch in macrophages that alters the cytokine/chemokine repertoire [373, 397]. Impaired

## Chapter 7: Phagocytosis and neutrophil efferocytosis by MDMs in IPF

efferocytosis may therefore reduce the capacity of IPF MDMs to inhibit inflammatory pathways that perpetuate tissue damage.

It can be hypothesised that the time point that efferocytosis occurs during macrophage differentiation and maturation may determine the subsequent role the cell plays in the process of wound repair and other pathological states. Inhibiting early efferocytosis in murine macrophages, for example, resulted in the persistence of an inflammatory phenotype and the development of emphysema [376]. Efferocytosis by MDMs that have entered the tissue after the initial repair phase following injury upregulate genes that inhibit further inflammation and promote matrix deposition [373]. Conversely, 'mature' MDMs that efferocytose dying cells during the later phases of healing may differentiate into 'pro-resolution' cells that secrete factors to terminate the repair process. It is conceivable that decreased efferocytic capacity by IPF MDMs that already display reparative characteristics may thus inhibit further differentiation to a 'pro-resolution' phenotype and predispose to fibrosis.

Over recent years, a large and diverse range of phagocytic scavenger receptors have been identified that serve to identify and clear cellular and particulate matter [344]. It is of interest therefore that of the four studied here all show a lower trend in expression by MDMs from IPF patients. Whilst statistical significance was seen only for *MSR-1* this may be due to the low numbers analysed. *MSR-1* does not bind ligands directly but instead forms a complex with other receptors to initiate phagocytic pathways [344]. In particular, it couples with the tyrosine protein kinase MERTK to form a functional complex that enables apoptotic cell uptake and promotes resolution of inflammation [398]. It could also potentiate pro-inflammatory processes depending on the co-receptor involved. For example, it can form a complex with TLR4 in the presence of LPS and mediate uptake of gram negative bacteria [344]. The decreased expression of this receptor can thus explain the reduced uptake of both neutrophils and *E coli* bioparticles observed in IPF MDMs. Indeed, a mouse study showed that increasing surface expression of *MSR-1* alongside MERTK on macrophages increased apoptotic cell clearance [383]. Interestingly, mice lacking this receptor who were exposed to a hepatotropic virus infection developed a greater inflammatory infiltrate followed by evidence of liver fibrosis [399].



## Chapter 7: Phagocytosis and neutrophil efferocytosis by MDMs in IPF

This chapter has demonstrated that day 7 MDMs from IPF patients have reduced capacity to perform both phagocytosis and efferocytosis. Whether IPF macrophages derived from monocytes exhibit similar characteristics within the lung is unknown but the potential mechanisms by which impaired efferocytosis could potentiate the pathophysiology of IPF are illustrated in the diagram below (Fig 7.11).

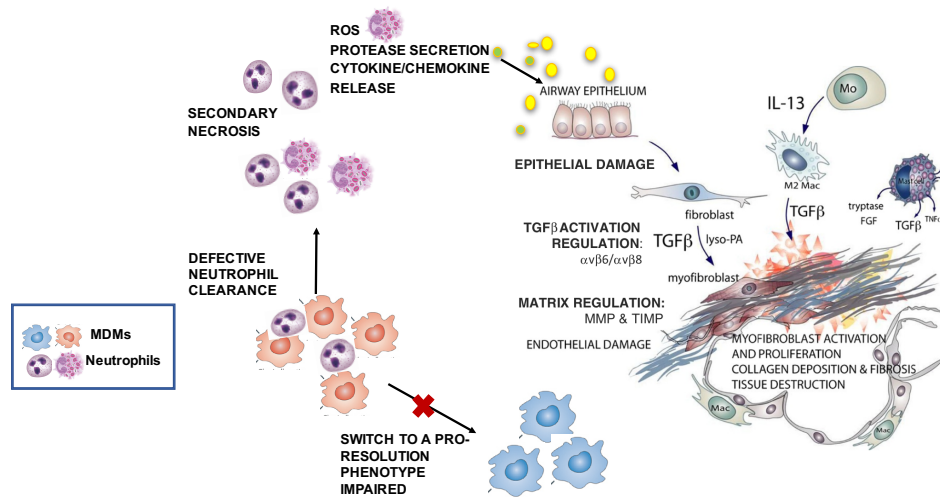


**Figure 7-11. Mechanisms by which impaired efferocytosis could potentiate the pathophysiology of IPF.**

Defective neutrophil clearance due to impaired efferocytosis by monocyte-derived macrophages (MDMs) may result in neutrophils undergoing secondary necrosis leading to the release of toxic mediators including ROS, proteases and cytokines/chemokines that promote AEC damage and potentiate fibrogenic pathways. Impaired efferocytosis may also prevent the differentiation of macrophages to an anti-inflammatory/pro-resolution phenotype.

## 8 Final discussion and future direction

### 8.1 Final discussion

The aim of this project was to characterise the phenotype of monocytes in patients with IPF based on the hypothesis that these cells contribute to the process of fibrotic over-repair in the lung. It has long been established that macrophages play important roles in inflammation and repair but the notion that monocytes and monocyte-derived-macrophages (MDMs) may drive fibrotic responses after injury follows the fairly recent understanding that macrophage populations differ significantly in health and disease. Research has revealed that the contribution of MDMs to the lung macrophage pool increases following injury and there is evidence that depending on the phase of repair, the phenotype and functionality of these infiltrating cells changes to direct the process accordingly [25, 126, 192, 235]. Monocytes and their macrophage derivatives may promote inflammation, fibrogenesis or healing resolution responses, depending on the environmental milieu and possibly pre-programmed characteristics acquired during BM development [182, 270]. I thus hypothesised that differences in the phenotype of monocytes may impact on the function of these cells within the lung and potentiate the process of fibrosis.

To test this, I first studied the phenotype of monocytes freshly isolated from the blood. The most common method of subdividing monocyte populations into classical, intermediate and non-classical subtypes did not reveal differences between controls and IPF patients, but expression of receptors more commonly associated with macrophage phenotypes revealed a significant increase in CD64 expression in IPF monocytes. This FcγR receptor is associated with activated and inflammatory monocyte functions including antibody-dependent cell-mediated cytotoxicity, phagocytosis and enhanced antigen presentation [220, 251, 253, 275]. Monocytes highly expressing CD64 are therefore likely to represent a particularly pro-inflammatory subgroup, of which a higher proportion exist in IPF. The preferential apoptosis of these CD64+CD163- monocytes in IPF after 24 hours suggests that these cells may represent a population of shorter lived monocytes that were not primed to differentiate into MDMs. Indeed, it has been revealed that monocytes are far more complex and heterogeneous than previously recognised. They may differentiate into MDMs or dendritic cells, but some remain as monocytes for their lifespan with evidence that they can traverse the endothelium to survey tissue and

## Chapter 8: Discussion and future direction

present antigen to cognate T cells [400]. CD64+CD163- monocytes may potentiate tissue damage within the lung without residing in the interstitium, providing a possible explanation for the paucity of inflammatory cells around fibroblastic foci. The activity of these 'pro-inflammatory' CD64+CD163- monocytes was not explored in this project but high CD64 expression has been correlated with clinical markers of disease activity in SLE and rheumatoid arthritis. Indeed, the binding of immune complexes to CD64/FcγR1 on monocytes within the kidney triggers an inflammatory response that is considered critical in the pathogenesis of lupus nephritis [160, 250, 253]. Although this is unlikely to be the mechanism in IPF, given that CD64 expression was significantly elevated in monocytes from treatment-naive patients only, it is probable that anti-fibrotic therapy perturbs pathways involved in monocyte activation, and by doing so, reduces their fibrogenic potential. Of interest, a study by Li *et al.* (2009) showed that CD64+ monocytes exhibited greater chemotaxis in response to MCP-1 [251]. MCP-1 levels are elevated in the BALF of IPF patients [245, 246] and thus it is plausible that CD64+CD163- monocytes may preferentially traffic to the lung and potentiate tissue damage.

In this project, MCP-1 was found to be highly expressed by monocytes in response to the viral PAMP, r848. Whilst not specific to IPF monocytes, this finding could be of significance given evidence that microbes may act as cofactors for disease development and progression [63, 64, 387, 389, 401, 402]. Viral infection within the lung may stimulate monocytes and macrophages within the locality to release MCP-1 resulting in the migration of monocytes in high numbers. Monocyte chemotaxis to the lung in response to infection enables the effective clearance of pathogens through phagocytosis and release of inflammatory mediators including ROS. In health, the subsequent apoptosis and clearance of these monocytes facilitates successful tissue resolution but in IPF, where an aberrant healing response has already been established, continual monocyte infiltration may occur and serve to enhance the fibrotic cascade further. Indeed, mouse models of non-resolving lung injury demonstrate the presence of an expanded MDM pool that is associated with tissue destruction and fibrosis [192].

The expression of genes by monocytes was found to differ between stable IPF and controls. *CD14*, *CD163* and *FGL2* were reduced in IPF monocytes with trends towards lower *TNFα* and *TGFβ1* expression alongside higher *IL-10*. Whilst this differential gene expression is likely to impact on monocyte behaviour, the up-regulated and down-regulated genes did not concur with the current concept of monocyte/macrophage phenotypes, which are based primarily on in vitro studies. The trend towards higher *IL-*

## Chapter 8: Discussion and future direction

10 and lower *TNF $\alpha$*  are suggestive of an immunomodulatory phenotype but the decreased expression of *CD14*, *CD163* and *FGL2*, do not fit with this phenotype [196, 197, 199, 220, 227]. Furthermore, CD14 protein was expressed more intensely on the cell surface of IPF monocytes and CD163 did not differ significantly between stable IPF and controls, demonstrating that gene transcription does not always correlate with translational changes (assuming that technical issues were not contributing factors). Thus, interpreting the significance and relevance of these findings is difficult. Retrospectively, the complicated phenotype of IPF monocytes is unsurprising given the complex pathological processes occurring, in which monocytes are likely to be subjected to an array of stimuli that modulates their differentiation and functional characteristics.

Despite the difficulty in classifying IPF monocytes into predefined phenotypic categories, the differential expression of protein receptors and genes is likely to be of relevance given the established roles that these cells play in injury and repair. The observation that IPF was associated with higher proportions of circulating monocytes and that levels correlated with fibrotic burden on CT also supports the hypothesis that these cells influence disease processes. Furthermore, the absence of correlation with radiological features that do not support a diagnosis of UIP (i.e. ground glass or consolidative change) suggests that monocytes are associated with fibrosis specifically, rather than a range of pathological processes. In concordance with this was a small human study that utilised a radiolabelled probe, which was preferentially taken up by monocytes. The authors then used positron-emission tomography (PET)/CT imaging to identify the location of the probe and found high uptake in the lungs of IPF patients that was not seen in either controls or patients with other forms of lung fibrosis [366].

There is evidence that the clinical manifestations of acute exacerbations of IPF are the result of an acceleration of the underlying disease process. It is probable that these events are triggered by a variety of external factors, of which infection is the most common [8, 15, 24, 64, 403, 404]. In this project, I studied the characteristics of 10 patients with AEIPF. I found that low baseline CPI, FVC and TLCO were more commonly seen in patients who had AE, consistent with the risk factors identified in other studies [248, 403]. In this project, I also noted that patients with AEIPF had a greater extent of lung fibrosis when graded on CT, reinforcing the notion that disease severity itself is a risk factor for the development of these events. To explore the hypothesis that monocytes in IPF are detrimental and possess an immunophenotype that potentiates fibrogenic activity, I was interested in determining whether perturbations in monocyte

## Chapter 8: Discussion and future direction

phenotype were exaggerated further during AE events. In support of this, I found that AEIPF patients had higher circulating monocyte levels than stable patients. Monocytes expressed CD163 more highly on their cell surface and genes associated with an 'M2' or reparative/immunomodulatory phenotype were up-regulated (*IL-10*, *IL-R2*, *CD163* and *THSB1*). Whilst these findings fitted well with the hypothesis that IPF monocytes are skewed towards a wound-healing phenotype, all patients sampled were concurrently receiving high dose corticosteroids as a therapeutic intervention. Steroids are recognised to polarise monocytes towards an 'M2' phenotype [199, 205, 383] and it was thus impossible to disentangle the drug effect from innate changes in monocytes induced in AEs. It may be of relevance, however, that the immunophenotype of monocytes exposed to steroids remained distinct (indicated by the high CD163 expression) following macrophage differentiation in culture over 7 days. Given that the phenotypic characteristics of these 'M2' MDMs are associated with the promotion of ECM deposition in the literature, it is possible that steroid administration may potentiate rather than inhibit the fibrogenic activity of monocytes in AEIPF [196, 199, 205].

Animal studies provide evidence that interstitial macrophages are replenished predominantly by monocytes following injury, and elicit inflammatory and fibrogenic cytokine responses not mounted by alveolar macrophages [170, 190, 191, 193, 269, 405]. Thus, to characterise monocytes further and study their potential influence on fibrogenic processes, I positively selected monocytes and differentiated them into macrophages using autologous serum. Whilst ex vivo culture could not simulate in vivo differentiation, I reasoned that analysing the phenotype and function of MDMs remained relevant because IPF is a lung-specific rather than a systemic disease. Therefore, the influences exerted by monocytes are most likely to be greatest following extravasation and differentiation into macrophages. Furthermore, given that the majority of monocytes have a relatively short lifespan [164], studying viable cells after the majority have undergone apoptosis may identify the populations predestined to enter the lung and mature into macrophages.

When the phenotypic characteristics of day 7 MDMs were analysed, those derived from IPF patients were found to differ considerably from controls. Firstly, the expression of the monocyte marker CD14 remained high whilst the macrophage scavenger receptor CD68 was reduced in IPF MDMs. Whilst the morphological changes associated with monocyte to macrophage differentiation did not differ between the groups, these results could indicate that a proportion of the IPF monocytes (which showed lower CD64 expression)

## Chapter 8: Discussion and future direction

exhibited delayed differentiation. In keeping with this was the finding that phagocytic ability, which typically increases during macrophage differentiation, actually showed the opposite trend to controls with decreasing capacity as IPF monocytes differentiated into macrophages. During the process of differentiation and maturation, research has demonstrated that MDMs exhibit less inflammatory potential and gradually start to resemble tissue resident macrophages within the lung [170, 190, 193]. Thus, it could be postulated that retention of monocytic characteristics in IPF MDMs may promote tissue damage following lung homing. Contrary to this hypothesis, however, was the finding that inflammatory markers CD64 and CD86 were reduced on IPF MDMs suggesting that they were in fact less, not more, pro-inflammatory than control MDMs. Furthermore, on balance, the gene expression data showed that genes associated with the later stages of repair were more highly expressed than those associated with inflammation.

Thus, whilst the MDM data was more consistent with a pro-repair phenotype than the monocyte results, the collective findings continued to evade classification into macrophage subsets associated with a specific phase of repair. An example of the difficulty in interpreting the data was seen in the expression of the inflammatory transcription factor *STAT1* which was up-regulated by IPF MDMs and should theoretically inhibit *STAT3* and *STAT6* pathways. However clear trends towards increased expression of all three transcription factors were found. Whilst this may simply demonstrate the common discrepancy between scientific doctrine and practical observation, it may also indicate that even after 7 days in uniform culture conditions, MDMs represent a heterogeneous population. The *ex-vivo* culture did not attempt to replicate the differentiation process within the body but the divergent expression of cell surface receptors and the often clustered differences seen in expression of genes between IPF and controls, indicates that monocytes followed distinct differentiation pathways, which may have been at least partially predetermined. Gibbings *et al.* (2015), showed that interstitial macrophages derived from monocytes in the heart, gut and lung shared a similar transcriptional profile regardless of the tissue in which they resided [190]. The preserved transcriptome seen in the monocyte-derived macrophages indicates that whilst susceptible to their microenvironment, monocytes retain some 'hardwired' characteristics acquired during BM development. In health, monocytes are not primed to enter and replenish macrophage populations within the lung tissue and there is evidence that the transcriptional profile of monocytes varies relatively little following extravasation [400]. Thus, the differentiation of healthy control monocytes to

## Chapter 8: Discussion and future direction

MDMs in culture may be more reproducible than monocytes from IPF patients, which are subjected to a wide array of pathological stimuli. Furthermore, as the disease is characterised by spatial and temporal heterogeneity with areas of established fibrosis adjacent to new lung injury and normal tissue [13], monocytes entering the lung are likely to be uniquely shaped by the environmental signals within their immediate locality.

Given the difficulty in interpreting how the phenotype of IPF and control MDMs might influence disease processes, I reasoned that a more informative approach might be to characterise MDMs according to their ability to undertake specialised functions relevant to injury and repair. Reactive oxygen species are produced by monocytes and macrophages in the early stages of tissue injury and contribute to inflammatory responses required for the clearance of invading pathogens. Oxidative stress induced by sustained or exuberant ROS production can, however, worsen tissue damage and in IPF there is evidence that oxidative stress contributes to fibrotic processes [124]. I thus questioned whether IPF MDMs may potentiate disease processes by generating enhanced ROS responses following stimulation. In contrast to my hypothesis, IPF MDMs that were viable on day 7 were found to generate less rather than more ROS compared to controls. Furthermore, inflammasome activation using LPS and Nigericin demonstrated no differences in the production of IL-1 $\beta$  by MDMs. However, whilst these findings did not support my theory that IPF MDMs potentiate fibrogenesis through these mechanisms, the in vitro nature of the assay and isolated time point used to assess MDM responses limited conclusions that could be drawn. Indeed, given that IPF monocytes possessed a more inflammatory phenotype than controls, repeating this assay on freshly isolated monocytes (prior to the apoptosis of CD64+CD163- monocytes) may have yielded different results.

I next questioned whether phagocytic responses differed given that the effective removal of pathogens and cellular debris is essential for successful repair. I found that the ability of IPF MDMs to phagocytose *E coli* bioparticles was significantly reduced. Furthermore, IPF MDMs exhibited reduced efferocytosis of aged neutrophils, a function essential for maintaining homeostasis and enabling the restoration of healthy tissue by the removal of redundant inflammatory cells [237, 371, 375]. By extrapolating the function of day 7 ex-vivo MDMs to in vivo responses following injury, the characteristics of IPF MDMs suggest that they may play a defective role during the earlier stages of tissue repair. Decreased ROS generation, a reduced ability to clear microbes and debris, as well as preferential apoptosis of inflammatory monocyte subsets may set the path for

## Chapter 8: Discussion and future direction

a defective healing response. Furthermore, as efferocytosis modulates macrophage phenotype and directs its functionality towards repair and resolution [373, 406], defective capacity may inhibit this process, as well as result in the persistence of cellular material contributing to non-resolving lesions.

There are several possible explanations for the divergent differentiation patterns observed in IPF MDMs. Firstly, the expression of genes differed in freshly isolated ex-vivo monocytes and these inherent transcriptional differences may lead to translational changes (such as increased production of IL-10) that then influence subsequent differentiation patterns. Secondly, the preferential apoptosis of CD64<sup>+</sup>CD163<sup>-</sup> monocytes from IPF patients at 24 hours probably skewed the phenotype of the viable MDM population later analysed. Thirdly, the differential ability of monocytes and MDMs to undertake efferocytosis may have modulated their phenotypic characteristics. Lastly, and probably most significantly, was the influence exerted by the elevated concentrations of M-CSF in the serum of IPF patients. As monocytes were cultured in autologous serum, this cytokine is highly likely to have influenced their differentiation profiles. Indeed, there are several protocols that advocate the use of M-CSF to polarise in vitro monocytes to 'M2', and injecting M-CSF into monkeys elevated levels of circulating monocytes [407]. M-CSF, in addition to IL-10, was shown in one study to synergistically increase the expression of CD14 and CD64 on monocytes [208]. Interestingly, research has also linked M-CSF to enhanced FcγR-mediated phagocytosis, antigen presentation and ROS production [206, 408]. The increased levels of monocytes, high CD14 and CD64 expression and trend towards superior phagocytosis in IPF monocytes would thus be consistent with exposure to higher concentrations of M-CSF. The in vivo influence of this cytokine in modulating monocyte properties as they differentiate into macrophages is less clear but of relevance. In vitro work has shown that M-CSF 'primes' MDMs towards an 'M2' phenotype, which can be modulated depending on additional stimuli resulting in cells with mixed reparative/inflammatory signatures (section 1-3-4) [207, 209].

Elevated concentrations of M-CSF within the serum have been found in a number of different pathological processes including cancer, inflammation and infection. M-CSF influences the survival, differentiation and functional characteristics of monocytes and tissue resident macrophages [207]. The finding that this growth factor was increased in IPF patients is therefore likely to hold pathological and clinical significance beyond the phenotypic/functional changes identified in IPF monocytes/MDMs in this project.



## Chapter 8: Discussion and future direction

Inhibiting the receptor for M-CSF has been trialled in numerous disease models, with varying success [409]. Blocking CSF-1R in mice, however, significantly reduced the extent of pulmonary fibrosis following bleomycin instillation [309] suggesting that interrupting M-CSF signalling may be a potential therapeutic target in human lung fibrosis.

Whether the phenotypic differences observed in IPF monocytes and MDMs translate to a disease-enhancing, disease-inhibiting or neutral role was not established in this project. It is clear however that MDMs as a collective group exert a strong influence on fibroblastic activity. They substantially increased proliferation and up-regulated genes associated with an invasive phenotype. Differences, however, were not seen between controls and IPF MDMs which may indicate that the hypothesis that IPF monocytes are more fibrogenic than controls is incorrect. It may also be the result of an experimental set-up that was too simplistic to detect subtle differences between controls and IPF MDMs. Alternatively, it is plausible that the phenotypic differences observed in monocytes and MDMs only translate to differences in fibrogenic endpoints when these cells are exposed to additional factors within the IPF lung. Indeed, monocytes that are directly pro-fibrogenic would cause exuberant scar formation following injury and widespread fibrosis in multiple organs. Thus, given that IPF is a lung-specific disease, the abnormal interstitium itself or factors released within the tissue may trigger the evolution of a pro-fibrogenic phenotype in monocytes that facilitates fibroblast activity locally. Exploring the interaction of monocytes and fibroblasts on a fibrotic interstitium in a way that recapitulates the disease processes in IPF is technically challenging and the lack of a representative animal model for the disease hampers investigation in this area further.

The results presented in this project show clear differences between IPF and controls but raise more questions than can be answered completely by our current understanding of monocyte biology. Whilst it is important not to over-interpret individual results, particularly given that *ex vivo* differentiation is far removed from processes that occur in the body, collectively there is sufficient evidence to support the hypothesis that IPF monocytes are likely to impact on fibrogenic processes differently to healthy controls. Whether this is pathogenic or otherwise has not been established and requires further work.

## 8.2 Future work

To fully elucidate how phenotypically distinct monocyte populations impact on fibrogenic processes, an *in vivo* model is necessary. As discussed previously, however, this is problematic as the bleomycin mouse model most commonly used to study lung fibrosis induces pathological manifestations that are distinct from those occurring in IPF. Work that builds on the pilot study undertaken by Collard *et al.* (2016) involving the labelling and tracking of monocytes in healthy volunteers and IPF patients (as well as those with other lung diseases), would determine the extent to which monocytes home to the lung but would not provide information as to their role within the tissue. More feasible, and currently being undertaken by members of our group, is to ascertain the presence of monocytes and monocyte-derived cells within IPF and healthy lung biopsy samples. Identification of CD14 positive cells and their proximity to areas of active fibrosis would strengthen the hypothesis that monocytes are involved in IPF fibrogenesis. Micro-dissecting these cells and undertaking techniques such as Nanostring to analyse their gene expression profiles would enable comparison with their peripheral blood counterparts and help determine how the transcriptome differs in health and disease. Single-cell RNA sequencing on circulating monocytes could also provide detailed information on how IPF monocytes differ from controls and overcome issues associated with monocyte heterogeneity when analysed as a collective group.


This study has demonstrated a link between monocyte levels and extent of fibrotic burden in IPF. Patients with acute exacerbations of disease were found to have the highest levels of circulating monocytes and it is possible that elevated monocyte levels contribute to acceleration of disease and thus predict those at high risk of disease worsening. Further work looking at monocyte levels in individuals over the time course of their disease would confirm whether levels may be used as a predictor of exacerbation risk or a more aggressive disease course. Given the high mortality associated with AEIPF, further work to unravel the mechanisms that lead to these events is urgently needed. Studying the immunophenotypic characteristics of monocytes and other circulating immune cells at the start of exacerbations, prior to the administration of steroids, may identify changes in cellular characteristics that could be of pathological significance. If changes in monocyte or other peripheral immune cell phenotype were linked to exacerbation or progression, the development of agents that inhibit or modulate the activity of these cells may be a potential therapeutic strategy. Equally, determining

## Chapter 8: Discussion and future direction

how corticosteroids modulate monocyte functionality and influence the trajectory of the disease clinically would advance our understanding of the pathophysiology of AEs and potentially alter our management approach. The finding that CD64 was significantly elevated on IPF monocytes is also of interest and possibly merits further investigation, particularly given that expression was most intense on treatment-naïve patients. It was not ascertained whether CD64 expression correlated with favourable responses to treatment but given the adverse side-effect profile associated with anti-fibrotic therapy, a biological marker that predicted a positive therapeutic response and identified those who were likely to benefit from ongoing treatment would be highly beneficial.

It would be of scientific interest and of potential clinical relevance to determine whether the phenotypic characteristics of IPF monocytes and MDMs are observed in other types of fibrotic disease. It is probable that the physical environment or mediators released during fibrogenesis itself modulate the monocyte phenotype. It is also possible, however, that polymorphisms in monocyte genes or epigenetic changes occurring at the precursor cell level predispose individuals to fibrosis. Depending on the subsequent environmental trigger and the organ affected, patients may go on to develop fibrosis in the corresponding locality. Thus, a study to determine whether monocytes from patients with other forms of fibrotic disease share a similar monocyte profile to IPF would provide evidence of a 'fibrotic signature' and strengthen the assertion that these cells are important in the process of fibrogenesis.

# Appendix

Oxford University Hospitals 

HH/RA/JC/10748

Dr Lin-Pei Ho  
HEFCE Senior Lecturer & Consultant in  
Respiratory Medicine  
Weatherall Institute of Molecular Medicine  
John Radcliffe Hospital  
Headington  
Oxford OX3 9DS

26<sup>th</sup> January 2015

Dear Dr Ho

NHS Trust  
From the R & D Lead  
OUH Research & Development  
Joint Research Office  
Block 60, Churchill Hospital  
Old Road, Headington  
Oxford OX3 7LE

Tel: (01865) (5)72386  
Fax: (01865) (5)72242  
James.Church@ouh.nhs.uk

**Re: The role of immune cells in control of disease progression in lung fibrosis**

**NIHR CSP Reference: 121881  
Research and Development Reference: 10748  
Research Ethics Committee Reference: 14/SC/1060**

#### **Confirmation of Trust Management Approval**

On behalf of the Oxford University Hospitals NHS Trust, I am pleased to confirm Trust Management Approval and Indemnity for the above research on the basis described in the application, protocol and other supporting documents.

#### **Conditions of Approval**

Your attention is drawn to the attached conditions of approval. Breach of these conditions may result in Trust Management Approval being revoked.

#### **Recruitment**

**The agreed total recruitment target for your study at the OUH site is 350 participants by 30.06.2019 as specified in the contract.**

**Your first participant recruitment target date is 02.04.2015**

To support OUH Trust and national recruitment targets, R&D will monitor and publish recruitment for your study: 1. Performance against the 70 calendar day period benchmark from the time of receipt of a valid research application in R&D to the date of recruitment of first participant to your study; and for interventional trials; 2. Recruiting planned participants to time and target. The R&D office will contact you to request recruitment progress against both targets. If you recruit your first participant into the study then please send the date to [researchrecruitment@ouh.nhs.uk](mailto:researchrecruitment@ouh.nhs.uk). If you miss this target you will be required to give reasons that can be reported to the DOH/NIHR.

## References

1. Meltzer, E.B. and P.W. Noble, *Idiopathic pulmonary fibrosis*. Orphanet Journal of Rare Diseases, 2008. **3** 8.
2. Ley, B. and H.R. Collard, *Epidemiology of idiopathic pulmonary fibrosis*. Clin Epidemiol, 2013. **5** 483-492.
3. Collard, H.R., S.-Y. Chen, W.-S. Yeh, Q. Li, Y.-C. Lee, A. Wang, *et al.*, *Health Care Utilization and Costs of Idiopathic Pulmonary Fibrosis in U.S. Medicare Beneficiaries Aged 65 Years and Older*. Ann Am Thorac Soc, 2015. **12** 981-987.
4. Coghlan, M.A., A. Shifren, H.J. Huang, T.D. Russell, R.D. Mitra, Q. Zhang, *et al.*, *Sequencing of idiopathic pulmonary fibrosis-related genes reveals independent single gene associations*. BMJ Open Respir Res, 2014. **1** e000057.
5. Raghu, G., B. Rochwerg, Y. Zhang, C.A.C. Garcia, A. Azuma, J. Behr, *et al.*, *An Official ATS/ERS/JRS/ALAT Clinical Practice Guideline: Treatment of Idiopathic Pulmonary Fibrosis. An Update of the 2011 Clinical Practice Guideline*. Am J Respir Crit Care Med, 2015. **192** e3-e19.
6. NICE, *Idiopathic pulmonary fibrosis - nintedanib [ID752]: appraisal consultation*. <https://www.nice.org.uk/guidance/indevelopment/gid-tag491/documents>, 2015.
7. NICE, *The diagnosis and management of suspected idiopathic pulmonary fibrosis*. <http://www.nice.org.uk/guidance/cg163>, 2013.
8. Kim, D.S., *Acute Exacerbations in Patients with Idiopathic Pulmonary Fibrosis*. Respiratory Research, 2013. **14**.
9. King, K., J. Tooze, M. Schwartz, K. Brown, and R. Cherniack, *Predicting Survival in Idiopathic Pulmonary Fibrosis*. American Journal of Respiratory and Critical Care Medicine, 2001. **164** 1171-1181.
10. Saini, G., J. Porte, P.H. Weinreb, S.M. Violette, W.A. Wallace, T.M. McKeever, *et al.*,  *$\alpha\beta6$  integrin may be a potential prognostic biomarker in interstitial lung disease*. Eur Respir J, 2015. **46** 486.
11. Cottin, V., *The impact of emphysema in pulmonary fibrosis*. Eur Respir Rev, 2013. **22** 153-157.
12. Bradley, B., H.M. Branley, J.J. Egan, M.S. Greaves, D.M. Hansell, N.K. Harrison, *et al.*, *Interstitial lung disease guideline: the British Thoracic Society in collaboration with the Thoracic Society of Australia and New Zealand and the Irish Thoracic Society*. Thorax, 2008. **63 Suppl 5** v1-58.
13. Raghu, G., H.R. Collard, J.J. Egan, F.J. Martinez, J. Behr, K.K. Brown, *et al.*, *An official ATS/ERS/JRS/ALAT statement: idiopathic pulmonary fibrosis: evidence-based guidelines for diagnosis and management*. Am J Respir Crit Care Med, 2011. **183** 788-824.
14. Collard H, M.B., Flaherty K, *et al.*, *Acute Exacerbations of Idiopathic Pulmonary Fibrosis*. Am J Respir Crit Care Med, 2007. **176** 636–643.
15. Johannson, K. and H.R. Collard, *Acute Exacerbation of Idiopathic Pulmonary Fibrosis: A Proposal*. Current respiratory care reports, 2013. **2** 10.1007/s13665-13013-10065-x.

16. Collard, H.R., E. Yow, L. Richeldi, K.J. Anstrom, and C. Glazer, *Suspected acute exacerbation of idiopathic pulmonary fibrosis as an outcome measure in clinical trials*. *Respiratory Research*, 2013. **14** 73-73.
17. Kaarteenaho, R. and V.L. Kinnula, *Diffuse Alveolar Damage: A Common Phenomenon in Progressive Interstitial Lung Disorders*. *Pulmonary Medicine*, 2011. **2011** 10.
18. Richeldi, L., R.M. du Bois, G. Raghu, A. Azuma, K.K. Brown, U. Costabel, *et al.*, *Efficacy and safety of nintedanib in idiopathic pulmonary fibrosis*. *N Engl J Med*, 2014. **370** 2071-2082.
19. Cottin, V. and T. Maher, *Long-term clinical and real-world experience with pirfenidone in the treatment of idiopathic pulmonary fibrosis*. *European Respiratory Review*, 2015. **24** 58.
20. King, T.E., Jr., W.Z. Bradford, S. Castro-Bernardini, E.A. Fagan, I. Glaspole, M.K. Glassberg, *et al.*, *A phase 3 trial of pirfenidone in patients with idiopathic pulmonary fibrosis*. *N Engl J Med*, 2014. **370** 2083-2092.
21. NICE, *Pirfenidone for treating idiopathic pulmonary fibrosis*. <http://www.nice.org.uk/guidance/ta282>, 2013.
22. Macias-Barragan, J., A. Sandoval-Rodriguez, J. Navarro-Partida, and J. Armendariz-Borunda, *The multifaceted role of pirfenidone and its novel targets*. *Fibrogenesis Tissue Repair*, 2010. **3** 16.
23. Wollin, L., I. Maillet, V. Quesniaux, A. Holweg, and B. Ryffel, *Antifibrotic and anti-inflammatory activity of the tyrosine kinase inhibitor nintedanib in experimental models of lung fibrosis*. *J Pharmacol Exp Ther*, 2014. **349** 209-220.
24. Juarez, M.M., A.L. Chan, A.G. Norris, B.M. Morrissey, and T.E. Albertson, *Acute exacerbation of idiopathic pulmonary fibrosis—a review of current and novel pharmacotherapies*. *Journal of Thoracic Disease*, 2015. **7** 499-519.
25. Gibbons, M.A., A.C. MacKinnon, P. Ramachandran, K. Dhaliwal, R. Duffin, A.T. Phythian-Adams, *et al.*, *Ly6Chi monocytes direct alternatively activated profibrotic macrophage regulation of lung fibrosis*. *Am J Respir Crit Care Med*, 2011. **184** 569-581.
26. Borzone, G., R. Moreno, R. Urrea, M. Meneses, M. OyarzÚN, and C. Lisboa, *Bleomycin-Induced Chronic Lung Damage Does Not Resemble Human Idiopathic Pulmonary Fibrosis*. *American Journal of Respiratory and Critical Care Medicine*, 2001. **163** 1648-1653.
27. Martinez, F.J., S. Safrin, D. Weycker, K.M. Starko, W.Z. Bradford, T.E. King, *et al.*, *The clinical course of patients with idiopathic pulmonary fibrosis*. *Ann Intern Med*, 2005. **142**.
28. Adamson, I.Y., L. Young, and D.H. Bowden, *Relationship of alveolar epithelial injury and repair to the induction of pulmonary fibrosis*. *Am J Pathol*, 1988. **130** 377-383.
29. Schmidt, S.L., N. Tayob, M.K. Han, C. Zappala, D. Kervitsky, S. Murray, *et al.*, *Predicting pulmonary fibrosis disease course from past trends in pulmonary function*. *Chest*, 2014. **145** 579-585.
30. Baumgartner, K.B., J.M. Samet, D.B. Coultas, C.A. Stidley, W.C. Hunt, T.V. Colby, *et al.*, *Occupational and environmental risk factors for idiopathic pulmonary fibrosis: a multicenter case-control study*. *Collaborating Centers*. *Am J Epidemiol*, 2000. **152**.

31. Kolb, M. and H.R. Collard, *Staging of idiopathic pulmonary fibrosis: past, present and future*. Eur Respir Rev, 2014. **23** 220-224.
32. Fingerlin, T.E., E. Murphy, W. Zhang, A.L. Peljto, K.K. Brown, M.P. Steele, *et al.*, *Genome-wide association study identifies multiple susceptibility loci for pulmonary fibrosis*. Nature genetics, 2013. **45** 613-620.
33. Alder, J.K., J.J.L. Chen, L. Lancaster, S. Danoff, S.-c. Su, J.D. Cogan, *et al.*, *Short telomeres are a risk factor for idiopathic pulmonary fibrosis*. Proceedings of the National Academy of Sciences of the United States of America, 2008. **105** 13051-13056.
34. Armanios, M.Y., J.J. Chen, J.D. Cogan, J.K. Alder, R.G. Ingersoll, C. Markin, *et al.*, *Telomerase mutations in families with idiopathic pulmonary fibrosis*. N Engl J Med, 2007. **356**.
35. Renzoni, E., V. Srihari, and P. Sestini, *Pathogenesis of idiopathic pulmonary fibrosis: review of recent findings*. F1000Prime Reports, 2014. **6** 69.
36. Tsakiri, K.D., J.T. Cronkhite, P.J. Kuan, C. Xing, G. Raghu, J.C. Weissler, *et al.*, *Adult-onset pulmonary fibrosis caused by mutations in telomerase*. Proceedings of the National Academy of Sciences, 2007. **104** 7552-7557.
37. Dall'Aglio, P.P., A. Pesci, G. Bertorelli, E. Brianti, and S. Scarpa, *Study of Immune Complexes in Bronchoalveolar Lavage Fluids*. Respiration, 1988. **54(suppl 1)** 36-41.
38. listed], N.a., *Bronchoalveolar lavage constituents in healthy individuals, idiopathic pulmonary fibrosis, and selected comparison groups. The BAL Cooperative Group Steering Committee*. American Review of Respiratory Disease, 1990. **141** S169-S170.
39. Pechkovsky, D.V., A. Prasse, F. Kollert, K.M. Engel, J. Dentler, W. Luttmann, *et al.*, *Alternatively activated alveolar macrophages in pulmonary fibrosis-mediator production and intracellular signal transduction*. Clin Immunol, 2010. **137** 89-101.
40. Prasse, A., V. Pechkovsky Dmitri, B. Toews Galen, M. Schäfer, S. Eggeling, C. Ludwig, *et al.*, *CCL18 as an indicator of pulmonary fibrotic activity in idiopathic interstitial pneumonias and systemic sclerosis*. Arthritis & Rheumatism, 2007. **56** 1685-1693.
41. Prasse, A., D.V. Pechkovsky, G.B. Toews, W. Jungraithmayr, F. Kollert, T. Goldmann, *et al.*, *A vicious circle of alveolar macrophages and fibroblasts perpetuates pulmonary fibrosis via CCL18*. Am J Respir Crit Care Med, 2006. **173** 781-792.
42. Fernandez, I.E., F.R. Greffo, M. Frankenberger, J. Bandres, K. Heinzelmann, C. Neurohr, *et al.*, *Peripheral blood myeloid-derived suppressor cells reflect disease status in idiopathic pulmonary fibrosis*. European Respiratory Journal, 2016. **48** 1171.
43. Guiot, J., C. Moermans, M. Henket, J.-L. Corhay, and R. Louis, *Blood Biomarkers in Idiopathic Pulmonary Fibrosis*. Lung, 2017. **195** 273-280.
44. Parker, M.W., D. Rossi, M. Peterson, K. Smith, K. Sikstrom, E.S. White, *et al.*, *Fibrotic extracellular matrix activates a profibrotic positive feedback loop*. J Clin Invest, 2014. **124** 1622-1635.
45. Flaherty, K.R., W.D. Travis, T.V. Colby, G.B. Toews, E.A. Kazerooni, B.H. Gross, *et al.*, *Histopathologic variability in usual and nonspecific interstitial pneumonias*. Am J Respir Crit Care Med, 2001. **164**.

46. Bjraker, J.A., J.H. Ryu, M.K. Edwin, J.L. Myers, H.D. Tazelaar, D.R. Schroeder, *et al.*, *Prognostic significance of histopathologic subsets in idiopathic pulmonary fibrosis*. *Am J Respir Crit Care Med*, 1998. **157**.
47. Specks, U., A. Nerlich, T.V. Colby, I. Wiest, and R. Timpl, *Increased expression of type VI collagen in lung fibrosis*. *American Journal of Respiratory and Critical Care Medicine*, 1995. **151** 1956-1964.
48. Raghu, G., K.K. Brown, W.Z. Bradford, K. Starko, P.W. Noble, D.A. Schwartz, *et al.*, *A placebo-controlled trial of interferon gamma-1b in patients with idiopathic pulmonary fibrosis*. *N Engl J Med*, 2004. **350**.
49. Jackson, R.M. and C.D. Fell, *Etanercept for Idiopathic Pulmonary Fibrosis*. *American Journal of Respiratory and Critical Care Medicine*, 2008. **178** 889-891.
50. Selman, M., T.E. King, and A. Pardo, *Idiopathic pulmonary fibrosis: prevailing and evolving hypotheses about its pathogenesis and implications for therapy*. *Ann Intern Med*, 2001. **134**.
51. Selman, M. and A. Pardo, *Role of epithelial cells in idiopathic pulmonary fibrosis: from innocent targets to serial killers*. *Proc Am Thorac Soc*, 2006. **3** 364-372.
52. Selman, M. and A. Pardo, *Revealing the Pathogenic and Aging-related Mechanisms of the Enigmatic Idiopathic Pulmonary Fibrosis. An Integral Model*. *Am J Respir Crit Care Med*, 2014. **189** 1161-1172.
53. Carter, B.W., *Hermansky-Pudlak syndrome complicated by pulmonary fibrosis*. *Proceedings (Baylor University. Medical Center)*, 2012. **25** 76-77.
54. Mason, R.J., *Biology of alveolar type II cells*. *Respirology*, 2006. **11** S12-S15.
55. Maitra, M., Y. Wang, R.D. Gerard, C.R. Mendelson, and C.K. Garcia, *Surfactant Protein A2 Mutations Associated with Pulmonary Fibrosis Lead to Protein Instability and Endoplasmic Reticulum Stress*. *Journal of Biological Chemistry*, 2010. **285** 22103-22113.
56. Tanjore, H., T.S. Blackwell, and W.E. Lawson, *Emerging evidence for endoplasmic reticulum stress in the pathogenesis of idiopathic pulmonary fibrosis*. *American Journal of Physiology - Lung Cellular and Molecular Physiology*, 2012. **302** L721-L729.
57. Pardo, A., S. Cabrera, M. Maldonado, and M. Selman, *Role of matrix metalloproteinases in the pathogenesis of idiopathic pulmonary fibrosis*. *Respiratory Research*, 2016. **17** 23.
58. Batista, L.F.Z., M.F. Pech, F.L. Zhong, H.N. Nguyen, K.T. Xie, A.J. Zaugg, *et al.*, *Telomere shortening and loss of self-renewal in dyskeratosis congenita induced pluripotent stem cells*. *Nature*, 2011. **474** 399-402.
59. Aubert, G. and P.M. Lansdorp, *Telomeres and Aging*. *Physiological Reviews*, 2008. **88** 557-579.
60. Liu, T., Y. Nozaki, and S.H. Phan, *Regulation of Telomerase Activity in Rat Lung Fibroblasts*. *American Journal of Respiratory Cell and Molecular Biology*, 2002. **26** 534-540.
61. Waisberg, D.R., E.R. Parra, J.V. Barbas-Filho, S. Fernezlian, and V.L. Capelozzi, *Increased fibroblast telomerase expression precedes myofibroblast  $\alpha$ -smooth muscle actin expression in idiopathic pulmonary fibrosis*. *Clinics*, 2012. **67** 1039-1046.
62. Lawson, W.E., D.-S. Cheng, A.L. Degryse, H. Tanjore, V.V. Polosukhin, X.C. Xu, *et al.*, *Endoplasmic reticulum stress enhances fibrotic remodeling in the lungs*.



- Proceedings of the National Academy of Sciences of the United States of America, 2011. **108** 10562-10567.
63. Molyneaux, P.L., M.J. Cox, S.A. Willis-Owen, P. Mallia, K.E. Russell, A.M. Russell, *et al.*, *The role of bacteria in the pathogenesis and progression of idiopathic pulmonary fibrosis*. *Am J Respir Crit Care Med*, 2014. **190** 906-913.
  64. Molyneaux, P.L. and T.M. Maher, *The role of infection in the pathogenesis of idiopathic pulmonary fibrosis*. *Eur Respir Rev*, 2013. **22** 376-381.
  65. Cabrera-Benitez, N.E., J.G. Laffey, M. Parotto, P.M. Spieth, J. Villar, H. Zhang, *et al.*, *Mechanical Ventilation-associated Lung Fibrosis in Acute Respiratory Distress Syndrome A Significant Contributor to Poor Outcome*. *Anesthesiology*, 2014. **121** 189-198.
  66. Savarino, E., R. Carbone, E. Marabotto, M. Furnari, L. Sconfienza, M. Ghio, *et al.*, *Gastro-oesophageal reflux and gastric aspiration in idiopathic pulmonary fibrosis patients*. *Eur Respir J*, 2013. **42** 1322-1331.
  67. Lee, J.S., J.W. Song, P.J. Wolters, B.M. Elicker, T.E. King, D.S. Kim, *et al.*, *Bronchoalveolar lavage pepsin in acute exacerbation of idiopathic pulmonary fibrosis*. *Eur Respir J*, 2012. **39** 352.
  68. Lee, J.S., H.R. Collard, K.J. Anstrom, F.J. Martinez, I. Noth, R.S. Roberts, *et al.*, *Anti-acid treatment and disease progression in idiopathic pulmonary fibrosis: an analysis of data from three randomised controlled trials*. *Lancet Respir med*, 2013. **1** 369-376.
  69. Irving, W.L., S. Day, and I.D. Johnston, *Idiopathic pulmonary fibrosis and hepatitis C virus infection*. *Am Rev Respir Dis*, 1993. **148**.
  70. Egan, J.J., J.P. Stewart, P.S. Hasleton, J.R. Arrand, K.B. Carroll, and A.A. Woodcock, *Epstein-Barr virus replication within pulmonary epithelial cells in cryptogenic fibrosing alveolitis*. *Thorax*, 1995. **50**.
  71. Kuwano, K., Y. Nomoto, R. Kunitake, N. Hagimoto, T. Matsuba, Y. Nakanishi, *et al.*, *Detection of adenovirus E1A DNA in pulmonary fibrosis using nested polymerase chain reaction*. *Eur Respir J*, 1997. **10**.
  72. Sime, P.J., Z. Xing, F.L. Graham, K.G. Csaky, and J. Gauldie, *Adenovector-mediated gene transfer of active transforming growth factor-beta1 induces prolonged severe fibrosis in rat lung*. *The Journal of Clinical Investigation*, 1997. **100** 768-776.
  73. Lok, S.S., Y. Haider, D. Howell, J.P. Stewart, P.S. Hasleton, and J.J. Egan, *Murine gammaherpes virus as a cofactor in the development of pulmonary fibrosis in bleomycin resistant mice*. *European Respiratory Journal*, 2002. **20** 1228-1232.
  74. Tang, Y.W., J.E. Johnson, P.J. Browning, R.A. Cruz-Gervis, A. Davis, B.S. Graham, *et al.*, *Herpesvirus DNA Is Consistently Detected in Lungs of Patients with Idiopathic Pulmonary Fibrosis*. *Journal of Clinical Microbiology*, 2003. **41** 2633-2640.
  75. Mora, A.L., C.R. Woods, A. Garcia, J. Xu, M. Rojas, S.H. Speck, *et al.*, *Lung infection with gamma-herpesvirus induces progressive pulmonary fibrosis in Th2-biased mice*. *Am J Physiol Lung Cell Mol Physiol*, 2005. **289**.
  76. Isler, J.A., A.H. Skalet, and J.C. Alwine, *Human cytomegalovirus infection activates and regulates the unfolded protein response*. *J virol*, 2005. **79** 6890-6899.

77. Lawson, W.E., P.F. Crossno, V.V. Polosukhin, J. Roldan, D.-S. Cheng, K.B. Lane, *et al.*, *Endoplasmic reticulum stress in alveolar epithelial cells is prominent in IPF: association with altered surfactant protein processing and herpesvirus infection*. *Am J Physiol Lung Cell Mol Physiol*, 2008. **294** L1119-L1126.
78. Wilson, M.S. and T.A. Wynn, *Pulmonary fibrosis: pathogenesis, etiology and regulation*. *Mucosal immunology*, 2009. **2** 103-121.
79. Wynn, T.A., *Integrating mechanisms of pulmonary fibrosis*. *J Exp Med*, 2011. **208** 1339-1350.
80. Wynn, T.A. and T.R. Ramalingam, *Mechanisms of fibrosis: therapeutic translation for fibrotic disease*. *Nat Med*, 2012. **18** 1028-1040.
81. Tatler, A.L. and G. Jenkins, *TGF- $\beta$  Activation and Lung Fibrosis*. *Proceedings of the American Thoracic Society*, 2012. **9** 130-136.
82. Derynck, R. and Y.E. Zhang, *Smad-dependent and Smad-independent pathways in TGF- $\beta$  family signalling*. *Nature*, 2003. **425** 577.
83. Schneider, A., U. Panzer, G. Zahner, U. Wenzel, G. Wolf, F. Thaiss, *et al.*, *Monocyte chemoattractant protein-1 mediates collagen deposition in experimental glomerulonephritis by transforming growth factor- $\beta$* . *Kidney International*, 1999. **56** 135-144.
84. Lafyatis, R., *Transforming growth factor  $\beta$ —at the centre of systemic sclerosis*. *Nature Reviews Rheumatology*, 2014. **10** 706.
85. Dooley, S. and P. ten Dijke, *TGF- $\beta$  in progression of liver disease*. *Cell and Tissue Research*, 2012. **347** 245-256.
86. Coker, R.K., G.J. Laurent, P.K. Jeffery, R.M. du Bois, C.M. Black, and R.J. McAnulty, *Localisation of transforming growth factor  $\beta$  and  $\beta$  mRNA transcripts in normal and fibrotic human lung*. *Thorax*, 2001. **56** 549.
87. Kisseleva, T., H. Uchinami, N. Feirt, O. Quintana-Bustamante, J.C. Segovia, R.F. Schwabe, *et al.*, *Bone marrow-derived fibrocytes participate in pathogenesis of liver fibrosis*. *Journal of Hepatology*, 2006. **45** 429-438.
88. Mehrad, B., M.D. Burdick, D.A. Zisman, M.P. Keane, J.A. Belperio, and R.M. Strieter, *Circulating peripheral blood fibrocytes in human fibrotic interstitial lung disease*. *Biochemical and Biophysical Research Communications*, 2007. **353** 104-108.
89. Phillips, R.J., M.D. Burdick, K. Hong, M.A. Lutz, L.A. Murray, Y.Y. Xue, *et al.*, *Circulating fibrocytes traffic to the lungs in response to CXCL12 and mediate fibrosis*. *J Clin Invest*, 2004. **114**.
90. Quan, T.E., S. Cowper, S.P. Wu, L.K. Bockenstedt, and R. Bucala, *Circulating fibrocytes: collagen-secreting cells of the peripheral blood*. *Int J Biochem Cell Biol*, 2004. **36**.
91. Zhang, Y.E., *Non-Smad pathways in TGF- $\beta$  signaling*. *Cell Res*, 2008. **19** 128.
92. Lamouille, S., J. Xu, and R. Derynck, *Molecular mechanisms of epithelial–mesenchymal transition*. *Nature reviews. Molecular cell biology*, 2014. **15** 178-196.
93. Nair, G.B., A. Matela, D. Kurbanov, and G. Raghu, *Newer developments in idiopathic pulmonary fibrosis in the era of anti-fibrotic medications*. *Expert Rev Respir Med*, 2016. **10** 699-711.
94. Varga, J. and B. Pasche, *Anti-TGF- $\beta$  Therapy in Fibrosis: Recent Progress and Implications for Systemic Sclerosis*. *Curr opin rheum*, 2008. **20** 720-728.

95. Wells, A.U., *The revised ATS/ERS/JRS/ALAT diagnostic criteria for idiopathic pulmonary fibrosis (IPF)--practical implications*. *Respir Res*, 2013. **14 Suppl 1** S2.
96. Bringardner, B.D., C.P. Baran, T.D. Eubank, and C.B. Marsh, *The Role of Inflammation in the Pathogenesis of Idiopathic Pulmonary Fibrosis*. *Antioxidants & redox signaling*, 2008. **10** 287-301.
97. Loveman, E., V.R. Copley, J. Colquitt, D.A. Scott, A. Clegg, J. Jones, *et al.*, *The clinical effectiveness and cost-effectiveness of treatments for idiopathic pulmonary fibrosis: a systematic review and economic evaluation*. *Health Technol Assess*, 2015. **19** i-xxiv, 1-336.
98. Zhang, Y., T.C. Lee, B. Guillemin, M.C. Yu, and W.N. Rom, *Enhanced IL-1 beta and tumor necrosis factor-alpha release and messenger RNA expression in macrophages from idiopathic pulmonary fibrosis or after asbestos exposure*. *The Journal of Immunology*, 1993. **150** 4188.
99. Rincon, M. and C.G. Irvin, *Role of IL-6 in Asthma and Other Inflammatory Pulmonary Diseases*. *International Journal of Biological Sciences*, 2012. **8** 1281-1290.
100. Le, T.-T.T., H. Karmouty-Quintana, E. Melicoff, T.-T.T. Le, T. Weng, N.-Y. Chen, *et al.*, *Blockade of IL-6 Signaling Attenuates Pulmonary Fibrosis*. *The Journal of Immunology*, 2014. **193** 3755.
101. Kinder, B.W., K.K. Brown, M.I. Schwarz, J.H. Ix, A. Kervitsky, and T.E. King, *Baseline BAL Neutrophilia Predicts Early Mortality in Idiopathic Pulmonary Fibrosis*. *Chest*, 2008. **133** 226-232.
102. Sumikawa, H., T. Johkoh, T.V. Colby, K. Ichikado, M. Suga, H. Taniguchi, *et al.*, *Computed Tomography Findings in Pathological Usual Interstitial Pneumonia*. *American Journal of Respiratory and Critical Care Medicine*, 2008. **177** 433-439.
103. Sumikawa, H., T. Johkoh, K. Fujimoto, H. Arakawa, T.V. Colby, J. Fukuoka, *et al.*, *Pathologically Proved Nonspecific Interstitial Pneumonia: CT Pattern Analysis as Compared with Usual Interstitial Pneumonia CT Pattern*. *Radiology*, 2014. **272** 549-556.
104. Piguet, P.F., C. Ribaux, V. Karpuz, G.E. Grau, and Y. Kapanci, *Expression and localization of tumor necrosis factor-alpha and its mRNA in idiopathic pulmonary fibrosis*. *The American Journal of Pathology*, 1993. **143** 651-655.
105. Miyazaki, Y., K. Araki, C. Vesin, I. Garcia, Y. Kapanci, J.A. Whitsett, *et al.*, *Expression of a tumor necrosis factor-alpha transgene in murine lung causes lymphocytic and fibrosing alveolitis. A mouse model of progressive pulmonary fibrosis*. *The Journal of Clinical Investigation*, 1995. **96** 250-259.
106. Piguet, P.F., G.E. Grau, and P. Vassalli, *Subcutaneous perfusion of tumor necrosis factor induces local proliferation of fibroblasts, capillaries, and epidermal cells, or massive tissue necrosis*. *The American Journal of Pathology*, 1990. **136** 103-110.
107. Liu, R.-M., *Oxidative Stress, Plasminogen Activator Inhibitor 1, and Lung Fibrosis*. *Antioxidants & redox signaling*, 2008. **10** 303-319.
108. Kotani, I., A. Sato, H. Hayakawa, T. Urano, Y. Takada, and A. Takada, *Increased procoagulant and antifibrinolytic activities in the lungs with idiopathic pulmonary fibrosis*. *Thrombosis Research*, 1995. **77** 493-504.

109. Kolb, M., P.J. Margetts, D.C. Anthony, F. Pitossi, and J. Gauldie, *Transient expression of IL-1 $\beta$  induces acute lung injury and chronic repair leading to pulmonary fibrosis*. *The Journal of Clinical Investigation*, 2001. **107** 1529-1536.
110. Eder, C., *Mechanisms of interleukin-1 $\beta$  release*. *Immunobiology*, 2009. **214** 543-553.
111. Abderrazak, A., T. Syrovets, D. Couchie, K. El Hadri, B. Friguet, T. Simmet, et al., *NLRP3 inflammasome: From a danger signal sensor to a regulatory node of oxidative stress and inflammatory diseases*. *Redox Biology*, 2015. **4** 296-307.
112. Bergsbaken, T., S.L. Fink, and B.T. Cookson, *Pyroptosis: host cell death and inflammation*. *Nature Reviews Microbiology*, 2009. **7** 99.
113. Wilson, M.S., S.K. Madala, T.R. Ramalingam, B.R. Gochoico, I.O. Rosas, A.W. Cheever, et al., *Bleomycin and IL-1 $\beta$ -mediated pulmonary fibrosis is IL-17A dependent*. *The Journal of Experimental Medicine*, 2010. **207** 535-552.
114. Heinrich, P.C., J.V. Castell, and T. Andus, *Interleukin-6 and the acute phase response*. *Biochem J*, 1990. **265** 621-636.
115. Barnes, T., M. Anderson, and R. Moots, *The Many Faces of Interleukin-6: The Role of IL-6 in Inflammation, Vasculopathy, and Fibrosis in Systemic Sclerosis*. *International Journal of Rheumatology*, 2011. **2011**.
116. Hunter, C.A. and S.A. Jones, *IL-6 as a keystone cytokine in health and disease*. *Nat Immunol*, 2015. **16** 448-457.
117. Sundararaj, K.P., D.J. Samuvel, Y. Li, J.J. Sanders, M.F. Lopes-Virella, and Y. Huang, *Interleukin-6 Released from Fibroblasts Is Essential for Up-regulation of Matrix Metalloproteinase-1 Expression by U937 Macrophages in Coculture: CROSS-TALKING BETWEEN FIBROBLASTS AND U937 MACROPHAGES EXPOSED TO HIGH GLUCOSE*. *The Journal of Biological Chemistry*, 2009. **284** 13714-13724.
118. Tomos, I., E. Manali, A. Karakatsani, A. Spathis, I. Korbila, A. Analitis, et al., *IL-6 and IL-8 in stable and exacerbated IPF patients and their association to outcome*. *Eur Respir J*, 2016. **48**.
119. Feghali, C.A., K.L. Bost, D.W. Boulware, and L.S. Levy, *Control of Il-6 Expression and Response in Fibroblasts from Patients with Systemic Sclerosis*. *Autoimmunity*, 1994. **17** 309-318.
120. Narazaki, M., T. Tanaka, and T. Kishimoto, *The role and therapeutic targeting of IL-6 in rheumatoid arthritis*. *Expert Review of Clinical Immunology*, 2017. **13** 535-551.
121. Borthwick, L.A., *The IL-1 cytokine family and its role in inflammation and fibrosis in the lung*. *Seminars in Immunopathology*, 2016. **38** 517-534.
122. Summers, C., S.M. Rankin, A.M. Condliffe, N. Singh, A.M. Peters, and E.R. Chilvers, *Neutrophil kinetics in health and disease*. *Trends in Immunology*, 2010. **31** 318-324.
123. Ray, P.D., B.-W. Huang, and Y. Tsuji, *Reactive oxygen species (ROS) homeostasis and redox regulation in cellular signaling*. *Cellular Signalling*, 2012. **24** 981-990.
124. Cheresh, P., S.-J. Kim, S. Tulasiram, and D.W. Kamp, *Oxidative Stress and Pulmonary Fibrosis*. *Biochimica et biophysica acta*, 2013. **1832** 1028-1040.
125. Kliment, C.R. and T.D. Oury, *Oxidative stress, extracellular matrix targets, and idiopathic pulmonary fibrosis*. *Free Radical Biology and Medicine*, 2010. **49** 707-717.

126. Wynn, Thomas A. and Kevin M. Vannella, *Macrophages in Tissue Repair, Regeneration, and Fibrosis*. Immunity, 2016. **44** 450-462.
127. Davalli, P., T. Mitic, A. Caporali, A. Lauriola, and D. D'Arca, *ROS, Cell Senescence, and Novel Molecular Mechanisms in Aging and Age-Related Diseases*. Oxidative Medicine and Cellular Longevity, 2016. **2016** 3565127.
128. Rahman, I., E. Skwarska, M. Henry, M. Davis, C.M. O'Connor, M.X. FitzGerald, *et al.*, *Systemic and pulmonary oxidative stress in idiopathic pulmonary fibrosis*. Free Radical Biology and Medicine, 1999. **27** 60-68.
129. Vyalov, S.L., G. Gabbiani, and Y. Kapanci, *Rat alveolar myofibroblasts acquire alpha-smooth muscle actin expression during bleomycin-induced pulmonary fibrosis*. The American Journal of Pathology, 1993. **143** 1754-1765.
130. Teke, T., E. Maden, A. Kiyici, C. Korkmaz, M. Gok, F. Ozer, *et al.*, *Cigarette smoke and bleomycin-induced pulmonary oxidative stress in rats*. Experimental and Therapeutic Medicine, 2012. **4** 121-124.
131. Psathakis, K., D. Mermigkis, G. Papatheodorou, S. Loukides, P. Panagou, V. Polychronopoulos, *et al.*, *Exhaled markers of oxidative stress in idiopathic pulmonary fibrosis*. European Journal of Clinical Investigation, 2006. **36** 362-367.
132. Kinnula, V.L., U.A. Hodgson, E.K. Lakari, R.J. Tan, R.T. Sormunen, Y.M. Soini, *et al.*, *Extracellular superoxide dismutase has a highly specific localization in idiopathic pulmonary fibrosis/usual interstitial pneumonia*. Histopathology, 2006. **49** 66-74.
133. Martinez, F.J., J.A. de Andrade, K.J. Anstrom, T.E. King, and G. Raghu, *Randomized Trial of N-acetylcysteine in Idiopathic Pulmonary Fibrosis*. The New England journal of medicine, 2014. **370** 2093-2101.
134. Micallef, L., N. Vedrenne, F. Bilet, B. Coulomb, I.A. Darby, and A. Desmouliere, *The myofibroblast, multiple origins for major roles in normal and pathological tissue repair*. Fibrogenesis Tissue Repair, 2012. **5** S5.
135. Kendall, R.T. and C.A. Feghali-Bostwick, *Fibroblasts in fibrosis: novel roles and mediators*. Frontiers in Pharmacology, 2014. **5** 123.
136. Mio, T., S. Nagai, M. Kitaichi, A. Kawatani, and T. Izumi, *Proliferative Characteristics of Fibroblast Lines Derived from Open Lung Biopsy Specimens of Patients with IPF (UIP)*. Chest, 1992. **102** 832-837.
137. Maher, T.M., I.C. Evans, S.E. Bottoms, P.F. Mercer, A.J. Thorley, A.G. Nicholson, *et al.*, *Diminished Prostaglandin E2 Contributes to the Apoptosis Paradox in Idiopathic Pulmonary Fibrosis*. American Journal of Respiratory and Critical Care Medicine, 2010. **182** 73-82.
138. Larsson, O., D. Diebold, D. Fan, M. Peterson, R.S. Nho, P.B. Bitterman, *et al.*, *Fibrotic Myofibroblasts Manifest Genome-Wide Derangements of Translational Control*. PLoS ONE, 2008. **3** e3220.
139. Willis, B.C., J.M. Liebler, K. Luby-Phelps, A.G. Nicholson, E.D. Crandall, R.M. du Bois, *et al.*, *Induction of epithelial-mesenchymal transition in alveolar epithelial cells by transforming growth factor-beta1: potential role in idiopathic pulmonary fibrosis*. Am J Pathol, 2005. **166**.
140. Kim, K.K., M.C. Kugler, P.J. Wolters, L. Robillard, M.G. Galvez, A.N. Brumwell, *et al.*, *Alveolar epithelial cell mesenchymal transition develops in vivo during pulmonary fibrosis and is regulated by the extracellular matrix*. Proc Natl Acad Sci U S A, 2006. **103**.

141. Rock, J.R., C.E. Barkauskas, M.J. Cronic, Y. Xue, J.R. Harris, J. Liang, *et al.*, *Multiple stromal populations contribute to pulmonary fibrosis without evidence for epithelial to mesenchymal transition*. Proceedings of the National Academy of Sciences of the United States of America, 2011. **108** E1475-E1483.
142. Kage, H. and Z. Borok, *EMT and Interstitial Lung Disease: A Mysterious Relationship*. Current opinion in pulmonary medicine, 2012. **18** 517-523.
143. Hoyne, G.F., H. Elliott, S.E. Mutsaers, and C.M. Prele, *Idiopathic pulmonary fibrosis and a role for autoimmunity*. Immunol Cell Biol, 2017.
144. Todd, N.W., R.G. Scheraga, J.R. Galvin, A.T. Iacono, E.J. Britt, I.G. Luzina, *et al.*, *Lymphocyte aggregates persist and accumulate in the lungs of patients with idiopathic pulmonary fibrosis*. Journal of Inflammation Research, 2013. **6** 63-70.
145. Marchal-Sommé, J., Y. Uzunhan, S. Marchand-Adam, D. Valeyre, V. Soumelis, B. Crestani, *et al.*, *Cutting Edge: Nonproliferating Mature Immune Cells Form a Novel Type of Organized Lymphoid Structure in Idiopathic Pulmonary Fibrosis*. The Journal of Immunology, 2006. **176** 5735.
146. Xue, J., D.J. Kass, J. Bon, L. Vuga, J. Tan, E. Csizmadia, *et al.*, *Plasma B Lymphocyte Stimulator and B Cell Differentiation in Idiopathic Pulmonary Fibrosis Patients*. The Journal of Immunology, 2013. **191** 2089.
147. Vuga, L.J., J.R. Tedrow, K.V. Pandit, J. Tan, D.J. Kass, J. Xue, *et al.*, *C-X-C Motif Chemokine 13 (CXCL13) Is a Prognostic Biomarker of Idiopathic Pulmonary Fibrosis*. American Journal of Respiratory and Critical Care Medicine, 2014. **189** 966-974.
148. Feghali-Bostwick, C.A., C.G. Tsai, V.G. Valentine, S. Kantrow, M.W. Stoner, J.M. Pilewski, *et al.*, *Cellular and Humoral Autoreactivity in Idiopathic Pulmonary Fibrosis*. The Journal of Immunology, 2007. **179** 2592.
149. Gilani, S.R., L.J. Vuga, K.O. Lindell, K.F. Gibson, J. Xue, N. Kaminski, *et al.*, *CD28 Down-Regulation on Circulating CD4 T-Cells Is Associated with Poor Prognoses of Patients with Idiopathic Pulmonary Fibrosis*. PLoS ONE, 2010. **5** e8959.
150. Kotsianidis, I., E. Nakou, I. Bouchliou, A. Tzouveleakis, E. Spanoudakis, P. Steiropoulos, *et al.*, *Global Impairment of CD4+CD25+FOXP3+ Regulatory T Cells in Idiopathic Pulmonary Fibrosis*. American Journal of Respiratory and Critical Care Medicine, 2009. **179** 1121-1130.
151. Nuovo, G.J., J.S. Hagood, C.M. Magro, N. Chin, R. Kapil, L. Davis, *et al.*, *The distribution of immunomodulatory cells in the lungs of patients with idiopathic pulmonary fibrosis*. Modern pathology : an official journal of the United States and Canadian Academy of Pathology, Inc, 2012. **25** 416-433.
152. Reilkoff, R.A., H. Peng, L.A. Murray, X. Peng, T. Russell, R. Montgomery, *et al.*, *Semaphorin 7a+ Regulatory T Cells Are Associated with Progressive Idiopathic Pulmonary Fibrosis and Are Implicated in Transforming Growth Factor- $\beta$ 1-induced Pulmonary Fibrosis*. American Journal of Respiratory and Critical Care Medicine, 2013. **187** 180-188.
153. Peng, X., M.W. Moore, H. Peng, H. Sun, Y. Gan, R.J. Homer, *et al.*, *CD4+CD25+FoxP3+ Regulatory Tregs inhibit fibrocyte recruitment and fibrosis via suppression of FGF-9 production in the TGF- $\beta$ 1 exposed murine lung*. Frontiers in Pharmacology, 2014. **5** 80.
154. Coombes, J.L., K.R.R. Siddiqui, C.V. Arancibia-Cárcamo, J. Hall, C.-M. Sun, Y. Belkaid, *et al.*, *A functionally specialized population of mucosal CD103(+) DCs*

- induces Foxp3(+) regulatory T cells via a TGF- $\beta$ - and retinoic acid-dependent mechanism.* The Journal of Experimental Medicine, 2007. **204** 1757-1764.
155. Fujita, J., N. Dobashi, Y. Ohtsuki, I. Yamadori, T. Yoshinouchi, T. Kamei, *et al.*, *Elevation of Anti-cytokeratin 19 Antibody in Sera of the Patients With Idiopathic Pulmonary Fibrosis and Pulmonary Fibrosis Associated With Collagen Vascular Disorders.* Lung, 1999. **177** 311-319.
  156. Dobashi, N., J. Fujita, Y. Ohtsuki, I. Yamadori, T. Yoshinouchi, T. Kamei, *et al.*, *Circulating Cytokeratin 8:Anti-Cytokeratin 8 Antibody Immune Complexes in Sera of Patients with Pulmonary Fibrosis.* Respiration, 2000. **67** 397-401.
  157. Dobashi, N., J. Fujita, M. Murota, Y. Ohtsuki, I. Yamadori, T. Yoshinouchi, *et al.*, *Elevation of Anti-Cytokeratin 18 Antibody and Circulating Cytokeratin 18: Anti-Cytokeratin 18 Antibody Immune Complexes in Sera of Patients with Idiopathic Pulmonary Fibrosis.* Lung, 2000. **178** 171-179.
  158. Kahloon, R.A., J. Xue, A. Bhargava, E. Csizmadia, L. Otterbein, D.J. Kass, *et al.*, *Patients with Idiopathic Pulmonary Fibrosis with Antibodies to Heat Shock Protein 70 Have Poor Prognoses.* American Journal of Respiratory and Critical Care Medicine, 2012. **187** 768-775.
  159. Vittal, R., E.A. Mickler, A.J. Fisher, C. Zhang, K. Rothhaar, H. Gu, *et al.*, *Type V Collagen Induced Tolerance Suppresses Collagen Deposition, TGF- $\beta$  and Associated Transcripts in Pulmonary Fibrosis.* PLOS ONE, 2013. **8** e76451.
  160. Yung, S., D.Y.H. Yap, and T.M. Chan, *Recent advances in the understanding of renal inflammation and fibrosis in lupus nephritis.* F1000Research, 2017. **6** 874.
  161. Derksen, V.F.A.M., T.W.J. Huizinga, and D. van der Woude, *The role of autoantibodies in the pathophysiology of rheumatoid arthritis.* Seminars in Immunopathology, 2017. **39** 437-446.
  162. Loveman, E., V.R. Copley, J.L. Colquitt, D.A. Scott, A.J. Clegg, J. Jones, *et al.*, *The effectiveness and cost-effectiveness of treatments for idiopathic pulmonary fibrosis: systematic review, network meta-analysis and health economic evaluation.* BMC Pharmacol Toxicol, 2014. **15** 63.
  163. Moore, M.W. and E.L. Herzog, *Regulatory T Cells in Idiopathic Pulmonary Fibrosis: Too Much of a Good Thing?* The American Journal of Pathology, 2016. **186** 1978-1981.
  164. Patel, A.A., Y. Zhang, J.N. Fullerton, L. Boelen, A. Rongvaux, A.A. Maini, *et al.*, *The fate and lifespan of human monocyte subsets in steady state and systemic inflammation.* The Journal of Experimental Medicine, 2017.
  165. Ziegler-Heitbrock, L., P. Ancuta, S. Crowe, M. Dalod, V. Grau, D.N. Hart, *et al.*, *Nomenclature of monocytes and dendritic cells in blood.* Blood, 2010. **116** e74.
  166. Ingersoll, M.A., R. Spanbroek, C. Lottaz, E.L. Gautier, M. Frankenberger, R. Hoffmann, *et al.*, *Comparison of gene expression profiles between human and mouse monocyte subsets.* Blood, 2010. **115** e10.
  167. Nguyen, K.D., S.J. Fentress, Y. Qiu, K. Yun, J.S. Cox, and A. Chawla, *Circadian Gene *Bmal1* Regulates Diurnal Oscillations of *Ly6C<sup>hi</sup>* Inflammatory Monocytes.* Science, 2013. **341** 1483.
  168. Jakubzick, C.V., G.J. Randolph, and P.M. Henson, *Monocyte differentiation and antigen-presenting functions.* Nature Reviews Immunology, 2017. **17** 349.

169. Thomas, G., R. Tacke, C.C. Hedrick, and R.N. Hanna, *Nonclassical Patrolling Monocyte Function in the Vasculature*. *Arteriosclerosis, thrombosis, and vascular biology*, 2015. **35** 1306-1316.
170. Yona, S., K.-W. Kim, Y. Wolf, A. Mildner, D. Varol, M. Breker, *et al.*, *Fate Mapping Reveals Origins and Dynamics of Monocytes and Tissue Macrophages under Homeostasis*. *Immunity*, 2013. **38** 79-91.
171. Guillems, M., F. Ginhoux, C. Jakubzick, S.H. Naik, N. Onai, B.U. Schraml, *et al.*, *Dendritic cells, monocytes and macrophages: a unified nomenclature based on ontogeny*. *Nat Rev Immunol*, 2014. **14** 571-578.
172. Buscher, K., P. Marcovecchio, C.C. Hedrick, and K. Ley, *Patrolling Mechanics of Non-Classical Monocytes in Vascular Inflammation*. *Frontiers in Cardiovascular Medicine*, 2017. **4** 80.
173. Rogacev, K.S., B. Cremers, A.M. Zawada, S. Seiler, N. Binder, P. Ege, *et al.*, *CD14<sup>++</sup>CD16<sup>+</sup> Monocytes Independently Predict Cardiovascular Events: A Cohort Study of 951 Patients Referred for Elective Coronary Angiography*. *Journal of the American College of Cardiology*, 2012. **60** 1512-1520.
174. ElAli, A. and N. Jean LeBlanc, *The Role of Monocytes in Ischemic Stroke Pathobiology: New Avenues to Explore*. *Frontiers in Aging Neuroscience*, 2016. **8** 29.
175. Kaito, M., S.-I. Araya, Y. Gondo, M. Fujita, N. Minato, M. Nakanishi, *et al.*, *Relevance of Distinct Monocyte Subsets to Clinical Course of Ischemic Stroke Patients*. *PLOS ONE*, 2013. **8** e69409.
176. Mukherjee, R., P. Kanti Barman, P. Kumar Thatoi, R. Tripathy, B. Kumar Das, and B. Ravindran, *Non-Classical monocytes display inflammatory features: Validation in Sepsis and Systemic Lupus Erythematosus*. *Scientific Reports*, 2015. **5** 13886.
177. Ghattas, A., H.R. Griffiths, A. Devitt, G.Y.H. Lip, and E. Shantsila, *Monocytes in Coronary Artery Disease and Atherosclerosis: Where Are We Now?* *Journal of the American College of Cardiology*, 2013. **62** 1541-1551.
178. Dayyani, F., K.-U. Belge, M. Frankenberger, M. Mack, T. Berki, and L. Ziegler-Heitbrock, *Mechanism of glucocorticoid-induced depletion of human CD14<sup>+</sup>CD16<sup>+</sup> monocytes*. *Journal of Leukocyte Biology*, 2003. **74** 33-39.
179. Villani, A.-C., R. Satija, G. Reynolds, S. Sarkizova, K. Shekhar, J. Fletcher, *et al.*, *Single-cell RNA-seq reveals new types of human blood dendritic cells, monocytes, and progenitors*. *Science*, 2017. **356**.
180. Notta, F., S. Zandi, N. Takayama, S. Dobson, O.I. Gan, G. Wilson, *et al.*, *Distinct routes of lineage development reshape the human blood hierarchy across ontogeny*. *Science*, 2016. **351**.
181. Yáñez, A., S.G. Coetzee, A. Olsson, D.E. Muench, B.P. Berman, D.J. Hazelett, *et al.*, *Granulocyte-Monocyte Progenitors and Monocyte-Dendritic Cell Progenitors Independently Produce Functionally Distinct Monocytes*. *Immunity*, 2017. **47** 890-902.e894.
182. Askenase, Michael H., S.-J. Han, Allyson L. Byrd, D. Morais da Fonseca, N. Bouladoux, C. Wilhelm, *et al.*, *Bone-Marrow-Resident NK Cells Prime Monocytes for Regulatory Function during Infection*. *Immunity*, 2015. **42** 1130-1142.
183. Hoeffel, G. and F. Ginhoux, *Ontogeny of Tissue-Resident Macrophages*. *Frontiers in Immunology*, 2015. **6** 486.



184. Bigley, V., M. Haniffa, S. Doulatov, X.-N. Wang, R. Dickinson, N. McGovern, *et al.*, *The human syndrome of dendritic cell, monocyte, B and NK lymphoid deficiency*. *The Journal of Experimental Medicine*, 2011.
185. Collin, M.P., D.N.J. Hart, G.H. Jackson, G. Cook, J. Cavet, S. Mackinnon, *et al.*, *The fate of human Langerhans cells in hematopoietic stem cell transplantation*. *The Journal of Experimental Medicine*, 2006. **203** 27-33.
186. Varol, C., A. Vallon-Eberhard, E. Elinav, T. Aychek, Y. Shapira, H. Luche, *et al.*, *Intestinal Lamina Propria Dendritic Cell Subsets Have Different Origin and Functions*. *Immunity*, 2009. **31** 502-512.
187. Italiani, P. and D. Boraschi, *From Monocytes to M1/M2 Macrophages: Phenotypical vs. Functional Differentiation*. *Frontiers in Immunology*, 2014. **5** 514.
188. Kopf, M., C. Schneider, and S.P. Nobs, *The development and function of lung-resident macrophages and dendritic cells*. *Nat Immunol*, 2015. **16** 36-44.
189. Hussell, T. and T.J. Bell, *Alveolar macrophages: plasticity in a tissue-specific context*. *Nat Rev Immunol*, 2014. **14** 81-93.
190. Gibbings, S.L., R. Goyal, A.N. Desch, S.M. Leach, M. Prabagar, S.M. Atif, *et al.*, *Transcriptome analysis highlights the conserved difference between embryonic and postnatal-derived alveolar macrophages*. *Blood*, 2015. **126** 1357.
191. Gibbings, S.L., S.M. Thomas, S.M. Atif, A.L. McCubbrey, A.N. Desch, T. Danhorn, *et al.*, *Three Unique Interstitial Macrophages in the Murine Lung at Steady State*. *American Journal of Respiratory Cell and Molecular Biology*, 2017. **57** 66-76.
192. Janssen, W.J., L. Barthel, A. Muldrow, R.E. Oberley-Deegan, M.T. Kearns, C. Jakubzick, *et al.*, *Fas Determines Differential Fates of Resident and Recruited Macrophages during Resolution of Acute Lung Injury*. *American Journal of Respiratory and Critical Care Medicine*, 2011. **184** 547-560.
193. Misharin, A.V., L. Morales-Nebreda, P.A. Reyfman, C.M. Cuda, J.M. Walter, A.C. McQuattie-Pimentel, *et al.*, *Monocyte-derived alveolar macrophages drive lung fibrosis and persist in the lung over the life span*. *The Journal of Experimental Medicine*, 2017. **214** 2387.
194. Hashimoto, D., A. Chow, C. Noizat, P. Teo, M.B. Beasley, M. Leboeuf, *et al.*, *Tissue resident macrophages self-maintain locally throughout adult life with minimal contribution from circulating monocytes*. *Immunity*, 2013. **38** 10.1016/j.immuni.2013.1004.1004.
195. Röszer, T., *Understanding the Biology of Self-Renewing Macrophages*. *Cells*, 2018. **7** 103.
196. Martinez, F.O. and S. Gordon, *The M1 and M2 paradigm of macrophage activation: time for reassessment*. *F1000Prime Reports*, 2014. **6** 13.
197. Martinez, F.O., S. Gordon, M. Locati, and A. Mantovani, *Transcriptional Profiling of the Human Monocyte-to-Macrophage Differentiation and Polarization: New Molecules and Patterns of Gene Expression*. *The Journal of Immunology*, 2006. **177** 7303.
198. Martinez, F.O., L. Helming, and S. Gordon, *Alternative activation of macrophages: an immunologic functional perspective*. *Annu Rev Immunol*, 2009. **27**.

199. Murray, P.J., J.E. Allen, S.K. Biswas, E.A. Fisher, D.W. Gilroy, S. Goerdts, *et al.*, *Macrophage activation and polarization: nomenclature and experimental guidelines*. *Immunity*, 2014. **41** 14-20.
200. Murray, P.J. and T.A. Wynn, *Protective and pathogenic functions of macrophage subsets*. *Nat Rev Immunol*, 2011. **11** 723-737.
201. Lawrence, T. and G. Natoli, *Transcriptional regulation of macrophage polarization: enabling diversity with identity*. *Nat Rev Immunol*, 2011. **11** 750-761.
202. Gordon, S., *Alternative activation of macrophages*. *Nat Rev Immunol*, 2003. **3**.
203. Varin A, G.S., *Alternative activation of macrophages: Immune function and cellular biology*. *Immunobiology*, 2009. **214** 630-641.
204. Stein, M., S. Keshav, N. Harris, and S. Gordon, *Interleukin 4 potentially enhances murine macrophage mannose receptor activity: a marker of alternative immunologic macrophage activation*. *J Exp Med*, 1992. **176**.
205. Ehrchen, J., L. Steinmüller, K. Barczyk, K. Tenbrock, W. Nacken, M. Eisenacher, *et al.*, *Glucocorticoids induce differentiation of a specifically activated, anti-inflammatory subtype of human monocytes*. *Blood*, 2007. **109** 1265.
206. Chitu, V. and E.R. Stanley, *Colony-stimulating factor-1 in immunity and inflammation*. *Current Opinion in Immunology*, 2006. **18** 39-48.
207. Hamilton, T.A., C. Zhao, P.G. Pavicic, and S. Datta, *Myeloid Colony-Stimulating Factors as Regulators of Macrophage Polarization*. *Frontiers in Immunology*, 2014. **5** 554.
208. Ji, X.H., T. Yao, J.C. Qin, S.K. Wang, H.J. Wang, and K. Yao, *Interaction between M-CSF and IL-10 on productions of IL-12 and IL-18 and expressions of CD14, CD23, and CD64 by human monocytes*. *Acta Pharmacologica Sinica*, 2004. **25** 1361-1365.
209. Jaguin, M., N. Houlbert, O. Fardel, and V. Lecreur, *Polarization profiles of human M-CSF-generated macrophages and comparison of M1-markers in classically activated macrophages from GM-CSF and M-CSF origin*. *Cell Immunol*, 2013. **281** 51-61.
210. Mia, S., A. Warnecke, X.M. Zhang, V. Malmström, and R.A. Harris, *An optimized Protocol for Human M2 Macrophages using M-CSF and IL-4/IL-10/TGF- $\beta$  Yields a Dominant Immunosuppressive Phenotype*. *Scandinavian Journal of Immunology*, 2014. **79** 305-314.
211. Mantovani, A., B. Bottazzi, F. Colotta, S. Sozzani, and L. Ruco, *The origin and function of tumor-associated macrophages*. *Immunology Today*, 1992. **13** 265-270.
212. Mantovani, A., P. Allavena, A. Sica, and F. Balkwill, *Cancer-related inflammation*. *Nature*, 2008. **454** 436.
213. Noy, R. and Jeffrey W. Pollard, *Tumor-Associated Macrophages: From Mechanisms to Therapy*. *Immunity*, 2014. **41** 49-61.
214. Qian, B.-Z. and J.W. Pollard, *Macrophage Diversity Enhances Tumor Progression and Metastasis*. *Cell*, 2010. **141** 39-51.
215. Biswas, Subhra K., *Metabolic Reprogramming of Immune Cells in Cancer Progression*. *Immunity*, 2015. **43** 435-449.
216. Biswas, S.K. and A. Mantovani, *Macrophage plasticity and interaction with lymphocyte subsets: cancer as a paradigm*. *Nat Immunol*, 2010. **11** 889-896.

217. Mantovani, A., F. Marchesi, A. Malesci, L. Laghi, and P. Allavena, *Tumour-associated macrophages as treatment targets in oncology*. Nature Reviews Clinical Oncology, 2017. **14** 399.
218. Ino, Y., R. Yamazaki-Itoh, K. Shimada, M. Iwasaki, T. Kosuge, Y. Kanai, et al., *Immune cell infiltration as an indicator of the immune microenvironment of pancreatic cancer*. British Journal of Cancer, 2013. **108** 914-923.
219. Pyonteck, S.M., L. Akkari, A.J. Schuhmacher, R.L. Bowman, L. Sevenich, D.F. Quail, et al., *CSF-1R inhibition alters macrophage polarization and blocks glioma progression*. Nature Medicine, 2013. **19** 1264.
220. Ambarus, C.A., S. Krausz, M. van Eijk, J. Hamann, T.R. Radstake, K.A. Reedquist, et al., *Systematic validation of specific phenotypic markers for in vitro polarized human macrophages*. J Immunol Methods, 2012. **375** 196-206.
221. Wang, N., H. Liang, and K. Zen, *Molecular Mechanisms That Influence the Macrophage M1–M2 Polarization Balance*. Frontiers in Immunology, 2014. **5** 614.
222. Benoit, M., B. Desnues, and J.-L. Mege, *Macrophage Polarization in Bacterial Infections*. The Journal of Immunology, 2008. **181** 3733.
223. Stempin, C.C., L.R. Dulgerian, V.V. Garrido, and F.M. Cerban, *Arginase in Parasitic Infections: Macrophage Activation, Immunosuppression, and Intracellular Signals*. Journal of Biomedicine and Biotechnology, 2010. **2010** 683485.
224. Gordon, S. and A. Plüddemann, *Tissue macrophages: heterogeneity and functions*. BMC Biology, 2017. **15** 53.
225. Mylonas, K.J., M.G. Nair, L. Prieto-Lafuente, D. Paape, and J.E. Allen, *Alternatively activated macrophages elicited by helminth infection can be reprogrammed to enable microbial killing*. J Immunol, 2009. **182** 3084-3094.
226. Noel, W., G. Raes, G. Hassanzadeh Ghasabeh, P. De Baetselier, and A. Beschin, *Alternatively activated macrophages during parasite infections*. Trends Parasitol, 2004. **20** 126-133.
227. Lech, M. and H.-J. Anders, *Macrophages and fibrosis: How resident and infiltrating mononuclear phagocytes orchestrate all phases of tissue injury and repair*. Biochimica et Biophysica Acta (BBA) - Molecular Basis of Disease, 2013. **1832** 989-997.
228. Meszaros, A.J., J.S. Reichner, and J.E. Albina, *Macrophage-Induced Neutrophil Apoptosis*. The Journal of Immunology, 2000. **165** 435-441.
229. Koh, T.J. and L.A. DiPietro, *Inflammation and wound healing: the role of the macrophage*. Expert Rev Mol Med, 2011. **13** e23.
230. Knipper, J.A., S. Willenborg, J. Brinckmann, W. Bloch, T. Maaß, R. Wagener, et al., *Interleukin-4 Receptor  $\alpha$  Signaling in Myeloid Cells Controls Collagen Fibril Assembly in Skin Repair*. Immunity, 2015. **43** 803-816.
231. Zhu, J., Z. Xu, X. Chen, S. Zhou, W. Zhang, Y. Chi, et al., *Parasitic antigens alter macrophage polarization during Schistosoma japonicum infection in mice*. Parasites & Vectors, 2014. **7** 122-122.
232. Ramachandran P, P.A., Vernon MA, et al, *Differential Ly-6C expression identifies the recruited macrophage phenotype, which orchestrates the regression of murine liver fibrosis*. PNAS, 2012. **109**.
233. Popov, Y., D.Y. Sverdlov, K.R. Bhaskar, A.K. Sharma, G. Millonig, E. Patsenker, et al., *Macrophage-mediated phagocytosis of apoptotic cholangiocytes*

- contributes to reversal of experimental biliary fibrosis. American Journal of Physiology - Gastrointestinal and Liver Physiology*, 2010. **298** G323.
234. Nahrendorf, M., F.K. Swirski, E. Aikawa, L. Stangenberg, T. Wurdinger, J.L. Figueiredo, *et al.*, *The healing myocardium sequentially mobilizes two monocyte subsets with divergent and complementary functions. J Exp Med*, 2007. **204** 3037-3047.
235. Duffield, J.S., S.J. Forbes, C.M. Constandinou, S. Clay, M. Partolina, S. Vuthoori, *et al.*, *Selective depletion of macrophages reveals distinct, opposing roles during liver injury and repair. The Journal of Clinical Investigation*, 2005. **115** 56-65.
236. Murray, L.A., R. Rosada, A.P. Moreira, A. Joshi, M.S. Kramer, D.P. Hesson, *et al.*, *Serum amyloid P therapeutically attenuates murine bleomycin-induced pulmonary fibrosis via its effects on macrophages. PLoS One*, 2010. **5** e9683.
237. Morimoto, K., W.J. Janssen, and M. Terada, *Defective efferocytosis by alveolar macrophages in IPF patients. Respiratory medicine*, 2012. **106** 1800-1803.
238. Hancock A, A.L., Gama R, Millar A, *Production of Interleukin 13 by Alveolar Macrophages from Normal and Fibrotic Lung. Am. J. Respir. Cell Mol. Biol*, 1998. **18** 60–65.
239. Lucas, T., A. Waisman, R. Ranjan, J. Roes, T. Krieg, W. Müller, *et al.*, *Differential Roles of Macrophages in Diverse Phases of Skin Repair. The Journal of Immunology*, 2010. **184** 3964.
240. Schupp, J.C., H. Binder, B. Jäger, G. Cillis, G. Zissel, J. Müller-Quernheim, *et al.*, *Macrophage Activation in Acute Exacerbation of Idiopathic Pulmonary Fibrosis. PLoS ONE*, 2015. **10** e0116775.
241. Mora, A.L., E. Torres-González, M. Rojas, C. Corredor, J. Ritzenthaler, J. Xu, *et al.*, *Activation of Alveolar Macrophages via the Alternative Pathway in Herpesvirus-Induced Lung Fibrosis. American Journal of Respiratory Cell and Molecular Biology*, 2006. **35** 466-473.
242. Zhou, Y., H. Peng, H. Sun, X. Peng, C. Tang, Y. Gan, *et al.*, *Chitinase 3-Like 1 Suppresses Injury and Promotes Fibroproliferative Responses in Mammalian Lung Fibrosis. Science Translational Medicine*, 2014. **6** 240ra276.
243. Daniil, Z.D., E. Papageorgiou, A. Koutsokera, K. Kostikas, T. Kiriopoulos, A.I. Papaioannou, *et al.*, *Serum levels of oxidative stress as a marker of disease severity in idiopathic pulmonary fibrosis. Pulmonary Pharmacology & Therapeutics*, 2008. **21** 26-31.
244. Negash, A.A., H.J. Ramos, N. Crochet, D.T.Y. Lau, B. Doehle, N. Papic, *et al.*, *IL-1 $\beta$  Production through the NLRP3 Inflammasome by Hepatic Macrophages Links Hepatitis C Virus Infection with Liver Inflammation and Disease. PLOS Pathogens*, 2013. **9** e1003330.
245. Shinoda, H., S. Tasaka, S. Fujishima, W. Yamasawa, K. Miyamoto, Y. Nakano, *et al.*, *Elevated CC Chemokine Level in Bronchoalveolar Lavage Fluid Is Predictive of a Poor Outcome of Idiopathic Pulmonary Fibrosis. Respiration*, 2009. **78** 285-292.
246. Suga, M., K. Iyonaga, H. Ichiyasu, N. Saita, H. Yamasaki, and M. Ando, *Clinical significance of MCP-1 levels in BALF and serum in patients with interstitial lung diseases. European Respiratory Journal*, 1999. **14** 376.
247. Wells, A.U., S.R. Desai, M.B. Rubens, N.S. Goh, D. Cramer, A.G. Nicholson, *et al.*, *Idiopathic pulmonary fibrosis: a composite physiologic index derived from*

- disease extent observed by computed tomography. *Am J Respir Crit Care Med*, 2003. **167** 962-969.
248. Song, J.W., S.B. Hong, C.M. Lim, Y. Koh, and D.S. Kim, *Acute exacerbation of idiopathic pulmonary fibrosis: incidence, risk factors and outcome*. *European Respiratory Journal*, 2011. **37** 356.
249. Richeldi, L., V. Cottin, K.R. Flaherty, M. Kolb, Y. Inoue, G. Raghu, *et al.*, *Design of the INPULSIS trials: two phase 3 trials of nintedanib in patients with idiopathic pulmonary fibrosis*. *Respir Med*, 2014. **108** 1023-1030.
250. Matt, P., U. Lindqvist, and S. Kleinau, *Elevated Membrane and Soluble CD64: A Novel Marker Reflecting Altered FcγR Function and Disease in Early Rheumatoid Arthritis That Can Be Regulated by Anti-Rheumatic Treatment*. *PLOS ONE*, 2015. **10** e0137474.
251. Li, Y., P.Y. Lee, E.S. Sobel, S. Narain, M. Satoh, M.S. Segal, *et al.*, *Increased expression of FcγRI/CD64 on circulating monocytes parallels ongoing inflammation and nephritis in lupus*. *Arthritis Research & Therapy*, 2009. **11** R6-R6.
252. Cros, J., N. Cagnard, K. Woollard, N. Patey, S.-Y. Zhang, B. Senechal, *et al.*, *Human CD14(dim) Monocytes Patrol and Sense Nucleic Acids and Viruses via TLR7 and TLR8 Receptors*. *Immunity*, 2010. **33** 375-386.
253. Matt, P., U. Lindqvist, and S. Kleinau, *Up-regulation of CD64-expressing monocytes with impaired FcγR function reflects disease activity in polyarticular psoriatic arthritis*. *Scandinavian Journal of Rheumatology*, 2015. **44** 464-473.
254. Brancato, S.K. and J.E. Albina, *Wound macrophages as key regulators of repair: origin, phenotype, and function*. *Am J Pathol*, 2011. **178** 19-25.
255. Klass, B.R., A.O. Grobbelaar, and K.J. Rolfe, *Transforming growth factor beta1 signalling, wound healing and repair: a multifunctional cytokine with clinical implications for wound repair, a delicate balance*. *Postgrad Med J*, 2009. **85**.
256. Akira, S. and K. Takeda, *Toll-like receptor signalling*. *Nat Rev Immunol*, 2004. **4** 499-511.
257. Krutzik, S.R., B. Tan, H. Li, M.T. Ochoa, P.T. Liu, S.E. Sharfstein, *et al.*, *TLR activation triggers the rapid differentiation of monocytes into macrophages and dendritic cells*. *Nat Med*, 2005. **11** 653-660.
258. Byrne, A.J., T.M. Maher, and C.M. Lloyd, *Pulmonary Macrophages: A New Therapeutic Pathway in Fibrosing Lung Disease?* *Trends in Molecular Medicine*, 2016. **22** 303-316.
259. Moore, B.B., C. Fry, Y. Zhou, S. Murray, M.K. Han, F.J. Martinez, *et al.*, *Inflammatory leukocyte phenotypes correlate with disease progression in idiopathic pulmonary fibrosis*. *Front Med*, 2014. **1**.
260. Naik, P.K., P.D. Bozyk, J.K. Bentley, A.P. Popova, C.M. Birch, C.A. Wilke, *et al.*, *Periostin promotes fibrosis and predicts progression in patients with idiopathic pulmonary fibrosis*. *American Journal of Physiology - Lung Cellular and Molecular Physiology*, 2012. **303** L1046.
261. Desai, B., J. Mattson, H. Paintal, M. Nathan, F. Shen, M. Beaumont, *et al.*, *Differential expression of monocyte/macrophage-selective markers in human idiopathic pulmonary fibrosis*. *Experimental Lung Research*, 2011. **37** 227-238.
262. Hofer, T.P., A.M. Zawada, M. Frankenberger, K. Skokann, A.A. Satz, W. Gesierich, *et al.*, *slan-defined subsets of CD16-positive monocytes: impact of*

- granulomatous inflammation and M-CSF receptor mutation*. *Blood*, 2015. **126** 2601.
263. Hoeve, M.A., A.A. Nash, D. Jackson, R.E. Randall, and I. Dransfield, *Influenza Virus A Infection of Human Monocyte and Macrophage Subpopulations Reveals Increased Susceptibility Associated with Cell Differentiation*. *PLOS ONE*, 2012. **7** e29443.
264. Zhang, J.-Y., Z.-S. Zou, A. Huang, Z. Zhang, J.-L. Fu, X.-S. Xu, *et al.*, *Hyper-Activated Pro-Inflammatory CD16+ Monocytes Correlate with the Severity of Liver Injury and Fibrosis in Patients with Chronic Hepatitis B*. *PLOS ONE*, 2011. **6** e17484.
265. Raghu, G., D. Weycker, J. Edelsberg, W.Z. Bradford, and G. Oster, *Incidence and prevalence of idiopathic pulmonary fibrosis*. *Am J Respir Crit Care Med*, 2006. **174** 810-816.
266. Ambrosini, V., A. Cancellieri, M. Chilosi, M. Zompatori, R. Trisolini, L. Saragoni, *et al.*, *Acute exacerbation of idiopathic pulmonary fibrosis: report of a series*. *Eur Respir J*, 2003. **22**.
267. Xu, H., A. Manivannan, I. Crane, R. Dawson, and J. Liversidge, *Critical but divergent roles for CD62L and CD44 in directing blood monocyte trafficking in vivo during inflammation*. *Blood*, 2008. **112** 1166-1174.
268. Ji, W.J., Y.Q. Ma, X. Zhou, Y.D. Zhang, R.Y. Lu, H.Y. Sun, *et al.*, *Temporal and spatial characterization of mononuclear phagocytes in circulating, lung alveolar and interstitial compartments in a mouse model of bleomycin-induced pulmonary injury*. *J Immunol Methods*, 2014. **403** 7-16.
269. Misharin, A.V., L. Morales-Nebreda, G.M. Mutlu, G.R.S. Budinger, and H. Perlman, *Flow Cytometric Analysis of Macrophages and Dendritic Cell Subsets in the Mouse Lung*. *American Journal of Respiratory Cell and Molecular Biology*, 2013. **49** 503-510.
270. Arts, R.J.W., A. Carvalho, C. La Rocca, C. Palma, F. Rodrigues, R. Silvestre, *et al.*, *Immunometabolic Pathways in BCG-Induced Trained Immunity*. *Cell Reports*, 2016. **17** 2562-2571.
271. Allaire, M.A., B. Tanne, S.C. Cote, and N. Dumais, *Prostaglandin E 2 Does Not Modulate CCR7 Expression and Functionality after Differentiation of Blood Monocytes into Macrophages*. *Int J Inflam*, 2013. **2013** 918016.
272. Shi, C. and E.G. Pamer, *Monocyte recruitment during infection and inflammation*. *Nat Rev Immunol*, 2011. **11** 762-774.
273. Hunninghake, G.W., J.E. Gadek, T.J. Lawley, and R.G. Crystal, *Mechanisms of neutrophil accumulation in the lungs of patients with idiopathic pulmonary fibrosis*. *The Journal of Clinical Investigation*, 1981. **68** 259-269.
274. Groselj-Grenc, M., A. Ihan, and M. Derganc, *Neutrophil and Monocyte CD64 and CD163 Expression in Critically Ill Neonates and Children with Sepsis: Comparison of Fluorescence Intensities and Calculated Indexes*. *Mediators of Inflammation*, 2008. **2008** 202646.
275. Devaraj, S., X. Chen, B. Adams-Huet, and I. Jialal, *Increased Expression of Fc- $\gamma$  Receptors on Monocytes in Patients With Nascent Metabolic Syndrome*. *The Journal of Clinical Endocrinology & Metabolism*, 2013. **98** E1510-E1515.
276. Swirski, F.K., M. Nahrendorf, M. Etzrodt, M. Wildgruber, V. Cortez-Retamozo, P. Panizzi, *et al.*, *Identification of Splenic Reservoir Monocytes and Their Deployment to Inflammatory Sites*. *Science*, 2009. **325** 612.

277. Fang, L., X.-L. Moore, A.M. Dart, and L.-M. Wang, *Systemic inflammatory response following acute myocardial infarction*. Journal of Geriatric Cardiology : JGC, 2015. **12** 305-312.
278. Klonz, A., K. Wonigeit, R. Pabst, and J. Westermann, *The Marginal Blood Pool of the Rat Contains not only Granulocytes, but also Lymphocytes, NK-Cells and Monocytes: a Second Intravascular Compartment, its Cellular Composition, Adhesion Molecule Expression and Interaction with the Peripheral Blood Pool*. Scandinavian Journal of Immunology, 1996. **44** 461-469.
279. Mathai, S.K., M. Gulati, X. Peng, T.R. Russell, A.C. Shaw, A.N. Rubinowitz, et al., *Circulating monocytes from systemic sclerosis patients with interstitial lung disease show an enhanced profibrotic phenotype*. Lab Invest, 2010. **90** 812-823.
280. Konishi, K., K.F. Gibson, K.O. Lindell, T.J. Richards, Y. Zhang, R. Dhir, et al., *Gene Expression Profiles of Acute Exacerbations of Idiopathic Pulmonary Fibrosis*. American Journal of Respiratory and Critical Care Medicine, 2009. **180** 167-175.
281. Yang, H., H. Wang, Y.A. Levine, M.K. Gunasekaran, Y. Wang, M. Addorisio, et al., *Identification of CD163 as an antiinflammatory receptor for HMGB1-haptoglobin complexes*. JCI Insight, 2016. **1**.
282. Fabrick, B.O., R. van Bruggen, D.M. Deng, A.J.M. Ligtenberg, K. Nazmi, K. Schornagel, et al., *The macrophage scavenger receptor CD163 functions as an innate immune sensor for bacteria*. Blood, 2009. **113** 887.
283. du Bois, R.M., D. Weycker, C. Albera, W.Z. Bradford, U. Costabel, A. Kartashov, et al., *Forced vital capacity in patients with idiopathic pulmonary fibrosis: test properties and minimal clinically important difference*. Am J Respir Crit Care Med, 2011. **184** 1382-1389.
284. Chetta, A., E. Marangio, and D. Olivieri, *Pulmonary Function Testing in Interstitial Lung Diseases*. Respiration, 2004. **71** 209-213.
285. Best, A.C., A.M. Lynch, C.M. Bozic, D. Miller, G.K. Grunwald, and D.A. Lynch, *Quantitative CT Indexes in Idiopathic Pulmonary Fibrosis: Relationship with Physiologic Impairment*. Radiology, 2003. **228** 407-414.
286. Best, A.C., J. Meng, A.M. Lynch, C.M. Bozic, D. Miller, G.K. Grunwald, et al., *Idiopathic Pulmonary Fibrosis: Physiologic Tests, Quantitative CT Indexes, and CT Visual Scores as Predictors of Mortality*. Radiology, 2008. **246** 935-940.
287. Desai, S.R., S. Veeraraghavan, D.M. Hansell, A. Nikolakopoulou, N.S. Goh, A.G. Nicholson, et al., *CT features of lung disease in patients with systemic sclerosis: comparison with idiopathic pulmonary fibrosis and nonspecific interstitial pneumonia*. Radiology, 2004. **232**.
288. Collins, C.D., A.U. Wells, D.M. Hansell, R.A. Morgan, J.E. MacSweeney, R.M. du Bois, et al., *Observer variation in pattern type and extent of disease in fibrosing alveolitis on thin section computed tomography and chest radiography*. Clin Radiol, 1994. **49**.
289. Oda, K., H. Ishimoto, K. Yatera, K. Naito, T. Ogoshi, K. Yamasaki, et al., *High-resolution CT scoring system-based grading scale predicts the clinical outcomes in patients with idiopathic pulmonary fibrosis*. Respiratory Research, 2014. **15** 10-10.
290. Desai, S.R., S. Veeraraghavan, D.M. Hansell, A. Nikolakopoulou, N.S.L. Goh, A.G. Nicholson, et al., *CT Features of Lung Disease in Patients with Systemic*

- Sclerosis: Comparison with Idiopathic Pulmonary Fibrosis and Nonspecific Interstitial Pneumonia*. *Radiology*, 2004. **232** 560-567.
291. Edey, A.J., A.A. Devaraj, R.P. Barker, A.G. Nicholson, A.U. Wells, and D.M. Hansell, *Fibrotic idiopathic interstitial pneumonias: HRCT findings that predict mortality*. *European Radiology*, 2011. **21** 1586-1593.
  292. Judge, E.P., A. Fabre, H.I. Adamali, and J.J. Egan, *Acute exacerbations and pulmonary hypertension in advanced idiopathic pulmonary fibrosis*. *European Respiratory Journal*, 2012. **40** 93.
  293. De Martinis, M., M. Modesti, and L. Ginaldi, *Phenotypic and functional changes of circulating monocytes and polymorphonuclear leucocytes from elderly persons*. *Immunol Cell Biol*, 2004. **82** 415-420.
  294. Wallace, W.A., S.N. Roberts, H. Caldwell, E. Thornton, A.P. Greening, D. Lamb, et al., *Circulating antibodies to lung protein(s) in patients with cryptogenic fibrosing alveolitis*. *Thorax*, 1994. **49** 218.
  295. Takeda, Y., K. Tsujino, T. Kijima, and A. Kumanogoh, *Efficacy and safety of pirfenidone for idiopathic pulmonary fibrosis*. Patient preference and adherence, 2014. **8** 361-370.
  296. Hansell, D.M., J.G. Goldin, T.E. King, Jr., D.A. Lynch, L. Richeldi, and A.U. Wells, *CT staging and monitoring of fibrotic interstitial lung diseases in clinical practice and treatment trials: a Position Paper from the Fleischner society*. *The Lancet Respiratory Medicine*, 2015. **3** 483-496.
  297. Davies, L.C., S.J. Jenkins, J.E. Allen, and P.R. Taylor, *Tissue-resident macrophages*. *Nat Immunol*, 2013. **14** 986-995.
  298. Landsman, L. and S. Jung, *Lung Macrophages Serve as Obligatory Intermediate between Blood Monocytes and Alveolar Macrophages*. *The Journal of Immunology*, 2007. **179** 3488.
  299. Epelman, S., Kory J. Lavine, Anna E. Beaudin, Dorothy K. Sojka, Javier A. Carrero, B. Calderon, et al., *Embryonic and Adult-Derived Resident Cardiac Macrophages Are Maintained through Distinct Mechanisms at Steady State and during Inflammation*. *Immunity*, 2014. **40** 91-104.
  300. Gundra, U.M., N.M. Girgis, D. Ruckerl, S. Jenkins, L.N. Ward, Z.D. Kurtz, et al., *Alternatively activated macrophages derived from monocytes and tissue macrophages are phenotypically and functionally distinct*. *Blood*, 2014. **123** e110.
  301. Zahuczky G, K.f.E., Majai G, Fe'su's L, *Differentiation and Glucocorticoid Regulated Apopto- Phagocytic Gene Expression Patterns in Human Macrophages. Role of Mertk in Enhanced Phagocytosis*. *PLoS ONE* 2011. **6** e21349.
  302. Bindreither, D., S. Ecker, B. Gschirr, A. Kofler, R. Kofler, and J. Rainer, *The synthetic glucocorticoids prednisolone and dexamethasone regulate the same genes in acute lymphoblastic leukemia cells*. *BMC Genomics*, 2014. **15** 662.
  303. Herold, S., K. Mayer, and J. Lohmeyer, *Acute Lung Injury: How Macrophages Orchestrate Resolution of Inflammation and Tissue Repair*. *Frontiers in Immunology*, 2011. **2** 65.
  304. Zhang, M.-Z., B. Yao, S. Yang, L. Jiang, S. Wang, X. Fan, et al., *CSF-1 signaling mediates recovery from acute kidney injury*. *The Journal of Clinical Investigation*, 2012. **122** 4519-4532.



305. Zaiss, D.M.W., W.C. Gause, L.C. Osborne, and D. Artis, *Emerging functions of amphiregulin in orchestrating immunity, inflammation and tissue repair*. *Immunity*, 2015. **42** 216-226.
306. Nishi, Y., H. Sano, T. Kawashima, T. Okada, T. Kuroda, K. Kikkawa, *et al.*, *Role of Galectin-3 in Human Pulmonary Fibrosis*. *Allergology International*, 2007. **56** 57-65.
307. [https://www.ncbi.nlm.nih.gov/gene?cmd=Retrieve&dopt=full\\_report&list\\_uids=3623](https://www.ncbi.nlm.nih.gov/gene?cmd=Retrieve&dopt=full_report&list_uids=3623) - additional-links. *INHA inhibin alpha subunit [ Homo sapiens (human) ]*. 2017.
308. Buchacher, T., A. Ohradanova-Repic, H. Stockinger, M.B. Fischer, and V. Weber, *M2 Polarization of Human Macrophages Favors Survival of the Intracellular Pathogen Chlamydia pneumoniae*. *PLOS ONE*, 2015. **10** e0143593.
309. Baran, C.P., J.M. Opalek, S. McMaken, C.A. Newland, J.M. O'Brien, Jr., M.G. Hunter, *et al.*, *Important roles for macrophage colony-stimulating factor, CC chemokine ligand 2, and mononuclear phagocytes in the pathogenesis of pulmonary fibrosis*. *Am J Respir Crit Care Med*, 2007. **176** 78-89.
310. Kiemle-Kallee, J.K., K Radzun HJ, *Alveolar macrophages in IPF display a more monocyte-like immunophenotype and an increased release of free oxygen radicals*. *ERJ*, 1991. **4** 400-408.
311. Guo, H., J.B. Callaway, and J.P.Y. Ting, *Inflammasomes: mechanism of action, role in disease, and therapeutics*. *Nat Med*, 2015. **21** 677-687.
312. He, Y., H. Hara, and G. Núñez, *Mechanism and Regulation of NLRP3 Inflammasome Activation*. *Trends in Biochemical Sciences*, 2016. **41** 1012-1021.
313. Franchi, L., R. Munoz-Planillo, and G. Nunez, *Sensing and reacting to microbes through the inflammasomes*. *Nat Immunol*, 2012. **13** 325-332.
314. Devitt, A., O.D. Moffatt, C. Raykundalia, J.D. Capra, D.L. Simmons, and C.D. Gregory, *Human CD14 mediates recognition and phagocytosis of apoptotic cells*. *Nature*, 1998. **392** 505-509.
315. Jersmann, H.P.A., *Time to abandon dogma: CD14 is expressed by non-myeloid lineage cells*. *Immunol Cell Biol*, 2005. **83** 462-467.
316. Ferrero, E., D. Jiao, B.Z. Tsuberi, L. Tesio, G.W. Rong, A. Haziot, *et al.*, *Transgenic mice expressing human CD14 are hypersensitive to lipopolysaccharide*. *Proceedings of the National Academy of Sciences*, 1993. **90** 2380-2384.
317. Knuefermann, P., S. Nemoto, A. Misra, N. Nozaki, G. Defreitas, S.M. Goyert, *et al.*, *CD14-Deficient Mice Are Protected Against Lipopolysaccharide-Induced Cardiac Inflammation and Left Ventricular Dysfunction*. *Circulation*, 2002. **106** 2608.
318. Tarzi, R.M., J. Liu, S. Schneiter, N.R. Hill, T.H. Page, H.T. Cook, *et al.*, *CD14 expression is increased on monocytes in patients with anti-neutrophil cytoplasm antibody (ANCA)-associated vasculitis and correlates with the expression of ANCA autoantigens*. *Clinical and Experimental Immunology*, 2015. **181** 65-75.
319. Ding, L., T. Liu, Z. Wu, B. Hu, T. Nakashima, M. Ullenbruch, *et al.*, *Bone Marrow CD11c<sup>+</sup> Cell-Derived Amphiregulin Promotes Pulmonary Fibrosis*. *The Journal of Immunology*, 2016. **197** 303.

320. Zhou, Y., J.-Y. Lee, C.-M. Lee, W.-K. Cho, M.-J. Kang, J.L. Koff, *et al.*, *Amphiregulin, an Epidermal Growth Factor Receptor Ligand, Plays an Essential Role in the Pathogenesis of Transforming Growth Factor- $\beta$ -induced Pulmonary Fibrosis*. *Journal of Biological Chemistry*, 2012. **287** 41991-42000.
321. Li, L.-c., J. Li, and J. Gao, *Functions of Galectin-3 and Its Role in Fibrotic Diseases*. *Journal of Pharmacology and Experimental Therapeutics*, 2014. **351** 336.
322. Thomas, A.L., C. Coarfa, J. Qian, J.J. Wilkerson, K. Rajapakshe, N.L. Krett, *et al.*, *Identification of potential glucocorticoid receptor therapeutic targets in multiple myeloma*. *Nuclear Receptor Signaling*, 2015. **13** e006.
323. Hoogsteden, H.C., J.J.M. van Dongen, B.T.W. van Hal, M. Delahaye, W. Hop, and C. Hilvering, *Phenotype of Blood Monocytes and Alveolar Macrophages in Interstitial Lung Disease*. *CHEST*, 1989. **95** 574-577.
324. Kalluri, R., *The biology and function of fibroblasts in cancer*. *Nat Rev Cancer*, 2016. **16** 582-598.
325. Hinz, B., G. Celetta, J.J. Tomasek, G. Gabbiani, and C. Chaponnier, *Alpha-Smooth Muscle Actin Expression Upregulates Fibroblast Contractile Activity*. *Molecular Biology of the Cell*, 2001. **12** 2730-2741.
326. LeBleu, V.S., Y. Teng, J.T. O'Connell, D. Charytan, G.A. Müller, C.A. Müller, *et al.*, *Identification of Human Epididymis Protein-4 as a Novel Fibroblast-Derived Mediator of Fibrosis*. *Nature medicine*, 2013. **19** 227-231.
327. González, L., N. Eiro, B. Fernandez-Garcia, L.O. González, F. Dominguez, and F.J. Vizoso, *Gene expression profile of normal and cancer-associated fibroblasts according to intratumoral inflammatory cells phenotype from breast cancer tissue*. *Molecular Carcinogenesis*, 2016. **55** 1489-1502.
328. Vancheri, C., M. Failla, N. Crimi, and G. Raghu, *Idiopathic pulmonary fibrosis: a disease with similarities and links to cancer biology*. *Eur Respir J*, 2010. **35** 496-504.
329. White, E.S., V.J. Thannickal, S.L. Carskadon, E.G. Dickie, D.L. Livant, S. Markwart, *et al.*, *Integrin  $\alpha(4)\beta(1)$  Regulates Migration across Basement Membranes by Lung Fibroblasts: A Role for Phosphatase and Tensin Homologue Deleted on Chromosome 10*. *American journal of respiratory and critical care medicine*, 2003. **168** 436-442.
330. Li, Y., D. Jiang, J. Liang, E.B. Meltzer, A. Gray, R. Miura, *et al.*, *Severe lung fibrosis requires an invasive fibroblast phenotype regulated by hyaluronan and CD44*. *The Journal of Experimental Medicine*, 2011. **208** 1459-1471.
331. Jakubzick, C., E.S. Choi, K.J. Carpenter, S.L. Kunkel, H. Evanoff, F.J. Martinez, *et al.*, *Human Pulmonary Fibroblasts Exhibit Altered Interleukin-4 and Interleukin-13 Receptor Subunit Expression in Idiopathic Interstitial Pneumonia*. *The American Journal of Pathology*, 2004. **164** 1989-2001.
332. Wolters, P.J., H.R. Collard, and K.D. Jones, *Pathogenesis of idiopathic pulmonary fibrosis*. *Annu Rev Pathol*, 2014. **9** 157-179.
333. Suki, B., S. Ito, D. Stamenović, K.R. Lutchen, and E.P. Ingenito, *Biomechanics of the lung parenchyma: critical roles of collagen and mechanical forces*. *Journal of Applied Physiology*, 2005. **98** 1892.
334. Raghu, G., S. Masta, D. Meyers, and A.S. Narayanan, *Collagen Synthesis by Normal and Fibrotic Human Lung Fibroblasts and the Effect of Transforming Growth Factor- $\beta$* . *American Review of Respiratory Disease*, 1989. **140** 95-100.

335. Chapman, H.A., *Epithelial-Mesenchymal Interactions in Pulmonary Fibrosis*. Annual Review of Physiology, 2011. **73** 413-435.
336. Hashimoto, N., H. Jin, T. Liu, S.W. Chensue, and S.H. Phan, *Bone marrow-derived progenitor cells in pulmonary fibrosis*. J Clin Invest, 2004. **113**.
337. Liu, Y. and X. Cao, *The origin and function of tumor-associated macrophages*. Cell Mol Immunol, 2015. **12** 1-4.
338. Franklin, R.A., W. Liao, A. Sarkar, M.V. Kim, M.R. Bivona, K. Liu, *et al.*, *The cellular and molecular origin of tumor-associated macrophages*. Science, 2014. **344** 921.
339. Wang, Y.-C., F. He, F. Feng, X.-W. Liu, G.-Y. Dong, H.-Y. Qin, *et al.*, *Notch Signaling Determines the M1 versus M2 Polarization of Macrophages in Antitumor Immune Responses*. Cancer Research, 2010. **70** 4840.
340. Xue, J., V. Sharma, M.H. Hsieh, A. Chawla, R. Murali, S.J. Pandol, *et al.*, *Alternatively activated macrophages promote pancreatic fibrosis in chronic pancreatitis*. 2015. **6** 7158.
341. Zheng, X., H. Baker, W.S. Hancock, F. Fawaz, M. McCaman, and E. Pungor, *Proteomic Analysis for the Assessment of Different Lots of Fetal Bovine Serum as a Raw Material for Cell Culture. Part IV. Application of Proteomics to the Manufacture of Biological Drugs*. Biotechnology Progress, 2006. **22** 1294-1300.
342. Oida, T. and H.L. Weiner, *Depletion of TGF- $\beta$  from fetal bovine serum*. Journal of immunological methods, 2010. **362** 195-198.
343. Filby, A., J. Begum, M. Jalal, and W. Day, *Appraising the suitability of succinimidyl and lipophilic fluorescent dyes to track proliferation in non-quiescent cells by dye dilution*. Methods, 2015. **82** 29-37.
344. Canton, J., D. Neculai, and S. Grinstein, *Scavenger receptors in homeostasis and immunity*. Nat Rev Immunol, 2013. **13** 621-634.
345. Foster, K.A., C.G. Oster, M.M. Mayer, M.L. Avery, and K.L. Audus, *Characterization of the A549 Cell Line as a Type II Pulmonary Epithelial Cell Model for Drug Metabolism*. Experimental Cell Research, 1998. **243** 359-366.
346. Kasai, H., J.T. Allen, R.M. Mason, T. Kamimura, and Z. Zhang, *TGF- $\beta$ 1 induces human alveolar epithelial to mesenchymal cell transition (EMT)*. Respiratory Research, 2005. **6** 56-56.
347. Ren, Z.-X., H.-B. Yu, J.-S. Li, J.-L. Shen, and W.-S. Du, *Suitable parameter choice on quantitative morphology of A549 cell in epithelial-mesenchymal transition*. Bioscience Reports, 2015. **35** e00202.
348. Kawami, M., R. Harabayashi, M. Miyamoto, R. Harada, R. Yumoto, and M. Takano, *Methotrexate-Induced Epithelial-Mesenchymal Transition in the Alveolar Epithelial Cell Line A549*. Lung, 2016. **194** 923-930.
349. Wahab, N.A. and R.M. Mason, *A critical look at growth factors and epithelial-to-mesenchymal transition in the adult kidney. Interrelationships between growth factors that regulate EMT in the adult kidney*. Nephron Exp Nephrol, 2006. **104**.
350. Milman, N., M.S. Kristensen, and K. Bentsen, *Hyaluronan and procollagen type III aminoterminal peptide in serum and bronchoalveolar lavage fluid from patients with pulmonary fibrosis*. APMIS, 1995. **103** 749-754.
351. Rankin, K.S. and D. Frankel, *Hyaluronan in cancer - from the naked mole rat to nanoparticle therapy*. Soft Matter, 2016. **12** 3841-3848.

352. Nikitovic, D., M. Tzardi, A. Berdiaki, A. Tsatsakis, and G.N. Tzanakakis, *Cancer Microenvironment and Inflammation: Role of Hyaluronan*. *Frontiers in Immunology*, 2015. **6** 169.
353. Zeng, Q. and W. Chen, *The Functional Behavior of a Macrophage/Fibroblast Co-culture Model Derived from Normal and Diabetic Mice with a Marine Gelatin - Oxidized Alginate Hydrogel*. *Biomaterials*, 2010. **31** 5772-5781.
354. Fielding, Ceri A., Gareth W. Jones, Rachel M. McLoughlin, L. McLeod, Victoria J. Hammond, J. Uceda, *et al.*, *Interleukin-6 Signaling Drives Fibrosis in Unresolved Inflammation*. *Immunity*, 2014. **40** 40-50.
355. Zhong, H., L. Belardinelli, T. Maa, and D. Zeng, *Synergy between A2B Adenosine Receptors and Hypoxia in Activating Human Lung Fibroblasts*. *American Journal of Respiratory Cell and Molecular Biology*, 2005. **32** 2-8.
356. Deng, X., M. Xu, C. Yuan, L. Yin, X. Chen, X. Zhou, *et al.*, *Transcriptional regulation of increased CCL2 expression in pulmonary fibrosis involves nuclear factor- $\kappa$ B and activator protein-1*. *The International Journal of Biochemistry & Cell Biology*, 2013. **45** 1366-1376.
357. Moore, B.B., *Following the Path of CCL2 from Prostaglandins to Periostin in Lung Fibrosis*. *American Journal of Respiratory Cell and Molecular Biology*, 2014. **50** 848-852.
358. Raghu, G., F.J. Martinez, K.K. Brown, U. Costabel, V. Cottin, A.U. Wells, *et al.*, *CC-chemokine ligand 2 inhibition in idiopathic pulmonary fibrosis: a phase 2 trial of carlumab*. *European Respiratory Journal*, 2015. **46** 1740.
359. Murray, L.A., R.L. Argentieri, F.X. Farrell, M. Bracht, H. Sheng, B. Whitaker, *et al.*, *Hyper-responsiveness of IPF/UIP fibroblasts: Interplay between TGF $\beta$ 1, IL-13 and CCL2*. *The International Journal of Biochemistry & Cell Biology*, 2008. **40** 2174-2182.
360. Uhal, B.D., C. Ramos, I. Joshi, A. Bifero, A. Pardo, and M. Selman, *Cell size, cell cycle, and  $\alpha$ -smooth muscle actin expression by primary human lung fibroblasts*. *American Journal of Physiology - Lung Cellular and Molecular Physiology*, 1998. **275** L998.
361. Yoon, Y.-S., Y.-J. Lee, Y.-H. Choi, Y.M. Park, and J.L. Kang, *Macrophages programmed by apoptotic cells inhibit epithelial-mesenchymal transition in lung alveolar epithelial cells via PGE2, PGD2, and HGF*. 2016. **6** 20992.
362. Shukla, M.N., J.L. Rose, R. Ray, K.L. Lathrop, A. Ray, and P. Ray, *Hepatocyte Growth Factor Inhibits Epithelial to Myofibroblast Transition in Lung Cells via Smad7*. *American Journal of Respiratory Cell and Molecular Biology*, 2009. **40** 643-653.
363. Polverini, P.J., R.S. Cotran, M.A. Gimbrone, and E.R. Unanue, *Activated macrophages induce vascular proliferation*. *Nature*, 1977. **269** 804-806.
364. Ikezumi, Y., L.A. Hurst, T. Masaki, R.C. Atkins, and D.J. Nikolic-Paterson, *Adoptive transfer studies demonstrate that macrophages can induce proteinuria and mesangial cell proliferation*. *Kidney International*, 2003. **63** 83-95.
365. Fu, X., H. Shi, Y. Qi, W. Zhang, and P. Dong, *M2 polarized macrophages induced by CSE promote proliferation, migration, and invasion of alveolar basal epithelial cells*. *International Immunopharmacology*, 2015. **28** 666-674.
366. Withana, N.P., X. Ma, H.M. McGuire, M. Verdoes, W.A. van der Linden, L.O. Ofori, *et al.*, *Non-invasive Imaging of Idiopathic Pulmonary Fibrosis Using Cathepsin Protease Probes*. *Scientific Reports*, 2016. **6** 19755.

367. Lucattelli, M., E. Cavarra, M. M. de Santi, T.D. Tetley, P.A. Martorana, and G. Lungarella, *Collagen phagocytosis by lung alveolar macrophages in animal models of emphysema*. European Respiratory Journal, 2003. **22** 728.
368. Kunkel, S.L., T. Standiford, K. Kasahara, and R.M. Strieter, *Interleukin-8 (IL-8): The Major Neutrophil Chemotactic Factor in the Lung*. Experimental Lung Research, 1991. **17** 17-23.
369. Dentener, M.A., V. Bazil, E.J.U. Vonasmuth, M. Ceska, and W.A. Buurman, *Involvement of Cd14 in Lipopolysaccharide-Induced Tumor-Necrosis-Factor-Alpha, Il-6 and Il-8 Release by Human Monocytes and Alveolar Macrophages*. Journal of Immunology, 1993. **150**.
370. Savill, J., I. Dransfield, C. Gregory, and C. Haslett, *A blast from the past: clearance of apoptotic cells regulates immune responses*. Nat Rev Immunol, 2002. **2** 965-975.
371. Jun, J.-I., K.-H. Kim, and L.F. Lau, *The matricellular protein CCN1 mediates neutrophil efferocytosis in cutaneous wound healing*. 2015. **6** 7386.
372. Silva, M.T., *Secondary necrosis: The natural outcome of the complete apoptotic program*. FEBS Letters, 2010. **584** 4491-4499.
373. Fadok, V.A., D.L. Bratton, A. Konowal, P.W. Freed, J.Y. Westcott, and P.M. Henson, *Macrophages that have ingested apoptotic cells in vitro inhibit proinflammatory cytokine production through autocrine/paracrine mechanisms involving TGF-beta, PGE2, and PAF*. Journal of Clinical Investigation, 1998. **101** 890-898.
374. Lee, Y.-J., C. Moon, S.H. Lee, H.-J. Park, J.-Y. Seoh, M.-S. Cho, *et al.*, *Apoptotic cell instillation after bleomycin attenuates lung injury through hepatocyte growth factor induction*. European Respiratory Journal, 2012. **40** 424.
375. McCubbrey, A.L. and J.L. Curtis, *Efferocytosis and Lung Disease*. Chest, 2013. **143** 1750-1757.
376. Yoshida, S., N. Minematsu, S. Chubachi, H. Nakamura, M. Miyazaki, K. Tsuduki, *et al.*, *Annexin V decreases PS-mediated macrophage efferocytosis and deteriorates elastase-induced pulmonary emphysema in mice*. American Journal of Physiology - Lung Cellular and Molecular Physiology, 2012. **303** L852.
377. Madsen, D.H., D. Leonard, A. Masedunskas, A. Moyer, H.J. Jürgensen, D.E. Peters, *et al.*, *M2-like macrophages are responsible for collagen degradation through a mannose receptor-mediated pathway*. The Journal of Cell Biology, 2013. **202** 951-966.
378. Underhill, D.M. and H.S. Goodridge, *Information processing during phagocytosis*. Nat Rev Immunol, 2012. **12** 492-502.
379. Kaufmann, S.H.E. and A. Dorhoi, *Molecular Determinants in Phagocyte-Bacteria Interactions*. Immunity, 2016. **44** 476-491.
380. Parakkal, P.F., *Involvement of macrophages in collagen resorption* The Journal of Cell Biology, 1969. **41** 345.
381. Cooper, J.A., *Effects of cytochalasin and phalloidin on actin*. The Journal of Cell Biology, 1987. **105** 1473-1478.
382. Rothlin, C.V., J.A. Leighton, and S. Ghosh, *Tyro3, Axl, and Mertk Receptor Signaling in Inflammatory Bowel Disease and Colitis-associated Cancer*. Inflammatory bowel diseases, 2014. **20** 1472-1480.

383. Zizzo, G., B.A. Hilliard, M. Monestier, and P.L. Cohen, *Efficient Clearance of Early Apoptotic Cells by Human Macrophages Requires M2c Polarization and MerTK Induction*. The Journal of Immunology, 2012. **189** 3508.
384. Józefowski, S., M. Arredouani, T. Sulahian, and L. Kobzik, *Disparate Regulation and Function of the Class A Scavenger Receptors SR-A/II and MARCO*. The Journal of Immunology, 2005. **175** 8032.
385. Stephen, S.L., K. Freestone, S. Dunn, M.W. Twigg, S. Homer-Vanniasinkam, J.H. Walker, *et al.*, *Scavenger Receptors and Their Potential as Therapeutic Targets in the Treatment of Cardiovascular Disease*. International Journal of Hypertension, 2010. **2010**.
386. Lipscomb, M.F., J. Hutt, J. Lovchik, T. Wu, and C.R. Lyons, *The Pathogenesis of Acute Pulmonary Viral and Bacterial Infections: Investigations in Animal Models*. Annual Review of Pathology: Mechanisms of Disease, 2010. **5** 223-252.
387. Pulkkinen, V., K. Salmenkivi, V.L. Kinnula, E. Sutinen, M. Halme, U. Hodgson, *et al.*, *A novel screening method detects herpesviral DNA in the idiopathic pulmonary fibrosis lung*. Annals of Medicine, 2012. **44** 178-186.
388. Lasithiotaki, I., K.M. Antoniou, V.-M. Vlahava, K. Karagiannis, D.A. Spandidos, N.M. Siafakas, *et al.*, *Detection of Herpes Simplex Virus Type-1 in Patients with Fibrotic Lung Diseases*. PLoS ONE, 2011. **6** e27800.
389. Tang, Y.-W., J.E. Johnson, P.J. Browning, R.A. Cruz-Gervis, A. Davis, B.S. Graham, *et al.*, *Herpesvirus DNA Is Consistently Detected in Lungs of Patients with Idiopathic Pulmonary Fibrosis*. Journal of Clinical Microbiology, 2003. **41** 2633-2640.
390. Vidal, S., C. de la Horra, J. Martín, M.A. Montes-Cano, E. Rodríguez, N. Respaldiza, *et al.*, *Pneumocystis jirovecii colonisation in patients with interstitial lung disease*. Clinical Microbiology and Infection, 2006. **12** 231-235.
391. Ding, K., A. Shibui, Y. Wang, M. Takamoto, T. Matsuguchi, and K. Sugane, *Impaired recognition by Toll-like receptor 4 is responsible for exacerbated murine Pneumocystis pneumonia*. Microbes and Infection, 2005. **7** 195-203.
392. Wang, S.-H., C. Zhang, M.E. Lasbury, C.-P. Liao, P.J. Durant, D. Tschang, *et al.*, *Decreased inflammatory response in Toll-like receptor 2 knockout mice is associated with exacerbated Pneumocystis pneumonia*. Microbes and infection / Institut Pasteur, 2008. **10** 334-341.
393. Kelly, M.N. and J.E. Shellito, *Current understanding of Pneumocystis immunology*. Future microbiology, 2010. **5** 43-65.
394. Heron, M., J.C. Grutters, K.M. ten Dam-Molenkamp, D. Hijdra, A. van Heugten-Roeling, A.M.E. Claessen, *et al.*, *Bronchoalveolar lavage cell pattern from healthy human lung*. Clinical and Experimental Immunology, 2012. **167** 523-531.
395. Carré, P.C., R.L. Mortenson, T.E. King, P.W. Noble, C.L. Sable, and D.W. Riches, *Increased expression of the interleukin-8 gene by alveolar macrophages in idiopathic pulmonary fibrosis. A potential mechanism for the recruitment and activation of neutrophils in lung fibrosis*. Journal of Clinical Investigation, 1991. **88** 1802-1810.
396. Gregory, A.D., C.R. Kliment, H.E. Metz, K.-H. Kim, J. Kargl, B.A. Agostini, *et al.*, *Neutrophil elastase promotes myofibroblast differentiation in lung fibrosis*. Journal of Leukocyte Biology, 2015. **98** 143-152.
397. Soehnlein, O. and L. Lindbom, *Phagocyte partnership during the onset and resolution of inflammation*. Nat Rev Immunol, 2010. **10** 427-439.

398. Todt, J.C., B. Hu, and J.L. Curtis, *The scavenger receptor SR-A I/II (CD204) signals via the receptor tyrosine kinase Mertk during apoptotic cell uptake by murine macrophages*. *Journal of Leukocyte Biology*, 2008. **84** 510-518.
399. Labonte, A.C., S.S.J. Sung, L.T. Jennelle, A.P. Dandekar, and Y.S. Hahn, *Expression of scavenger receptor-AI promotes alternative activation of murine macrophages to limit hepatic inflammation and fibrosis*. *Hepatology (Baltimore, Md.)*, 2017. **65** 32-43.
400. Jakubzick, C., Emmanuel L. Gautier, Sophie L. Gibbings, Dorothy K. Sojka, A. Schlitzer, Theodore E. Johnson, *et al.*, *Minimal Differentiation of Classical Monocytes as They Survey Steady-State Tissues and Transport Antigen to Lymph Nodes*. *Immunity*, 2013. **39** 599-610.
401. Molyneaux, P., M. Cox, S. Willis-Owen, K. Russell, P. Mallia, A.-M. Russell, *et al.*, *High Bacterial Load Predicts Poor Outcomes in Patients with Idiopathic Pulmonary Fibrosis*. *bioRxiv*, 2014.
402. Mora, A.L., C.R. Woods, A. Garcia, J. Xu, M. Rojas, S.H. Speck, *et al.*, *Lung infection with gamma-herpesvirus induces progressive pulmonary fibrosis in Th2-biased mice*. *Am J Physiol Lung Cell Mol Physiol*, 2005. **289** L711-721.
403. Kakugawa, T., N. Sakamoto, S. Sato, H. Yura, T. Harada, S. Nakashima, *et al.*, *Risk factors for an acute exacerbation of idiopathic pulmonary fibrosis*. *Respiratory Research*, 2016. **17** 79.
404. Kim, D.S., J.H. Park, B.K. Park, J.S. Lee, A.G. Nicholson, and T. Colby, *Acute exacerbation of idiopathic pulmonary fibrosis: frequency and clinical features*. *Eur Respir J*, 2006. **27**.
405. Cai, Y., C. Sugimoto, M. Arainga, X. Alvarez-Hernandez, E.S. Didier, and M.J. Kuroda, *In vivo characterization of alveolar and interstitial lung macrophages in rhesus macaques: Implications for understanding lung disease in humans*. *Journal of immunology (Baltimore, Md. : 1950)*, 2014. **192** 2821-2829.
406. Arandjelovic, S. and K.S. Ravichandran, *Phagocytosis of apoptotic cells in homeostasis*. *Nat Immunol*, 2015. **16** 907-917.
407. Munn, D.H., M.B. Garnick, and N.K. Cheung, *Effects of parenteral recombinant human macrophage colony-stimulating factor on monocyte number, phenotype, and antitumor cytotoxicity in nonhuman primates*. *Blood*, 1990. **75** 2042.
408. Zhang, Y., S. Choksi, K. Chen, Y. Pobezienskaya, I. Linnola, and Z.-G. Liu, *ROS play a critical role in the differentiation of alternatively activated macrophages and the occurrence of tumor-associated macrophages*. *Cell Res*, 2013. **23** 898.
409. Hume, D.A. and K.P.A. MacDonald, *Therapeutic applications of macrophage colony-stimulating factor-1 (CSF-1) and antagonists of CSF-1 receptor (CSF-1R) signaling*. *Blood*, 2012. **119** 1810.